SEISMIC REGIONALIZATION TECHNIQUES AND STRONG MOTION RECORDINGS

Thesis

Submitted to the University of London
in partial fulfilment for the M. Phil
in Civil Engineering

by

Alexander A. Roussopoulos

November 1977

TABLE OF CONTENTS

Chapter	Title	page
	ACKNOWLEDGEMENTS	i
	ABSTRACT	1
	INTRODUCTION	2-8
I	STRONG MOTION RECORDINGS IN LEUKAS ISLAND (GREECE)	9-16
II	MICROZONING IN THE CITY OF LEUKAS	17-29
III	MICROZONING STUDIES IN THESSALONIKI	30-51
IV	FINAL CONCLUSIONS AND RECOMMENDATIONS	52-54
I	FIGURES	55-99
II	FIGURES	100-114
III	FIGURES	115-152
APPENDIX A	BASE LINE CORRECTION	153-158
APPENDIX B	RESPONSE SPECTRA	159-162
APPENDIX C	NUMERICAL CALCULATION OF SPECTRUM	163-165
APPENDIX D	COMPUTER PROGRAM	166-175
REFERENCES		176-179

ACKNOWLEDGEMENTS

Part of the work of this thesis was carried out in the Department of Civil Engineering (Engineering Seismology) of the Imperial College of Science and Technology, London, and was supported by UNESCO. The other part, especially the field work, was carried out in Greece.

Particularly the microzoning in the city of Thessaloniki was done within the frame of the UNESCO Project "Seismicity of the Balkan Region".

I am indebted to Professor N.Ambraseys for continuous encouragement, assistance and guidance during the whole period of the work. Many thanks are due to Mr. G. Leventakis for participating in the microtremor measurements and part of the calculations of the microzoning of Thessaloniki. Thanks are also due to Dr. Sarma for valuable comments.

The computational work was carried out at the CDC 6600 computer of the University of London.

A B S T R A C T

The results of the Leukas earthquake which occured on November 4, 1973, are discussed and the recorded strong motion accelerograms are analysed for the main shock and the aftershock.

The main characteristics of the ground motion are calculated giving information about the nature of the earthquake and the influence of the maximum peak acceleration 0,53g to the damage distribution.

A microzoning map of the city of Leukas is compiled by the use of microtremor measurements and the soil of the city is classified according to Kanai's proposals.

The influence of the subsoil condition and the water elevation is one of the main characteristics arising from the comparison of the microzoning map, the hydrological map and the damage distribution of the city of Leukas and the soil amplification factors are derived from the calculated predominant periods of the microtremors.

From the comparison of the strong motion records and the microtremors measurements some period correlations are observed but we cannot conclude from this case that microtremors can predict earthquake motions.

In the city of Thessaloniki several microzoning methods using microtremors were applied and microzoning maps were compiled which were compared to each other. From the results obtained and the comparisons, we may conclude a) that there is a general agreement between the microzoning maps compiled by Kobayashi (Japan) and the Greek team, and b) from an engineering point of view Sherif's (U.S.A.) microzoning map is not very practical and the evaluation of his results gave seismic coefficients for Thessaloniki which are considered as overestimated.

Finally as a concluding remark we may point out that from the 24 hours measurements in the city of Leukas and in Thessaloniki, microtremors are almost stationary in time and that for unfavourable soil conditions microtremor measurements are recommended for the compilation of microzoning maps.

INTRODUCTION

It has long been recognized that the intensity of ground shaking during earthquakes and the associated damage to buildings are seriously influenced by local geologic and soil conditions. This means that macroseismic data alone are inadequate to determine the effects of earthquakes on shaken areas, as they are not sufficient to describe the exact motion at each site with different geologic and soil conditions. Studies of the distribution of damage caused by earthquakes indicate that large differences in the extent of damage often occur over relatively short distances. This means that local geological and soil conditions influence greatly the transmission of seismic waves causing different damping effects, and magnification in the layered soil, resulting in foundation failures and differential settlements of structures.

Because of the fundamental importance of soil foundation problems to all aspects of earthquake resistant design, much attention should be given to soil conditions and local geology during earthquake ground shaking. Even at the same distance from the epicenter or fault, the magnitudes of the ground motion associated with a particular earthquake may vary significantly because of the influence of local inhomogeneities in geological structure or soil and subsoil conditions. On the other hand, both theoretical analyses and results of field measurements indicate that the characteristics of the motion at the surface of a soft, deep deposit may be different from those at the underlying bedrock or on neighbouring firm ground. The effects of such a layer are usually to lengthen the period of the dominant waves in the acceleration diagram and to increase the intensity, duration

and degree of periodicity of the motion.

The investigation of soil and subsoil conditions in relation with earthquake damage is therefore very important and useful for design purposes. From observations of some recent earthquakes the amount of damage is drastically changing over extremely short distances (Skopje, Poceski, 1969). It is evident therefore that these large variations of structural damage are due to local soil and foundation problems. The relation between soil type and earthquake damage can be investigated by considering a)the influence of soil type on the intensity and waveform of earthquake motion, b) the influence of soil type on the vibration damping properties of structures, and c) the decrease in the strength of soil when subjected to vibration.

From observations and detailed investigations of past strong earthquakes and their damage effects, two main categories of structural damage can be distinguished having a close relationship both with the type of soil and the type of structure : 1) Damage arising from foundation failures caused by settlement, liquefaction or failure of soil. This type of damage mainly concerns the structure as a whole and many observations and investigations were made after some characteristic earthquakes (Niigata 1964, Chili 1960). 2) Damage occuring by cracks on the main part of the body of the structure or by dislocations at the part connected with the ground. The first type of earthquake damage occurs mainly in flexible structures with large weight, on soft ground, while the second type occurs with rigid but brittle structures which are located on hard ground.

The development of instrumentation techniques enable today seismologists and engineers to record and study seismic parameters which are of primary importance for the determination of coefficients depending on the

local geologic and soil conditions. Ground accelerations, velocities and displacements provide the basis for more accurate calculations in determining the effect of the seismic waves travelling through the bedrock and the soil layers to the ground surface.

Strong motion records provide today the main characteristics of the ground motion during a strong earthquake. The most significant characteristics of the motion are : a) the peak values of accelerations, velocity, and displacement diagrams; b) the duration of the motion; c) the degree of regularity or periodicity of the dominant pulses; and d) the mean period of these pulses. The study and the analysis of these characteristics is considered as one of the fundamental steps in facing earthquake risk.

Ground acceleration, velocity and displacement form the basic data for spectral calculation which, as maximum response values, can be expressed in terms of acceleration, velocity and displacement for different dampings. The calculation of spectral values is very important for engineering purposes.

Modern computer methods facilitate immensely the use of the recorded data, their classification and the calculation of all the seismic parameters.

The nature of the ground movements at a site will depend on many factors such as the proximity of the site to the focal volume, the magnitude of the shock, the mechanism of the earthquake and the superficial geology of the site. More specifically, in addition to recording the motion of the ground at some point in the epicentral region of the earthquake, it is also of great engineering importance to record the motion on a variety of foundation materials, such as rock, firm alluvium of various depths, and

soft ground. Earthquake ground motions should be recorded on the different foundation conditions on which structures are built.

Seismic waves generated after the release of energy caused by an earthquake, propagate from the seismic source through the earth crust to the bedrock and then through the soil layers to the ground surface.

The behaviour of the materials through which the waves propagate is very important, but what is really very significant is the behaviour of the foundations materials due to the bedrock motion and the layer response to this motion.

In the alluvium ground, impedance is small in comparison to that in rock and diluvial ground; and moreover, since there are predominant periods, there is a possibility of particularly large vibrations occuring at the time of an earthquake. Maximum values of acceleration, velocity, and displacement are important characteristic values of earthquake motion, and it is necessary to know to what extent these are amplified by the existence of the surface layer. However, circumstances differ according to the case and it is difficult to state the matter in general terms (Ambraseys, 1970).

From various observations and results obtained, it is concluded that displacements in alluvial areas are considerably greater than those in rocky area . However, as the magnification ratio cannot be determined generally, the method of obtaining the surest results is to carry out individual geological surveys and to make detailed calculations.

If we consider seismic zoning on a general or global basis there would probably be a rough general agreement on the shape and size of three basic zones : a) a relatively high risk area, in which definite provisions should be made for protection from destructive earthquakes, b) a moderate risk area, in which destructive earthquakes may occur so rarely that the economic consequences can be easily absorbed by society with only minor protective measures, c) an almost aseismic region where practically no measures are taken.

However, this zoning classification is inadequate for engineering purposes since structural design requires seismic parameters which are related with local geology and soil and subsoil conditions at each specific site.

A first approach towards more detailed seismic zones is done with the seismic zoning maps which are usually prepared by seismologists following a major earthquake. These so called intensity maps are made on a basis of observation of damage, reactions of inhabitants, moving of objects and so forth. The region is divided into various zones of expected intensity (intencity experienced). More detailed maps would show how the expected intensity of ground shaking varies within a zone, taking into account proximity of faults, local geology and so on. In this most detailed form, the map would provide intensity evaluations for specific sites. However, even these maps are not always sufficient for engineering purposes, since they are not based on recorded ground motion. The engineering value of such earthquake intensity maps would be greatly enhanced if they could be based on a more meaningful definition of intensity than subjective assesements of building damage

and the like. On the other hand damage to structures is caused not only by seismic intensity but also by damage of soil and quality of structures.

Today, the limited number of strong motion accelerographs makes the exact knowledge of earthquake ground motion very difficult and consequently the compilation of a seismic map has to be based on other parameters.

The production of maps of seismic zoning, requires the depth of the earthquake foci, the relationship between energy at the focus and epicentral intensity, the correlation between magnitude and intensity, information concerning attenuation of intensity with distance and other data.

More detailed studies in earthquake engineering problems are necessary for seismic maps, which should indicate the relative danger from earthquake at any given locality. Such maps should consider: a) The general seismicity of the area occuring from the investigation of the geographical distribution of hypocenters of past earthquakes. b) The influence of the local geological conditions on ground motions associated with earthquakes. c) The details of local soil and subsoil foundation conditions.

Urban planning and industrial development of a region which is often subjected to strong earthquakes, requires a detailed investigation of the soil and the subsoil conditions before construction. In order to protect the national economy of a country which suffers from strong earthquakes, it is necessary to introduce technical criteria which will enable society to face dangerous earthquakes. If seismic

zoning considers distribution of earthquake hazard for the entire country or larger regions, seismic microzoning considers a more detailed distribution of earthquake hazard within each of the zones defined by the seismic zoning.

Among the various existing definitions, microzoning can be defined as the study of small land areas under local geology conditions and earthquake characteristics, serving as guide for safer land use and safer construction, according to the specified local differences in earthquake attack on structures.

Various microzoning techniques are used for the compilation of microzoning maps. These techniques applying microtremor measurements (Kanai) or measuring the ratio of earthquake damage, expressed in seismic intensity, and the rigidity of the surface soil layers (Medvedev) are used for the determination and evaluation of ground motion characteristics.

The installation of more strong motion instruments at seismic active regions and the application of the microzoning methods, will enable engineers and seismologists to get more accurate information and data for the compilation and evaluation of microzoning maps.

C H A P T E R I

STRONG MOTION RECORDINGS IN LEUKAS ISLAND (GREECE)

==========

I.1 General considerations

The region of the Ionian islands in Greece, is considered as one of the most seismic active regions of the Mediterranean area. Strong and severe earthquakes have shaken this region in the past with many human losses and heavy damages.

One of the most characteristic earthquakes which have shaken the Ionian islands was the earthquake which occured in August 1953, during which many people were killed and many buildings were destroyed. Namely the islands of Zakynthos, Cephalonia and Ithaca were almost completely destroyed, and the island of Leukas was seriously damaged. The shocks during that time were not recorded by strong motion seismographs and consequently ground accelerations were not obtained. However the observed maximum intensities for the zone including the islands Leukas, Zakynthos, Cephalonia are I > IX. The concentration of earthquake activity in this area has been attributed by A.Galanopoulos (1965a) to the intersection of the Ionian fault zone with the assumed prolongation of the North Anatolian shear fault zone.

Recently a strong motion network has been installed to these islands and the recorded accelerograms provided useful information for this area.

I.2 Leukas earthquake of November 4, 1973

On November 4, 1973 in 15:52(h:min) the island of Leukas was shaken by a strong earthquake of magnitude M = 6.0 with epicentral distance 18 km. The isoseismal map of the Leukas earthquake is shown in figure I.1.

This earthquake was recorded by the strong motion instrument type SMA-1 which was installed in the city of Leukas and the original accelerogram is shown in Fig. I.2a. The duration of this earthquake was 24 sec and it was recorded in two horizontal (N25W, N65E) and one vertical component. The maximum acceleration obtained was for the N25W component and was found equal to 0,53g, which is the highest acceleration ever recorded in Greece by a strong motion accelerograph.

After a while in 16:11 (h:min) another earthquake of magnitude M = 5.0 has shaken Leukas with maximum recorded acceleration 0,08g (N25W component). The duration of this earthquake was 12,5 sec, and the original record is shown in Fig.I.2b .

I.3 Digitization of the accelerograms

It was found that the accelerogram trace could be approximated quite closely by a series of straight line segments.

The digitizing process is carried out on a device which consists of a mechanical cross-head and cross-hair system which can be manually set to successive x - y coordinates on the record trace. By means of a magnetic read out head these x - y coordi-

nates are converted to digital position signals by an electronic counter and are stored in an accumulator system from which they can automatically read out to an electric typewriter.

Since there is no zero axis on the accelerogram, a temporary base line is drawn on the record and the coordinates of the intersection points of successive line segments are measured from this temporary base line and recorded.

If we enlarge the accelerogram which is shown in Fig.I.3 along with a plot of the same portion taken from the punched cards after digitizing, we can observe that the punched card trace follows the instrumental trace reasonably well, but it is clear that there is a circle of uncertainty about each intersection point. It is apparent that the width of the trace is large enough to leave an uncertainty as to the exact coordinates of any particular point. So different persons approximating the same accelerogram by broken line diagrams would use different numbers of line segments. Even if the same broken line diagrams were used by all, there would still be differences in reading the time and acceleration coordinates.

The original accelerograms of the Leukas earthquakes were enlarged three times and digitized.

I.4 Integration procedure

The integration procedure is based on the assumption that the accelerogram is a series of straight lines connecting the peaks. So the values of velocities and displacements can be determined by two successive integrations of the digitized accelerogram.

Symbols $\ddot{u}$, $\dot{u}$, u denote acceleration, velocity and displacement respectively.

Considering just the peaks we can write for the interval

$$t_{i-1} < t < t_i \quad , \quad \ddot{u} = a_i(t-t_{i-1}) + b_i$$

where a_i b_i are constants for the i'th segment of the record. Integrating once, we have

$$\dot{u} = \frac{a_i}{2}(t-t_{i-1})^2 + b_i(t-t_{i-1}) + c_i$$

at $t = t_{i-1}$, $\dot{u} = \dot{u}_{i-1}$

$$\dot{u} = \frac{a_i}{2}(t-t_{i-1})^2 + b_i(t-t_{i-1}) + \dot{u}_{i-1} \qquad \ldots (1.1)$$

If we integrate once more,

$$u = \frac{a_i}{6}(t-t_{i-1})^3 + \frac{b_i}{2}(t-t_{i-1})^2 + \dot{u}_{i-1}(t-t_{i-1}) + u_{i-1} \qquad \ldots (1.2)$$

Thus, starting from the beginning of the record with initial conditions at rest, i.e. at t=0, u=$\dot{u}$=0, the record can be integrated step by step to obtain the ground velocity and ground displacement at any required instant and also at the end of the event.

These calculations were carried out by the use of digital computers.

In principle it should be immaterial whether the displacements, velocities or accelerations of the ground are measured, since there is a simple mathematical relationship between them.

To obtain displacement from acceleration requires two integrations, whereas to obtain the acceleration from the displacement requires two differentiations. In practice, however, integrations can be carried out much more accurately than differentiations, since it is easier to determine the way in which the area under a complicated curve varies with time than it would be to measure the slope of the curve with the required accuracy. This can be seen clearly for any typical earthquake which gives the ground acceleration, velocity and displacement curves. To start from the displacement curve and then to repeat the process to obtain the very complicated acceleration curve would be a practically impossible undertaking. The inevitable loss of accuracy in the differentiation process cannot be avoided no matter how the process is carried out. We can thus reach the conclusion, that the basic measurement for earthquake engineering applications must be of the ground acceleration versus time. Once an accurate ground acceleration curve is available, the velocity and displacement curves can be obtained with a satisfactory accuracy, taking into consideration that the original accelerogram has no base line and that a base line correction is required for the determination of these values.

Figures I.4 to I.9 show the values of velocities before the base line correction for all the components of the main shock and the aftershock of the Leukas earthquakes.

I.5 Base line correction

One of the most important stages in the analysis of strong motion records is the base line correction. The procedure is described in details in Appendix A.

Introducing the mean square velocity technique for the base line correction we get the corrected values of acceleration, velocity and displacement.

A computer program has been prepared and the computer work was carried out at the CDC 6600 computer unit of Imperial College (See Appendix D).

The recorded accelerograms of the main shock and of the aftershock were analysed and the values of acceleration, velocity and displacement were obtained in the two horizontal components and the vertical component.

The results are shown in the following table I.1

TABLE I.1

MAIN SHOCK AND AFTERSHOCK OF NOV.4,1973 IN LEUKAS

	Component	Duration of earthquake in sec	Max acceleration in g.	Max velocity in cm/sec	Permanent displacement in cm
MAIN SHOCK	N25W	24	0,53	55	3,8
	N65E	24	0,27	26,8	1,1
	Vertical	24	0,11	8	1,3
AFTER-SHOCK	N25W	12,5	0,08	5	0,40
	N65E	12,5	0,05	3	0,40
	Vertical	12,5	0,03	1,8	0,40

The plots of the three components of the main shock and the aftershock for the values, corrected acceleration, corrected velocity, corrected displacement, are shown in figures I.10 to I.27.

I.6 Response spectra

The mathematical solution of response spectra is given in Appendix B. However, since the acceleration records can be approximated to a series of triangular pulses we can apply numerical calculations to the end of evaluating the integrals of the equations. The complete solution of the equation of motion for a linear, viscously damped, single degree of freedom oscillator, using numerical calculation is given in Appendix C.

A complete analysis of the three recorded components of both the main shock and the aftershock was accomplished and the corresponding results were plotted. The spectral values were calculated for different dampings, i.e. $\lambda_1 = 0$, $\lambda_2 = 0,01$, $\lambda_3 = 0,02$, $\lambda_4 = 0,05$, $\lambda_5 = 0,10$, $\lambda_6 = 0,20$. The time interval used was 0,02 sec.

The plots of the three components of the main shock and the aftershock of Leukas, for the values acceleration spectra, velocity spectra and displacement spectra are shown in figures I.28 to I.45.

I.7. Observations - conclusions on Leukas earthquake

1. The epicenter was located in the sea at a distance of 18 km northwest of the island.
2. The earthquake had shaken all the island with maximum intensity observed into the city of Leukas (Fig.I.1)
3. Cracks along the coast were observed and in some regions there were landslides.
4. Some houses were damaged including buildings of reinforced concrete.

5. As shown in figure I.10 the maximum acceleration of 0,53g was instantaneous and the following values of acceleration during the shock ranged from 0,13g to 0,06g. This explains the limited destruction which occured since the instantaneous duration of 0,53g was out of the range of the periods of the buildings.

6. It must be mentioned that the water level of the city of Leukas is very high. A possible result of this was a limited liquefaction of the soil which caused greater periods after the occurence of the peak acceleration.

7. Another interesting characteristic is the beginning of the main shock which as shown in the recorded accelerograms of the vertical component (Fig.I.16), the ground started moving vertically. This was confirmed by the inhabitants. A possible reason may be the small epicentral distance.

8. From the various buildings which were examined after the earthquake, it was observed that damages were considerably heavy in new buildings made of reinforced concrete. On the other hand old and simple flexible houses which were constructed 150-200 years ago, were slightly damaged or even undamaged. This is due to the method of construction with the characteristic wooden elements distributed to the vertical, horizontal and diagonal directions among the main body of the house and to the instantaneous peak acceleration.

C H A P T E R II

MICROZONING OF THE CITY OF LEUKAS

II.1 Microtremor measurements

Two main reasons lead us to experience microzoning techniques in the city of Leukas island. The first, because the earthquake of November 4, 1973 was recorded by the strong motion accelerograph and the analysis of the records gave much information about the characteristics of the ground motion. Consequently it was possible to compare some results obtained from the strong motion records and microtremor measurements. The second; because the soil conditions of the city of Leukas consist of deep alluvial deposits with high water level, and such conditions have to be studied very carefully.

The microzoning technique which was used in the city of Leukas was developed by Kanai who introduced microtremor measurements. Microtremors represent continuous vibrations of the ground having small amplitudes ranging from 0.1 to 1 micron. These vibrations are resulting from uncontrolled natural or artificial exitations such as wind, sea waves, traffic, industrial noise and similar causes. Kanai has recorded microtremors and earth shaking at a number of sites. Generally his results have been published in terms of period distribution curves in which the frequency of occurence was plotted against period.

The instrumentation system used in the city of Leukas consisted of three seismometers, one vertical and two horizontal, a three-channel amplifier, a four-channel, open reel magnetic tape recorder and a six-channel oscillograph which was recording the microtremor measurements on a photographic paper.

In the city of Leukas (Fig. II.1) 30 points were selected for microtremor measurements. The duration of each measurement was about 90 sec and the analysis of the recorded microtremors was extended up to 30 sec.

Kanai's microzoning technique which was used in the city of Leukas is based on two proposals.

The first uses the "mean" period and the "largest" period (that is the period of the largest amplitude wave), while the second method uses the largest amplitude of the recorded motion and the predominant period at the site. By this way subsoils are classified using the characteristics of the observed microtremors with the aid of the microzoning charts as shown in Fig.II.2 and II.3. The symbols I,II,III,IV represent the kinds of soil as they are used in the Building Code of Japan with the following standards for the designation:

Kind I : Ground consisting of rock, hard sand gravel etc., classified as tertiary or older strata over a considerable area around the structure.

Kind II : Ground consisting of sandy gravel, sandy hard clay etc., classified as diluvial, or gravelly alluvium, about 5 meters or more in thickness, over a considerable area around the structure.

Kind III : Ground consisting of alluvium 5 meters or more in thickness, which can be distinguished from the ground of Kind II

by bluff formation.

Kind IV : Alluvium consisting of soft delta deposits, topsoil, mud etc., exceeding 30 m. in depth. Land obtained by reclamation of marsh where more than 30 years have elapsed since time of reclamation.

The application of the above mentioned two proposals depends on the largest period, mean period, predominant period and largest amplitude of microtremors, and the evaluation of these ground parameters is achieved with the use of frequency-period distribution curves. The whole procedure is described in details in Chapter III.

In Fig. II.4 to II.11 tne plotted period distribution curves are shown and in Table II.1 the soil is classified according to Kanai's two proposals.

A microzoning map of the city of Leukas is compiled indicating the soil classification (Fig.II.12).

Also a map of the city showing the water level was compiled (Fig.II.13).

Finally a 24 hour microtremor measurements were carried out at the place where the strong motion record was installed with the following results :

In the amplitude versus time curve A=f(t) a maximum amplitude of 0,30μ appeared at 14,00h and a minimum of 0,16μ at 04,00 h . Fig.II.14a.

The corresponding predominant period during the 24 hour measurement showed very small variations from its constant value 0,25 sec. Fig.II.14b.

II.2 Discussion on Microzoning results of the city of Leukas

One of the main problems of microzoning using microtremors is the validity of them as compared to strong motion measurements. Accor-

TABLE II.1

CITY OF LEUKAS

MICROTREMOR MEASUREMENTS

Point No	Predominant Period (T_G) sec	Largest Period(T_L) sec	Mean Per.(T_M) sec	Largest Amplit(A) μ	Kind of soil T_L-T_M	Kind of soil T_G-A	SOIL
1	0,200	1,000	0,40	0,33	2 - 3	2	II
2	0,200	0,675	0,24	0,40	2	2 - 3	II
3	0,200	0,675	0,27	0,33	2	2 - 3	II
4	0,200	0,550	0,33	0,26	2	2	II
5	0,360	00,675	0,36	0,58	2 - 3	3	III
6	0,295	0,825	0,28	0,31	2	2 - 3	III
7	0,200	0,825	0,28	0,50	2	2 - 3	II
8	0,450	0,825	0,40	0,68	2 - 3	3	III
9	0,295	0,825	0,28	0,40	2	2 - 3	II
10	0,295	0,825	0,38	0,33	2 - 3	2 - 3	II-III
11	0,200	0,825	0,28	0,44	2	2 - 3	II
12	0,295	1,000	0,25	0,30	2 - 3	2 - 3	II-III
13	00,200	0,825	0,25	0,33	2	2 - 3	II
14	0,200	0,825	0,35	0,45	2	2 - 3	II
15	0,200	0,825	0,33	0,35	2	2	II
16	0,360	1,000	0,22	0,80	2 - 3	3	III
17	0,450	0,825	0,40	0,83	2 - 3	3	III
18	0,450	1,000	0,38	0,50	2 - 3	3	III
19	0,200	1,000	0,45	0,25	2 - 3	2	II
20	0,200	0,825	0,40	0,25	2 - 3	2	II
21	0,200	1,000	0,37	0,52	2 - 3	2 - 3	II-III
22	0,245	0,825	0,36	0,71	2 - 3	3	III
23	0,200	0,675	0,30	0,50	2	2 - 3	II
24	0,450	0,675	0,37	0,52	2 - 3	2 - 3	II-III
25	0,200	0,675	0,30	0,25	2	2	II
26	0 ,200	0,675	0,25	0,23	2	2	II
27	0,200	0,825	0,38	0,32	2 - 3	2	II
28	0,245	0,825	0,36	0,37	2 - 3	2 - 3	II-III
29	0 ,450	0,825	0,43	0,55	2 - 3	3	III
30	0,450	0,825	0,38	0,75	2 - 3	3	III

ding to F. Udwadia who studied this problem using the accelerograms of the El Centro earthquakes, little or no correlation could be established between the ground response to strong earthquakes and microtremor excitation. He reported that the analysis of accelerograms in the El Centro area indicates that ground motion caused by close-in earthquakes is dependent on many factors such as the source mechanism and geologic path along which the energy travels, and which often overshadow any effects of local site conditions.

According to the Japanese investigators (Kanai, Tanaka etc) there is a considerable correlation between strong motion records and microtremor measurements. More specifically, according to Kanai for earthquakes of magnitude greater than 6, the predominant period of earthquake motion is particular to each locality and the value coincides with that of the predominant period of microtremors.

From the above mentioned we may say that there is a disagreement about the validity of microtremors after investigations and measurements in U.S.A. and Japan. Therefore it is interesting and important to find which could be the causes of these differences, since microzoning techniques are very widely applied and recommended by many investigators especially for sites where important structures are expected to be built and for sites of industrial and urban planning.

The city of Leukas island provides a good case for comparison of strong motion records and microtremor measurements.

II.3 Microtremors

According to the soil classification of the city of Leukas using microtremor measurements, the city was divided in three zones, II, II-III, III (Fig.II.12).

One of the most important parameters of ground motion is the predominant period of the ground. According to the microtremor measurements at different points of the city of Leukas and from Table I.1, the average values of predominant periods T_G corresponding to the soil classification in zones II, II-III, III, were found as follows:

SOIL II $T_G = 0,2$ sec

SOIL II-III $T_G = 0,3$ sec

SOIL III $T_G = 0,4$ sec

In alluvial surface layers vibrations are amplified due to multi reflection phenomena. By combining the results of actual measurements and theoretical calculations, Kanai derived the following formula for the amplification factor:

$$G(T) = \frac{1}{\sqrt{\left[1-\left(\frac{T}{T_G}\right)^2\right]^2 + \left[\frac{0,2}{\sqrt{T_G}}\left(\frac{T}{T_G}\right)\right]^2}}$$

where T_G is the predominant period and T is the period of vibration. For $T = T_G$ the corresponding amplification factor for each of the kinds of soil are shown in Table II.2

TABLE II.2

Kind of soil	T_G	G(T)
II	0,2	2,3
II-III	0,3	2,7
III	0,4	3,1

From the points measured in the city of Leukas, point 21(Fig.II.12)

shows the location of the strong motion instrument which recorded the earthquake of November 4, 1973 and its aftershock. According to the soil classification the strong motion accelerograph is installed on soil kind II-III.

The predominant period of the ground at that point was found according to the period distribution curve T_G = 0,245 sec.

II.4 Comparison of microtremors and strong motion records

The Fourier analysis of the microtremor at point 21, place where the strong motion accelerograph was installed, gave predominant period 0,25 sec. This value coincides with that obtained from the period distribution curve.

From the Fourier analysis of the strong motion record, of the main shock (N25W) we obtained predominant period 0,32 sec.

The results are shown in Fig. II.15.

These results show that there are some but not marked period correlations between microtremors at Leukas and strong motion records.

II.5 Comparison of microzoning map and damage distribution from the earthquake

The heaviest damages which occured from the earthquake were observed in zones III and II-III. In zone II damages were considerably lighter than the other zones. This evidence shows the influence of subsoil conditions during this strong earthquake since the way of construction and the construction materials are the same in the whole city. This last observation does not include a small section of the

city where some new houses were recently built (Fig.II.12,section N).

II.6 Comparison between microzoning map and hydrological map of the city of Leukas

If we compare the microzoning map of the city of Leukas (Fig.I.12) and the map showing the water elevation (Fig.II.13), we observe many similarities existing between these two maps. This is an indication showing the influence of the water level in a microzoning study of an area.

The seismic rigidity method developed for seismic microzoning is based on the ratio of earthquake damages expressed in seismic intensity and the rigidity of the surface soil layers. It was found in general that if the soil rigidity decreases, the earthquake damage increases. Using the results from observations of earthquake damage and geophysical explorations of the longitudinal wave velocities of the surface layers, Medvedev proposed an empirical formula for evaluation of the increment of the seismic intensity :

$$\Delta I = 1{,}67 \log \frac{P_o V_o}{P_i V_i} + e^{-0.04 h_i^2}$$

where P_o, V_o and P_i, V_i are density and longitudinal wave velocity for standard and considered soil respectively. The second term $e^{-0.04 h_i^2}$ is the increment depending on the water table elevation (h_i is the corresponding depth under the surface).

On the basis of the above equation and empirical observations, Medvedev offers the following relationship showing increases in seismic

intensity with decreasing distance of water table from ground surface level for loams, loams and fine-grained sands :

TABLE II.3

Distance to water table (meters)	Intensity increment (units)
0 - 1	1
4	0,5
10	0

Fig. II.16 shows the relation between intensity increment ΔI and water depth h_i after Steinberg.

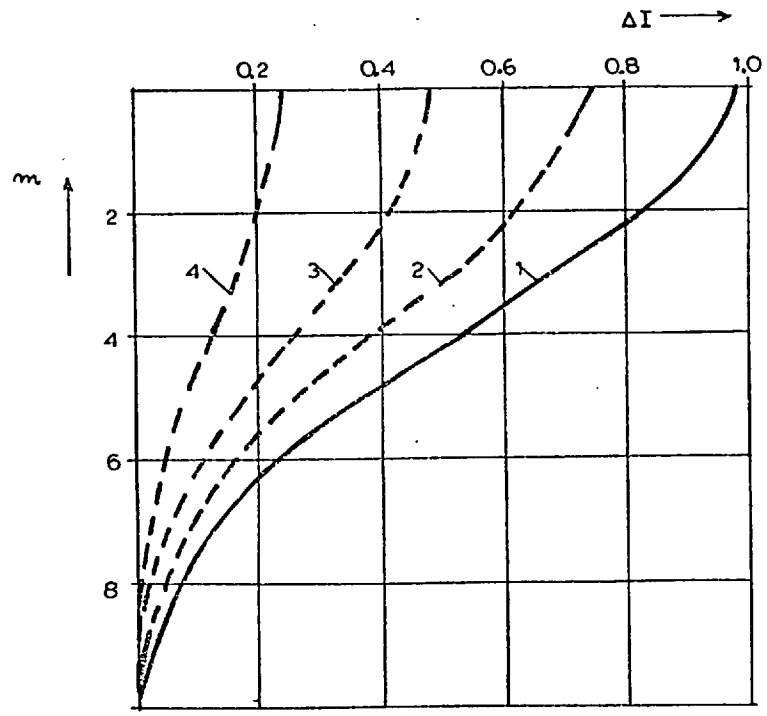


FIG II.16

Although the above figure does not necessarily apply in all cases, it does provide preliminary guidelines in assessing the earthquake damage potential of an area with respect to high water table levels.

Therefore for the city of Leukas and for zones III and II-III (Fig.II.12) the intensity increment due to water elevation was found to be $\Delta I = 1$.

II.8 Conclusions

The main results from Leukas microzonation reported in the previous section may be summarized in the following way :

1. The comparison of the microzoning map and the damage distribution showed that damages were extended mainly in the regions included in zones III and II-III according to the soil classification.Taking into consideration that the same construction techniques and building materials cover the whole city of Leukas, this evidence shows the influence of sub-soil conditions to the behaviour of the structures.

2. If to the above mentioned comparison we add the hydrological map of the city of Leukas, we observe many similarities between these maps. Namely there is a general agreement between zones III and II-III obtained from the soil classification and the zone of the hydrological map whose water depth is 0,20-0,50 m. and 0,50-1,00 m. respectively. Following Medvedev's formula the influence of water elevation is considerable for the region, giving an intensity increment $\Delta I = 1$.Although liquefaction characteristics were not observed at the region shaken, much attention must be paid since liquefaction potential is high.

3. Taking into consideration the results obtained by Uwadia concerning the comparison of microtremors and strong motion records for the El Centro region, and the results obtained from our investigation using microtremors and the strong motion records in the city of Leukas we may conclude the following :

a) Microtremors for the city of Leukas are almost stationary in time. This is in disagreement with Uwadia's conclusions for the El Centro region where he found that microtremors are not stationary in time.

b) The difference of the excitation level between microtremors and strong earthquakes is an important parameter which must be taken into consideration, when period correlations are compared.

c) According to Uwadia and for close-in earthquakes, ground motion is dependant on factors such as the source mechanism and the geological path which the energy travels, and which overshadow any effects of local site condition. The results obtained from the strong motion record in Leukas showing peak acceleration for the main shock 0,53g with earthquake magnitude M=6 show the influence of the local site conditions which have amplified the ground motion. It must be mentioned also here the case of the Skopje earthquake of 1963 which having a magnitude of M=6 destroyed the whole city. After studying the ground effects of this earthquake, Poceski (1969) concluded that the damage distribution was not significantly affected by the location of

the epicenter but was mainly due to the different amplification of the seismic motion to the surface.

d) Different site conditions seem to influence the results obtained from microtremors. According to the geological and geophysical investigations the El Centro region is consisted of hard rock. This is proved from the geological sections of the region (Uwadia 1972) and the high velocities measured at the upper ground layers.

The city of Leukas having deep alluvial soil with high water level is consisted of soft soil.

4. The recorded peak ground acceleration 0,53g cannot be considered as the effective acceleration. Its very short period of duration which in general puts it out of the range of the period of the buildings, and the amplification of the ground motion due to the site conditions are the main characteristics of the peak acceleration. Additionally to the analysis of the accelerogram the resulting value of response spectrum velocity is very high reaching up to 190 cm/sec (Fig. I29). Such a high response spectrum velocity from a low magnitude earthquake can only be the result of great amplification and energy release on a small area in a short-time period.

5. From the above mentioned we may say that for unfavourable soil conditions microtremors is a good technique for soil classification and the effect of water elevation according to Medvedev's formula plays an important role to the damage distribution in such soils. However, microtremor techniques are inadequate for the prediction of earthquake

spectra with ground motions of different excitation levels. Because of the small amplitude and short duration of the microtremors the amplification results cannot represent the amplification factors for strong ground motion. Quantitatively they are different from those found by Kanai's formula. However, qualitatively they would be in agreement.

C H A P T E R III

MICROZONING STUDIES IN THESSALONIKI

III.1 General considerations

(1) Introduction

The seismotectonic and geological condition in Thessaloniki, its local seismic activity, the engineering, geological and hydrological characteristics of the town, the subsoil conditions with materials of different dynamic, physical and mechanical properties, made it possible for Thessaloniki to represent a good seismological model for microzoning investigations where different microzoning techniques could be applied.

So Thessaloniki has been chosen as a site of a pilot microzoning study according to the plan of operation of the UNDP/UNESCO project "Seismicity of the Balkan Region".

Some preliminary studies and investigations were carried out for the concentration of the necessary data of the region which could make possible the microzoning study of Thessaloniki.

The microzoning investigations were carried out by different teams of experts who used various instruments and techniques. These techniques, the results and the comparison of the microzoning methods are discussed in this Chapter.

(2) Seismotectonics and geological characteristics of the region

The urban area of Thessaloniki is not aseismic. Many strong earth-

quakes have shaken the region with destructive results in the past. The most destructive earthquake for the city of Thessaloniki seems to have been the shock of July 5, 1902 with maximum intensity VIII-X of the Mercalli-Sieberg scale. The maximum intensity observed in the area of Thessaloniki over the period 1900-1972 is according to the existing map of isolines of maximum intensities of the region, IX degrees of the Mercalli scale (Fig.III.1).

Thessaloniki is near the center of the area bounded by parallels $40^{o}N$ - $41^{o}N$ and the meridians $22.5^{o}E$ - $23.5^{o}E$. The nearest foci around Thessaloniki which generated large earthquakes are at distances 15-30 km, but the strongest near destructive earthquakes are from 60 km epicentral distances. The return periods for shallow shocks which occured in the region of Thessaloniki are 18-23 years for M=5,5 , 45-55 years for M=6, 110-135 years for M=6,5 and 273-335 years for M=7 (Drakopoulos, 1971).

From the Seismotectonic Map of Greece (Fig.III.2) note that the city of Thessaloniki is surrounded by major fault lines along which several shallow focussed earthquakes ranging from magnitudes of 5 to 7 have occured during the last 170 years.

A geological map showing surficial soil deposits was compiled for the area of Thessaloniki (Fig.III.3). Symbol (L) denotes littoral deposits (sands, aggregates, clays) alluvium They extend from the docks of the harbour to the region of Kalohori. They also extend along the eastern coast of the city reaching a part of the cape where Kalamaria is located. Finally they extend to a smaller area behind the cape.

(Q_1) denotes red clays with carbonate concretions conglomerates which prevail near their base. They extend from the region above Kalohori, South-East to the center of the city along the harbour. They also extend East and South-East of the cape of Kalamaria.

(P_2) denotes sandy marls yellow alternating to microconglomerates and sandstone, marls sometimes compact within the sands. They occupy the main area of the region under investigation in the center of the city and a small part is extended South-East of the cape of Kalamaria.

(P_1) denotes red to tile coloured silty and marly clays with carbonate concretions. They occupy the region north of Kalohori at the surrounding area of the city and east of the cape.

(S) denotes the basement individed of schists, marbles, phyllites and metamorphosed and eruptive stones in general. They occupy the surrounding area of the city and they extend South-East.

Finally a hydrological map of Thessaloniki was compiled showing the regions with different water elevations (Fig.III.4).

III.2 Microzoning methods used in Thessaloniki

A. The Sherif-Bostrom method.

(1) Instrumentation

The Sherif-Bostrom (U.S.A.) microzoning method used in Thessaloniki, involved the operation of two three-component seismic stations with their associated power supplies, amplifiers and recorders. One of these stations was kept permanent on the bedrock and designated as the Base Station. The other portable seismic station was mobile and covered the whole area of the city of Thessaloniki.

The base station equipments included the following :

3 Ranger-type seismometers

2 Batteries connected in series to supply D.C. power

1 Topaz static invertor for converting D.C. power to A.C. signal.

3 Newport 60 amplifiers

1 Six-channel Ampex 1/2 inch tape recorder.

To preserve instrumental compatibility, the portable station consisted of exactly the same types of instruments as those at the base station except that an additional scope was used at the portable station to make sure, prior to recording, that all the equipments were operational every time they were moved from one place to the other.

The measurements took place at 69 locations of Thessaloniki. The data were acquired at all hours of the day. After ensuring that the base station was fully operational, the portable station equipments were placed in a station wagon and transported to predesigned locations for recording. To minimize non-stationarity, the signals at the base and at the portable station were recorded at exactly the same time for three minutes at 30-minutes intervals.

(2) Analysis and results

According to the measurements, the data were analysed by Fast Fourier Transform Power Spectra (Sherif 1973). The distribution of predominant frequencies at the various portable station sites was evaluated, and a map showing the predominant frequency distribution was plotted,

which divided the whole measured area into three different domains (D), with predominant frequencies (Hz) ranging as follows : (Fig.III.5).

D_1 : $0,5 \leq f < 2,5$

D_2 : $2,5 < f < 5,5$

D_3 : $5,5 < f < 8,0$

From the calculation of power spectra, the amplification ratio curves were plotted, which represent the ratio of the resultant of the power spectra obtained at various portable stations to that obtained at the base station, and in connection with the above frequency distribution the three domains were subdivided according to their amplification factors into zones I, I_2, I_3, II, II_2, II_3, III, III_2 (Fig. III.6). The final division into eight zones corresponds to the average resultant amplification curves from which the relationships between the average design acceleration and the approximate number of building stories are calculated according to the specifications given by the American aseismic building code of California where $T \cong 0,1\ N$. T is the natural period of the building and N the number of stories.

Assuming an average ground acceleration for the city of Thessaloniki 0,12g on uniform geologic conditions and no site amplification, and based on the calculated amplification factors, Sherif derived a relationship between the design acceleration levels and the corresponding number of building stories N for each zone within the city of Thessaloniki which can be summarized in Table III.1.

Finally the problem of liquefaction and densification for the city of Thessaloniki was faced. From the data available and the water

TABLE III.1

A SUMMARY OF RECOMMENDED AVERAGE DESIGN ACCELERATION LEVELS WITH RESPECT TO THE NUMBER OF BUILDING STORIES N, IN VARIOUS SEISMIC ZONES IN THESSALONIKI DETERMINED BY THE SHERIF-BOSTROM (U.S.A.) MICROZONATION METHOD

Zone No.	Recommended Average Design Acceleration Values g	No. of Building Stories, N	Remarks
I_1	0.12g	for all N	
I_2	0.12g 0.17g 0.25g	for $N \geq 16$ for $4 \geq N$, $15 \geq N \geq 12$ for $11 \geq N \geq 5$	Buildings with $9 \geq N \geq 7$ could be subjected to acceleration as high as 0.3g
I_3	0.2g 0.35g	for $N \geq 16$ for $N \leq 15$	Buildings with $12 \geq N \geq 6$ could be subject to acceleration as high as 0.45g
II_1	0.15g	for all N	
II_2	0.28g	for all N	
II_3	0.15g 0.20g 0.25g 0.35g	for $N \geq 11$ for $10 \geq N > 5$ for $2 > N$ for $5 \geq N \geq 2$	Buildings with N = 3 or N = 4 stories could be subjected to acceleration as high as 0.45g
III_1	0.12g 0.2g 0.15g	for N = 1 for $10 \geq N > 1$ for $N \geq 11$	
III_2	0.25g 0.15g	for N = 1 for $N \geq 2$	

(After M.A. Sherif)

elevation a map was compiled showing the liquifiable and densifiable regions (Fig.III.7).

B. Japanese microtremor measurements (Kabayashi)

(1) Instrumentation

The microtremor seismograph system which was used by Kabayashi in Thessaloniki consisted of three seismographs, cassette type magnetic tape recorder and pen-writing oscillograph.

a) Seismograph : Two horizontal components and one vertical. The pick-up has a pendulum with natural period 1,0 sec. and critical damping. The amplifier has an integrater in it and so its output, displacement of ground motion, is obtained.

b) Tape recorder : Four signals can be recorded by the magnetic tape recorder simultaneously. These signals are recorded in cassette type magnetic tape.

c) Pen-writing Osci-lograph : The output signal of the magnetic tape recorder is recorded by the pen-writing oscillograf.

The measurements covered the populated area and the outer part of the city, up to 9 km westwards and 12 km southwards of the center of Thessaloniki. In this area 187 points were chosen for microtremor measurements.

(2) Analysis and results

Kobayashi carried out a trial of a rapid analysis without computer. The analysis was carried out on 10 seconds records where mean periods of 10 seconds records presented the mean periods of Ka-

nai's method and largest amplitudes of 10 second records presented the largest amplitudes of Kanai's method. He called these values mean period T_{10A} and maximum amplitude A_{10}. He defined also mean period T_{10B} which is the mean period of a .10 seconds record with short periods excluded, just like the Ishimoto's zero-crossing method.

According to Kanai's method soil classification is based on his two proposals resulting from the estimation of largest periods, mean periods, predominant periods and largest amplitudes (Fig.II.2, II.3).

Instead of the first proposal of Kanai he assumed as follows:

Kind I	Mean period	T_{10A}	= 0 ∿ 0,22 sec
Kind II	" "	T_{10A}	= 0,12∿ 0,45 sec
Kind III	" "	T_{10A}	= 0,35∿ 0,75 sec
Kind IV	" "	T_{10A}	= 0,55∿ sec

This classification corresponds to the case of Kanai's method with the assumption that largest period is not so large. Instead of the second proposal he assumed that the mean period T_{10B} corresponds to the predominant period and the maximum amplitude A_{10} corresponds to Kanai's largest amplitude.

Using the above mentioned modified Kanai's proposals, Kobayashi compiled finally a microzoning map of Thessaloniki where the soil classification of the region is shown (Fig. III.8).

C. Greek microtremor measurements

(1) Instrumentation

The following seismograph system was used for the microtremor measurements :

a) 3 velocity type seismometers with natural period of 1 sec., sensitivity 3 V_{p-p} cm/sec and damping factor approximately 0,7. One seismometer is used for vertical and two for horizontal motions.

b) A three-channel IC's solid-state amplifier which offers four measuring modes by the built-in differentiator, the direct amplifier, the integrator and the double integrator. By this amplifier and the above mentioned seismometers it is possible to measure the acceleration, the velocity or displacement of the ground motion. The frequency range covers from 0,5 to 30 Hz with frequency response within 0,5 dB. Its gain is approximately 70 dB and has a 7 ranges attenuator.

c) A six-channel electromagnetic oscillograph using tungsten light as light source and records on photo-sensitive paper with speeds 1.5 , 10 and 50 cm/sec.

d) A portable magnetic tape recorder with three channels for the registration of signals and a fourth one for recording information and remarks from microphone.

The block diagram of the above mentioned instruments is shown in Fig. III.9

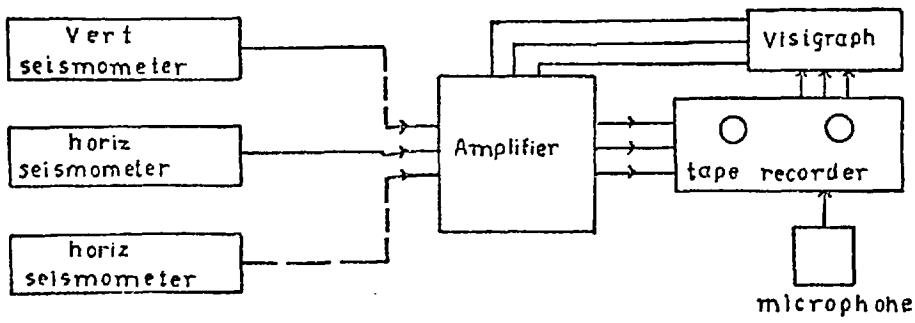


Fig. III. 9

In the urban area of Thessaloniki 100 points were selected for microtremor measurements.

The microtremor measurements were carried out on the ground surface and the duration of each record was 90 seconds.

A 24 hour measurement took place at the coastal area of Thessaloniki in order to check the stationarity of microtremors.

(2) Analysis and results

The records obtained have been analysed by Kanai's method and the analysis was extended up to 30 seconds.

A frequency period distribution curve was plotted for each of the points measured. Taking the 30 seconds portion of the record the interval of the wave crossing the zero line till its coming to zero line again is measured. Thus, the reading of time is doubled and considered as the period. Taking the period and the number of the waves for each period, and plotting them as abcissa and ordinate in that order, the frequency-period distribution curve of the tremor is plotted for each point. These curves give predominant periods and largest periods.

In order to find the mean period of the microtremors we use the formula $T_M = \frac{t}{\Sigma}$ where T_M is the mean period of tremors in sec., t is the total analysis time of the record and Σ is the sum of number of waves.

Largest amplitudes of microtremors are measured from the analysed records.

The first proposal of Kanai's method for ground classification depends on the relation between the largest and the mean period of microtremors.

TABLE III.2

THESSALONIKI

MICROTREMOR MEASUREMENTS

Point No	Predominant Period(T_G) sec	Largest Period(T_L) sec	Mean Per.(T_M) sec	Largest Amplit(A) μ	Kind of soil T_L-T_M	Kind of soil T_G-A	SOIL
(1)	(2)	(3)	(4)	(5)	(6)	(7)	(8)
1	0,200	0,550	0,312	0,20	2	2 - 3	II
2	0,055	0,450	0,210	0,042	1 - 2	1	I
3	0,360	0,675	0,280	0,099	2	2	II
4	0,450	1,000	0,39	0,60	3	2 - 3	III
5	0,135	0,450	0,22	0,07	1	1	I
6	0,450	1,000	0,40	0,80	2 - 3	3	III
7	0,450	1,000	0,396	1,00	2 - 3	3	III
8	0,450	1,200	0,35	0,30	3	2 - 3	III
9	0,675	1,000	0,66	0,32	3	2 - 3	III
10	0,450	0,825	0,21	0,183	2	2	II
11	0,090	0,450	0,16	0,92	1 - 2	2	II
12	0,200	0,550	0,29	0,173	2	2	II
13	0,090	0,450	0,12	0,047	1	1	I
14	0,135	0,550	0,25	0,15	2	1 - 2	II
15	0,200	0,550	0,32	0,148	2	1 - 2	II
16	0,360	0,675	0,20	0,117	1 - 2	2	II
17	0,450	0,825	0,23	0,11	2	2	II
18	0,135	0,450	0,27	0,080	1 - 2	1	I
19	0,200	1,200	0,298	0,40	2 - 3	3	III
20	0,360	0,825	0,25	0,13	1 - 2	2 - 3	II
21	0,245	0,675	0,22	0,19	2	2	II
22	0,200	0,675	0,23	0,21	2	2	II
23	0,200	0,675	0,19	0,133	2	2	II
24	0,675	1,000	0,34	0,21	2 - 3	2 - 3	II-III
25	0,245	0,825	0,18	0,263	2	2	II
26	0,055	1,000	0,265	0,12	2 - 3	2	II
27	0,295	1,000	0,327	0,17	2 - 3	2 - 3	II-III
28	0,200	0,675	0,26	0,10	2	2	II
29	0,675	1,000	0,377	0,25	2 - 3	2 - 3	II-III
30	0,825	1,40	0,50	0,20	3 - 4		III

(1)	(2)	(3)	(4)	(5)	(6)	(7)	(8)
31	0,450	0,825	0,375	0,65	2 - 3	3	III
32	0,450	1,000	0,40	0,60	2 - 3	3	III
33	0,450	0,695	0,350	0,40	2	2 -3	II
34	0,135	0,295	0,132	0,23	1 - 2	2	II
35	0,295	0,550	0,322	0,17	2	2	II
36	0,200	0,675	0,240	0,16	2	2	II
37	0,450	0,675	0,30	0,20	2	2 - 3	II
38	0,450	0,675	0,260	0,40	2 - 3	2 - 3	II-III
39	0,450	1,000	0,30	0,50	2 - 3	3	III
40	0,360	0,550	0,50	1,10	2 - 3	3	III
41	0,360	0,825	0,380	0,70	2 - 3	3	III
42	0,135	0,360	0,153	0,30	1 - 2	2	II
43	0,135	0,450	0,17	0,045	1	1	I
44	0,360	0,825	0,303	0,25	2	2	II
45	0,055	0,675	0,238	0,10	1 - 2	1	I
46	0,055	0,450	0,14	0,12	1	1 - 2	I
47	0,200	0,675	0,26	0,098	1 - 2	2	II
48	0,135	0,675	0,29	0,053	2	2	II
49	0,200	0,825	0,294	0,16	2	2	II
50	0,550	0,825	0,12	0,157	2	2	II
51	0,550	0,675	0,20	0,23	2	2	II
52	0,295	0,825	0,258	0,42	2	2 - 3	II
53	0,550	0,825	0,30	0,35	2	2 - 3	II
54	0,295	0,875	0,26	0,44	2	2 - 3	II
55	0,295	0,875	0,25	0,30	2	2	II
56	0,135	0,550	0,18	0,15	1 - 2	1 - 2	I-II
57	0,090	0,450	0,19	0,08	1 - 2	1	I
58	0,055	0,450	0,26	0,027	1	1	I
59	0,450	0,675	0,31	0,050	1 - 2	1 - 2	I-II
60	0,550	0,825	0,25	0,15	1 - 2	2	II
61	0,550	0,825	0,27	0,105	1 - 2	2	II
62	0,200	0,450	0,217	0,20	1 - 2	2	II
63	0,200	0,450	0,25	0,25	1 - 2	2	II
64	0,200	0,450	0,20	0,22	1 - 2	2	II
65	0,135	0,360	0,153	0,30	1 - 2	2	II

(1)	(2)	(3)	(4)	(5)	(6)	(7)	(8)
66	0,200	0,550	0,25	0,32	1 - 2	1 2	II
67	0,450	0,675	0,298	0,32	2	2 - 3	II
68	0,450	0,675	0,21	0,12	1 - 2	1 - 2	I-II
69	0,450	0,675	0,20	0,15	1 - 2	2	II
70	0,450	0,825	0,21	0,18	1 - 2	2	II
71	0,055	0,360	0,103	0,050	1	1	I
72	0,055	0,450	0,28	0,10	2	1 - 2	II
73	0,135	0,550	0,26	0,035	1	1	I
74	0,135	0,550	0,28	0,05	1	1	I
75	0,200	0,550	0,20	0,05	1 - 2	1	I
76	0,245	0,825	0,274	0,37	2	2 - 3	II
77	0,090	0,550	0,188	0,30	1 - 2	2	II
78	0,200	0,675	0,259	0,25	2	2	II
79	0,450	1,000	0,29	0,98	3	3	III
80	0,450	1,000	0,38	0,87	2 - 3	3	III
81	0,450	0,825	0,50	2,00	3	2 - 3	III
82	0,450	1,000	0,46	2,61	3	4	III
83	0,450	1,000	0,45	0,32	3	2 - 3	III
84	0,450	1,000	0,50	0,40	3	2 - 3	III
85	0,450	1,000	0,48	0,38	3	2 - 3	III
86	0,450	0,875	0,48	0,32	3	2 - 3	III
87	0,450	1,200	0,361	0,40	3	2 - 3	III
88	0,450	0,875	0,422	0,200	3	2 - 3	III
89	0,675	1,200	0,483	0,66	3	3	III
90	0,450	1,200	0,313	0,28	3 - 4	2 - 3	III
91	0,200	0,825	0,25	0,377	2	2 - 3	II
92	0,450	0,675	0,294	0,45	2	2 - 3	II
93	0,135	0,450	0,15	0,16	1	1 - 2	I
94	0,135	0,450	0,19	0,04	1 - 2	1	I
95	0,135	0,450	0,20	0,038	1 - 2	1	I
96	0,055	0,360	0,163	0,06	1 - 2	1	I
97	0,450	0,875	0,320	0,35	2	2 - 3	II
98	0,450	0,675	0,35	0,30	2	2 - 3	II
99	0,200	0,550	0,42	0,25	2 - 3	2	II

The second proposal of Kanai's method depends on the relation between the predominant period and the largest amplitude of microtremors.

In Fig. III.10 to III.34 are shown the plotted frequency-period distribution curves of the measured points. Each curve represents a point.

In Table III.2 are presented for each point the corresponding values of predominant period, mean period, largest period and largest amplitude according to the above mentioned calculations and measurements.

With the application of Kanai's two proposals we finally get the classification of soil (Table III.2). According to these two proposals, Thessaloniki was divided into various zones with different kind of soil. This classification is based on the depth of diluvium or alluvium surface layers which cover the rocky or hard ground basements.

From an engineering point of view, the predominant periods of microtremors are of primary importance since it seems that there is a close relationship between them and the predominant periods of the sites during earthquakes. Consequently, this gives a direct relation between soil deposits and structures built upon them during an earthquake.

Based on this remark and in relation to Kanai's two proposals, a map of Thessaloniki was finally compiled and the soil was classified into three kinds I,II,III (Fig. III35).

From the 24-hour microtremor measurements which took place at the coastal area of Thessaloniki, we obtained the following results :

In the amplitude versus time curve A = f(t) a maximum amplitude of 0,82 μ. appears at 12 h., and a minimum of 0,33 μ. between 02-04 h. (Fig.III.36a).

However the corresponding predominant period during the 24 hour measurement is not varying significantly from its constant value 0,45 sec. (Fig. III.36b).

(3) Amplification factor

As mentioned before from an engineering point of view predominant periods of microtremor measurements are very important. The average value of predominant periods corresponding to the classification of soil in Thessaloniki in zones I,II,III were found as follows :

Soil I T_G = 0,2 sec.

Soil II T_G = 0,4 sec.

Soil III T_G = 0,6 sec.

Applying Kanai's formula :

$$G(T) = \frac{1}{\sqrt{\left|1-\left(\frac{T}{T_G}\right)^2\right|^2 + \left|\frac{0,2}{\sqrt{T_G}}\left(\frac{T}{T_G}\right)\right|^2}}$$

and for $T = T_G$ the corresponding amplification factor for each of the kinds of soil founded I,II,III, are shown in Table III.3.

TABLE III.3

Kind of soil	T_G	G(T)
I	0,2	2,4
II	0,4	3,1
III	0,6	3,6

These amplification factors provide the basis for the choice of the coefficient which is depending on the effect of soil conditions in

order to chose the design value of a seismic load.

In any case the values of the soil condition coefficient must be specified in national codes according to the methods of considering the effect of geological and hydrogeological conditions on the parameters of design seismic loadings.

III.3 Comparison of results

(1) Comparison between soil classification by microtremors and Geological map of Thessaloniki

After the classification of the soil of the urban area of Thessaloniki into kinds I,II,III was completed, a comparison with the Geological map was possible (Fig. III.37).

Littoral deposits composed from sands, aggregates and clays (L) extend from the docks of the harbour to the region of Kalohori. They also extend along the eastern coast of the city reaching a part of the cape where Kalamaria is located. Finally they extend to a smaller area behind the cape.

The soft geological structure of that region correlates well with kind of soil III.

Red clays with carbonate concretions (Q1), sandy marls, and sandstone marls (P2) occupy the main area of the region under investigation. They occupy the center of the city and they extend to the north and to the east. The geological structure of that region and soil kind II are similar.

Finally, silty and marly days with carbonate concretions (P1), and the undivided basement in general composed of schistes, marbles, phylites and metamorphosed and eruptive stones (S), occupy the surrounding area of the city extending to North-West, to North, North-East and to the East.

The geological structure of that region and soil kind I are similar.

(2) Comparison between microtremor measurements of the Greek working group and Koyabashi's measurements (Japan).

The microtremor measurements of Koyabashi and of the Greek working group were taken in approximately the same area.

The instrumentation techniques were almost the same with some differences in recording. Koyabashi used a pen-writing oscillograph while the Greek working group used photographic paper, six-channel oscillograph.

Using a modified application of Kanai's method, Koyabashi carried out a rapid analysis of 10 seconds records.

The Greek working group carried out manually the analysis of the records, applying the zero-crossing method, and obtained the period distribution curves from these records.

The classification of soil was done by Kanai's method and there is a general agreement between Koyabashi's results and the Greek working group's results.

The soil of the urban area of Thessaloniki was classified into kinds I,II,III by both teams, and the main differences were limited in two

small regions (Fig.III38). The first difference was at the area of the railroad station where soil kind III according to Koyabashi's results was soil kind II according to Greek working group's results and the second at some regions of the coasts of the cape where soil kind III for Koyabashi was soil kind II for the Greek working group and soil kind I for Koyabashi was soil III for the Greek working group.

(3) Comparison between microtremor measurements by the Greek working group and measurements by the Sherif-Bostrom method (U.S.A.)

The measured area of Thessaloniki was divided according to the Sherif-Bostrom method into three different domains according to the predominant frequency distribution. These domains were subdivided according to their amplification factors (Ratio of amplification obtained at the various portable stations to that obtained at the base station).(Sherif, Microzonation of Thessaloniki, 1973).

The region of Kalohori was not measured by the Sherif's team.

In zone I_3 at the center of the city (after Sherif) the amplification factor A = 3.0 seems to have been influenced by traffic noise (Fig.III.39).

Also in the region of Kalamaria (at the cape), zones I_3, II_2, I_2 are not in accordance with soil kinds II, and I obtained by the Greek working group (Fig. III.39).

According to the existing bore hole data Sherif compiled a map delineating areas that are susceptible to liquefaction during strong earthquakes. As it is shown there, the whole coastal area of Thessaloniki extending from Kalohori to the cape and continuing to the East, is susceptible to liquefaction (Fig.III.7). However, the possibilities of

liquefaction are limited in some regions where the water level is not very high as is shown by the hydrological map of Thessaloniki (Fig. III.4).

III.4 Measurement of weak earthquakes in Thessaloniki

Three portable vertical components, seismographs model MEQ 801 with characteristics almost equivalent to those of the microtremor measurements seismograph had been installed on three different kinds of soil in the urban area of Thessaloniki during February 1974. The locations 1,2,3 of these seismometers are shown in Fig.III.35.

Seismometers were put on top soil and noise of the city did not allow magnification larger than 3,500 (minimum), which already was high during daytime since recorded amplitude of noise sometimes exceeded the distance between two successive lines of the record. The latter was small in order to obtain 24 hour records.

Some earthquakes, clearly recorded by all seismograph stations were analyzed. Predominant periods corresponding to the first P;P with largest amplitude , S and S with largest amplitude wave groups have been calculated for each seismogram. The results from 3 earthquakes are shown in Tables III.4, III.5, III.6. For the earthquakes of 12.2.1974 and 14.2.1974 with epicentral distances of 50 km and 100 km respectively and of magnitude less than 3, there is a systematic tendency of strong correlation between kinds of soil and predominant periods of all phases.

The softer the soil conditions, the larger the corresponding predominant periods for the above mentioned waves.

Predominant periods of microtremors at the points 1,2 and 3 where the portable seismographs were in operation are calculated for the

Z component as well as for the N-S component and their values are : T = 0, 110 sec. for point 1, T = 0, 450 sec. for point 2 and T = 0,675 sec. for point 3.

It must be mentioned that for the earthquake with epicentral distance of 340 km and magnitude M = 4,0 , station No.3 recorded very short periods compared to those of stations existing on harder soils. It must be also mentioned that there is some degree of stability in the predominant periods of the three earthquakes for zone III. Predominant period of microtremors for this zone coincides with that of S waves corresponding to the largest amplitude.

T A B L E III.4

12.2.1974 H=20^h28^m D=50 km

Predominant T(sec) First P	P Larg.Amp.	S	S Larg.Amp.	Kind of soil	Station
0.18	0.25	0.20	0.25	I	1
0.20	0.25	0.60	0.60	II	2
0.25	0.40	0.60	0.65	III	3

T A B L E III.5

14.2.1974 H=08^h01^m D=100 km

Predominant T(sec) First P	P Larg.Amp.	S	S Larg.Amp.	Kind of soil	Station
0.15	0.19	0.40	0.30	I	1
0.25	0.30	0.40	0.60	II	2
0.25	0.25	0.45	0.65	III	3

T A B L E III.6

17.2.1974 H=05^h03^m D=340 km

Predominant T(sec) First P	P Larg.Amp.	S	S Larg.Amp	Kind of soil	Station
0.22	0.40	0.45	0.70	I	1
0.46	0.55	0.7-0.8	0.85	II	2
0.29	0.40	0.50	0.55	III	3

III.5 Discussion on engineering aspects of microzoning

The analysis and comparison of the microtremor measurements in the area of Thessaloniki provided much useful information concerning the kind of soil and ground characteristics.

However, it must be pointed out that for the determination of seismic coefficients, the seismic parameters involved have to be very reliable and carefully checked before their application.

Sherif estimated the ground acceleration 0,12g for the city of Thessaloniki, assuming earthquake magnitude M=7 and hypocentral distance 20 km. According to the seismic activity of the region it seems that the assumed value of magnitude 7 is overestimated for epicentral distance 20 km. This is why the values of the design accelerations (Table III.I) for the different kinds of soil, based on the calculated soil amplification factors are considered very high for the region. For kinds of soil I_1, II_1 and III_1 the recommended average design acceleration values range from 0,12g to 0,2g. For kinds of soil I_2, II_2, III_2 the design accele-

ration values range from 0,12g to 0,28g. For kinds of soil I_3,II_3,III_3 the design acceleration values range from 0,2g to 0,35g. The variations of these values depends on the number of building stories N. For some special cases the design acceleration can reach the value of 0,45g.

On the other hand Sherif used the empirical formula T=0.1N for the calculation of the natural periods of buildings. Some countries have derived their own empirical formulaes relating natural period of buildings and building stories. For example T.Tanigichi showed that the natural periods of reinforced concrete structures for Japanese office buildings range from 0,07N to 0,09N, and for high-rise buildings with steel frames Japanese use the empirical formula T=0,1N.

The above mentioned indicate that the empirical formulaes relating natural periods of building and stories, differ from country to country according to their structural systems and structural materials.

According to the Greek regulations for aseismic constructions for the area of Thessaloniki, and considering three kinds of soil, the seismic design coefficients are 0.06, 0.08 and 0.12 respectively. Up to now buildings of reinforced concrete designed with the seismic coefficients corresponding to the soil conditions have resisted in satisfactory way to earthquakes.

Comparing thus the design coefficients derived from Sherif and those used in the Greek regulations, it seems that Sherif's values are overestimated.

Another point which should be discussed is the division of Thessaloniki into 8 different zones according to Sherif classification. We think that for design purposes the division of the city into fewer zones of different but broader characteristics, is more practical.

C H A P T E R IV

FINAL CONCLUSIONS AND RECOMMENDATIONS

Some conclusions concerning the analysis of the strong motion records of Leukas earthquake of November 4, 1973 and the microzoning study of the city of Leukas have been already reported.

Adding to these the results obtained from the pilot microzoning study of Thessaloniki with the methods already discussed some final conclusions and recommendations can be derived.

1) From the analysis of the strong motion accelerograms and the microzoning study in the city of Leukas it is concluded that the peak acceleration 0,53g which was recorded from an earthquake of magnitude M=6 was mainly due to the ground amplification. More strong motion recordings of the Leukas area are necessary in order to evaluate the effective design acceleration values and to compare them with the seismic design coefficients used according to the Greek aseismic regulations, and which have for three kinds of soil the values 0,08 , 0,12 , 0,16 respectively.

2) Microtremor measurements were proved to be a useful technique for soil classification, but not for the prediction of future earthquake motions. Microtremor measurements should be extended to areas of Greece where strong motion recordings are available and to areas which have experienced destructive earthquakes in the past. The comparison of damage distribution maps and microzoning maps is recommended.

3) Microtremor measurements provided very useful information for

the influence of subsoil conditions especially for the city of Leukas. The important role of the water elevation is pointed out.

4) According to the 24 hours measurements in Thessaloniki and Leukas and the results obtained, microtremors are almost stationary in time at these regions. However, since excitation levels differ from place to place, more measurements are required to check the stationarity of microtremors.

5) Medvedev's microzoning method is recommended for the comparison of results between different microzoning techniques and especially for regions with high water elevation.

6) The derivation of seismic design accelerations depends on the bedrock motion, and the amplification of the ground motion reaching the surface through the various layers. In this sense 1) much attention must be paid to the empirical formulaes relating the earthquake parameters such as magnitude, hypocentral and epicentral distances with bedrock accelerations, a n d 2) the application of different microzoning methods at the same sites is recommended for comparison of the results and for the checking of the amplification characteristics of layered soils.

7) Finally from an engineering point of view, soil and subsoil characteristics can be as mentioned before, some of the causes for damages to structures. However, we must point out here that structural materials, design methods, construction techniques, design standards and regulations, and the ability of the structural engineer, are some very important parameters which have to be taken into consideration for the compilation of a microzoning

map. In this sense, these maps could provide useful information for the causes of damages since isoseismal maps which are widely used today, can only summarize the results of damages on structures without any analysis on their causes.

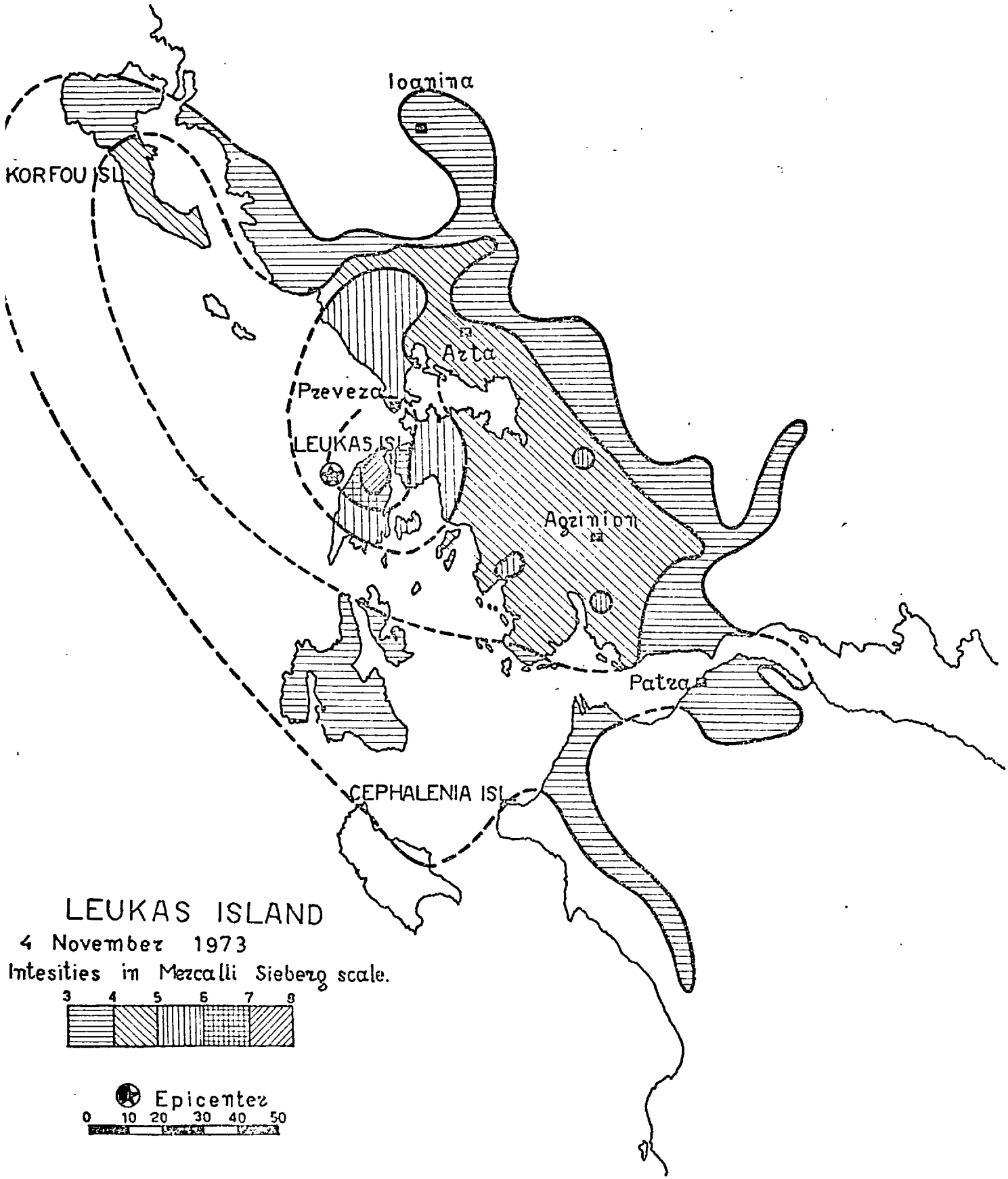
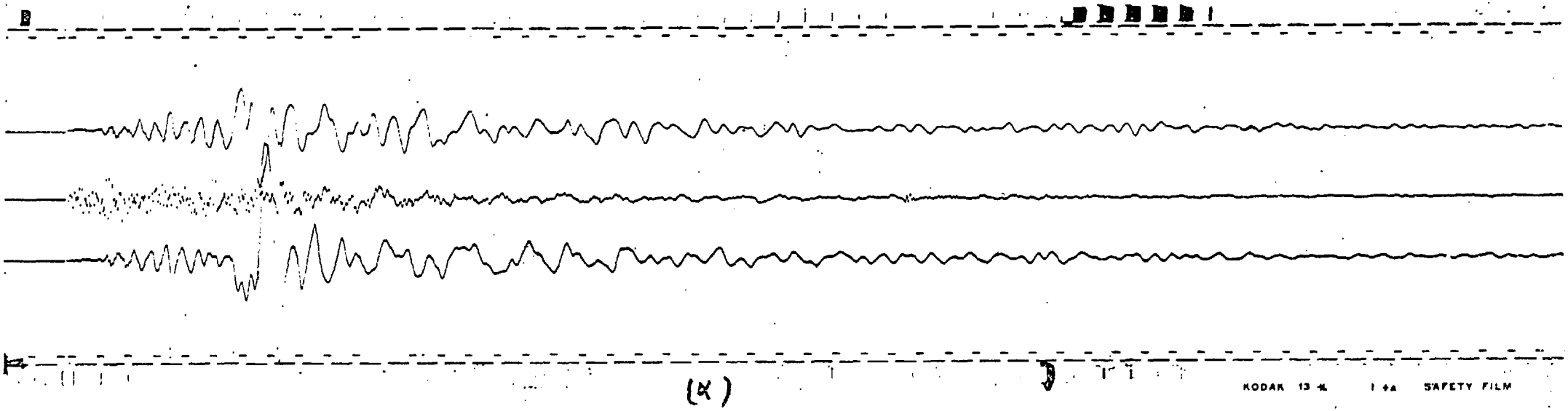


FIG.1. ISOSEISMAL MAP OF THE LEUKAS EARTHQUAKE OF NOVEMBER 4, 1973

(COMPILED BY A. IKONOMIDIS.)



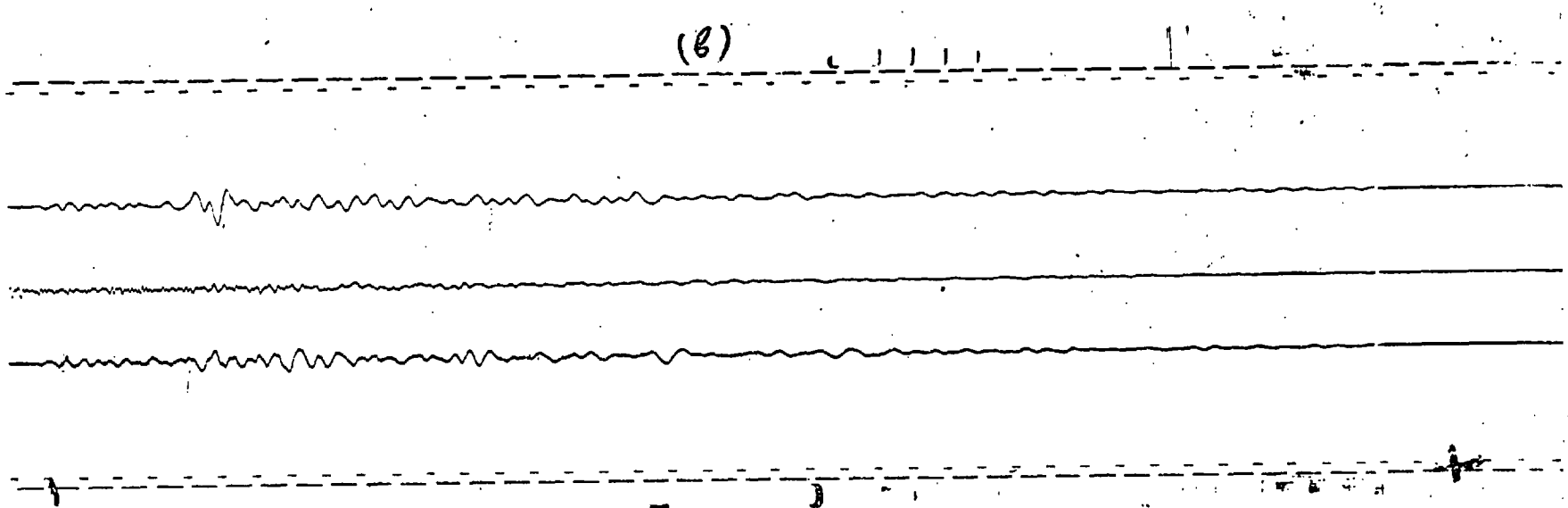
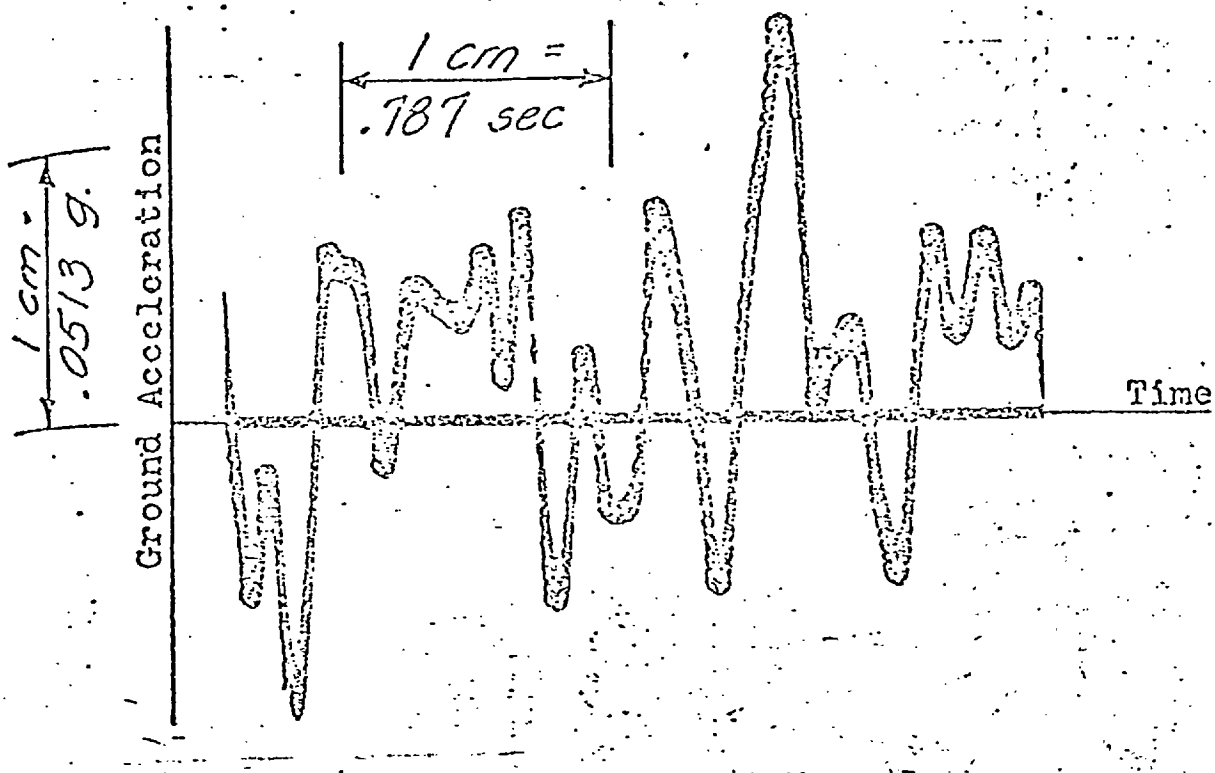
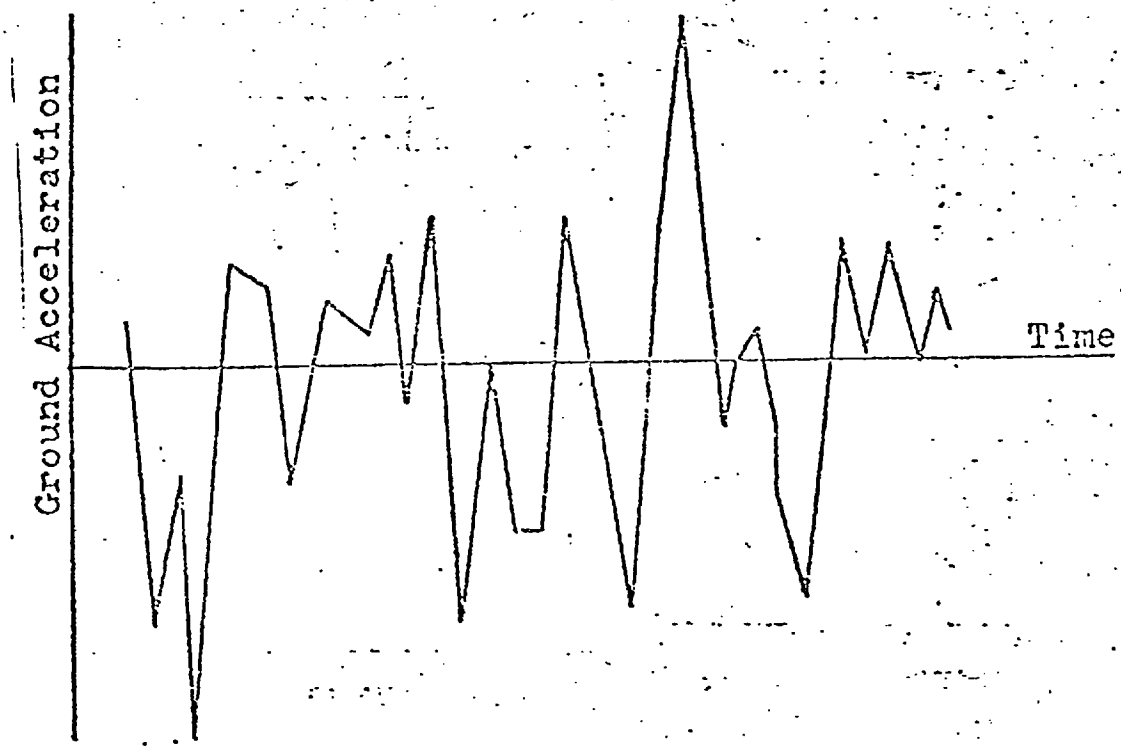


Fig I.2



(a) Original Accelerogram



(b) Plot of Punched Card Data.

Fig. I.3 Portion of accelerogram and punched Card Trace (Berg).

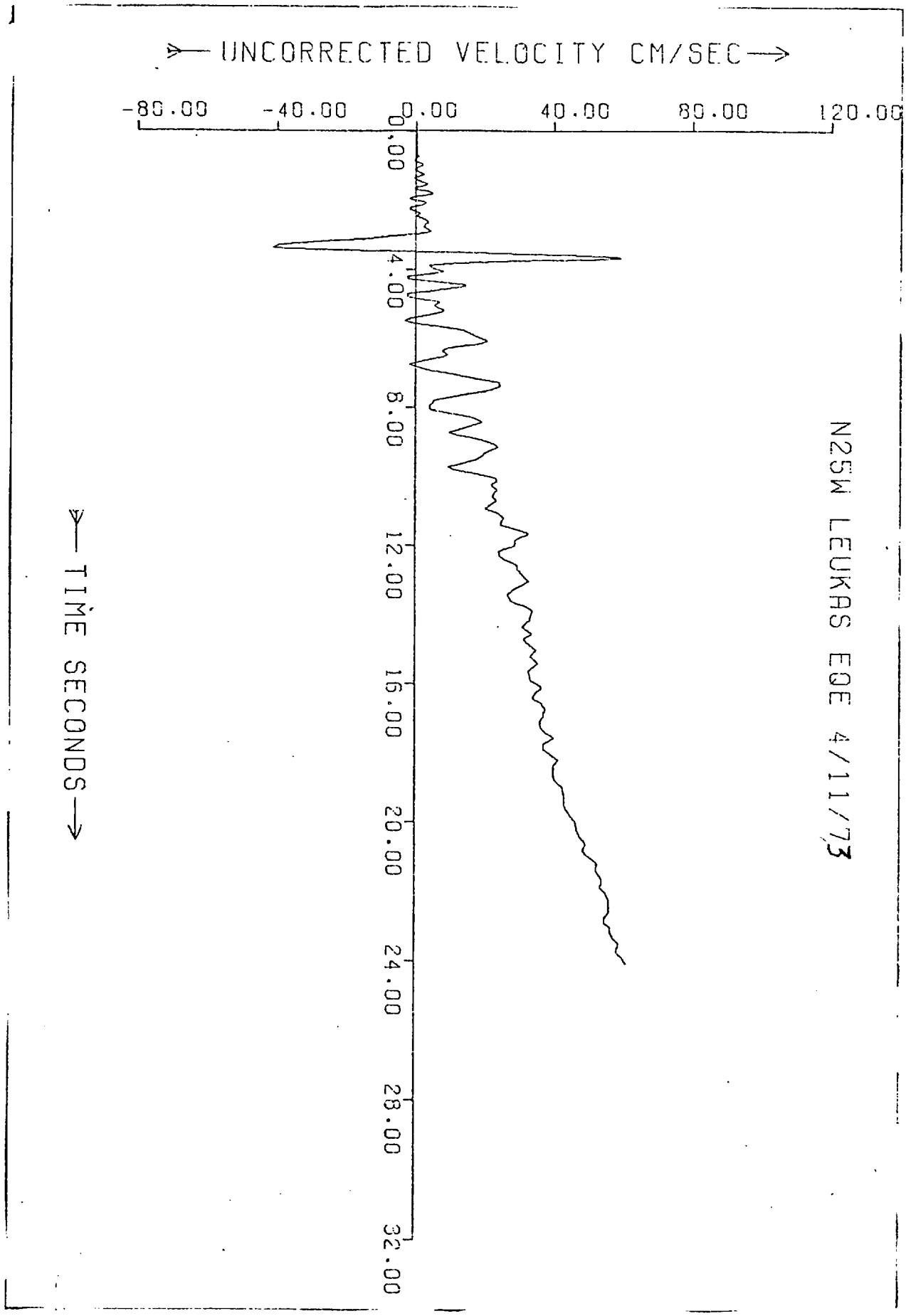

UNCORRECTED VELOCITY CM/SEC
-80.00
-40.00
0.00
40.00
80.00
120.00
0.00
4.00
8.00
12.00
16.00
20.00
24.00
28.00
32.00
TIME SECONDS
N25W LEUKAS EQE 4/11/73

Fig I.4

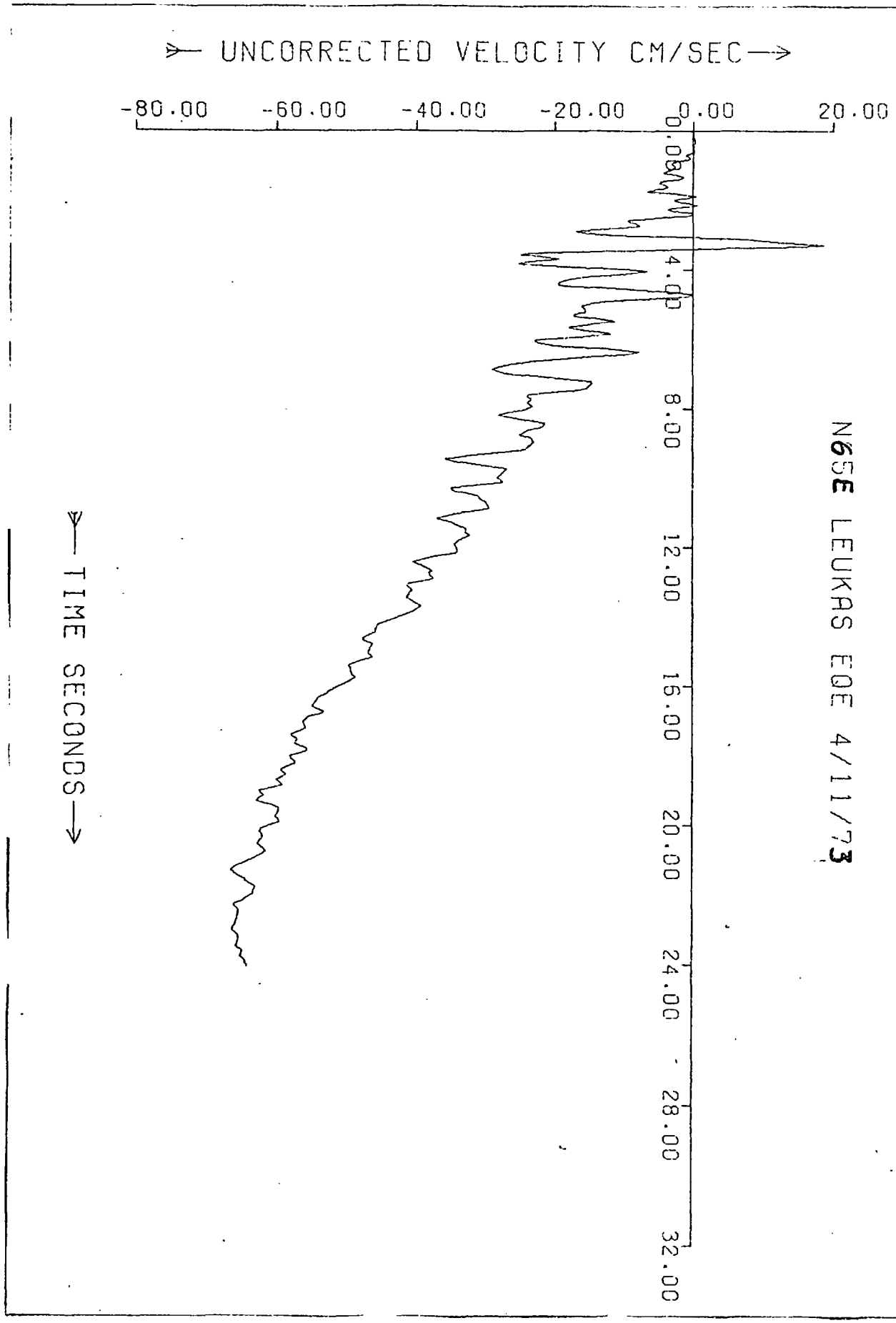

UNCORRECTED VELOCITY CM/SEC
-80.00
-60.00
-40.00
-20.00
0.00
20.00
0.00
4.00
8.00
12.00
16.00
20.00
24.00
28.00
32.00
TIME SECONDS
N65E LEUKAS EQE 4/11/73

Fig I.5

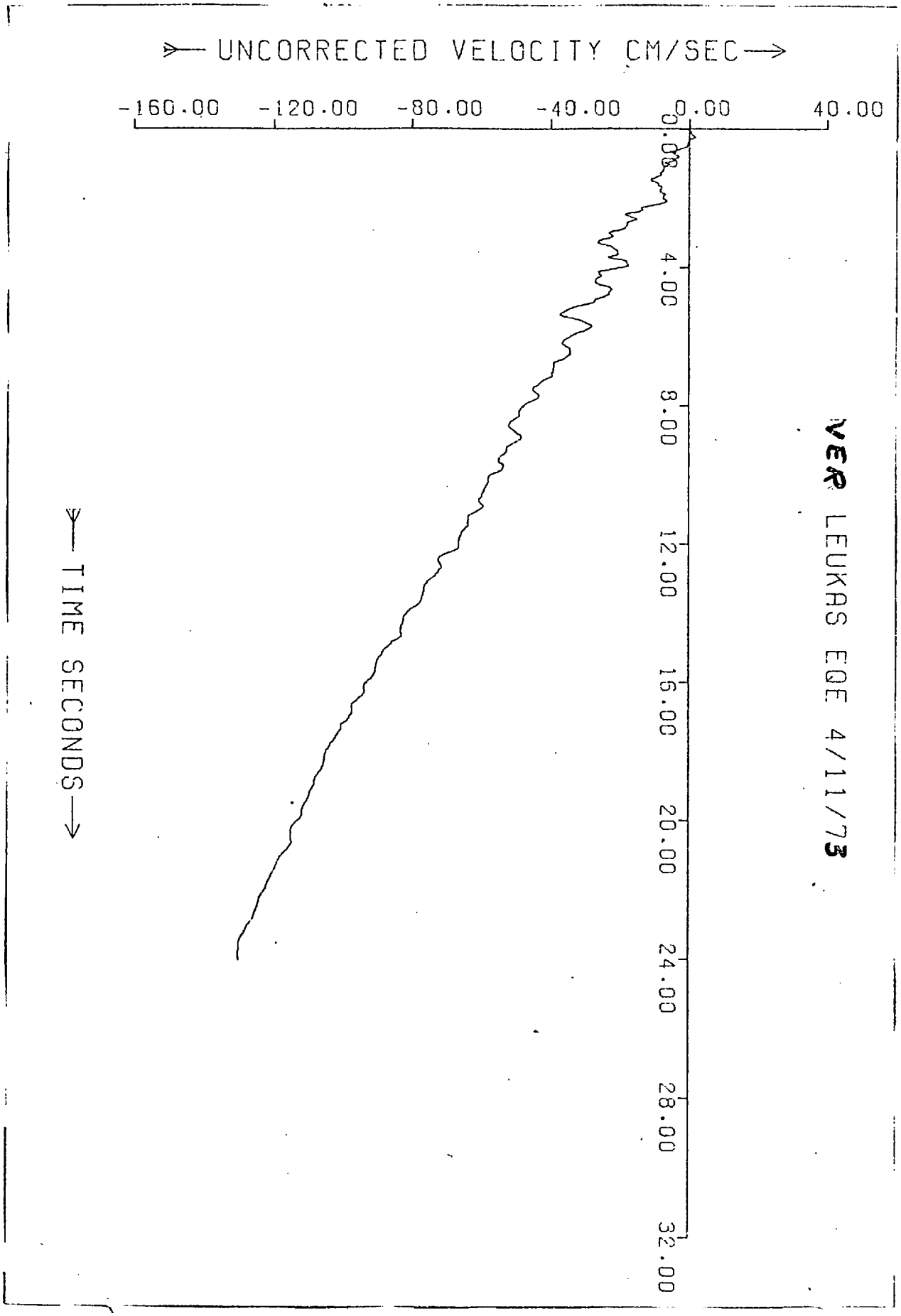

UNCORRECTED VELOCITY CM/SEC
-160.00
-120.00
-80.00
-40.00
0.00
40.00
0.00
4.00
8.00
12.00
16.00
20.00
24.00
28.00
32.00
TIME SECONDS
VER LEUKAS EQE 4/11/73

Fig I.6

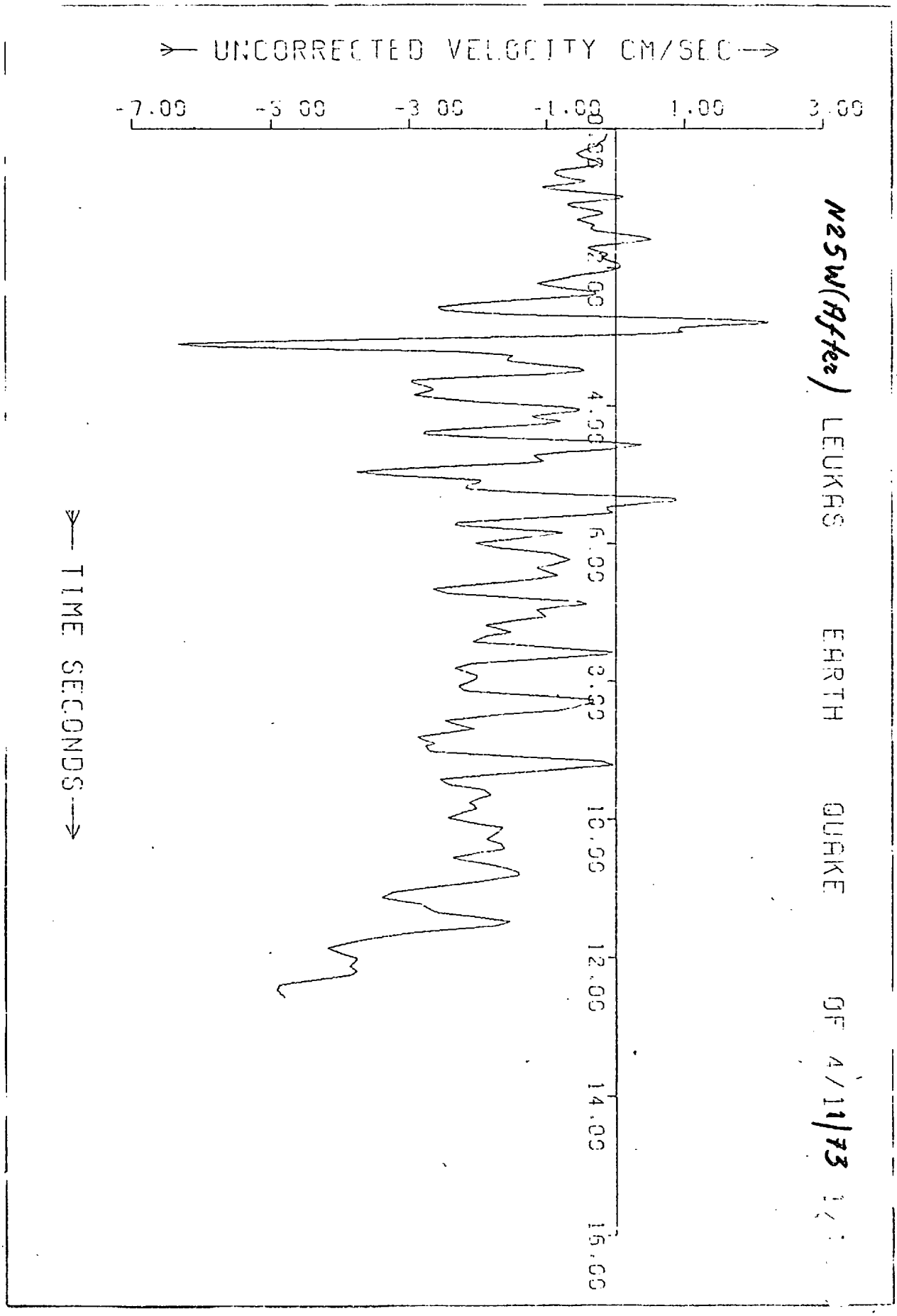

UNCORRECTED VELOCITY CM/SEC
-7.00
-5.00
-3.00
-1.00
1.00
3.00
2.00
4.00
6.00
8.00
10.00
12.00
14.00
16.00
TIME SECONDS
N25W(Reflex) LEUKAS EARTH QUAKE OF 4/11/73

Fig I.7

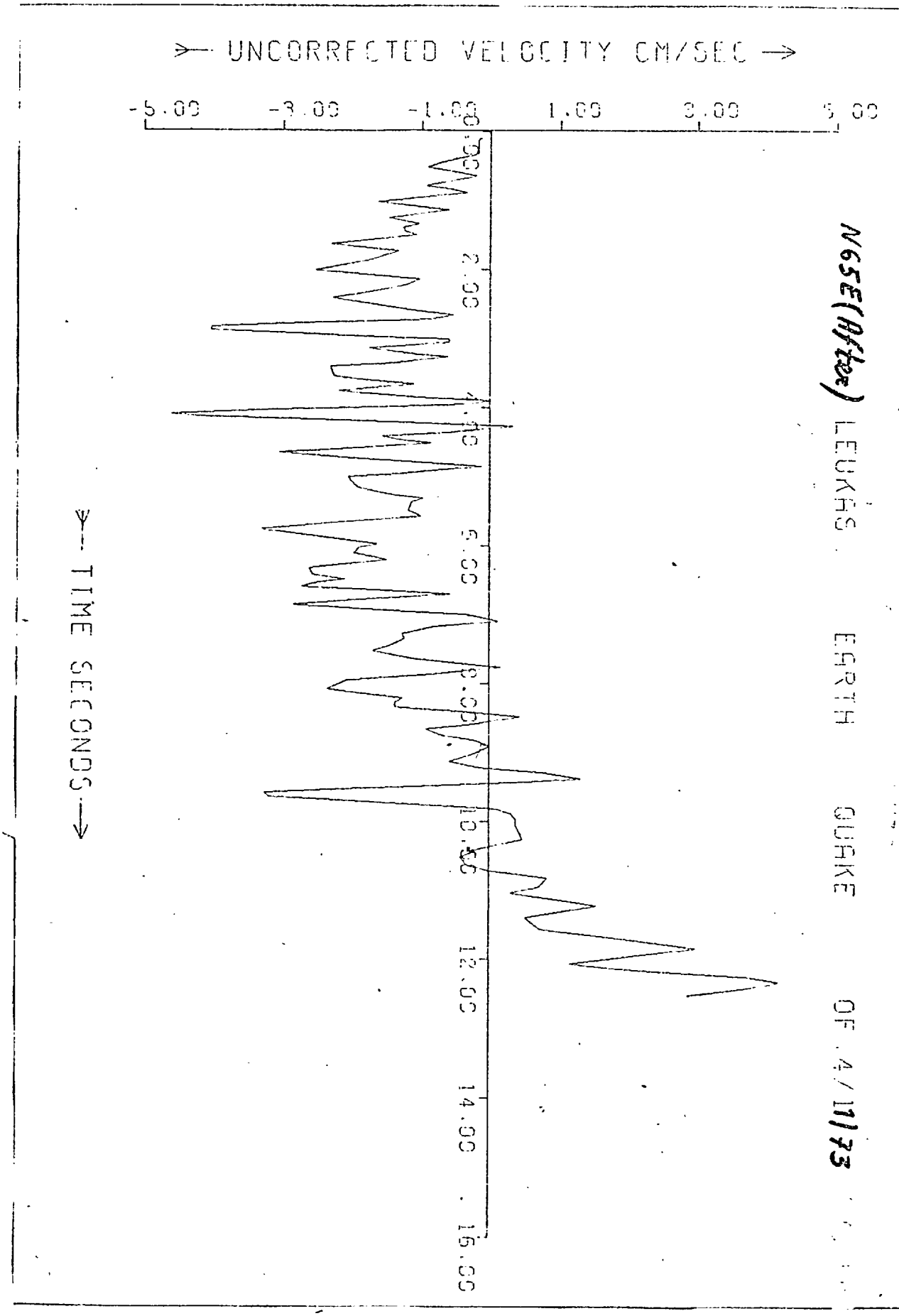

UNCORRECTED VELOCITY CM/SEC
-5.00
-3.00
-1.00
1.00
3.00
5.00
0.00
2.00
4.00
6.00
8.00
10.00
12.00
14.00
16.00
TIME SECONDS
N65E (Arthur) LEUKAS EARTH QUAKE OF 4/11/73

Fig I.8

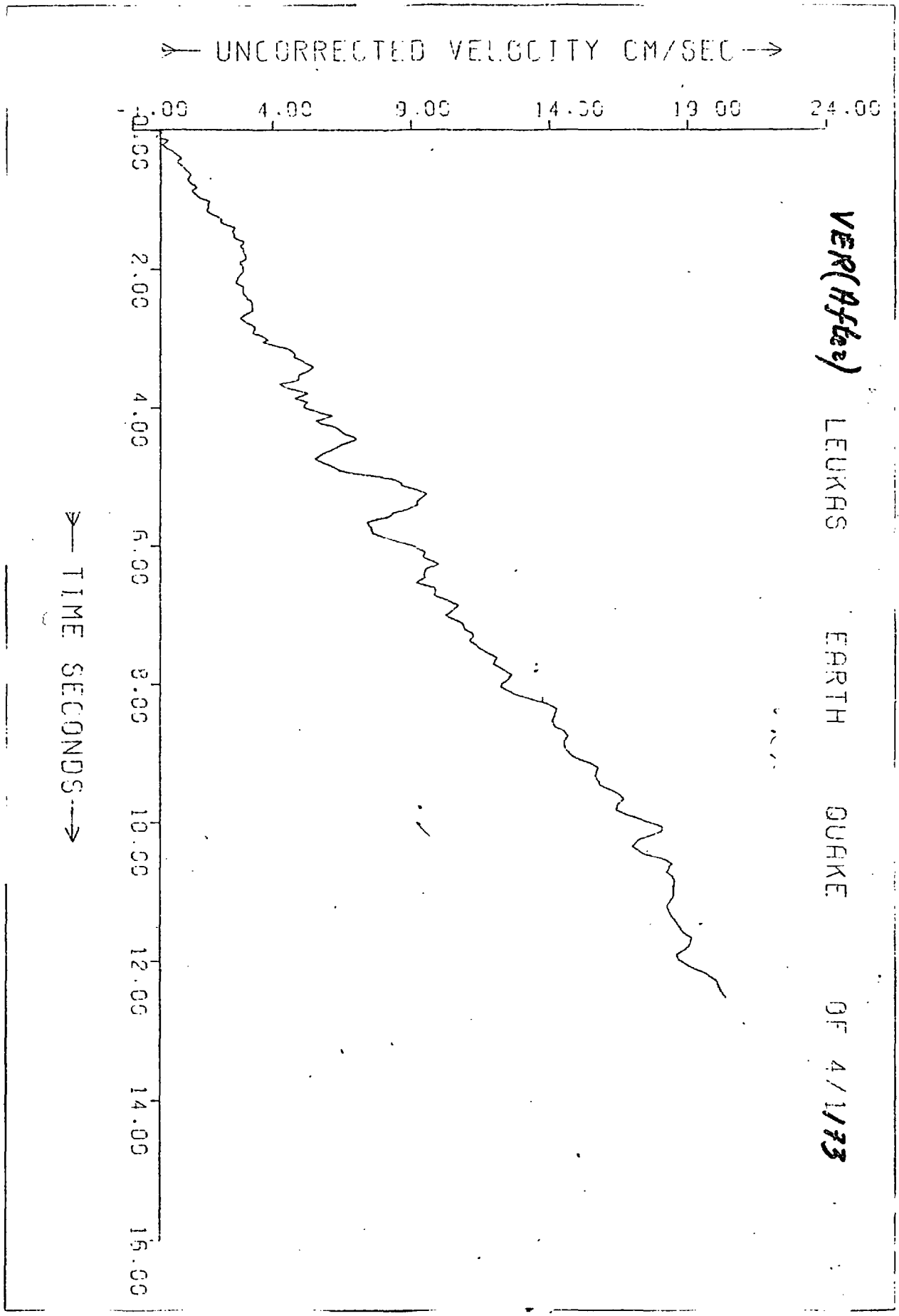

UNCORRECTED VELOCITY CM/SEC
-4.00
4.00
9.00
14.00
19.00
24.00
0.00
2.00
4.00
6.00
8.00
10.00
12.00
14.00
16.00
TIME SECONDS
VER(Hfbo)
LEUKAS
EARTH
QUAKE
OF 4/1/73

Fig I.9.

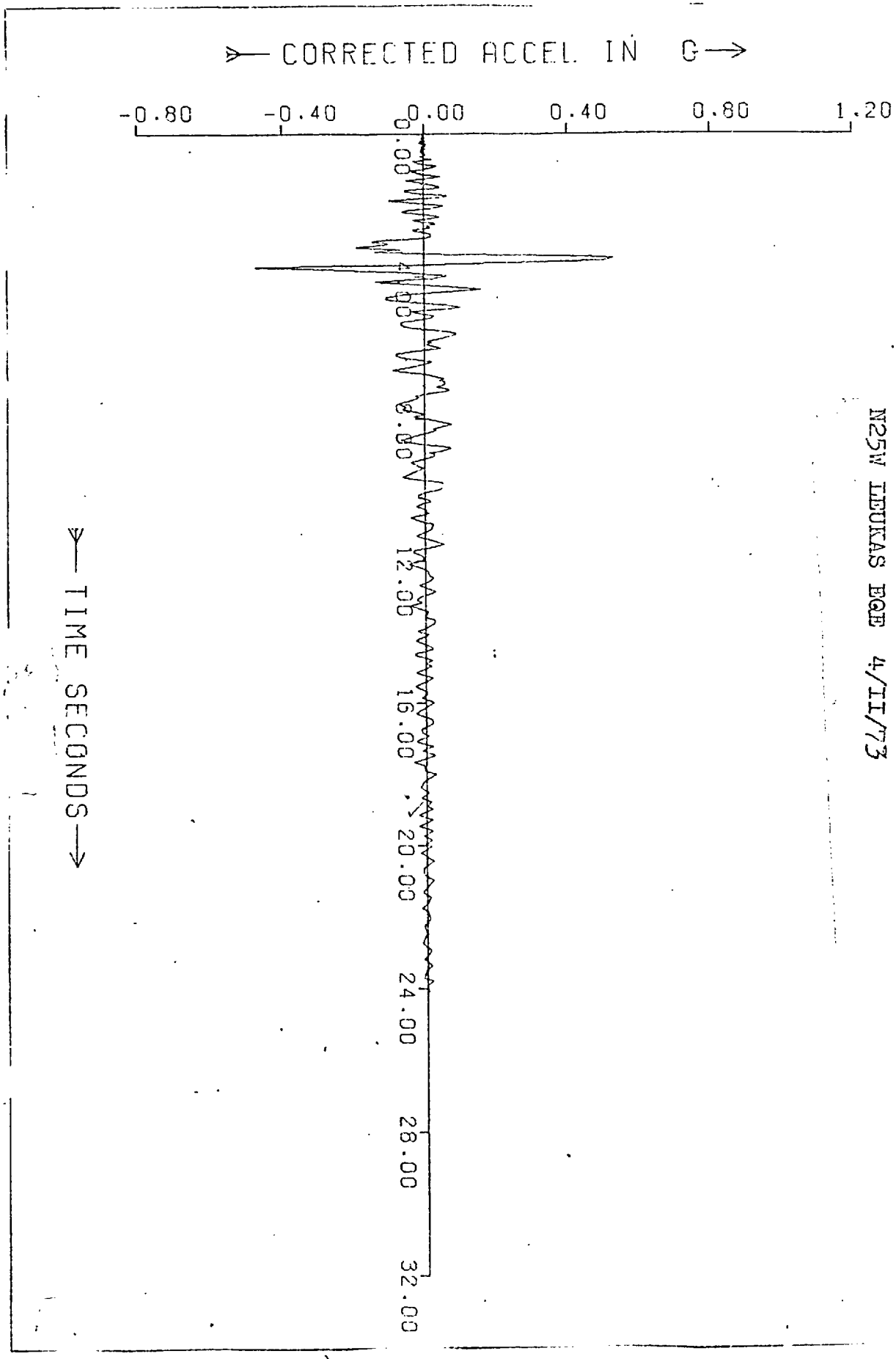

CORRECTED ACCEL. IN G
-0.80
-0.40
0.00
0.40
0.80
1.20
0.00
4.00
8.00
12.00
16.00
20.00
24.00
28.00
32.00
TIME SECONDS
N25W LEUKAS EQE 4/II/73

Fig I.10

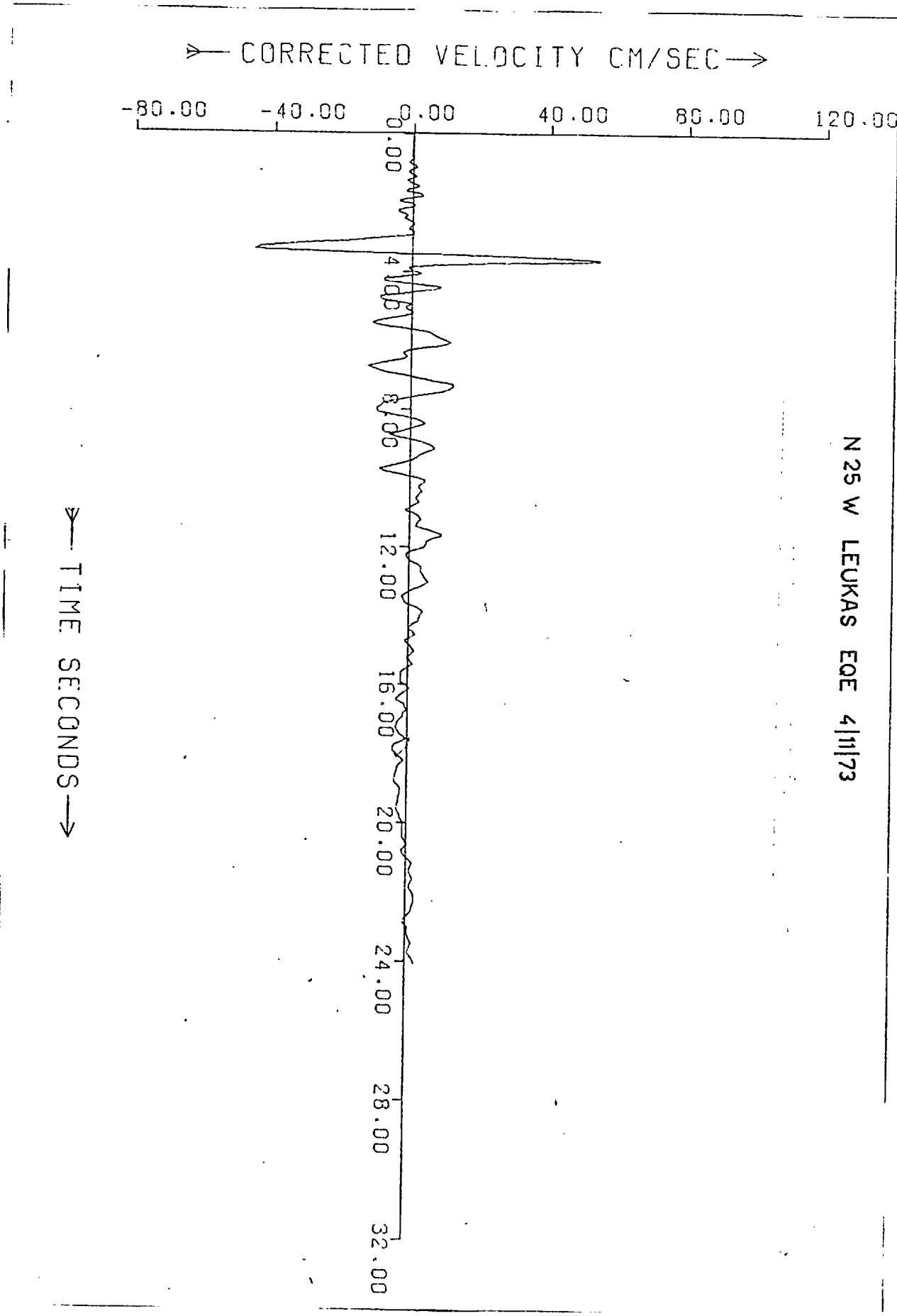

CORRECTED VELOCITY CM/SEC
-80.00
-40.00
0.00
40.00
80.00
120.00
0.00
4.00
8.00
12.00
16.00
20.00
24.00
28.00
32.00
TIME SECONDS
N 25 W LEUKAS EQE 4/11/73

Fig I.11

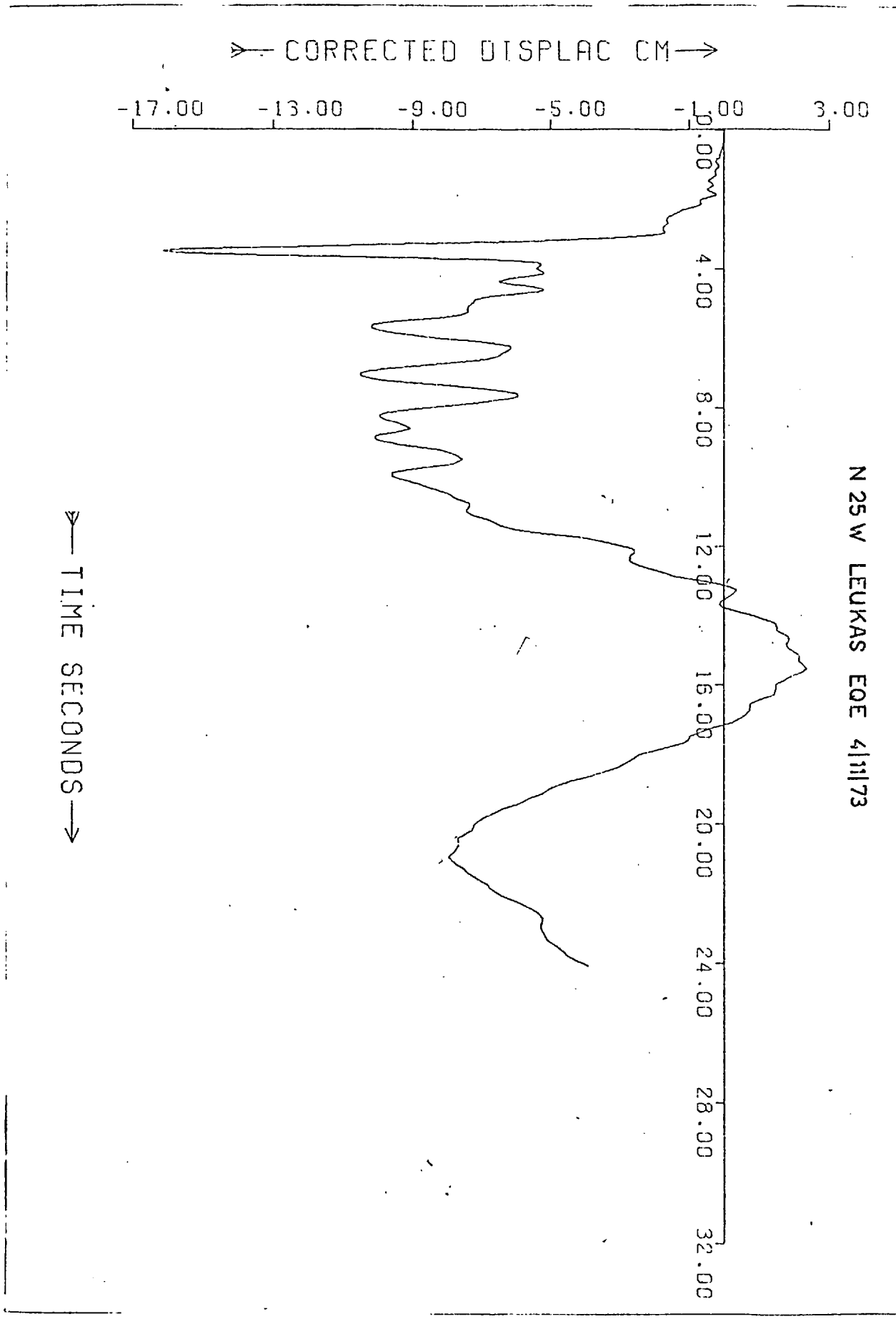

CORRECTED DISPLAC CM
-17.00
-13.00
-9.00
-5.00
-1.00
3.00
0.00
4.00
8.00
12.00
16.00
20.00
24.00
28.00
32.00
TIME SECONDS
N 25 W LEUKAS EQE 4|11|73

Fig I.12.

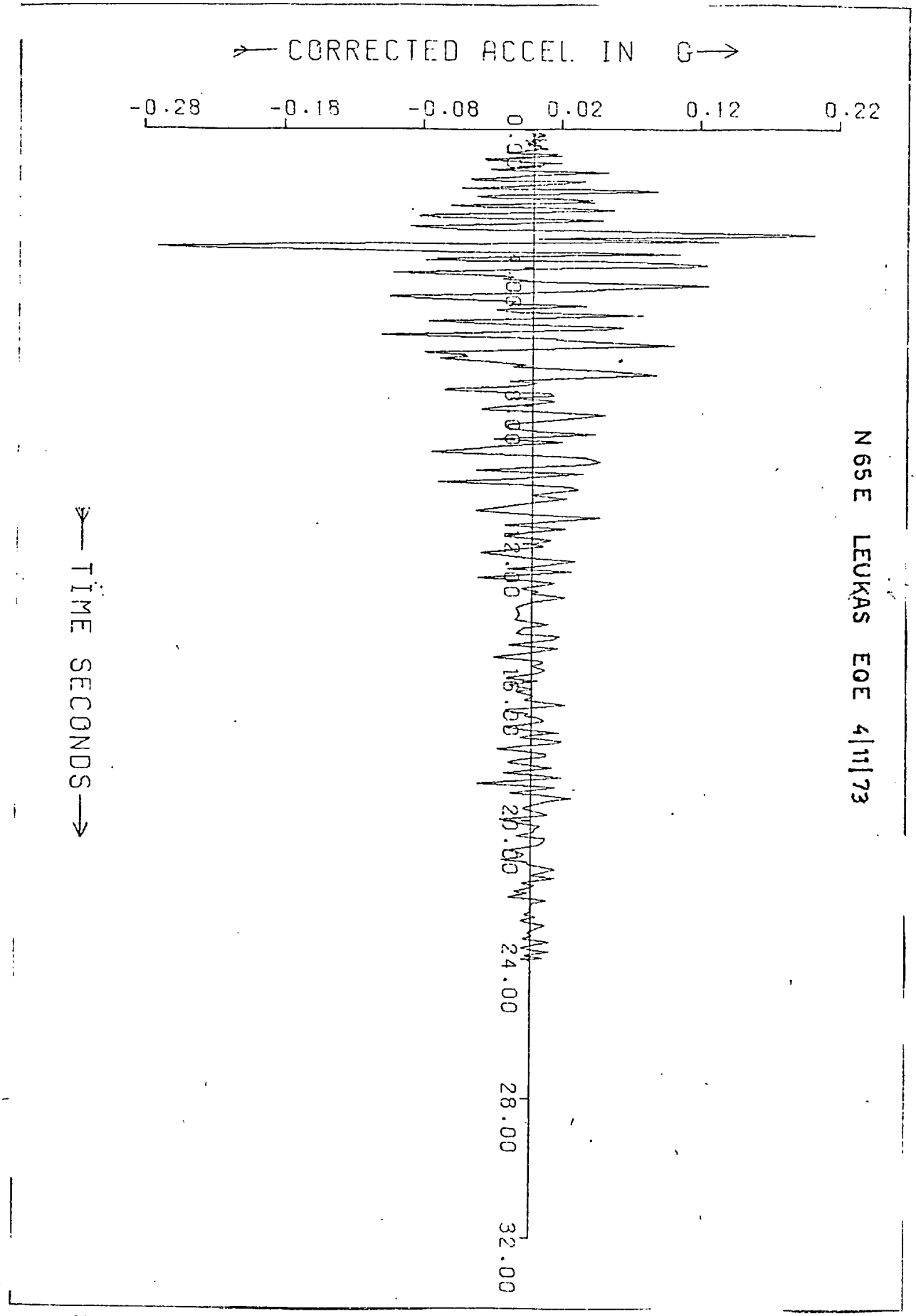

CORRECTED ACCEL. IN G
-0.28
-0.18
-0.08
0.02
0.12
0.22
0.00
4.00
8.00
12.00
16.00
20.00
24.00
28.00
32.00
TIME SECONDS
N 65 E LEUKAS EQE 4/11/73

Fig I.13

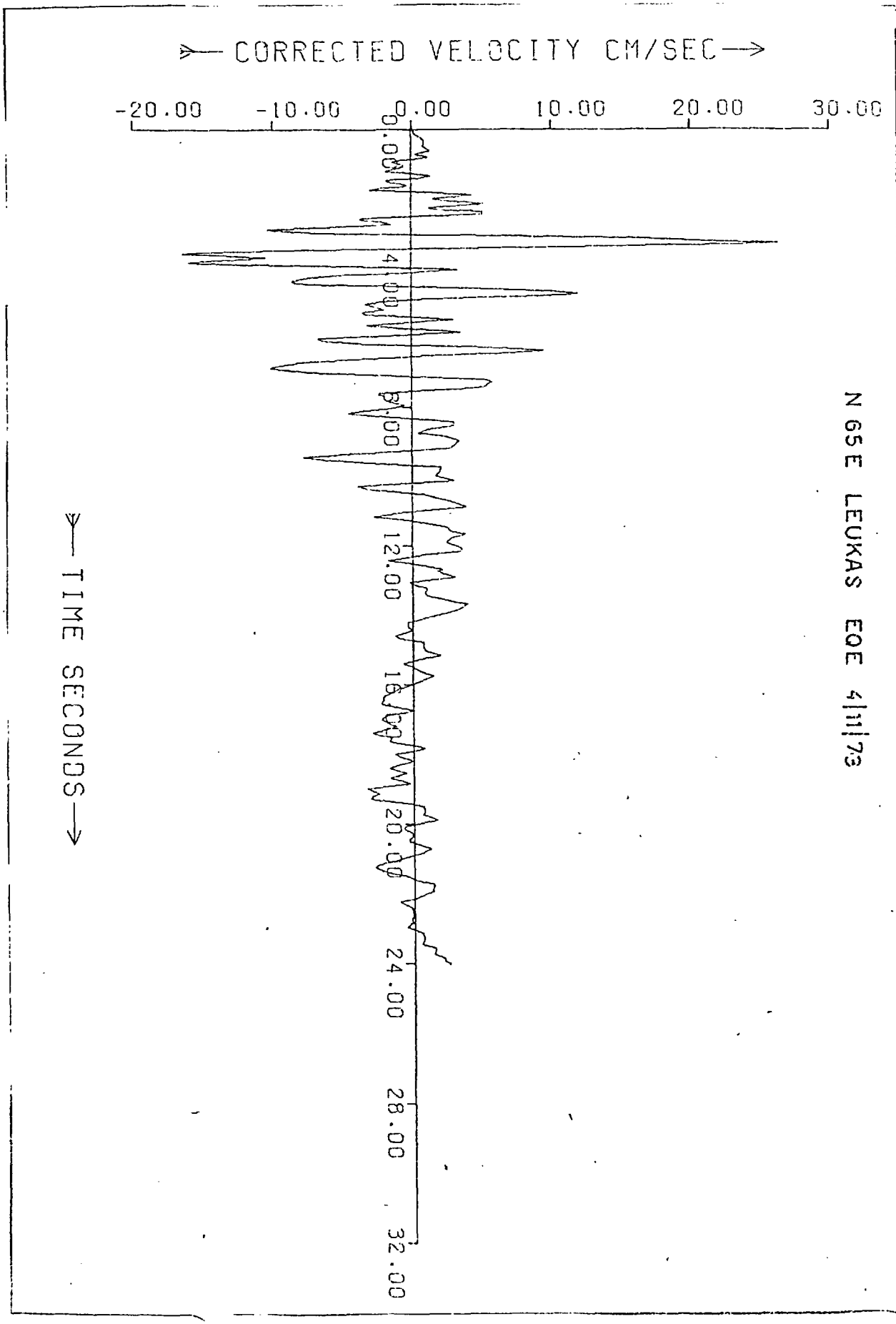

CORRECTED VELOCITY CM/SEC
-20.00
-10.00
0.00
10.00
20.00
30.00
0.00
4.00
8.00
12.00
16.00
20.00
24.00
28.00
32.00
TIME SECONDS
N 65 E LEUKAS EQE 4/11/73

Fig I.14

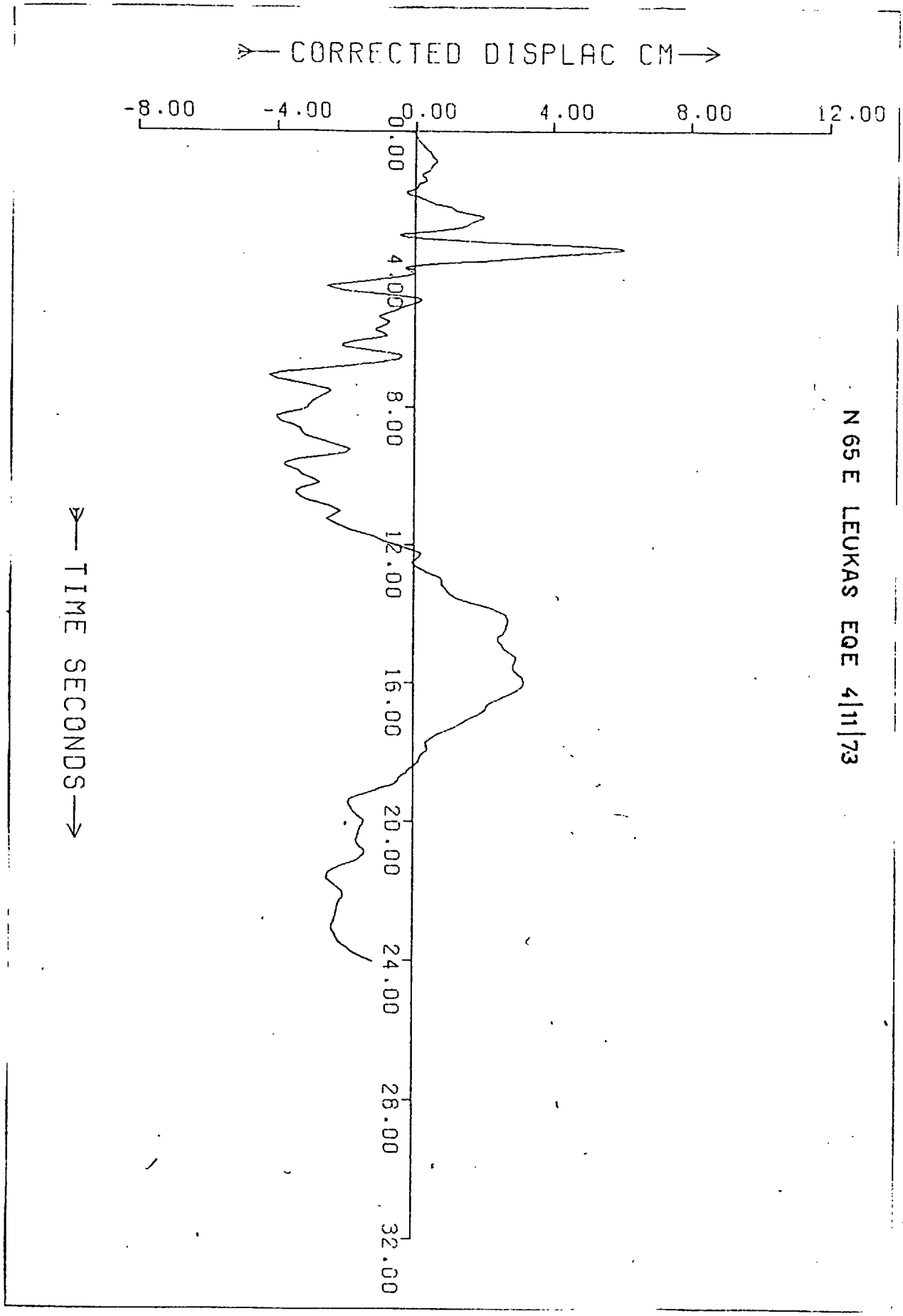

CORRECTED DISPLAC CM
-8.00
-4.00
0.00
4.00
8.00
12.00
0.00
4.00
8.00
12.00
16.00
20.00
24.00
26.00
32.00
TIME SECONDS
N 65 E LEUKAS EQE 4/11/73

Fig I. 15

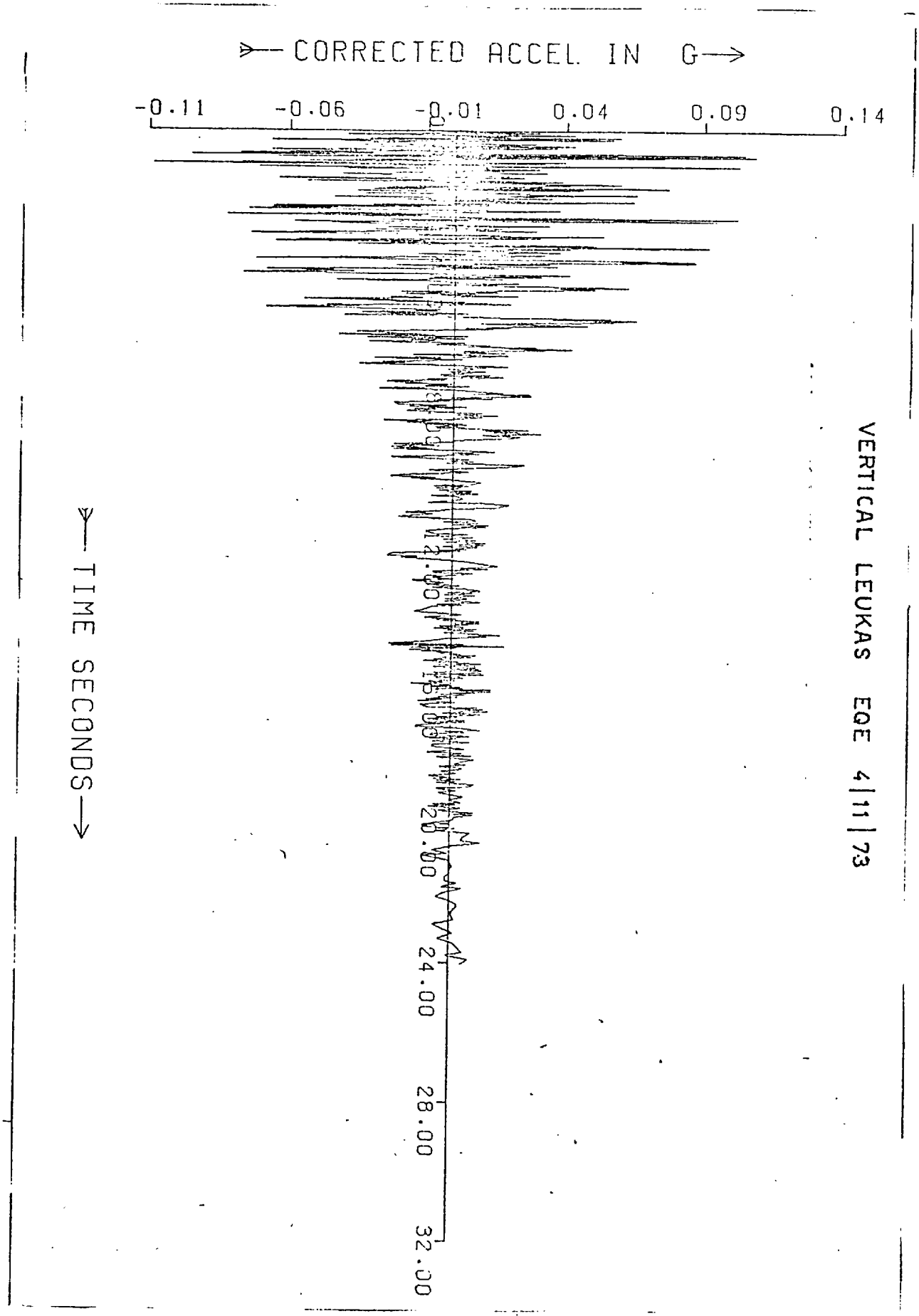

CORRECTED ACCEL. IN G
-0.11
-0.06
-0.01
0.04
0.09
0.14
TIME SECONDS
0.00
4.00
8.00
12.00
16.00
20.00
24.00
28.00
32.00
VERTICAL LEUKAS EQE 4|11|73

Fig I.16

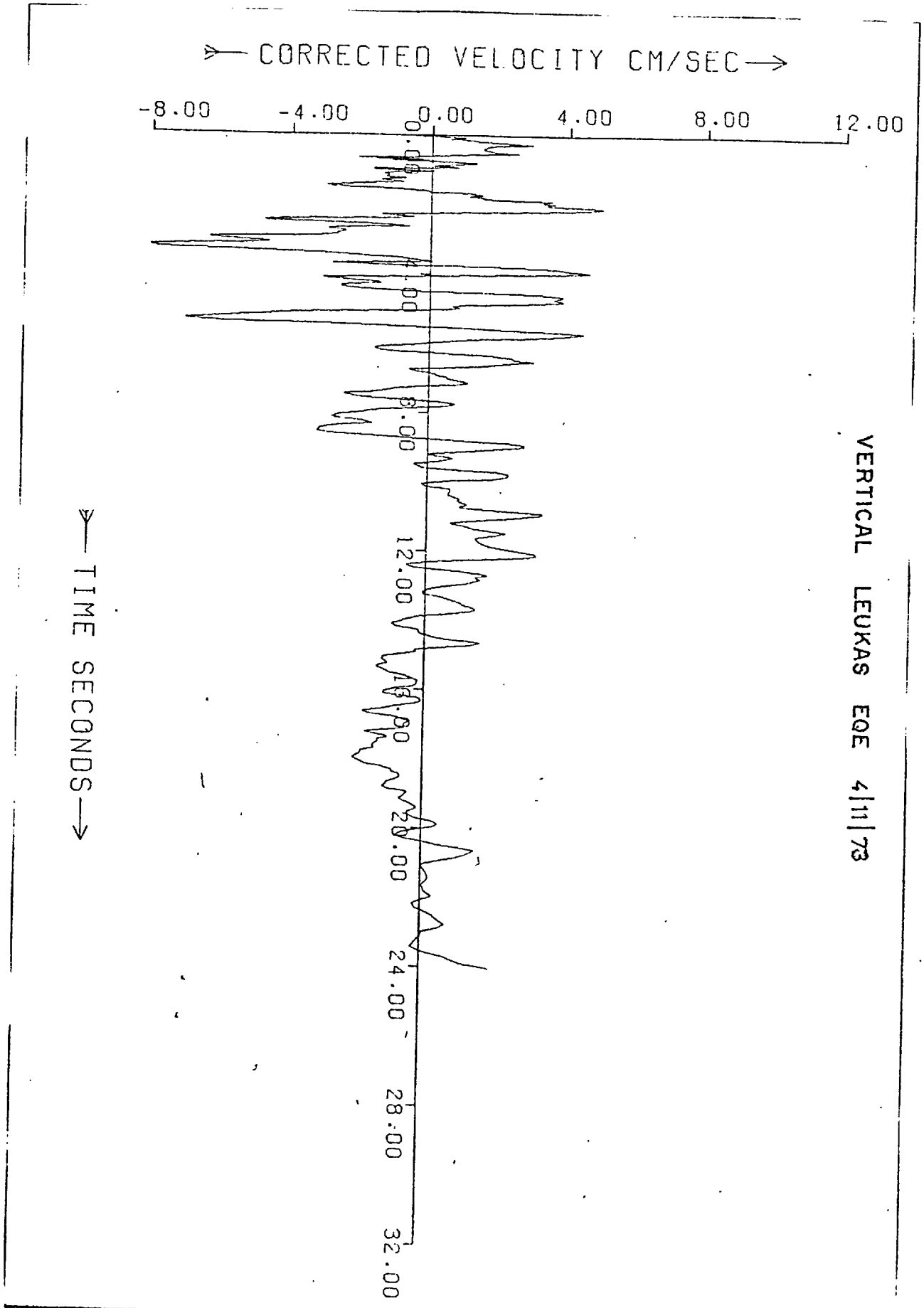

CORRECTED VELOCITY CM/SEC
-8.00
-4.00
0.00
4.00
8.00
12.00
0.00
4.00
8.00
12.00
16.00
20.00
24.00
28.00
32.00
TIME SECONDS
VERTICAL LEUKAS EQE 4/11/73

Fig I.17

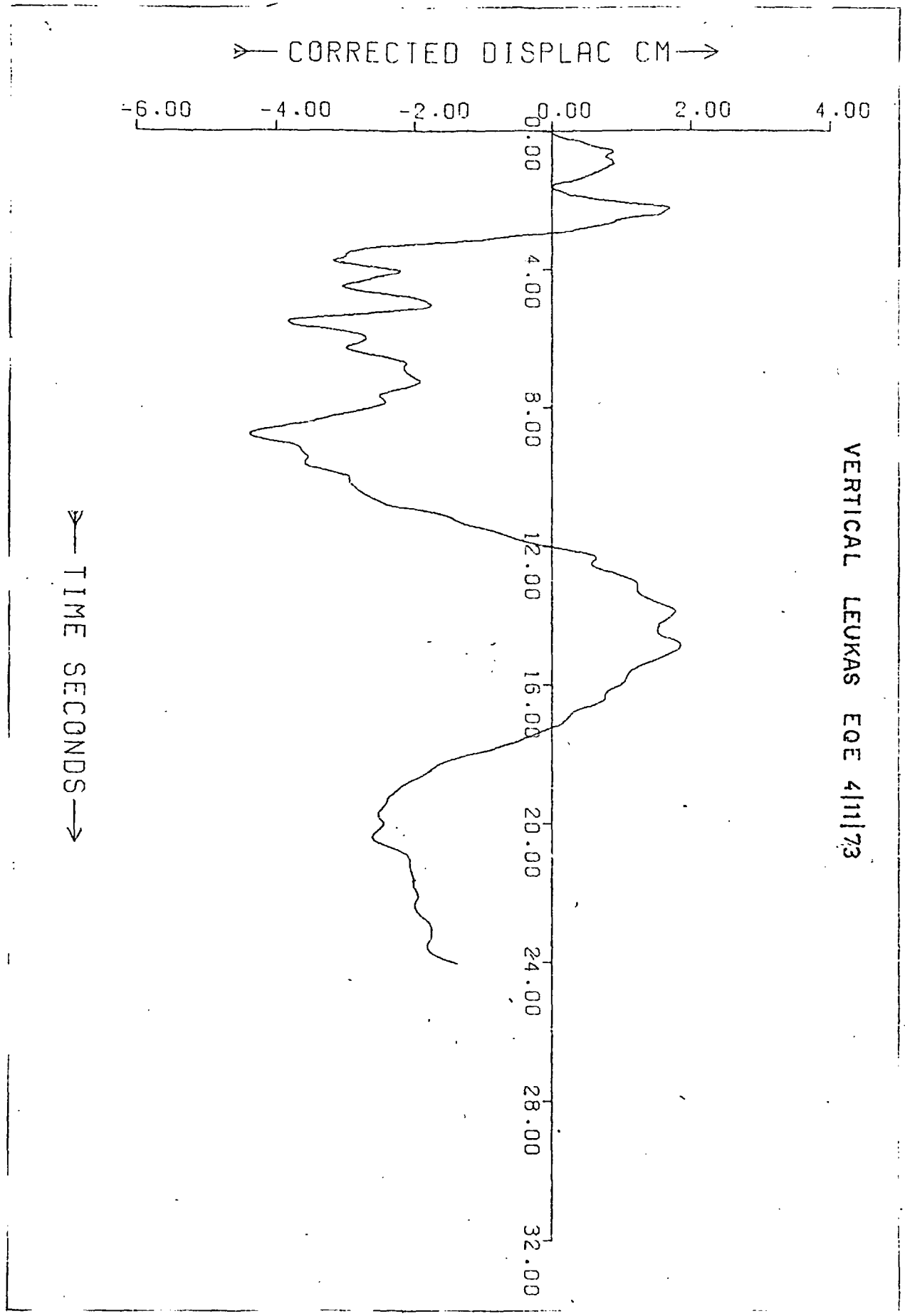

CORRECTED DISPLAC CM
-6.00
-4.00
-2.00
0.00
2.00
4.00
0.00
4.00
8.00
12.00
16.00
20.00
24.00
28.00
32.00
TIME SECONDS
VERTICAL LEUKAS EQE 4/11/73

Fig. I. 18

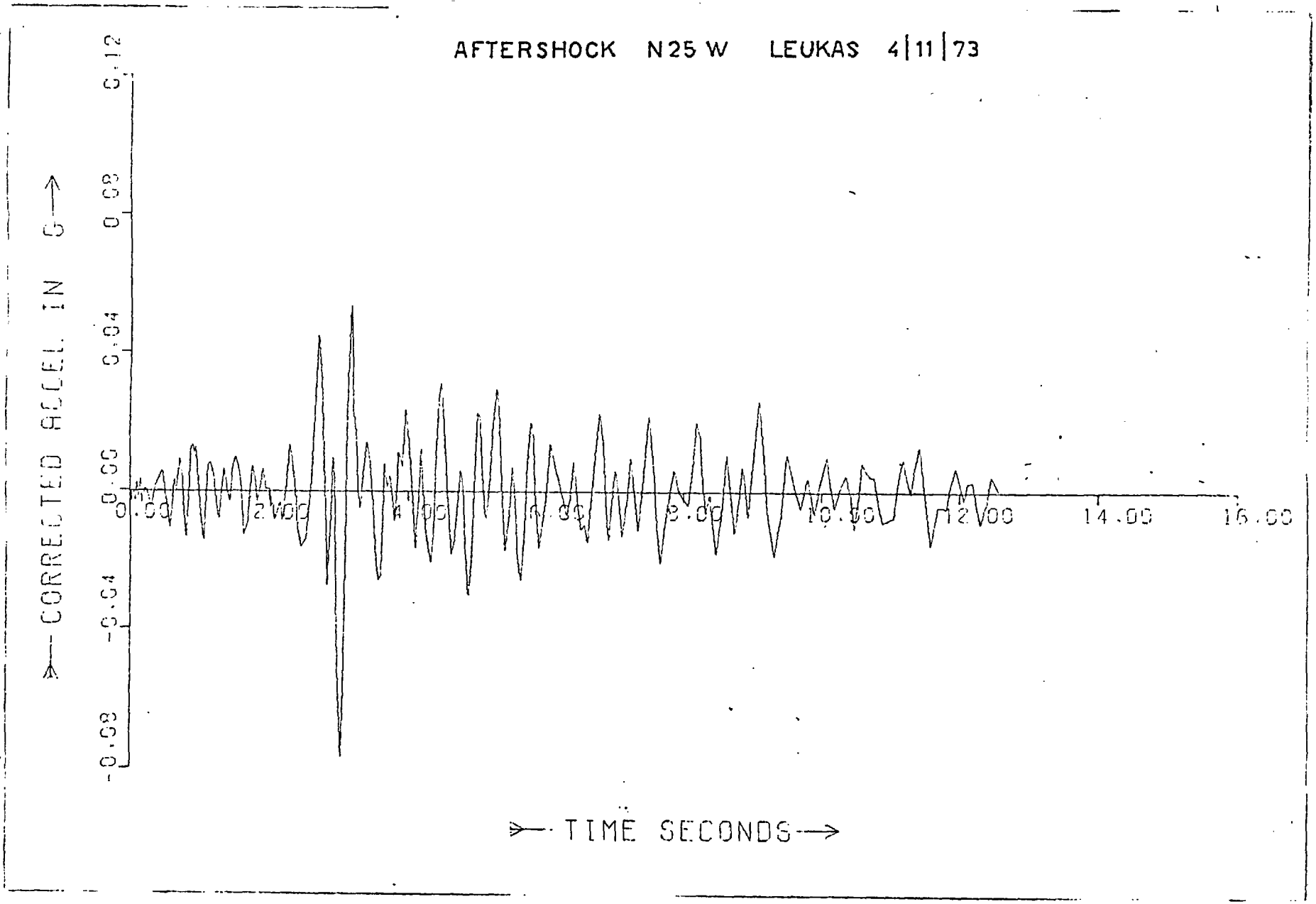

AFTERSHOCK N25 W LEUKAS 4|11|73
CORRECTED ACCEL IN G
0.12
0.08
0.04
0.00
-0.04
-0.08
0.00
2.00
4.00
6.00
8.00
10.00
12.00
14.00
16.00
TIME SECONDS

Fig I.19

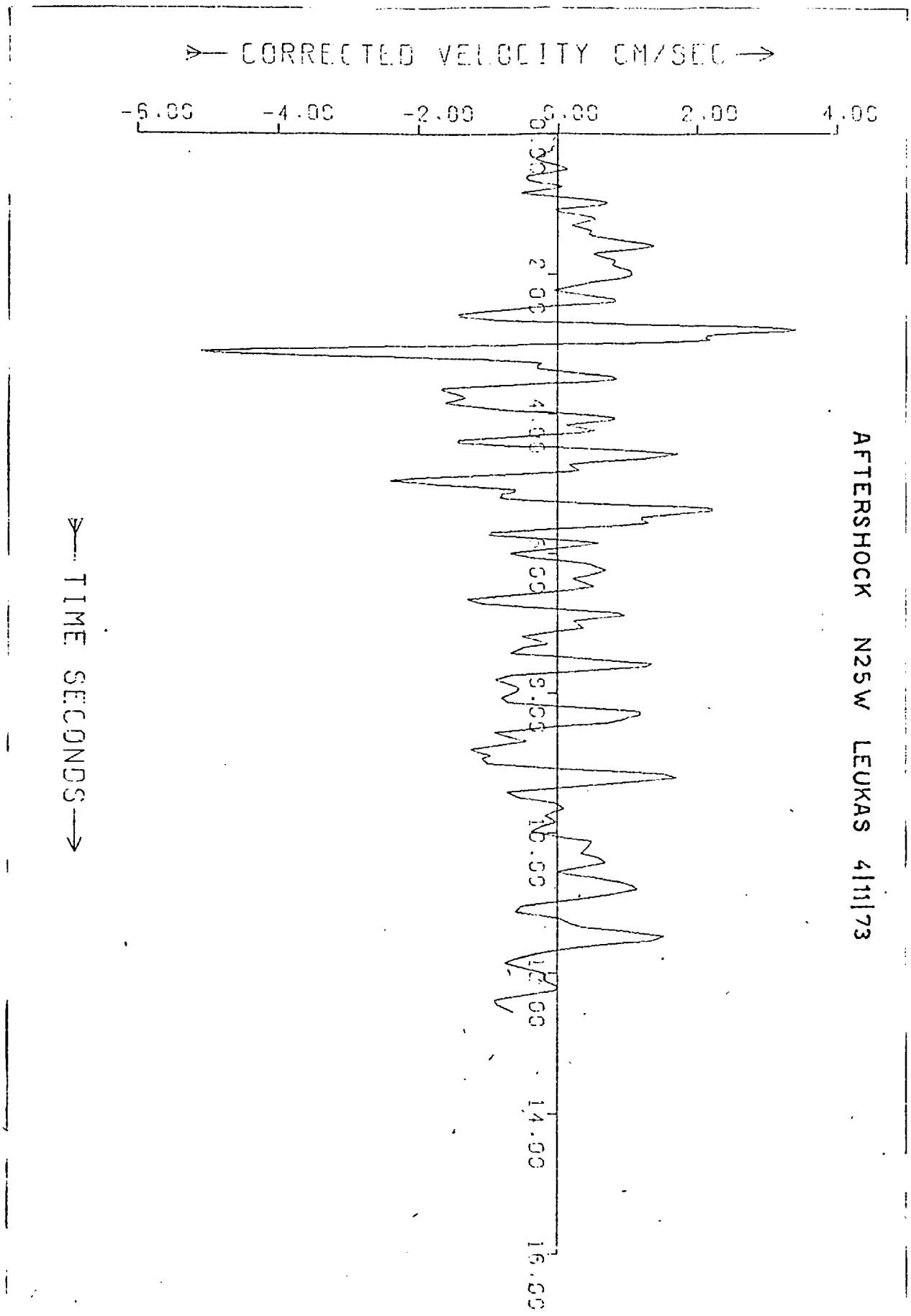

CORRECTED VELOCITY CM/SEC
-6.00
-4.00
-2.00
0.00
2.00
4.00
2.00
4.00
6.00
8.00
10.00
12.00
14.00
16.00
TIME SECONDS
AFTERSHOCK N25W LEUKAS 4|11|73

Fig I.20

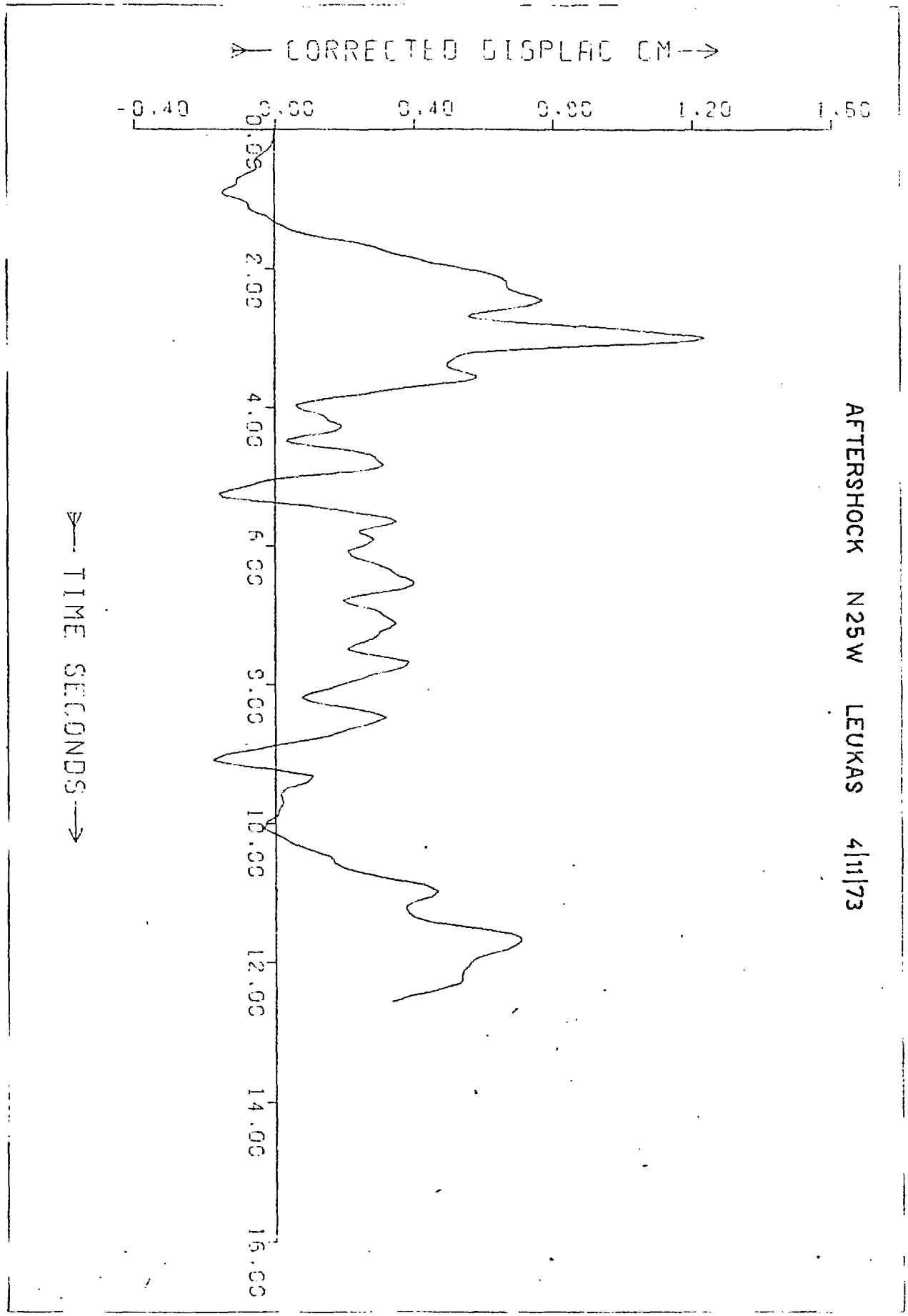

CORRECTED DISPLAC CM
-0.40
0.00
0.40
0.80
1.20
1.60
0.00
2.00
4.00
6.00
8.00
10.00
12.00
14.00
16.00
TIME SECONDS
AFTERSHOCK N25W LEUKAS 4/11/73

Fig I.21

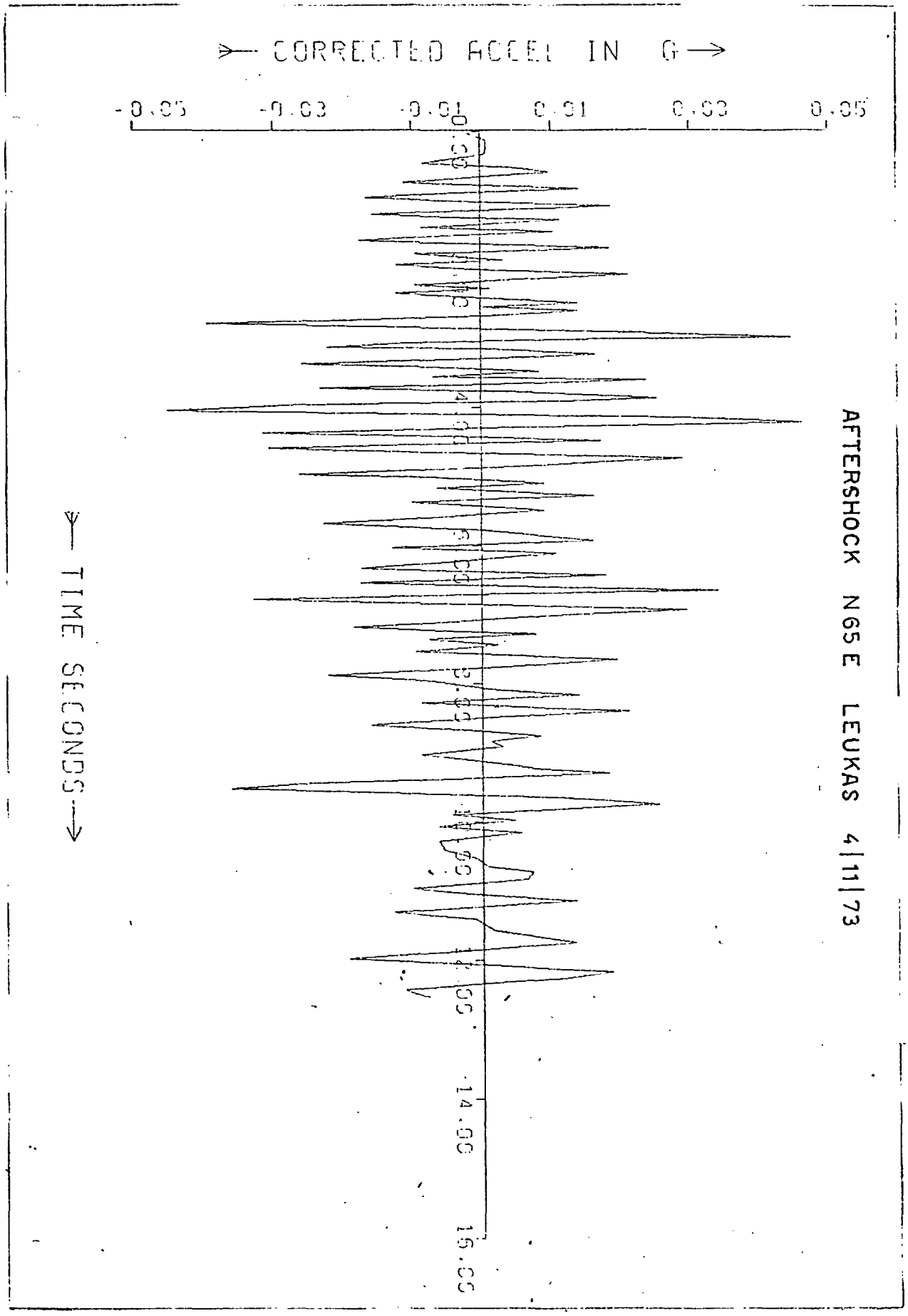

CORRECTED ACCEL IN G
-0.05
-0.03
-0.01
0.01
0.03
0.05
0.00
2.00
4.00
6.00
8.00
10.00
12.00
14.00
16.00
TIME SECONDS
AFTERSHOCK N65E LEUKAS 4|11|73

Fig I.22

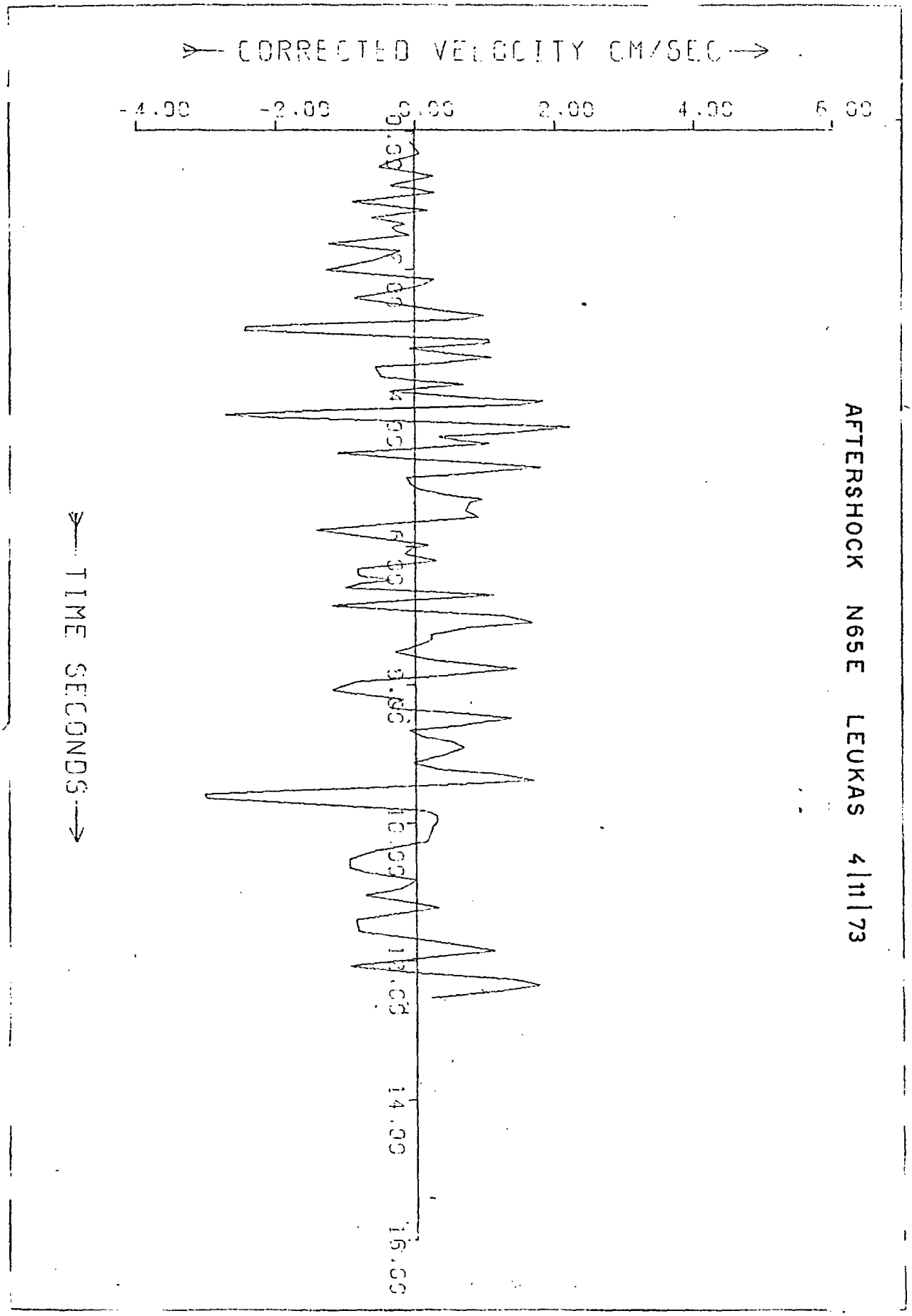

CORRECTED VELOCITY CM/SEC
-4.00
-2.00
0.00
2.00
4.00
6.00
TIME SECONDS
AFTERSHOCK N65E LEUKAS 4|11|73

Fig I.23

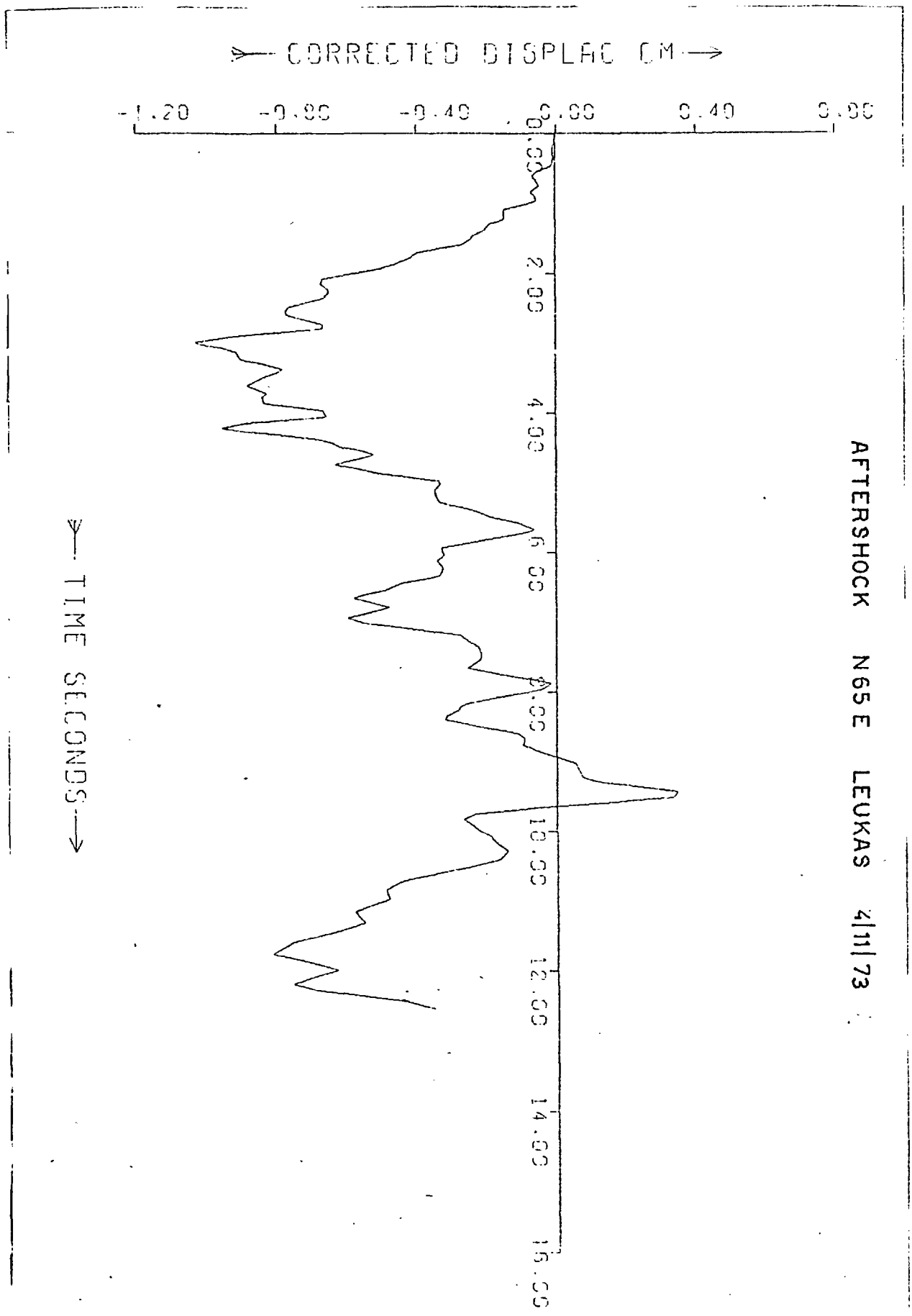

CORRECTED DISPLAC CM
-1.20
-0.80
-0.40
0.00
0.40
0.80
0.00
2.00
4.00
6.00
8.00
10.00
12.00
14.00
16.00
TIME SECONDS
AFTERSHOCK N65 E LEUKAS 4|11|73

Fig I.24

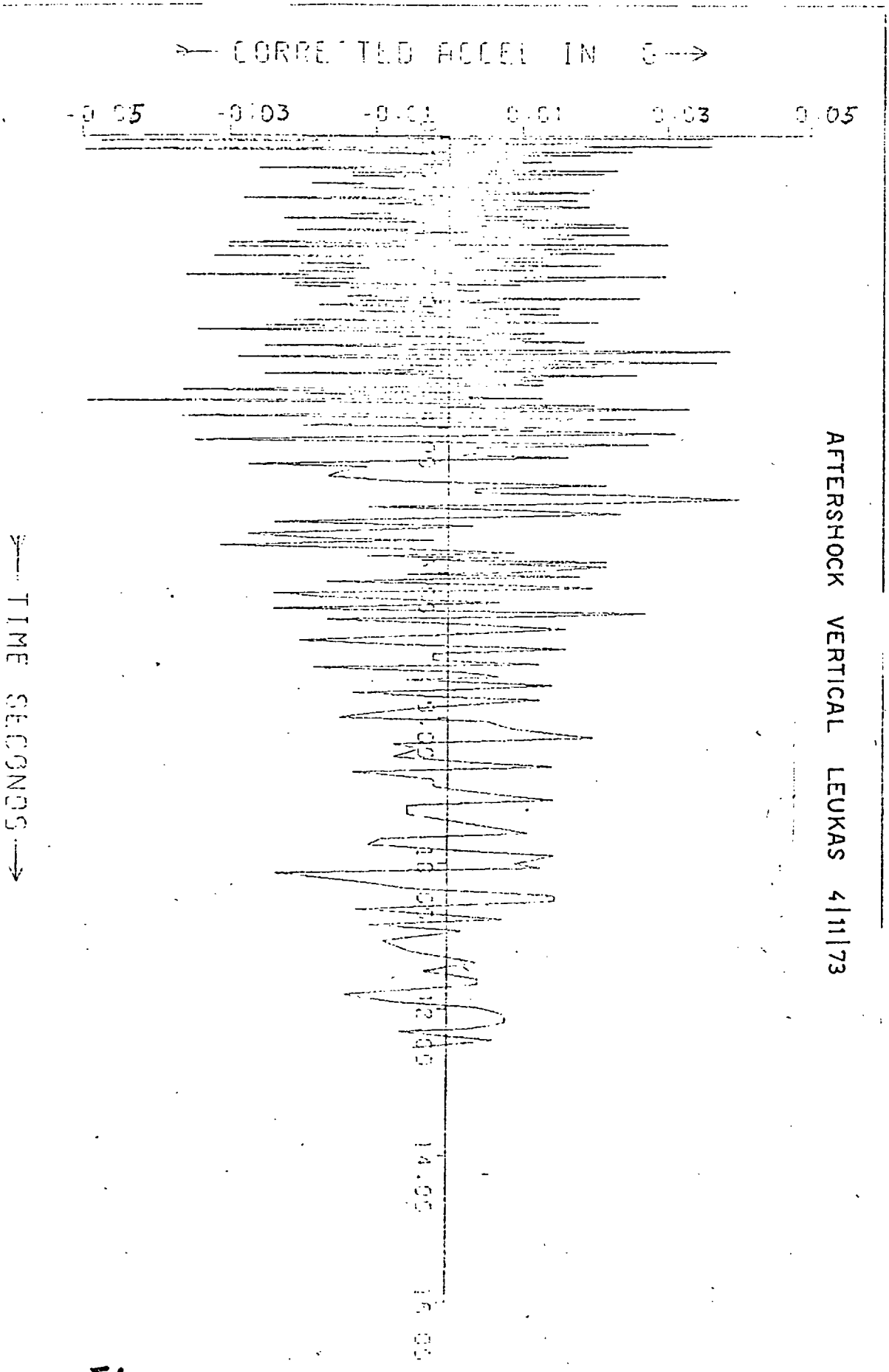

CORRECTED ACCEL IN G
-0.05
-0.03
-0.01
0.01
0.03
0.05
AFTERSHOCK VERTICAL LEUKAS 4/11/73
TIME SECONDS
0.00
2.00
4.00
6.00
8.00
10.00
12.00
14.00
16.00

Fig I.25

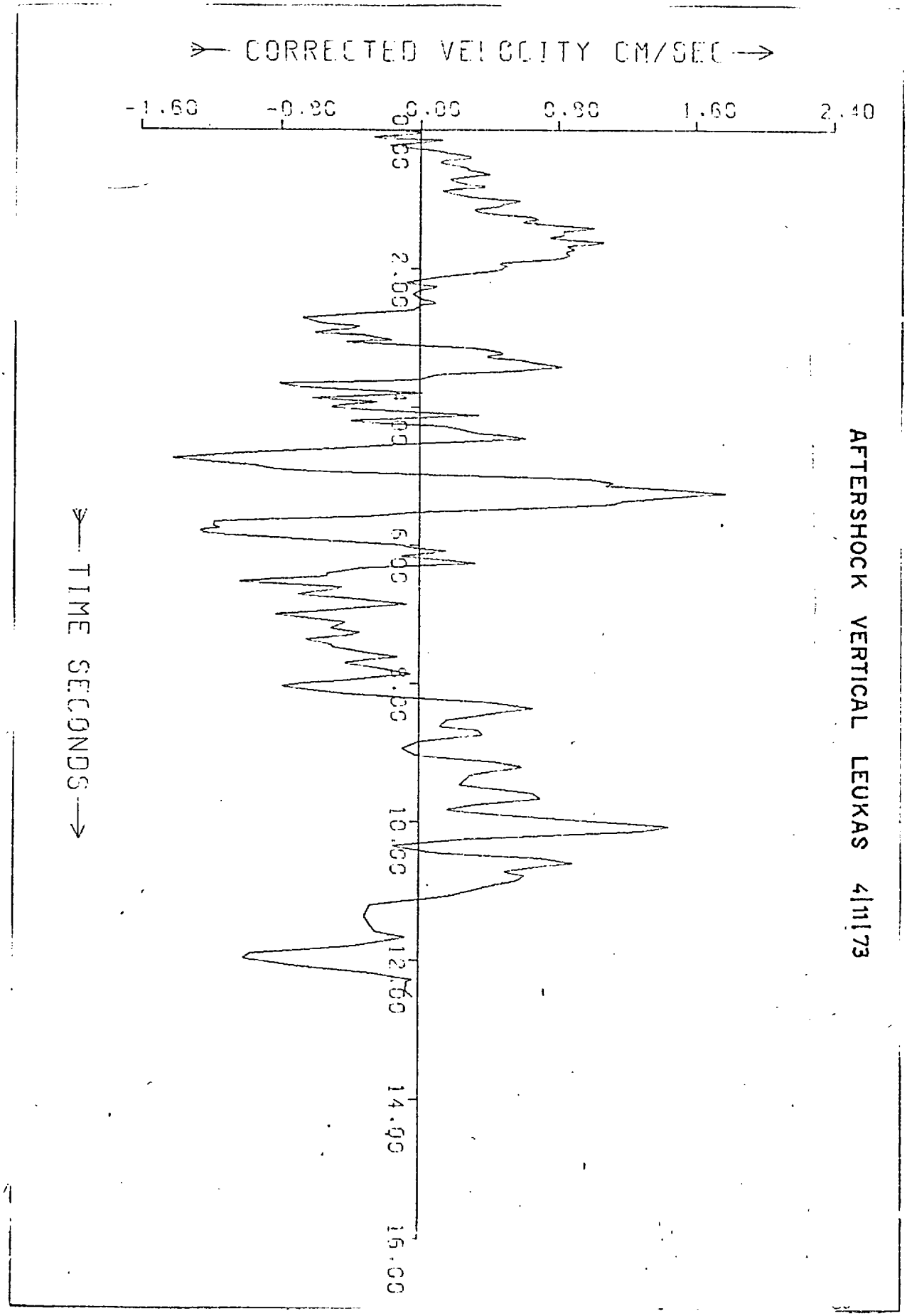

CORRECTED VELOCITY CM/SEC
-1.60
-0.80
0.00
0.80
1.60
2.40
0.00
2.00
4.00
6.00
8.00
10.00
12.00
14.00
16.00
TIME SECONDS
AFTERSHOCK VERTICAL LEUKAS 4/11/73

Fig I.25

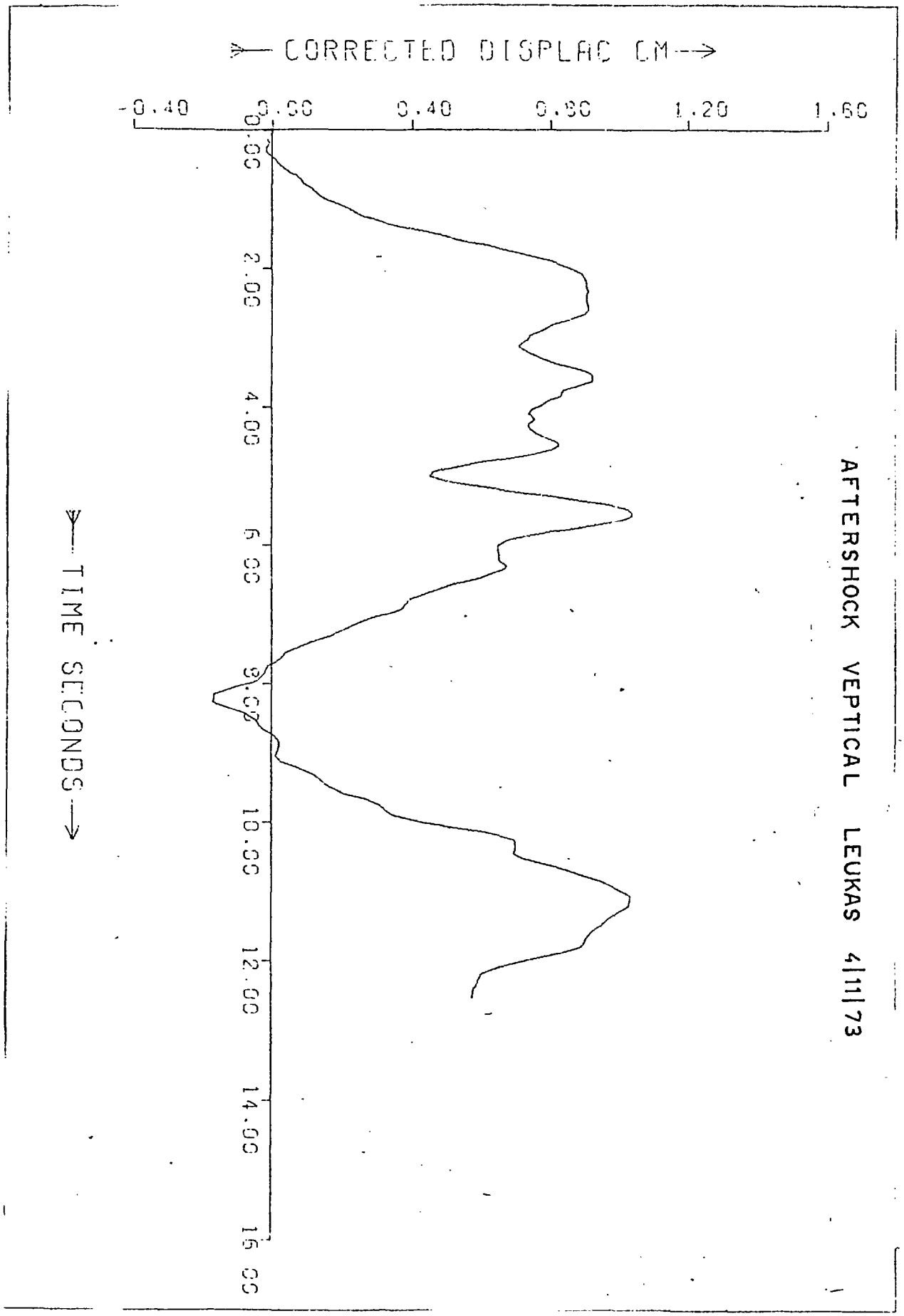

CORRECTED DISPLAC CM
-0.40
0.00
0.40
0.80
1.20
1.60
0
00.00
00.2
00.4
00.6
00.8
00.00
10.00
12.00
14.00
16.00
TIME SECONDS
AFTERSHOCK VEPTICAL LEUKAS 4|11|73

Fig I.27

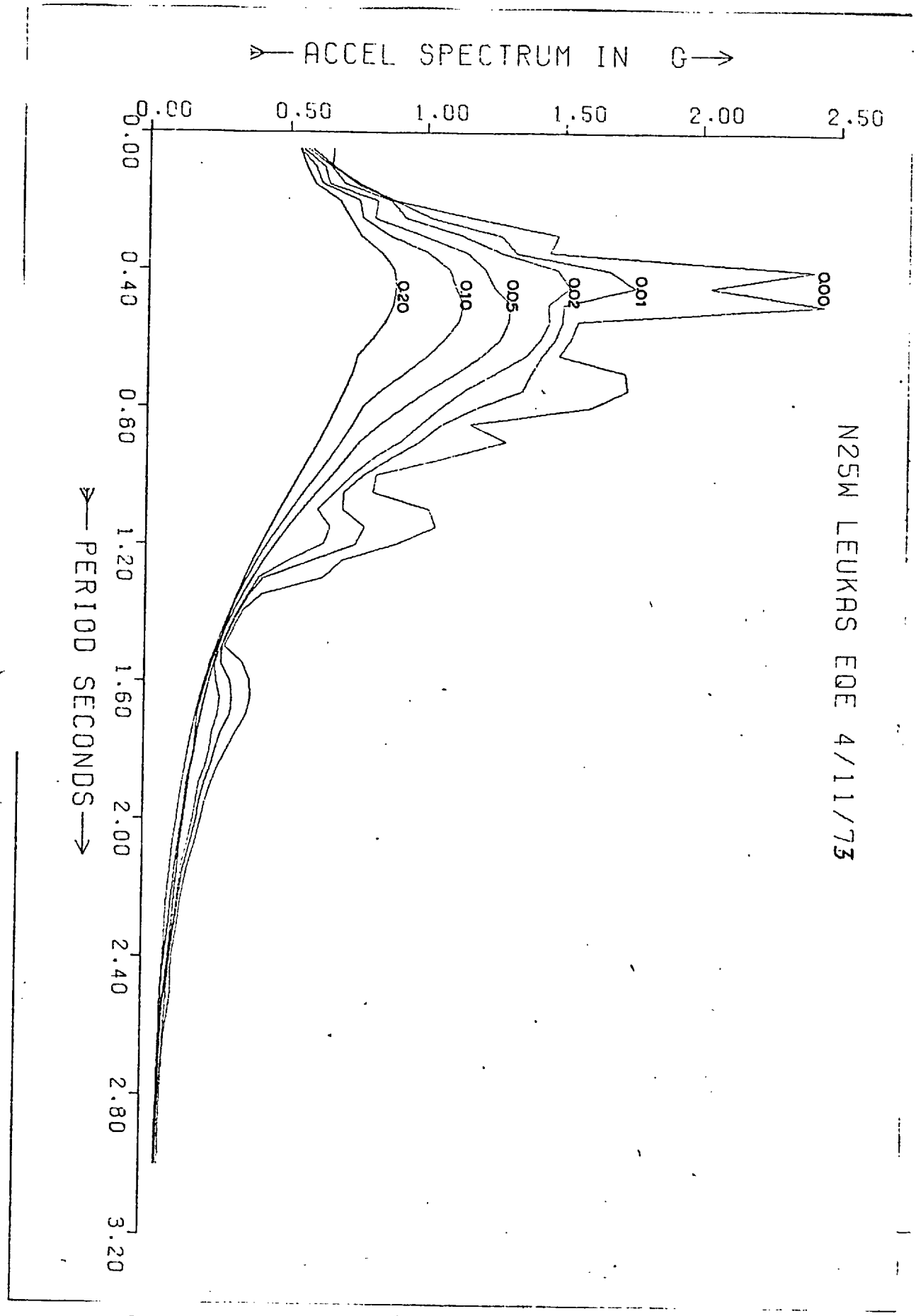

ACCEL SPECTRUM IN G
0.00
0.50
1.00
1.50
2.00
2.50
0.00
0.40
0.60
1.20
1.60
2.00
2.40
2.80
3.20
PERIOD SECONDS
020
010
005
002
001
000
N25W LEUKAS EQE 4/11/73

Fig I.28

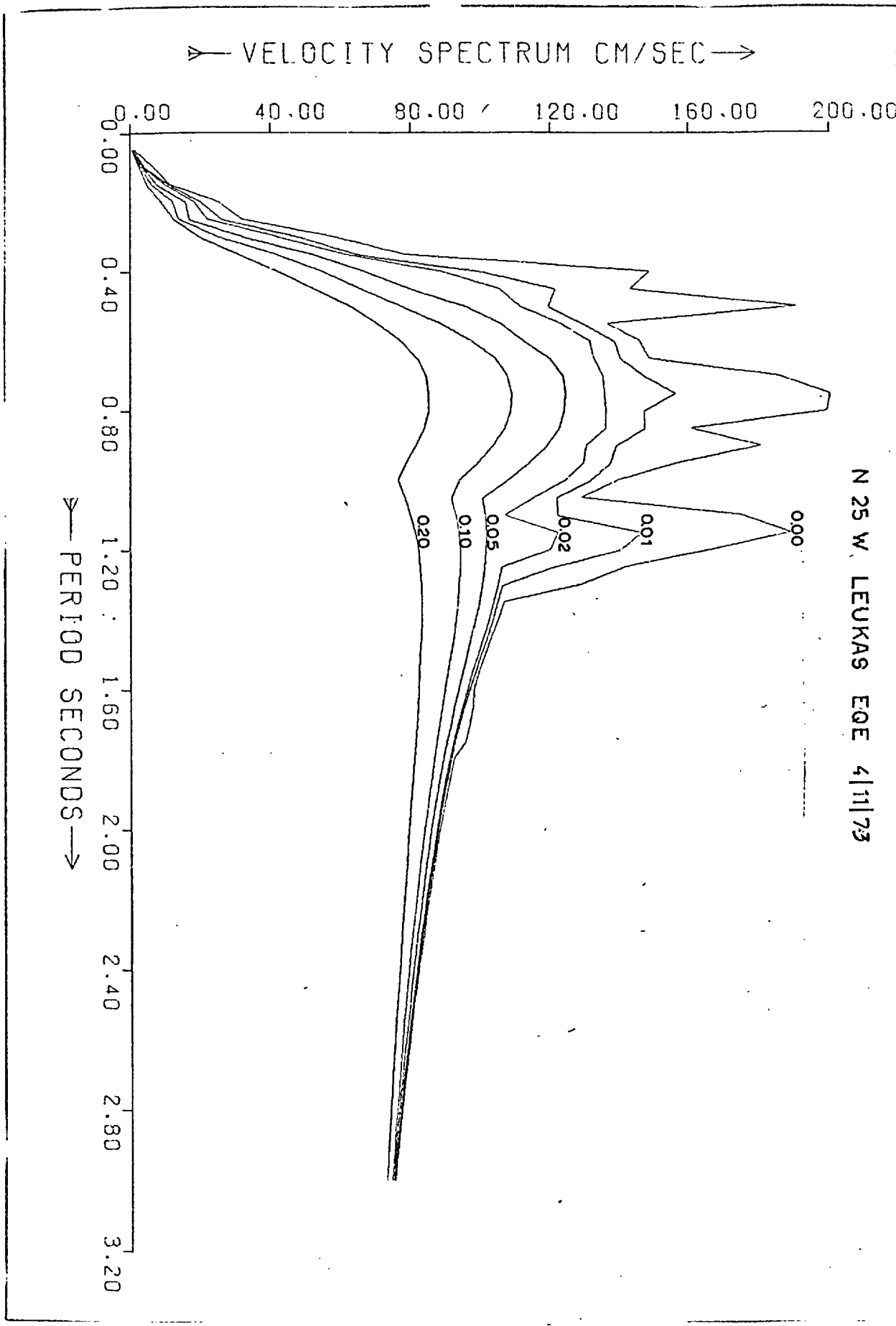

VELOCITY SPECTRUM CM/SEC
0.00
40.00
80.00
120.00
160.00
200.00
PERIOD SECONDS
0.00
0.40
0.80
1.20
1.60
2.00
2.40
2.80
3.20
0.20
0.10
0.05
0.02
0.01
0.00
N 25 W LEUKAS EQE 4|11|73

Fig I. 29

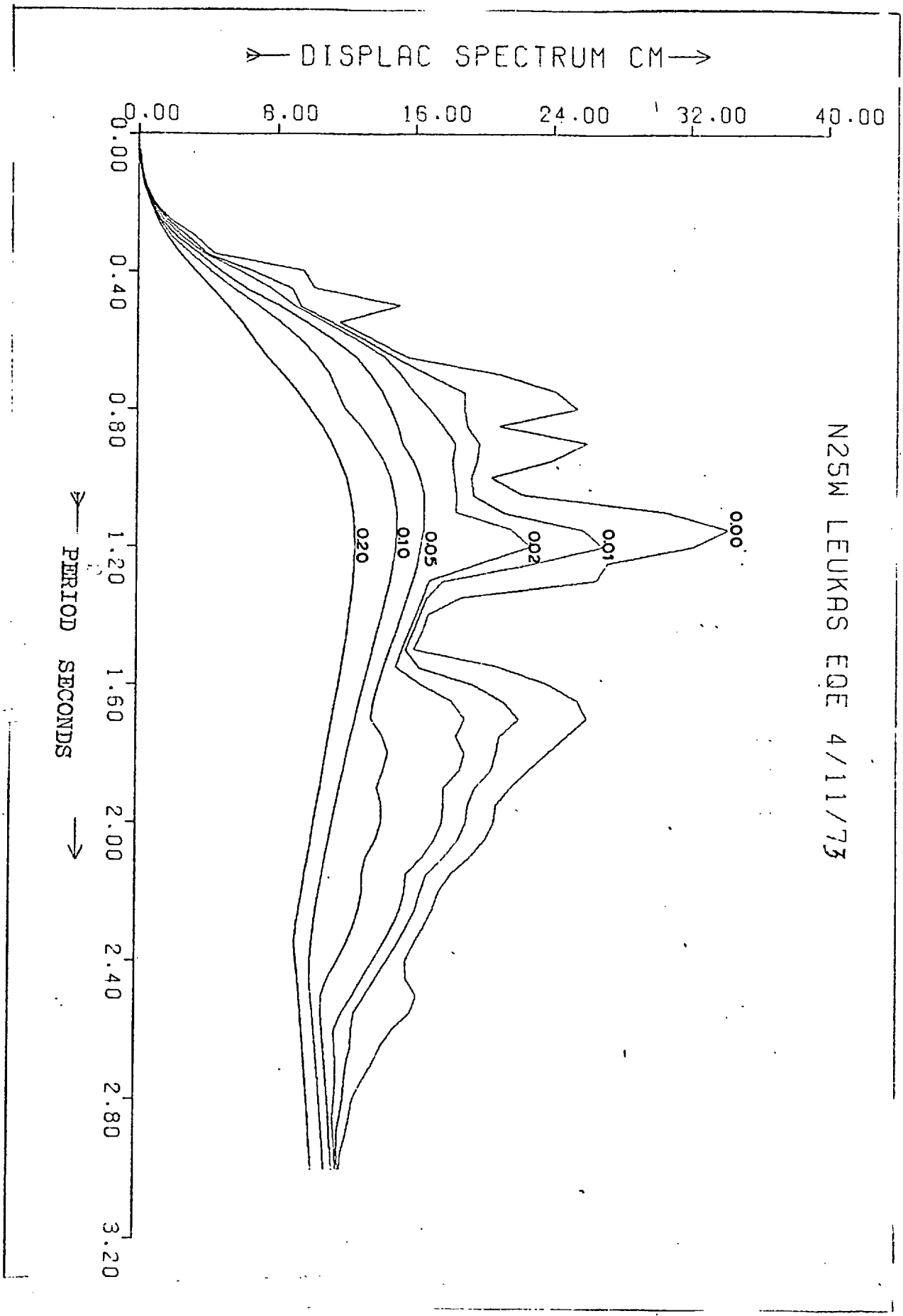

DISPLAC SPECTRUM CM
0.00
8.00
16.00
24.00
32.00
40.00
PERIOD SECONDS
0.00
0.40
0.80
1.20
1.60
2.00
2.40
2.80
3.20
0.20
0.10
0.05
0.02
0.01
0.00
N25W LEUKAS EQE 4/11/73

Fig I.30

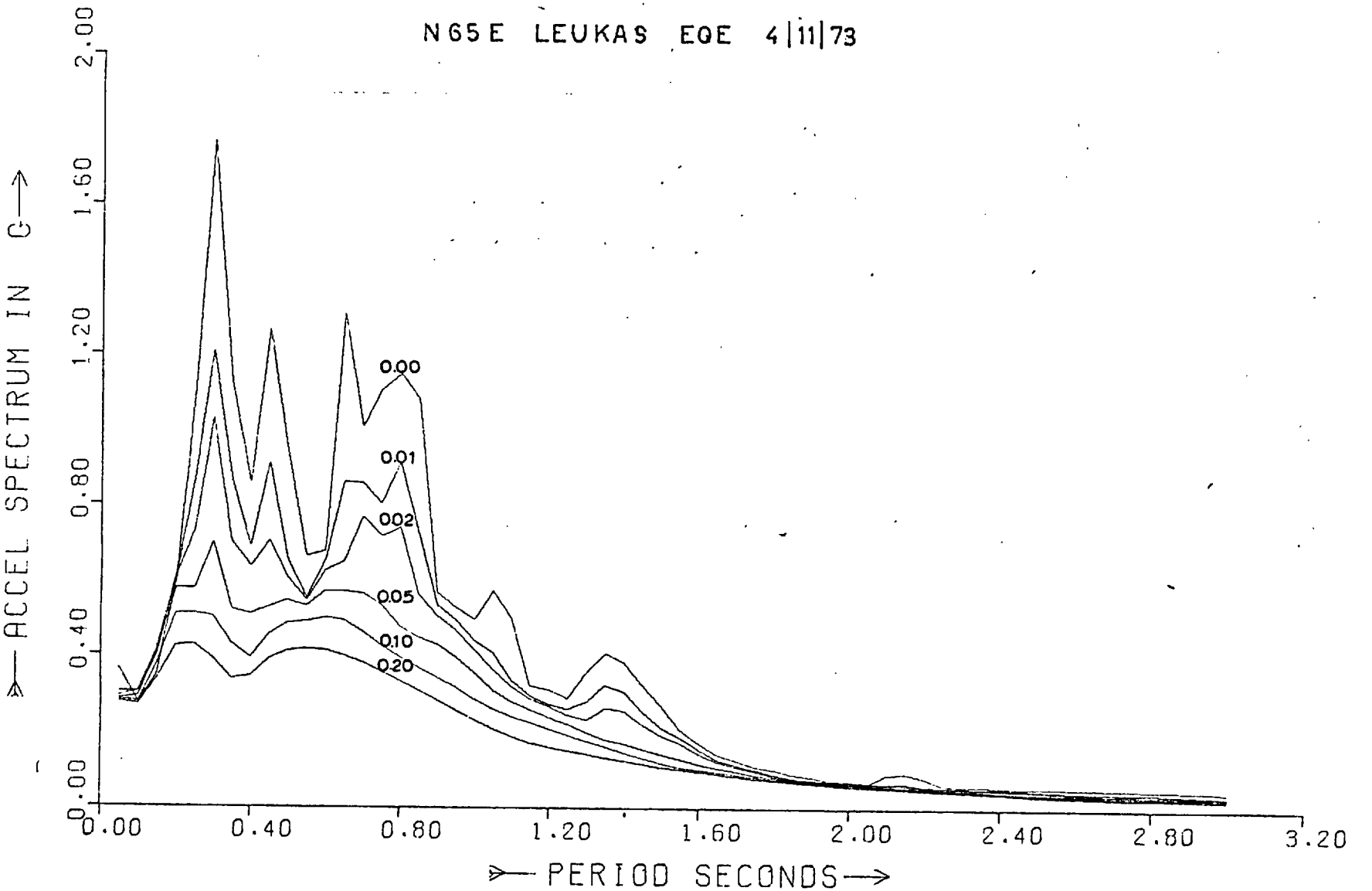

N65E LEUKAS EQE 4|11|73
ACCEL SPECTRUM IN C
PERIOD SECONDS
0.00
0.40
0.80
1.20
1.60
2.00
2.40
2.80
3.20
0.00
0.40
0.80
1.20
1.60
2.00
0.00
0.01
0.02
0.05
0.10
0.20

Fig I.31

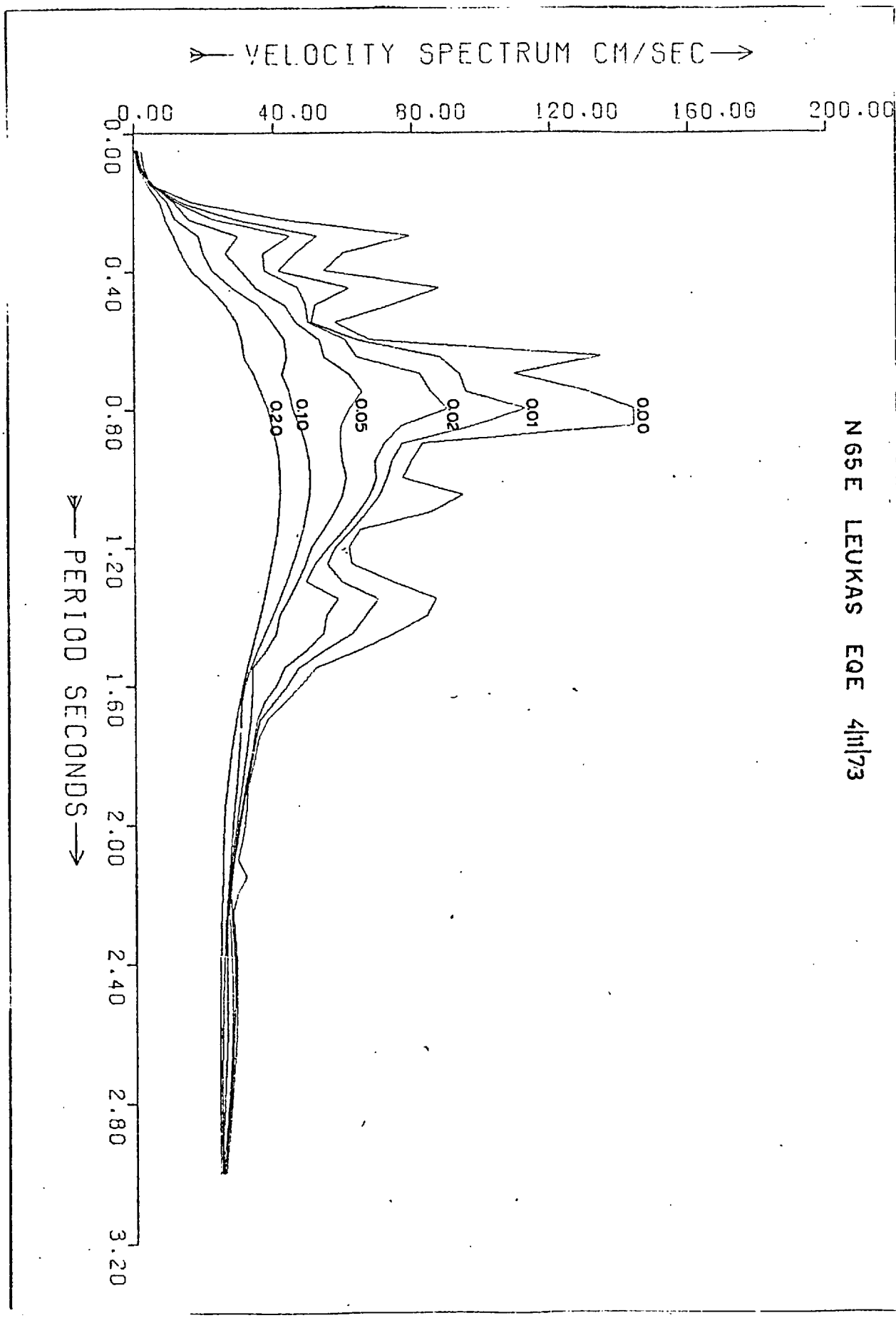

VELOCITY SPECTRUM CM/SEC
0.00
40.00
80.00
120.00
160.00
200.00
PERIOD SECONDS
0.00
0.40
0.80
1.20
1.60
2.00
2.40
2.80
3.20
0.20
0.10
0.05
0.02
0.01
0.00
N 65 E LEUKAS EQE 4/11/73

Fig I.32

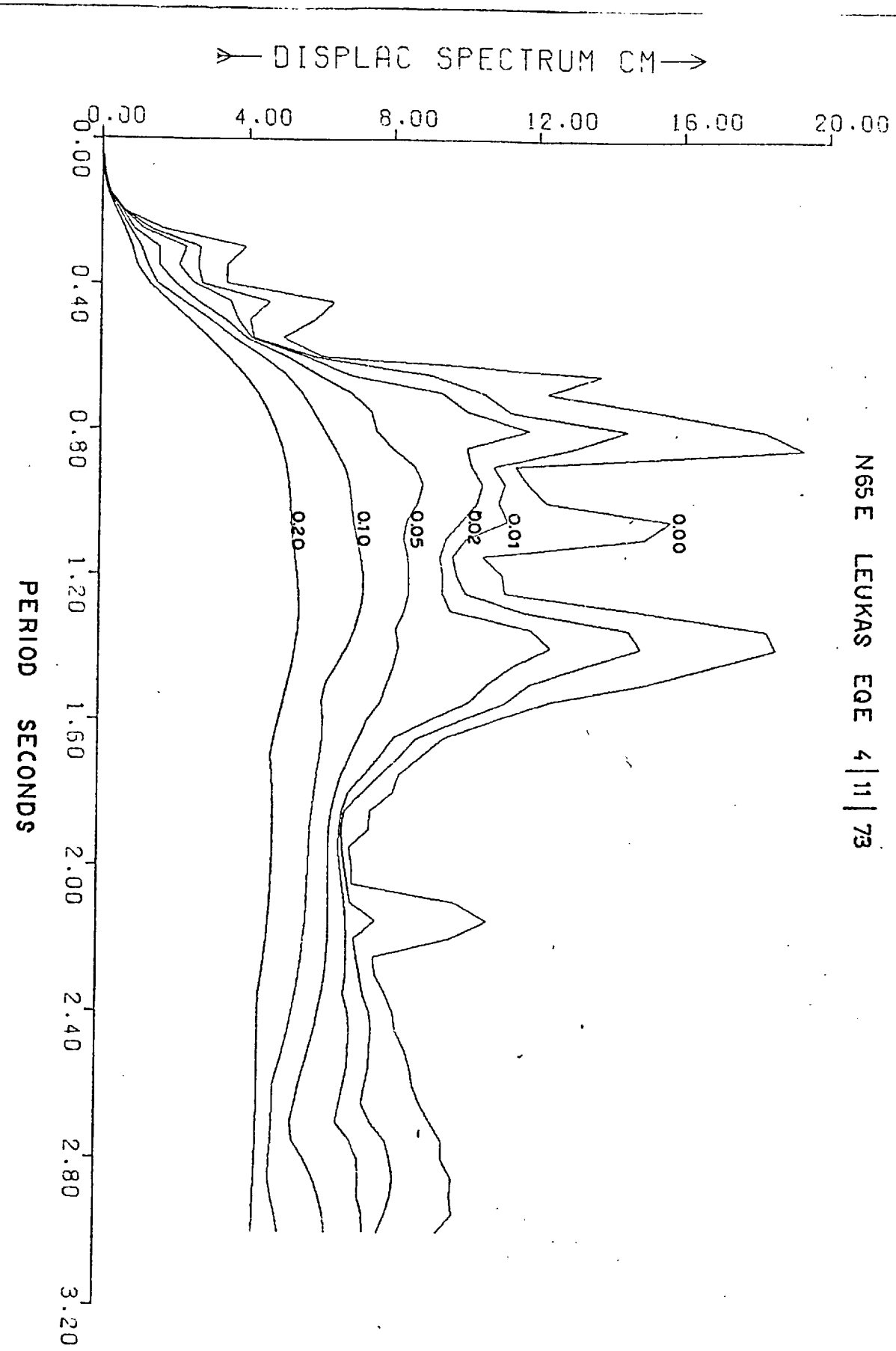

DISPLAC SPECTRUM CM
0.00
4.00
8.00
12.00
16.00
20.00
0.00
0.40
0.80
1.20
1.60
2.00
2.40
2.80
3.20
PERIOD SECONDS
0.20
0.10
0.05
0.02
0.01
0.00
N65E LEUKAS EQE 4|11|73

Fig I.33

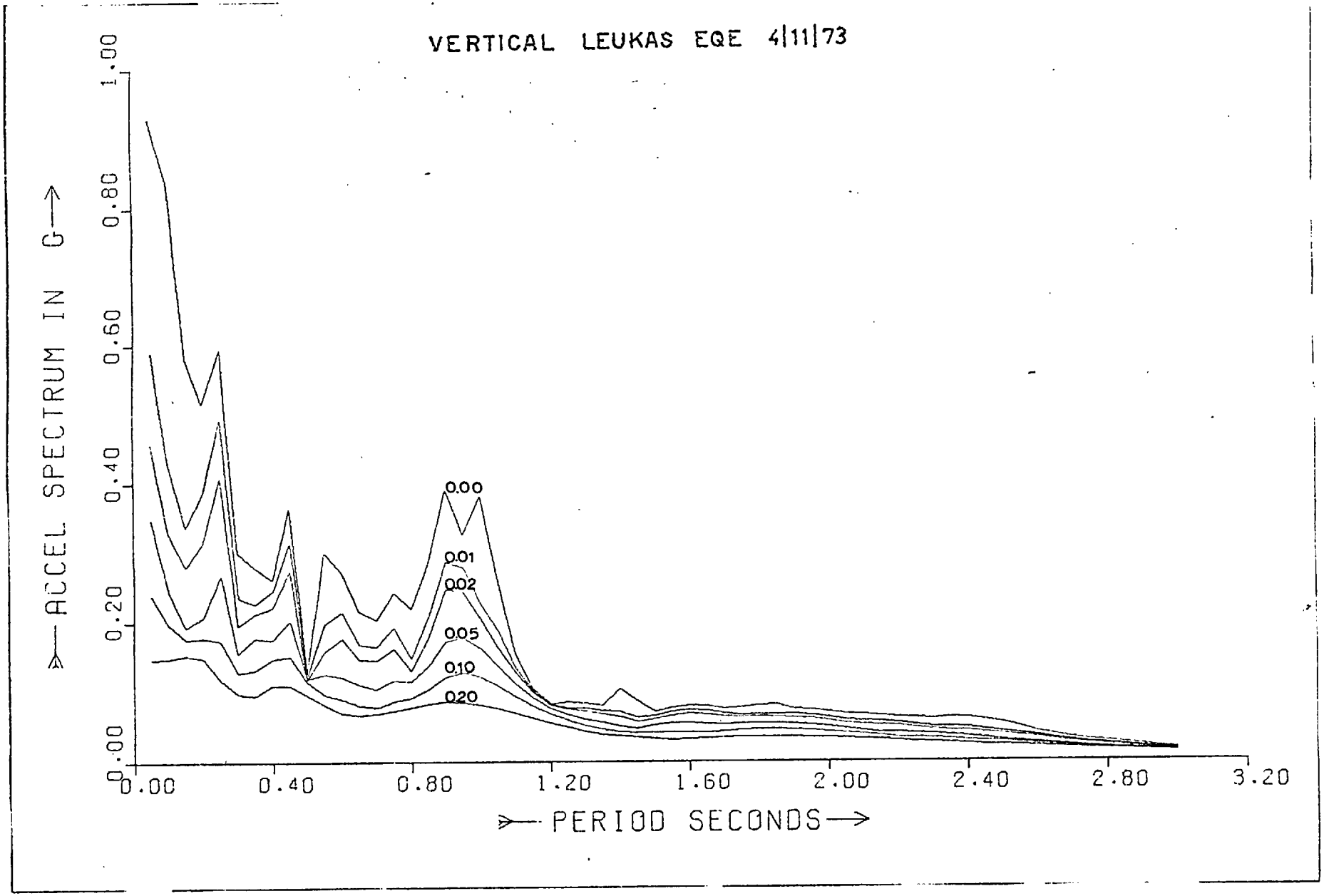

VERTICAL LEUKAS EQE 4|11|73
ACCEL SPECTRUM IN G
PERIOD SECONDS
0.00
0.20
0.40
0.60
0.80
1.00
0.00
0.40
0.80
1.20
1.60
2.00
2.40
2.80
3.20
0.00
0.01
0.02
0.05
0.10
0.20

Fig 7.34

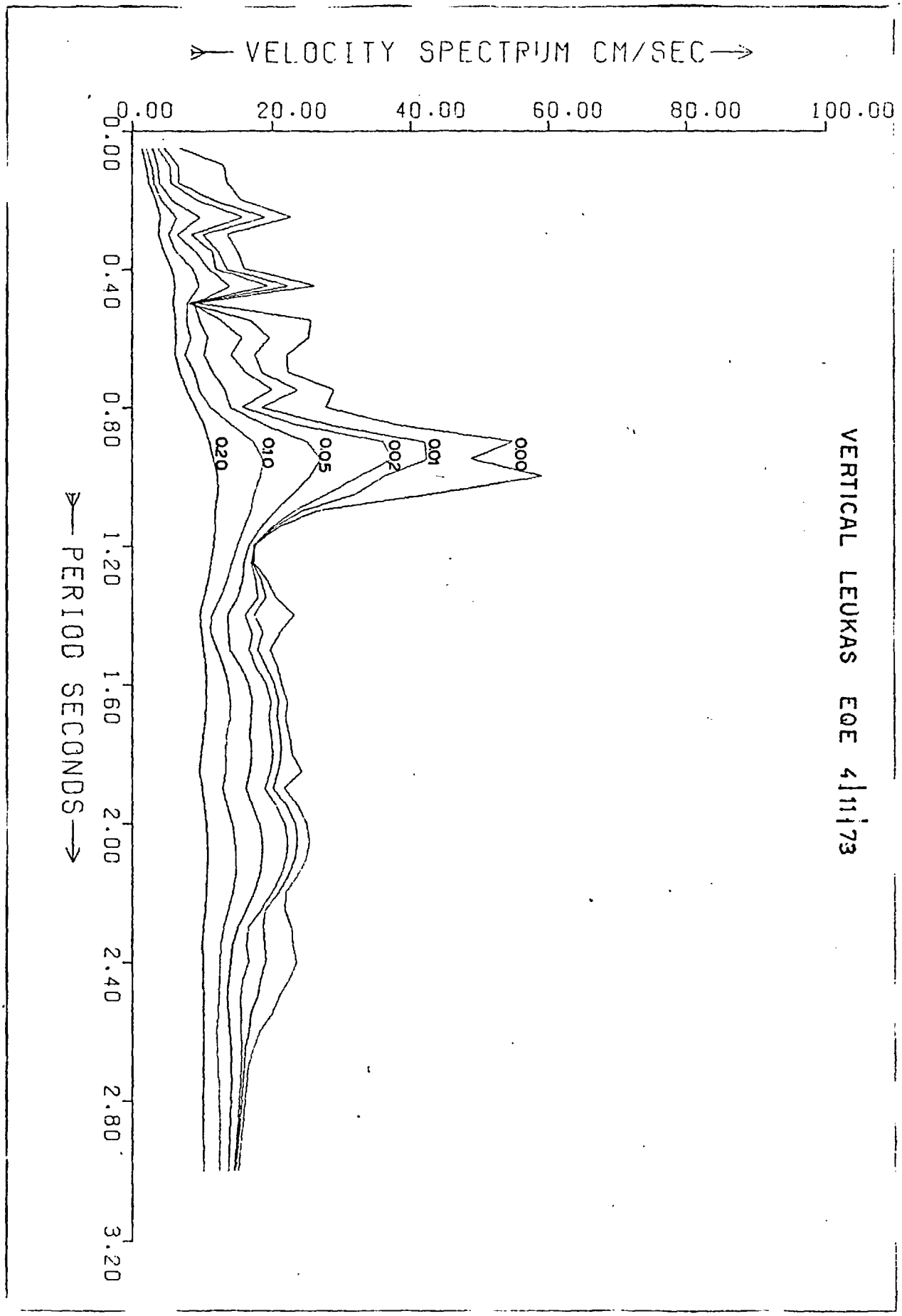

VELOCITY SPECTRUM CM/SEC
0.00
20.00
40.00
60.00
80.00
100.00
0.00
0.40
0.80
1.20
1.60
2.00
2.40
2.80
3.20
PERIOD SECONDS
020
010
005
002
001
000
VERTICAL LEUKAS EQE 4|11|73

Fig I.35

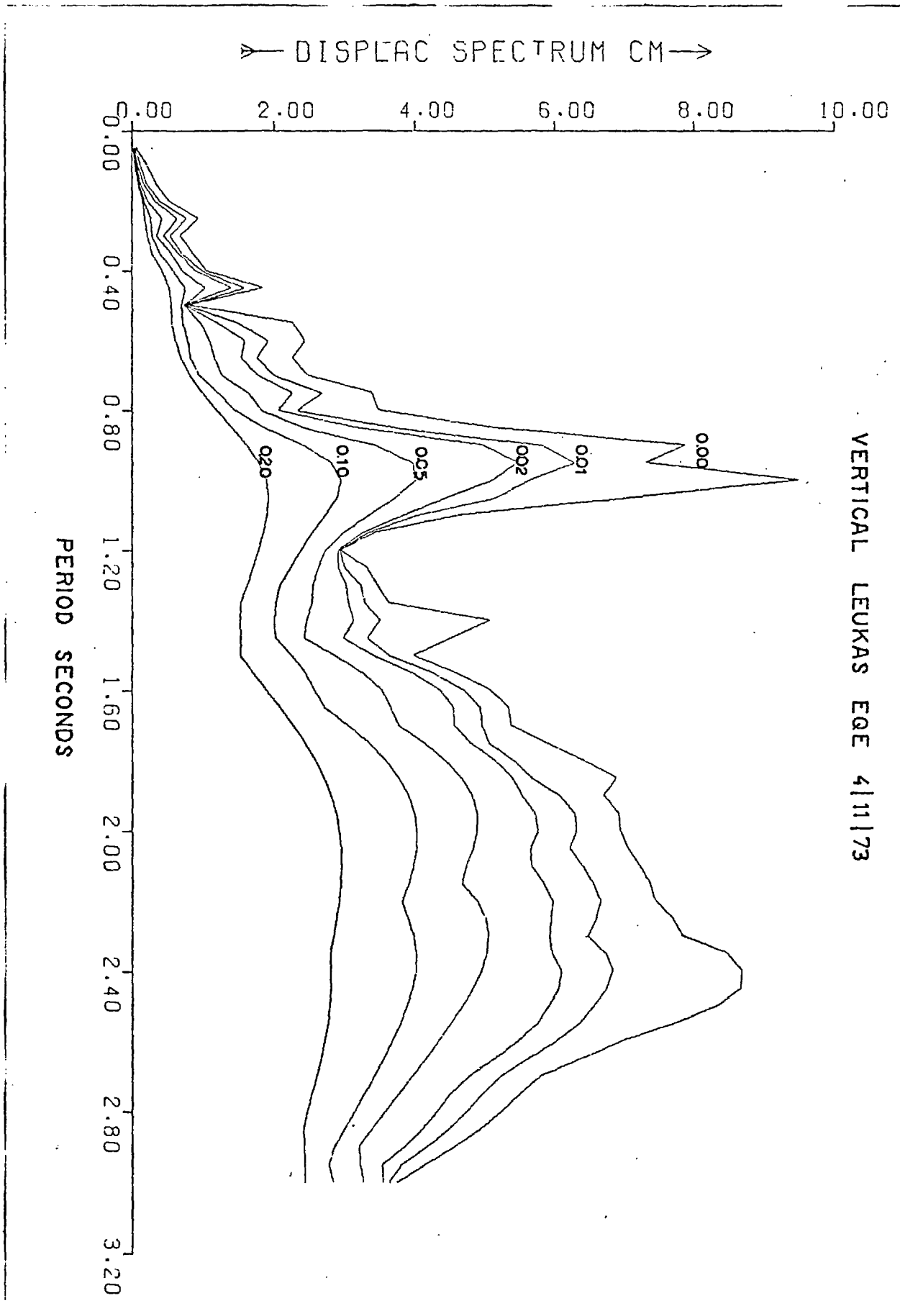

DISPLAC SPECTRUM CM
0.00
2.00
4.00
6.00
8.00
10.00
0.00
0.40
0.80
1.20
1.60
2.00
2.40
2.80
3.20
PERIOD SECONDS
0.20
0.10
0.05
0.02
0.01
0.00
VERTICAL LEUKAS EQE 4|11|73

Fig I.36

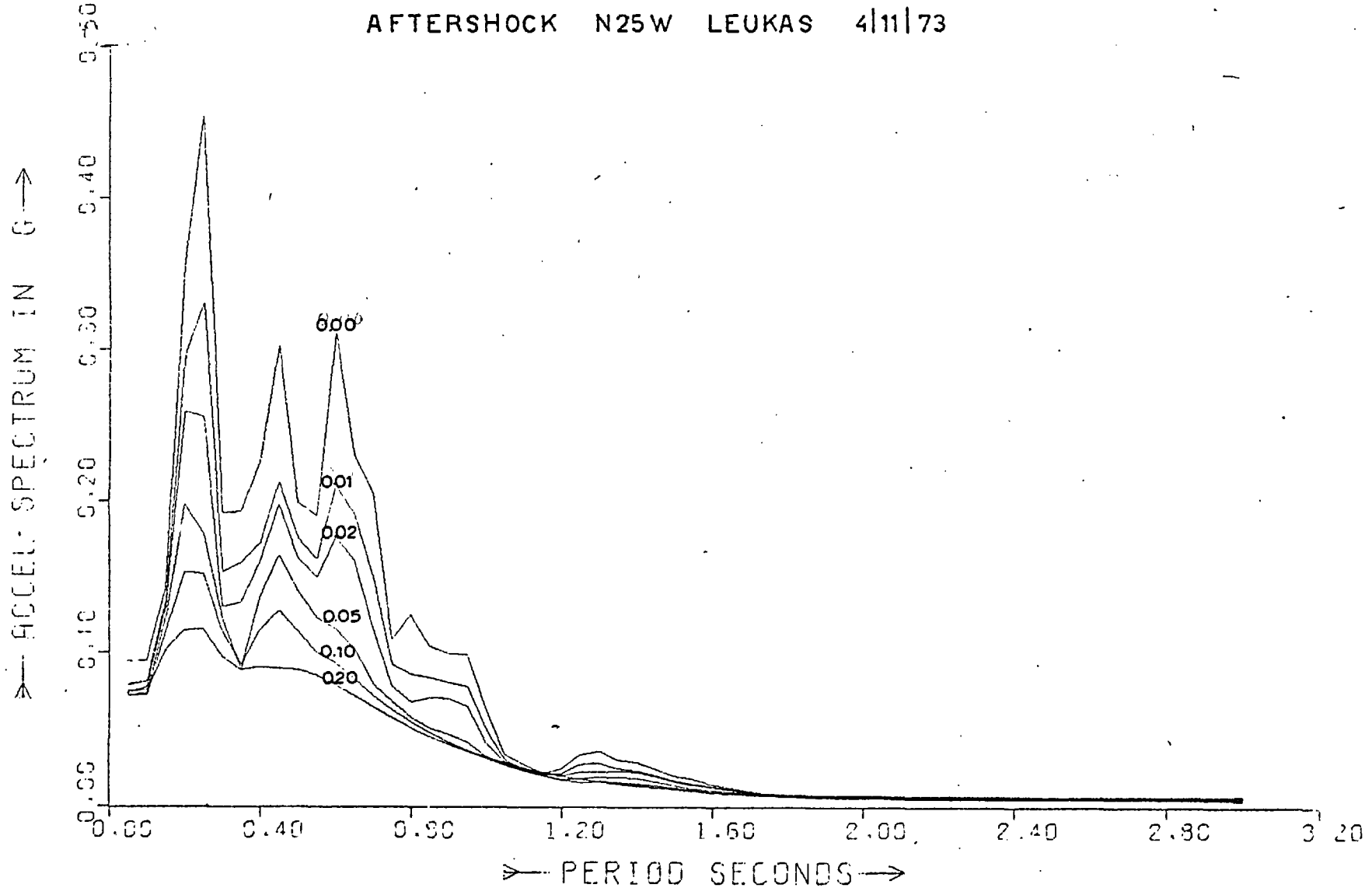

AFTERSHOCK N25W LEUKAS 4|11|73
ACCEL. SPECTRUM IN G
0.00
0.10
0.20
0.30
0.40
0.50
0.00
0.40
0.80
1.20
1.60
2.00
2.40
2.80
3.20
PERIOD SECONDS
0.00
0.01
0.02
0.05
0.10
0.20

Fig I.37

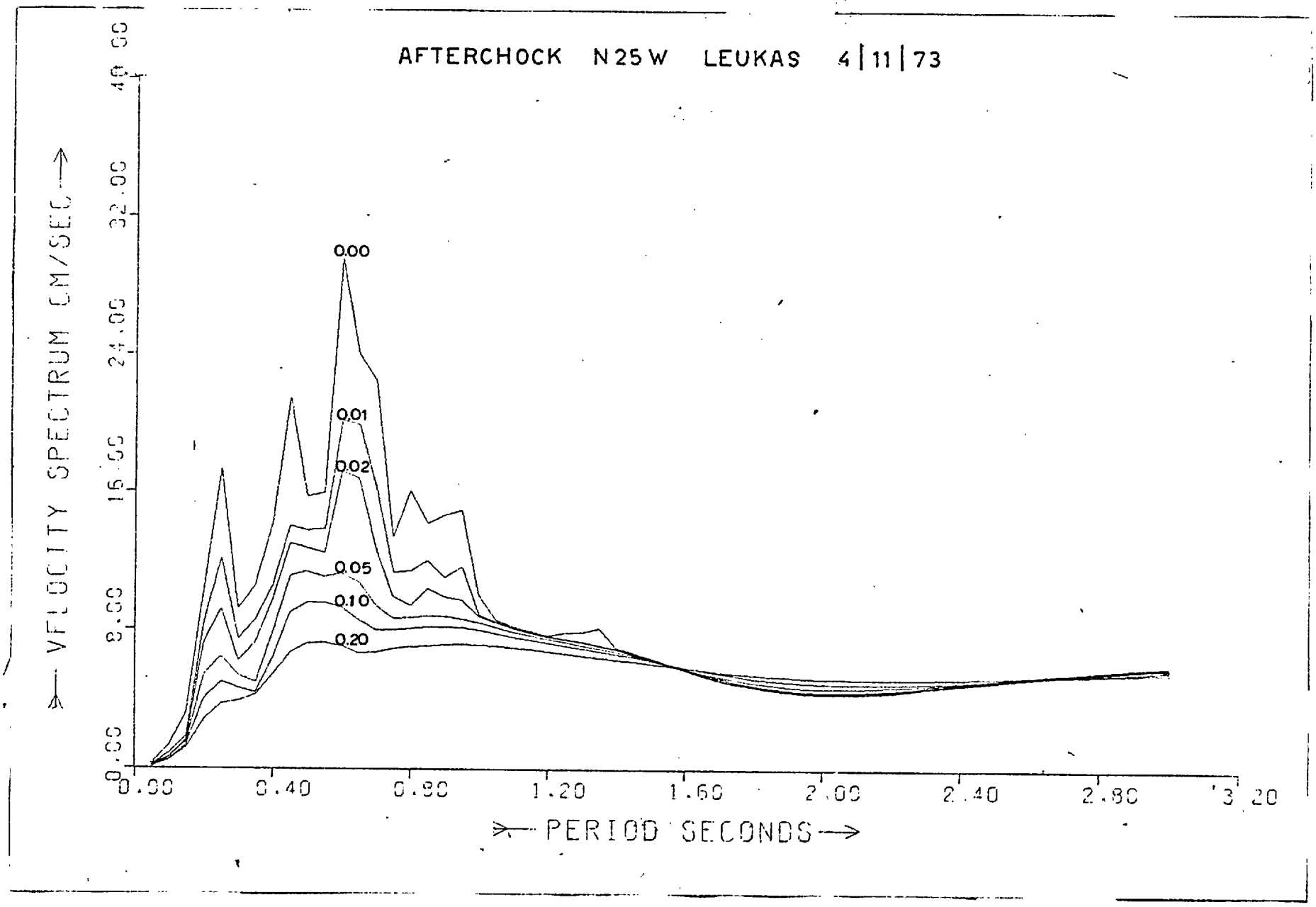

AFTERCHOCK N25W LEUKAS 4|11|73
VELOCITY SPECTRUM CM/SEC
0.00
8.00
16.00
24.00
32.00
40.00
0.00
0.40
0.80
1.20
1.60
2.00
2.40
2.80
3.20
PERIOD SECONDS
0.00
0.01
0.02
0.05
0.10
0.20

Fig I.38

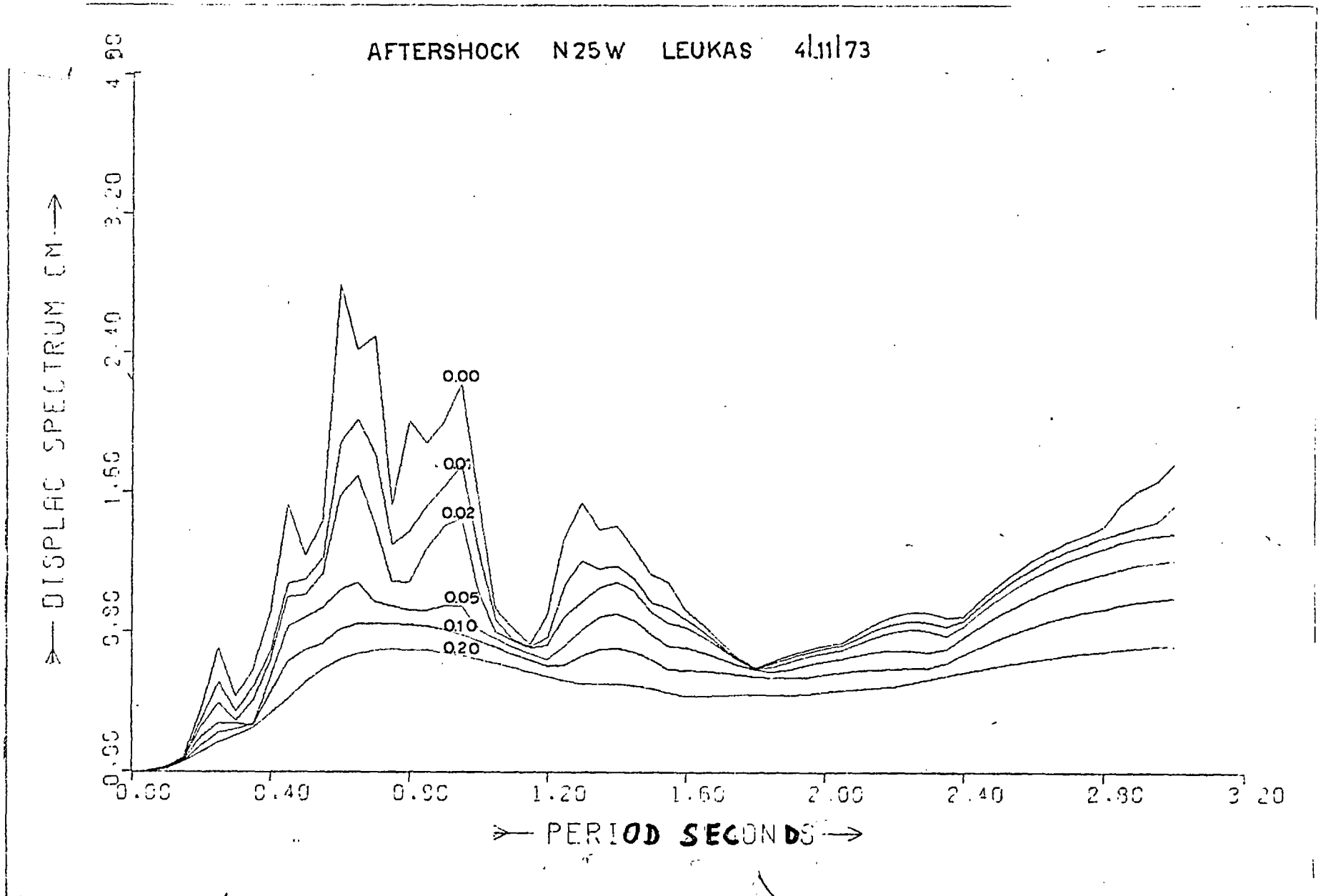

AFTERSHOCK N25W LEUKAS 4.11.73
DISPLAC SPECTRUM CM
PERIOD SECONDS
0.00
0.01
0.02
0.05
0.10
0.20
0.00
0.40
0.80
1.20
1.60
2.00
2.40
2.80
3.20
0.80
1.60
2.40
3.20
4.00

Fig I.39

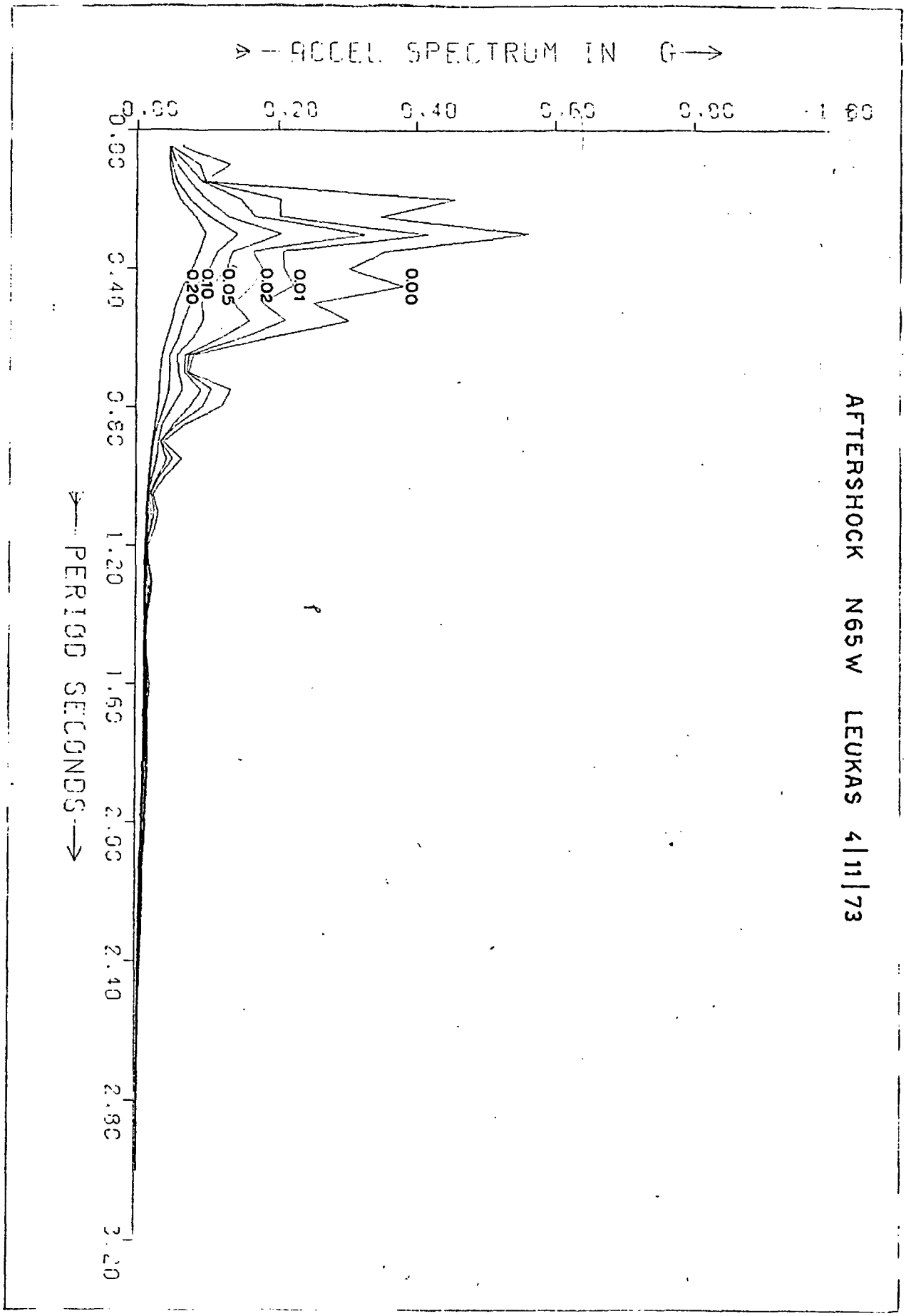

ACCEL SPECTRUM IN G
0.00
0.20
0.40
0.60
0.80
1.00
0.00
0.40
0.80
1.20
1.60
2.00
2.40
2.80
3.20
PERIOD SECONDS
0.00
0.01
0.02
0.05
0.10
0.20
AFTERSHOCK N65W LEUKAS 4/11/73

Fig I.40

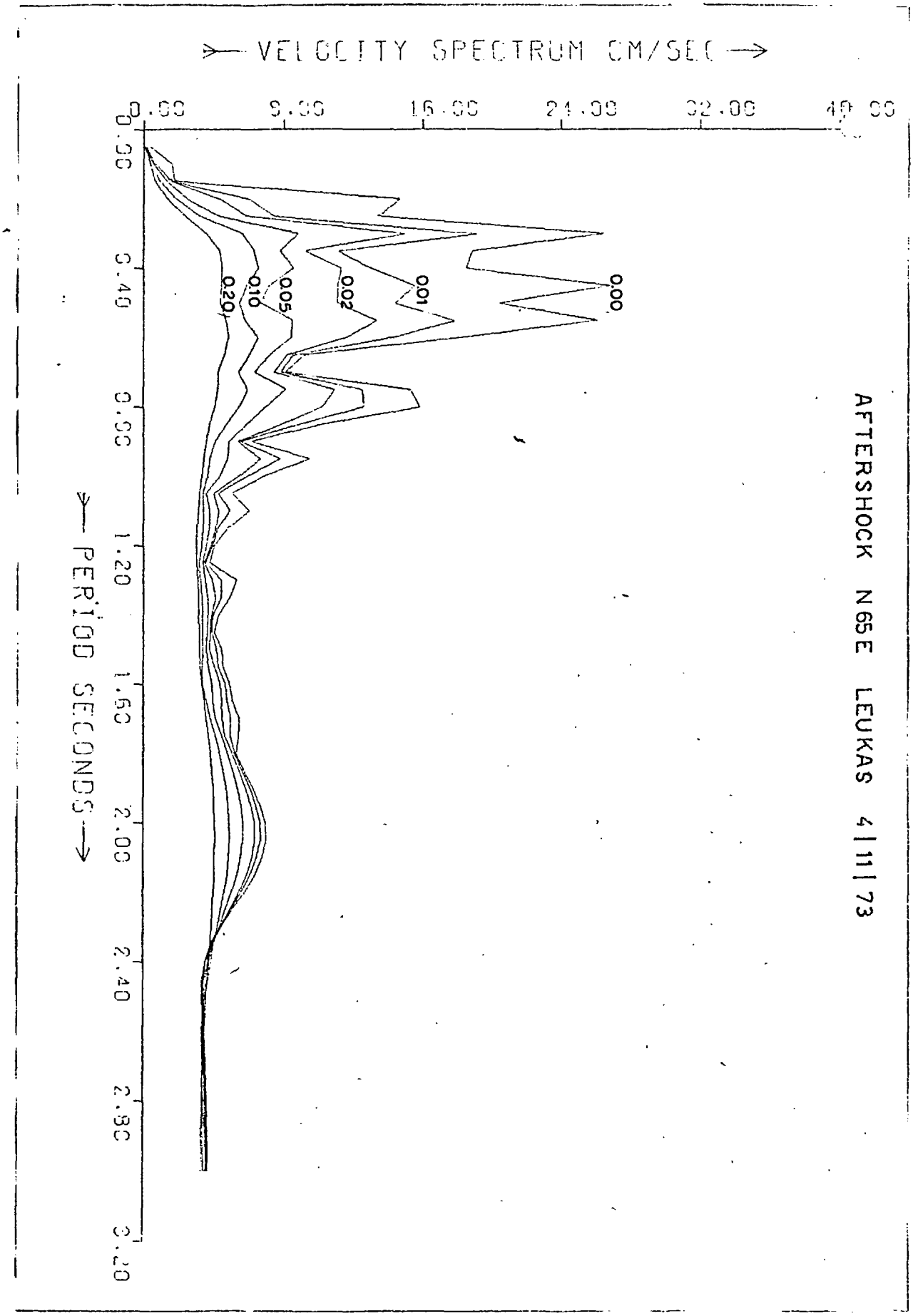

VELOCITY SPECTRUM CM/SEC
0.00
8.00
16.00
24.00
32.00
40.00
0.00
0.40
0.80
1.20
1.60
2.00
2.40
2.80
3.20
PERIOD SECONDS
0.20
0.10
0.05
0.02
0.01
0.00
AFTERSHOCK N65E LEUKAS 4|11|73

Fig I.41

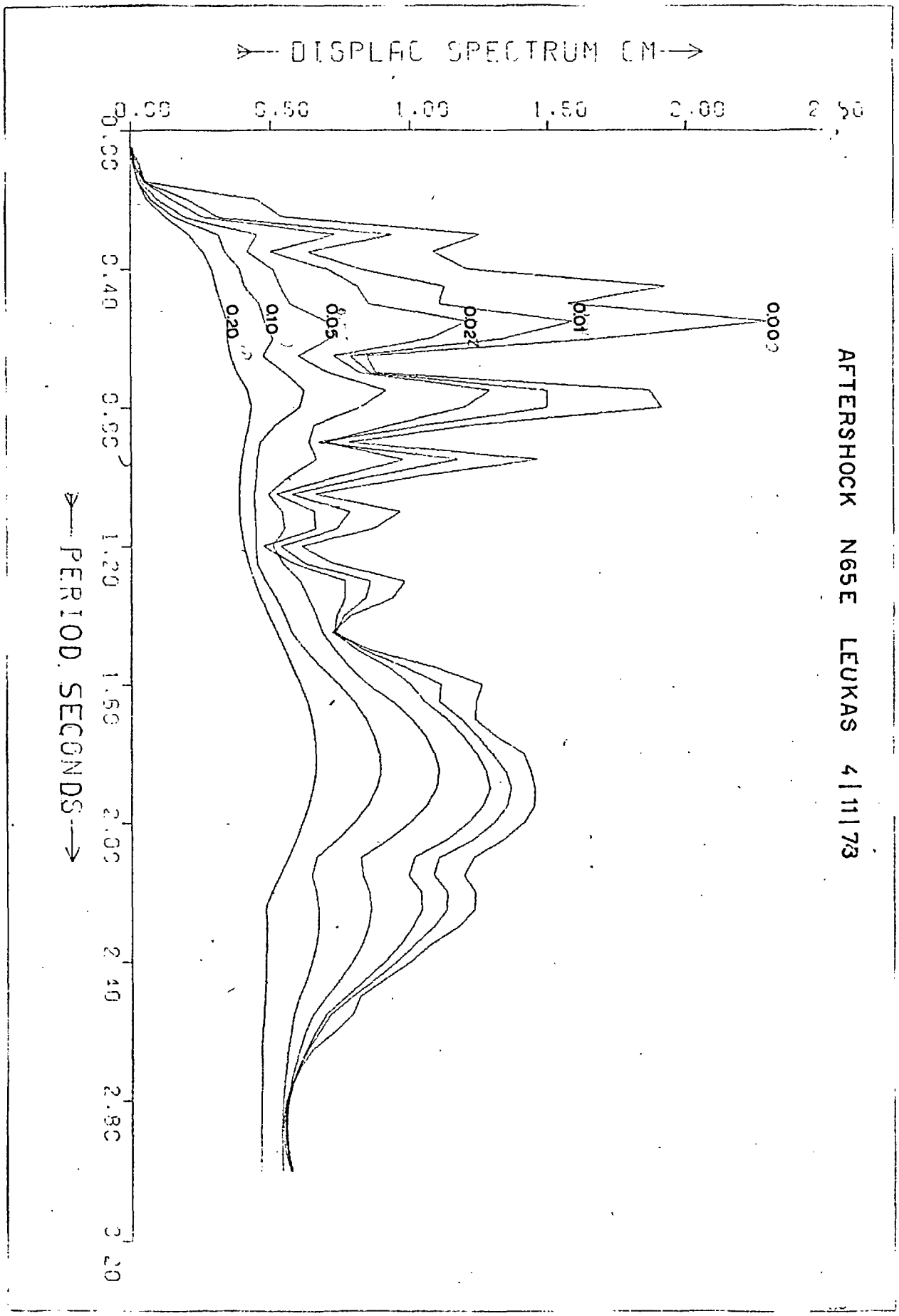

DISPLAC SPECTRUM CM
0.00
0.50
1.00
1.50
2.00
2.50
0.00
0.40
0.80
1.20
1.60
2.00
2.40
2.80
3.20
PERIOD SECONDS
0.20
0.10
0.05
0.02
0.01
0.00
AFTERSHOCK N65E LEUKAS 4 11 73

Fig I.42

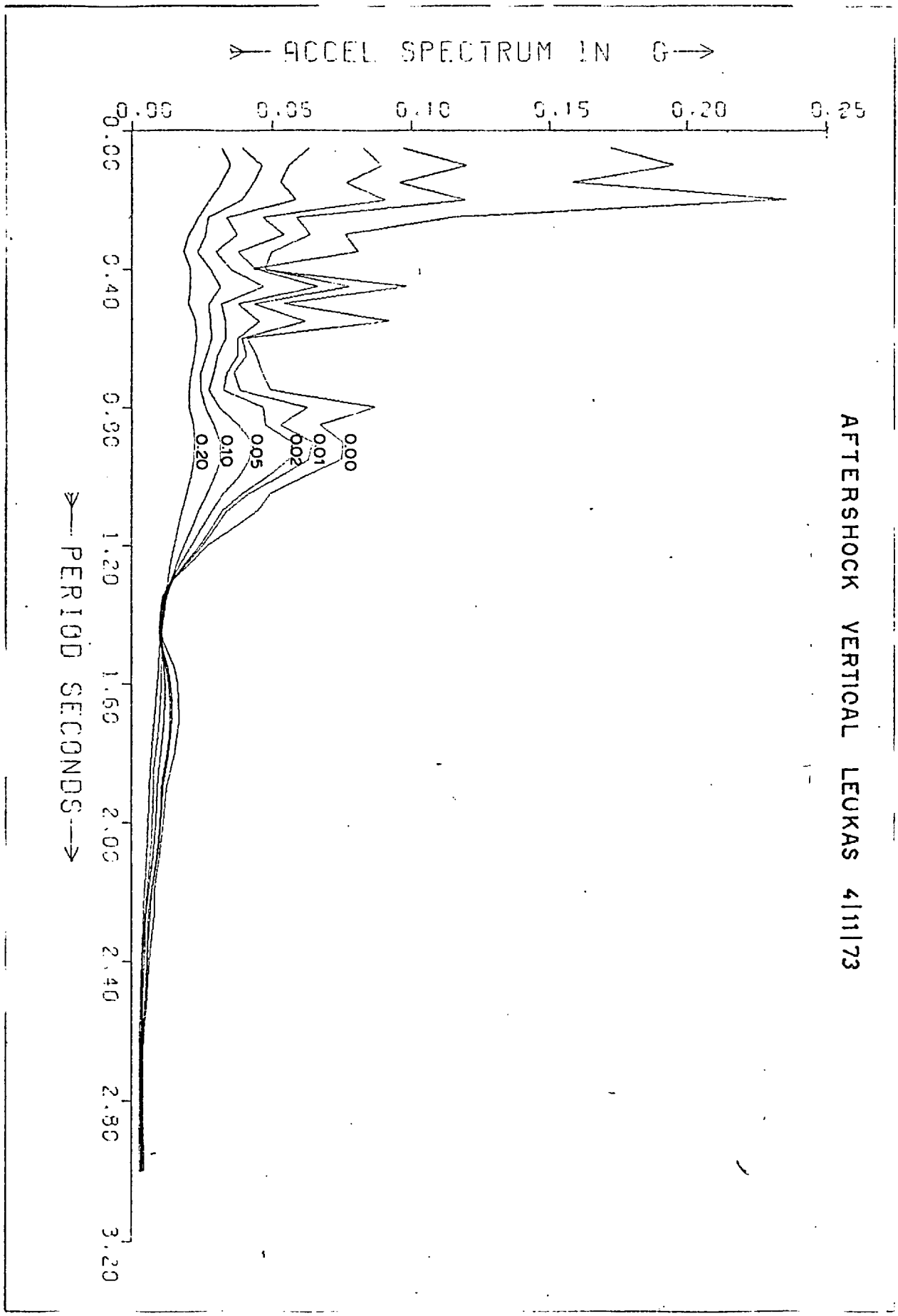

ACCEL SPECTRUM IN G
0.00
0.05
0.10
0.15
0.20
0.25
0.00
0.40
0.80
1.20
1.60
2.00
2.40
2.80
3.20
PERIOD SECONDS
0.20
0.10
0.05
0.02
0.01
0.00
AFTERSHOCK VERTICAL LEUKAS 4|11|73

Fig I.43

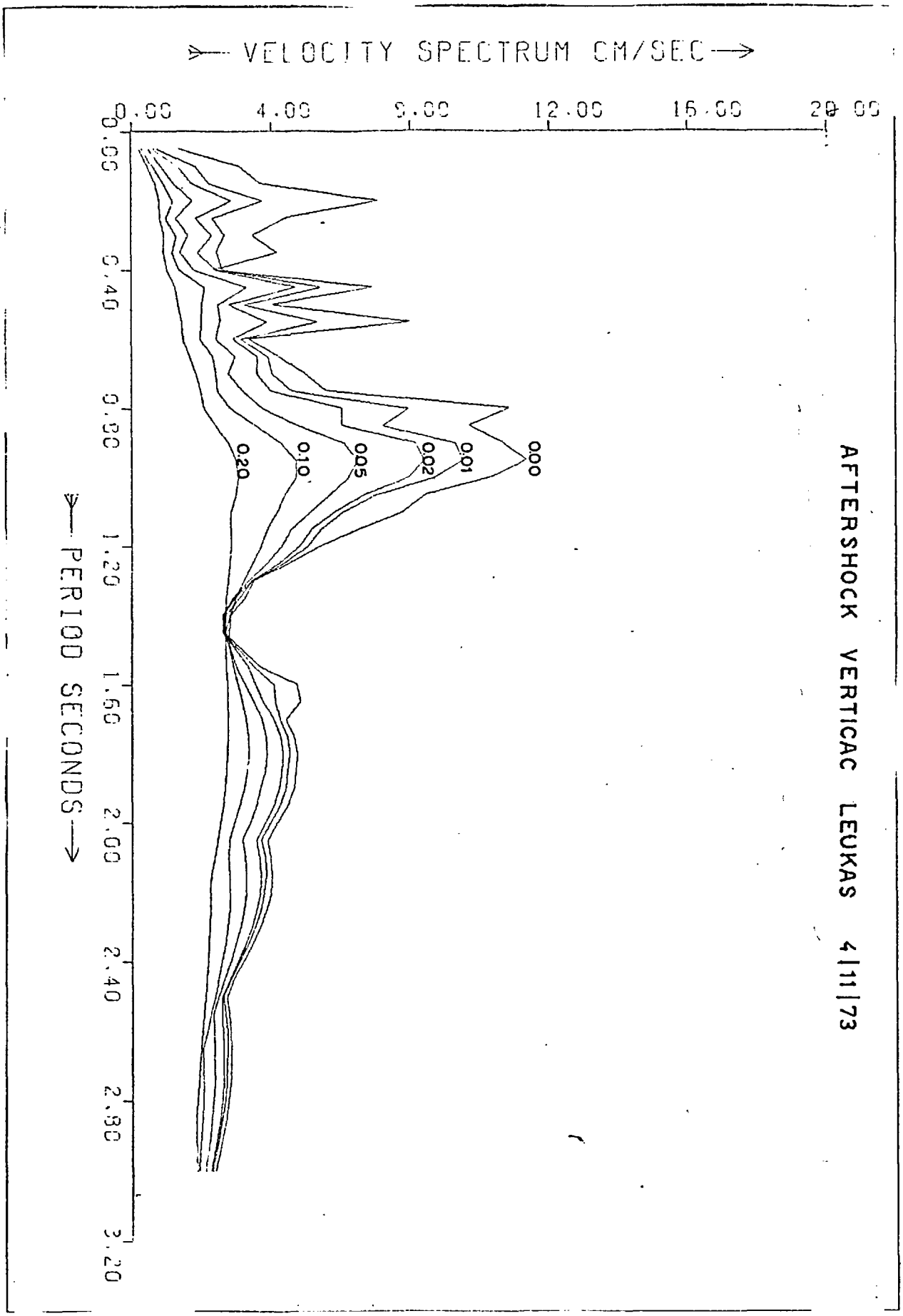

VELOCITY SPECTRUM CM/SEC
0.00
4.00
8.00
12.00
16.00
20.00
PERIOD SECONDS
0.00
0.40
0.80
1.20
1.60
2.00
2.40
2.80
3.20
0.20
0.10
0.05
0.02
0.01
0.00
AFTERSHOCK VERTICAC LEUKAS 4|11|73

Fig I.44

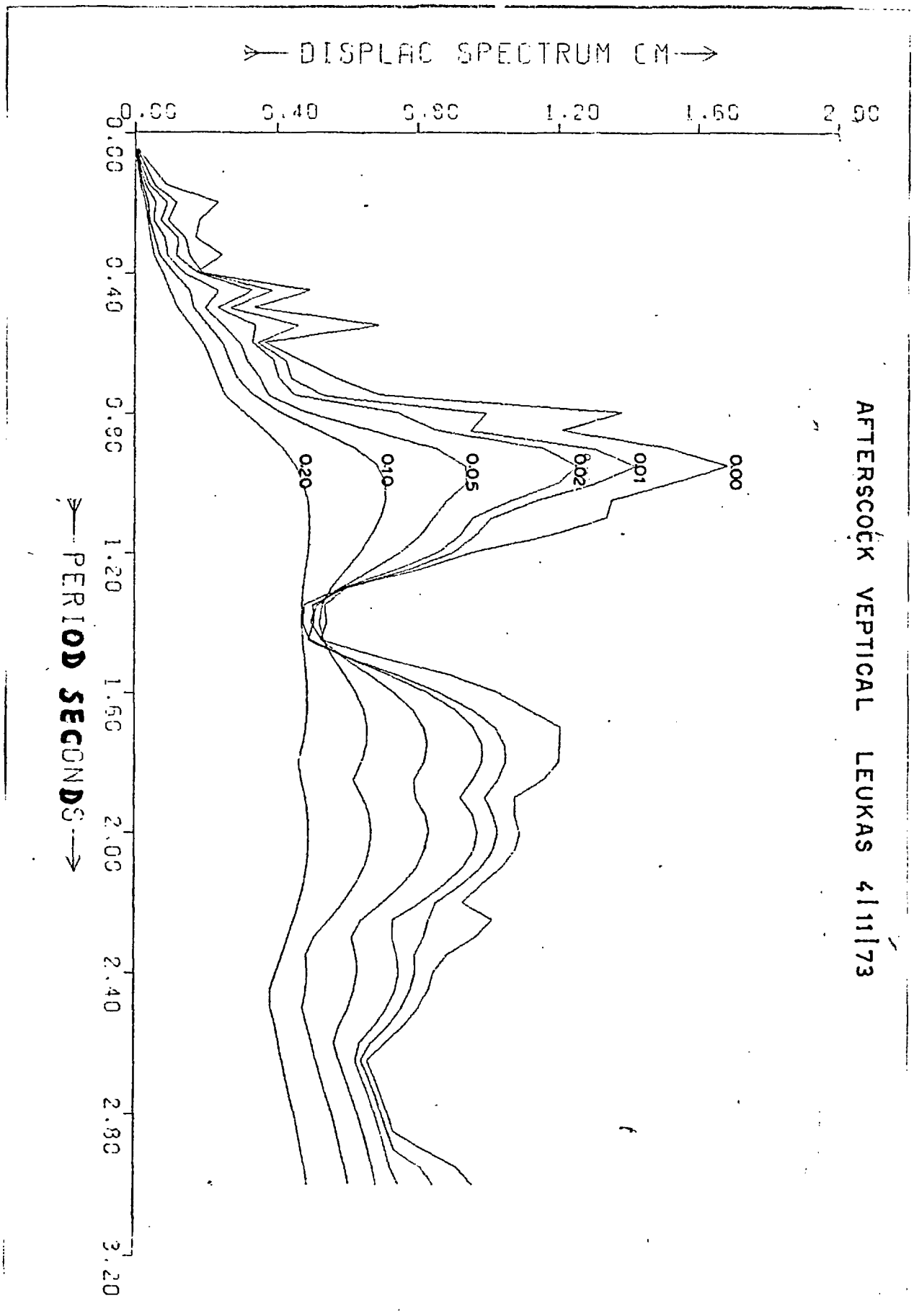

DISPLAC SPECTRUM CM
0.00
0.40
0.80
1.20
1.60
2.00
PERIOD SECONDS
0.00
0.40
0.80
1.20
1.60
2.00
2.40
2.80
3.20
0.20
0.10
0.05
0.02
0.01
0.00
AFTERSCOCK VEPTICAL LEUKAS 4/11/73

Fig 3.45



CITY OF LEUKAS
Fig B. 1

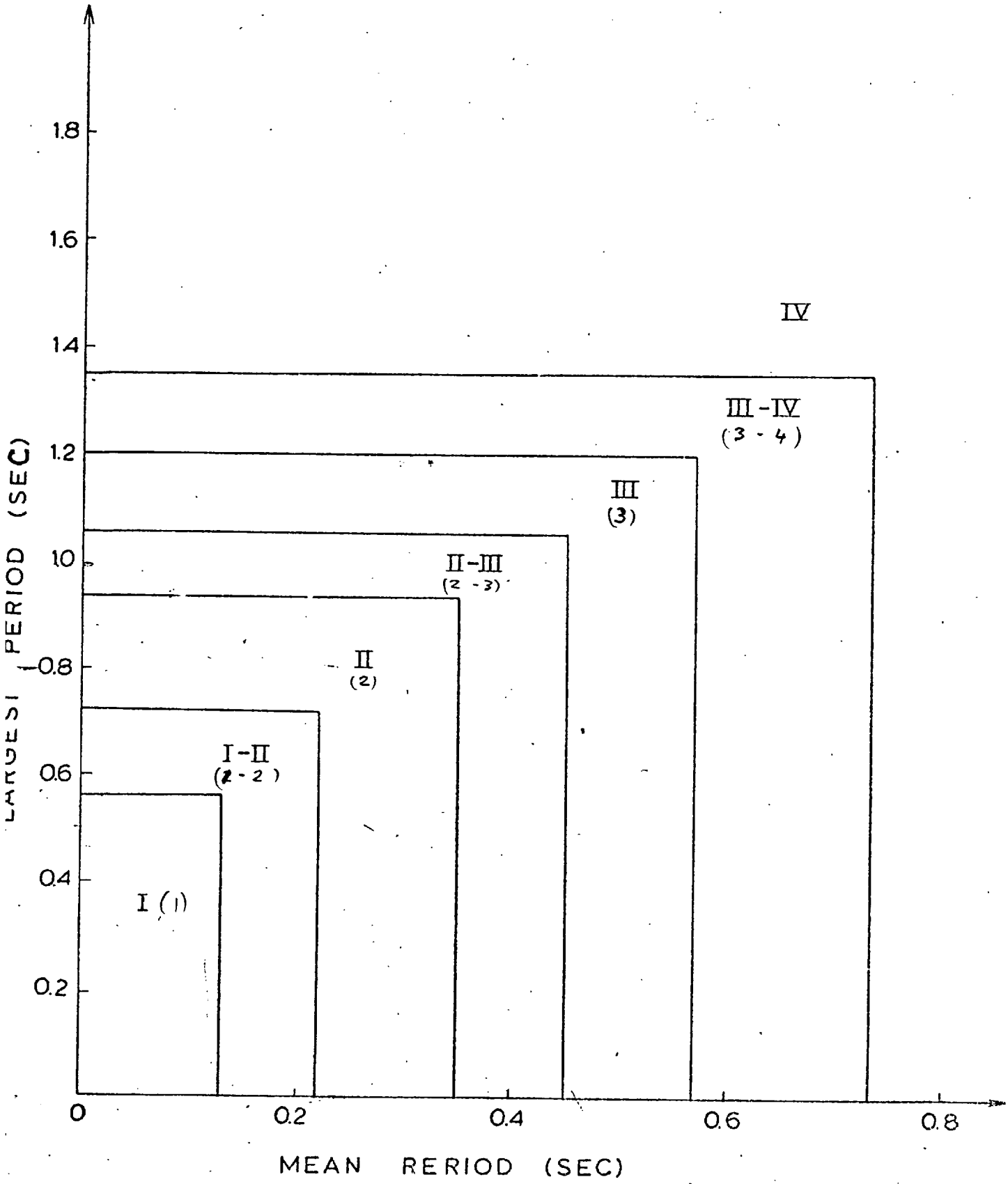

1.8
1.6
1.4
1.2
1.0
0.8
0.6
0.4
0.2
0
0.2
0.4
0.6
0.8
LARGEST PERIOD (SEC)
MEAN RERIOD (SEC)
I (1)
I-II (1-2)
II (2)
II-III (2-3)
III (3)
III-IV (3-4)
IV

FIG II. 2

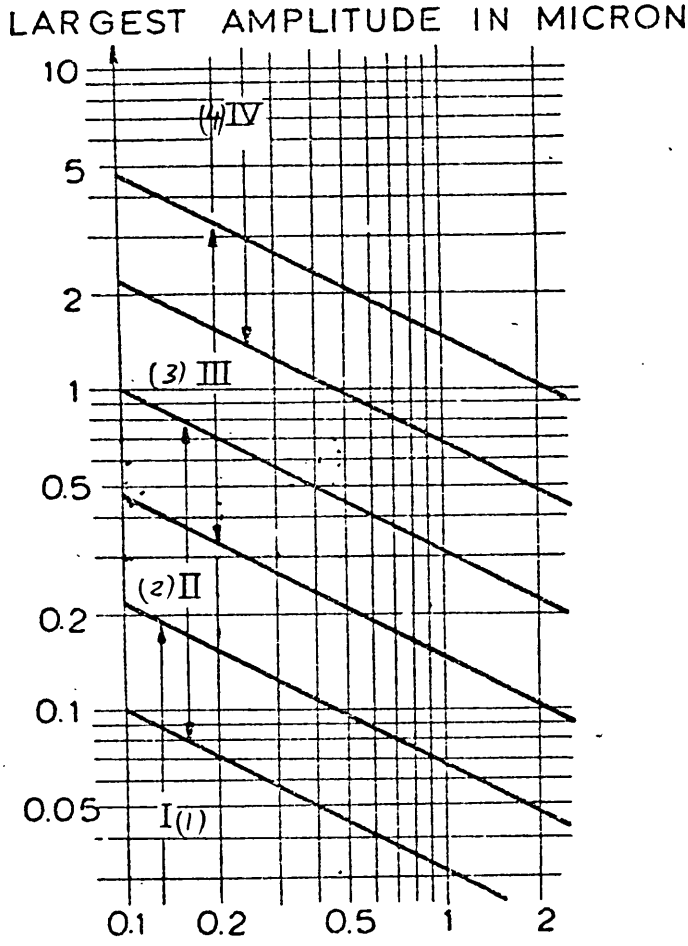
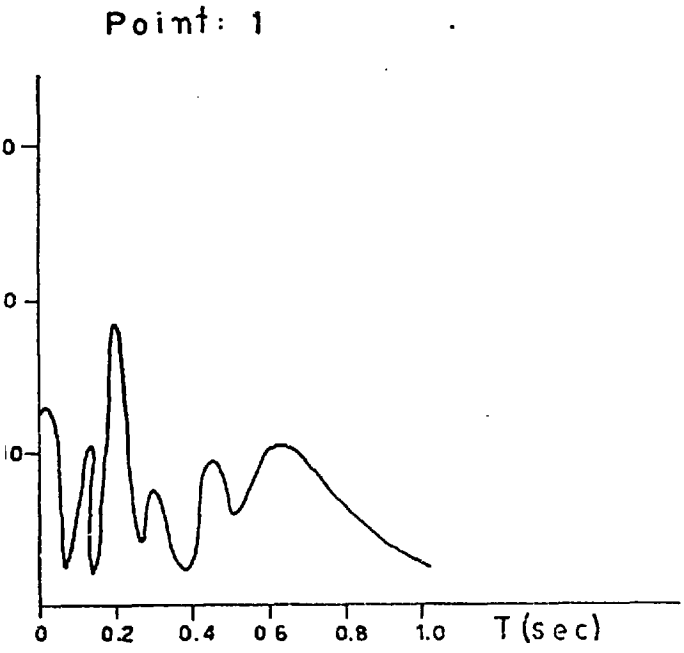
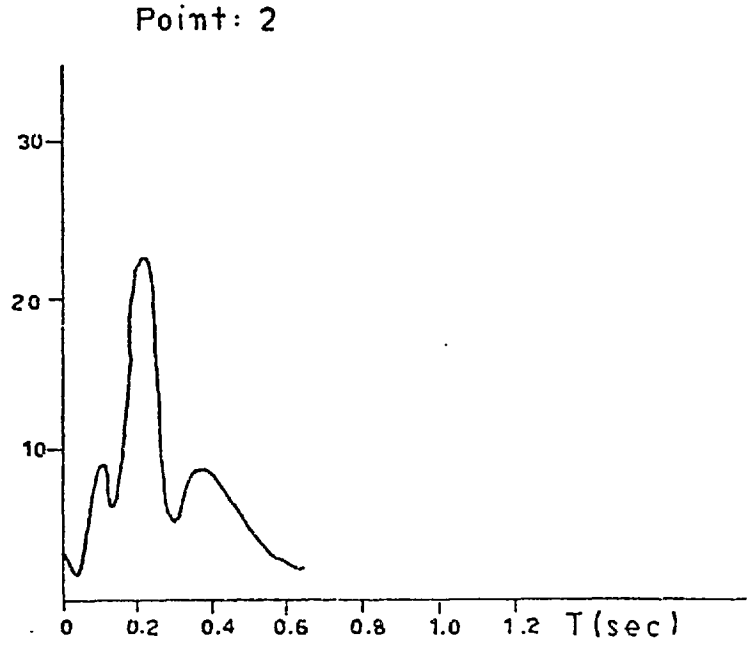
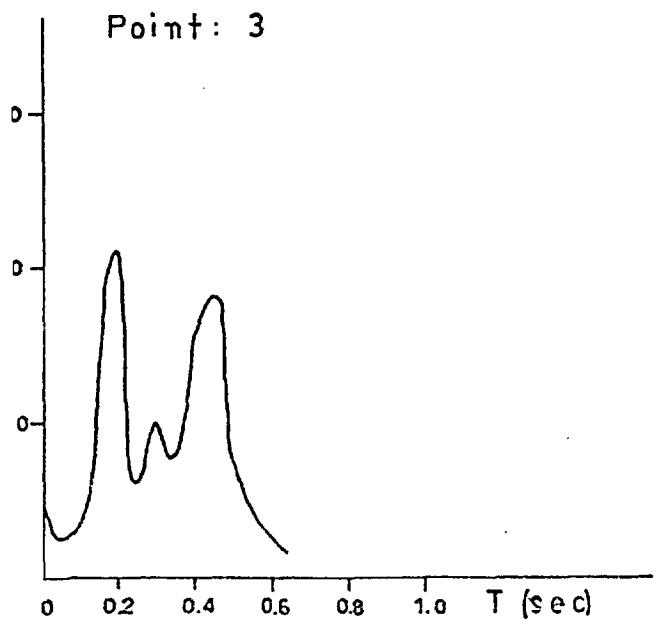

LARGEST AMPLITUDE IN MICRON
10
5
2
1
0.5
0.2
0.1
0.05
(4) IV
(3) III
(2) II
I (1)
0.1
0.2
0.5
1
2
PREDOMINANT PERIOD IN SEC

FIG II. 3


Point: 1
0
0
10
0 0.2 0.4 0.6 0.8 1.0 T (sec)


Point: 2
30
20
10
0 0.2 0.4 0.6 0.8 1.0 1.2 T (sec)


Point: 3
0
0
0
0 0.2 0.4 0.6 0.8 1.0 T (sec)

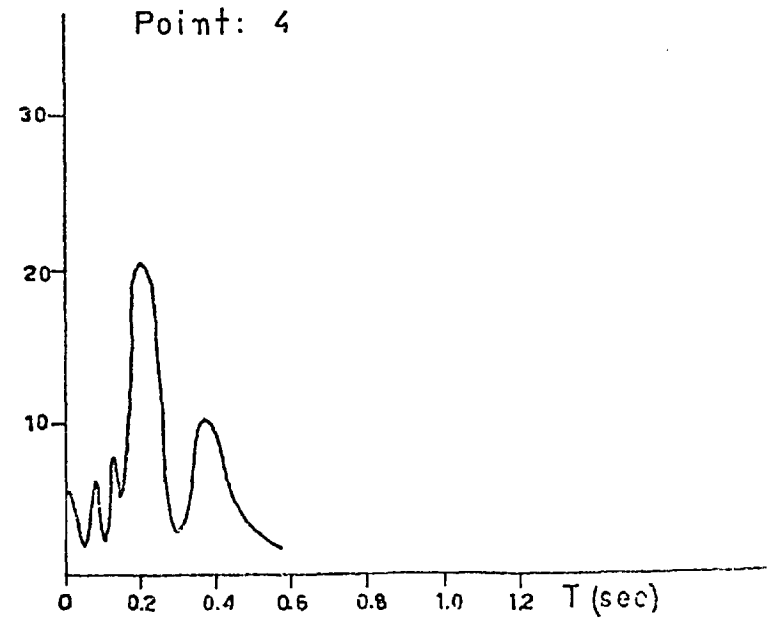
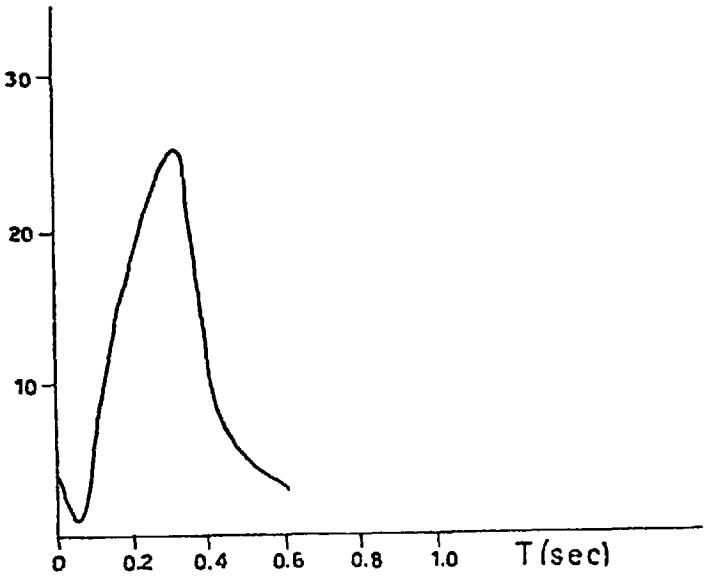
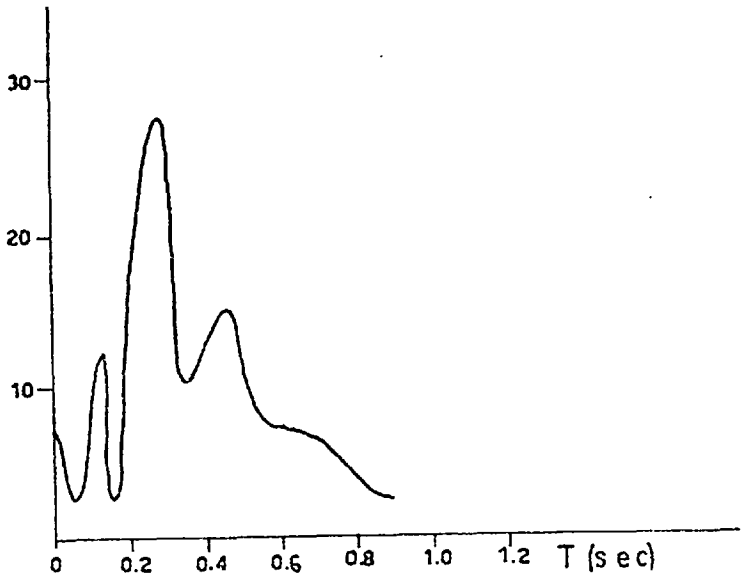

Point: 4
30
20
10
0 0.2 0.4 0.6 0.8 1.0 1.2 T (sec)

FIG 4

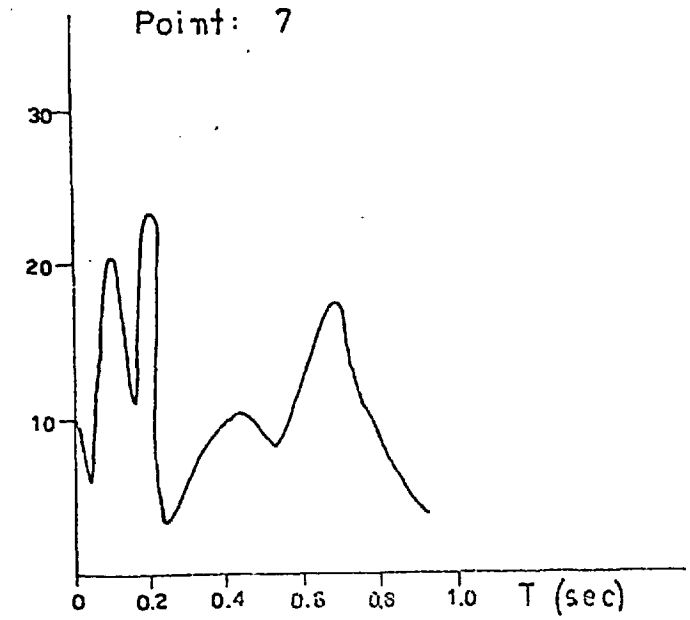
Point : 5



Point: 6



Point: 7



Point: 8

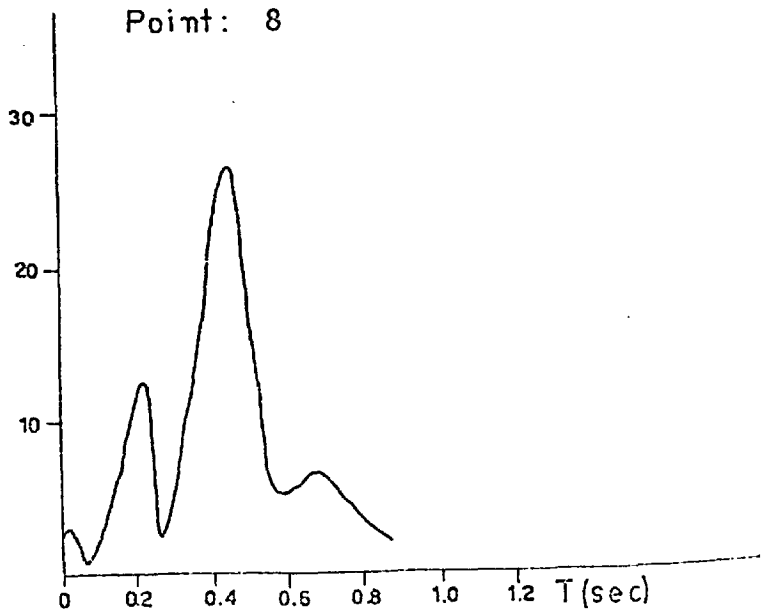
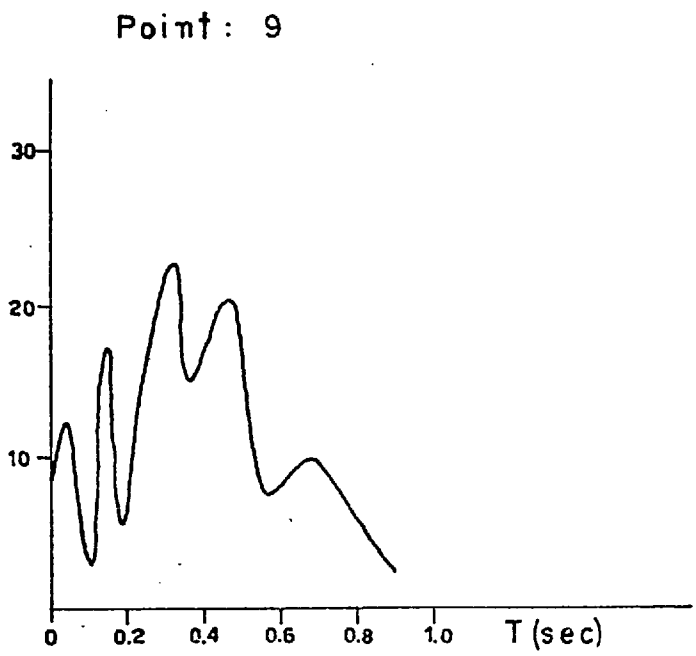
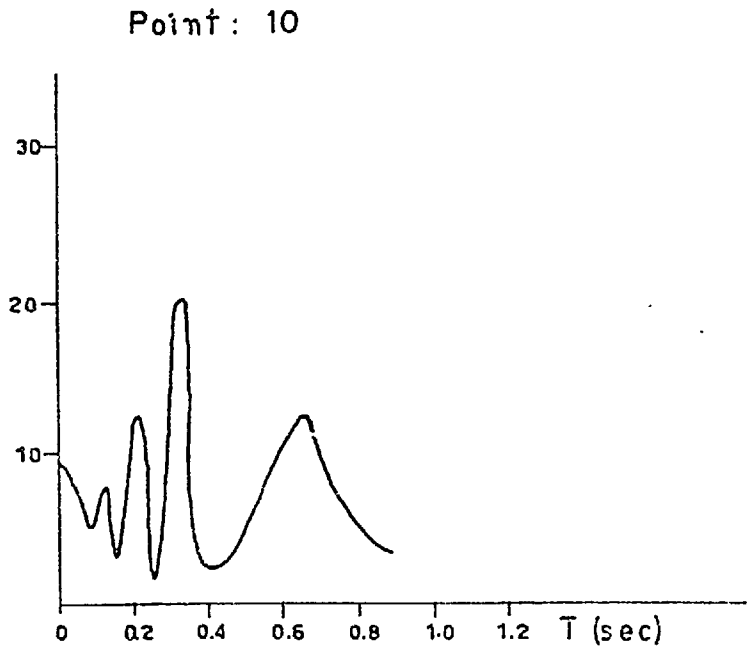
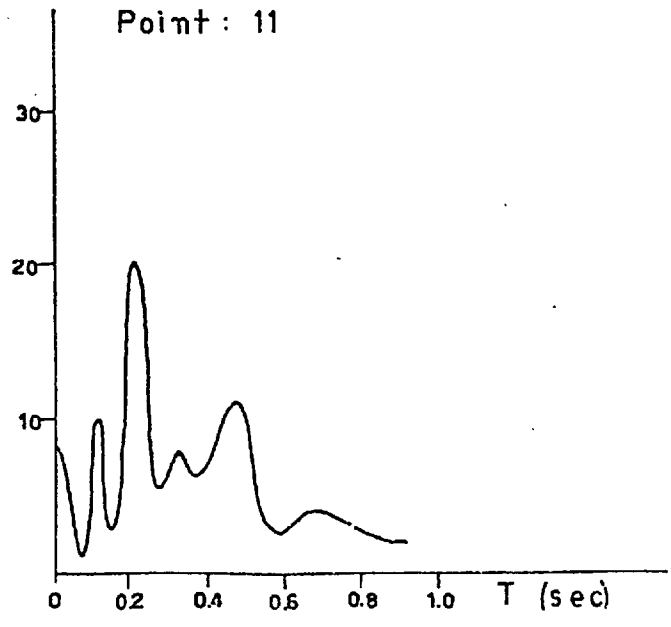


FIG II.5


Point : 9
30
20
10
0
0.2
0.4
0.6
0.8
1.0
T (sec)


Point : 10
30
20
10
0
0.2
0.4
0.6
0.8
1.0
1.2
T (sec)


Point : 11
30
20
10
0
0.2
0.4
0.6
0.8
1.0
T (sec)

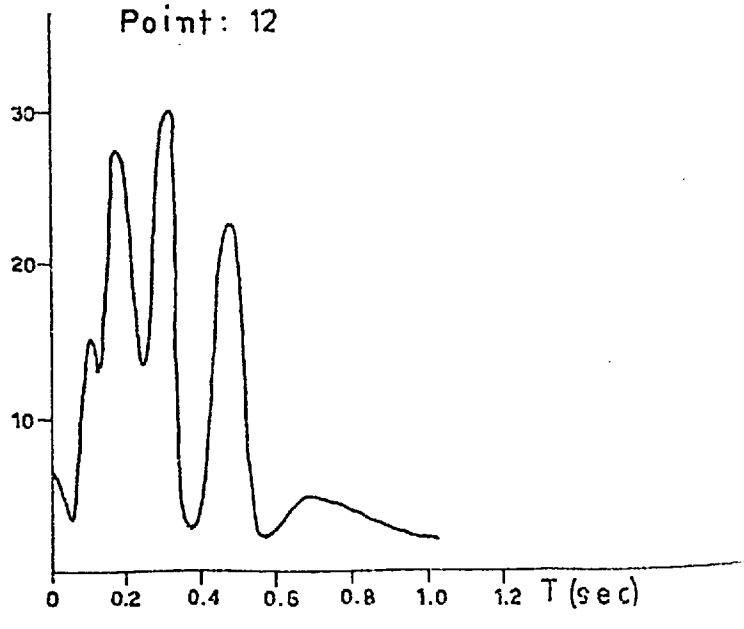
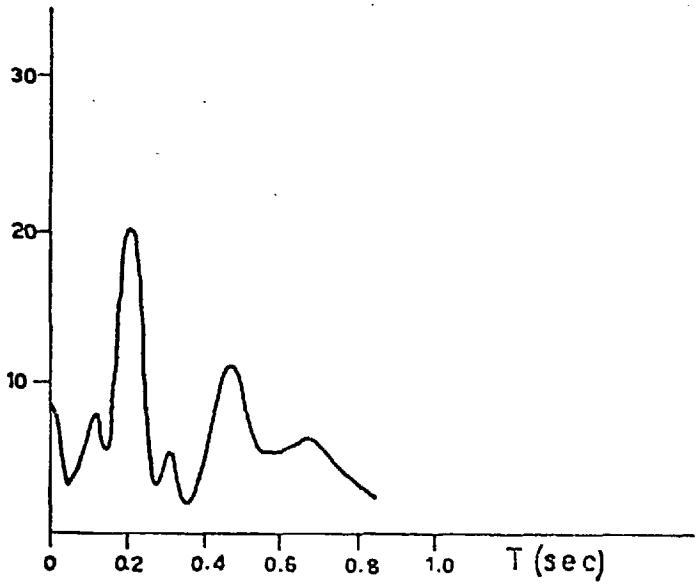
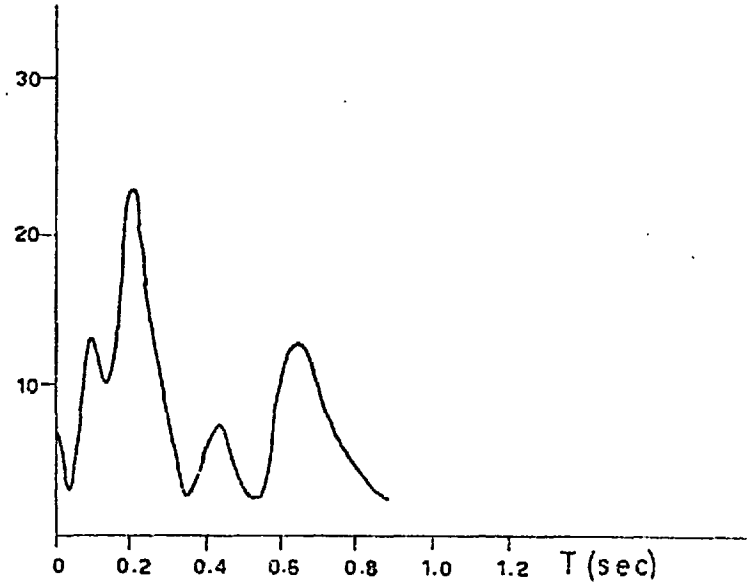

Point : 12
30
20
10
0
0.2
0.4
0.6
0.8
1.0
1.2
T (sec)

FIG.A.6

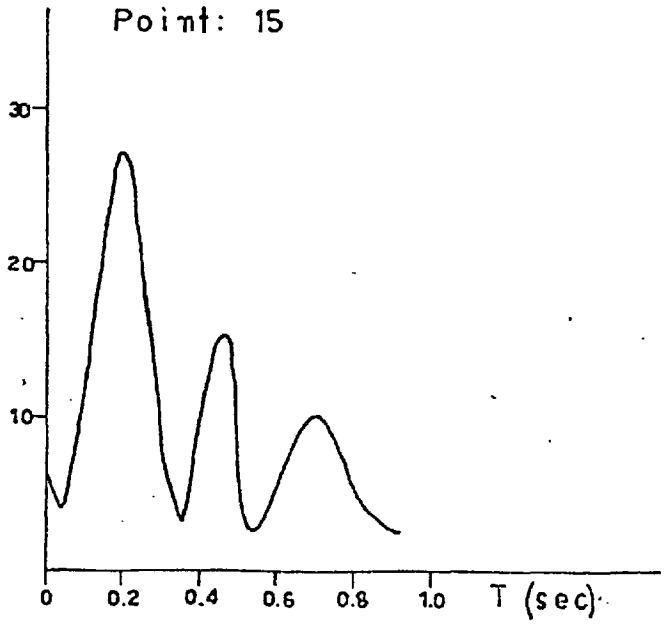
Point: 13



Point: 14



Point: 15



Point: 16

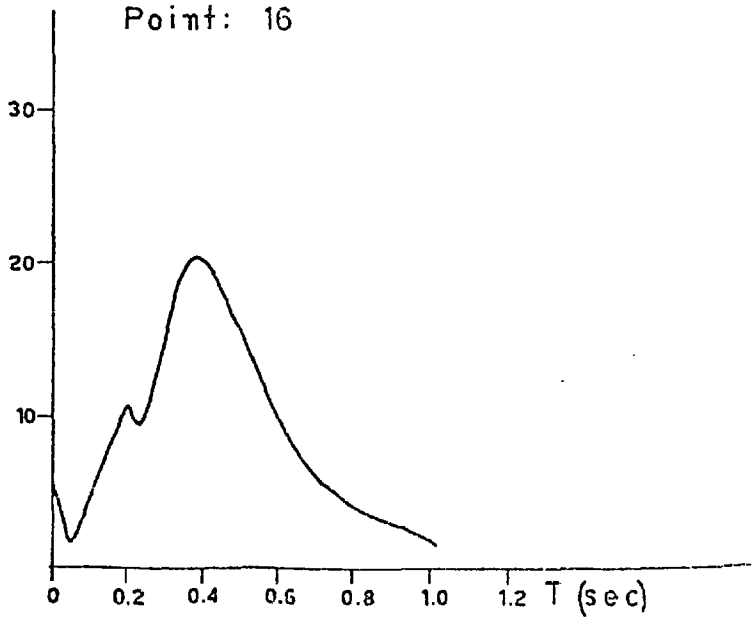
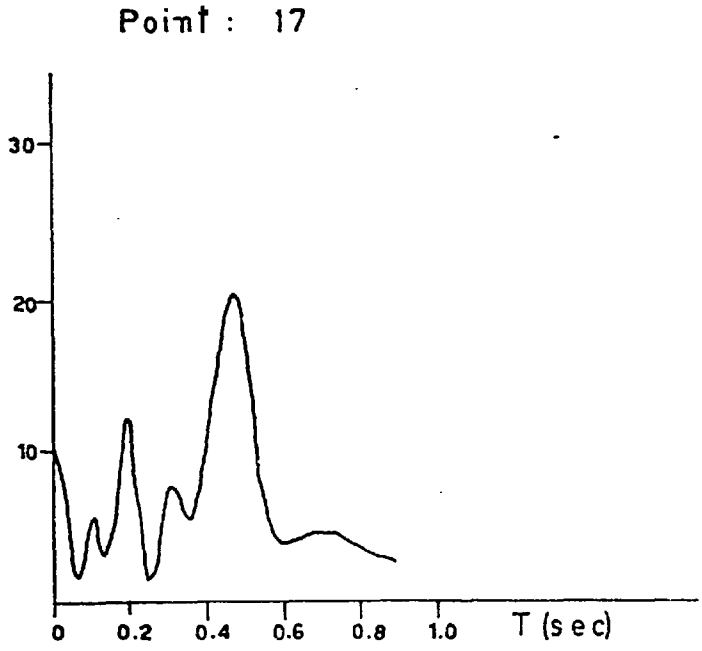
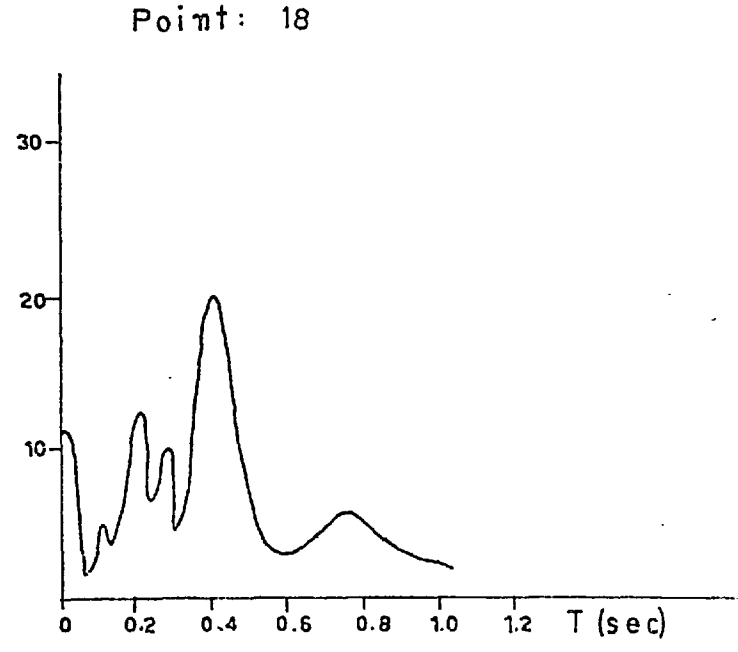
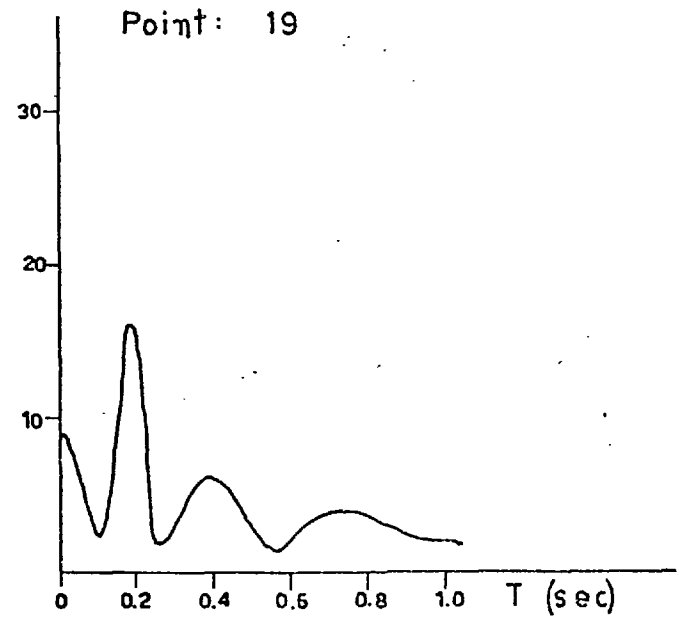


FIG. 3.7


Point : 17
30
20
10
0
0.2
0.4
0.6
0.8
1.0
T (sec)


Point : 18
30
20
10
0
0.2
0.4
0.6
0.8
1.0
1.2
T (sec)


Point : 19
30
20
10
0
0.2
0.4
0.6
0.8
1.0
T (sec)

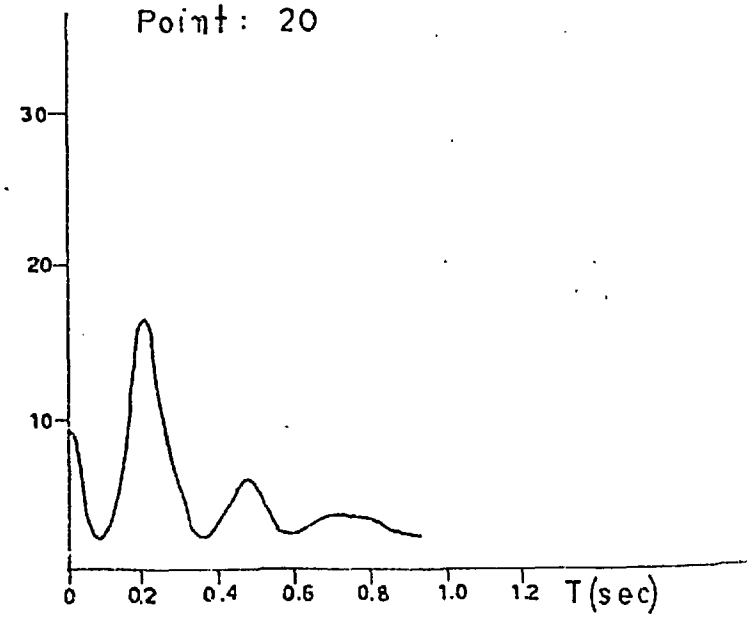
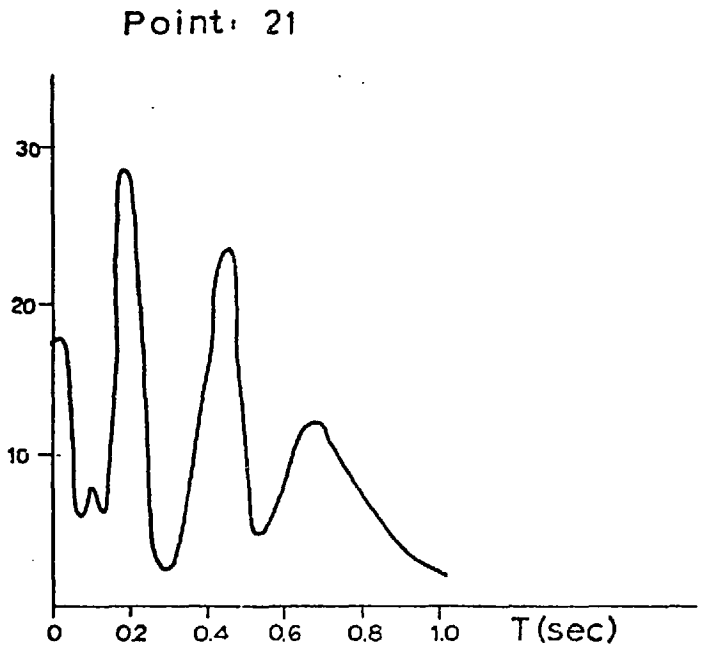
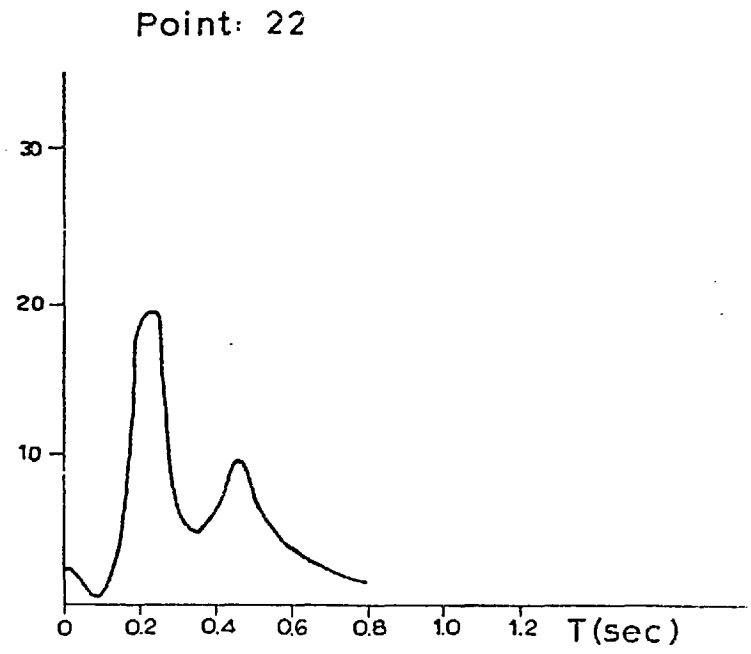
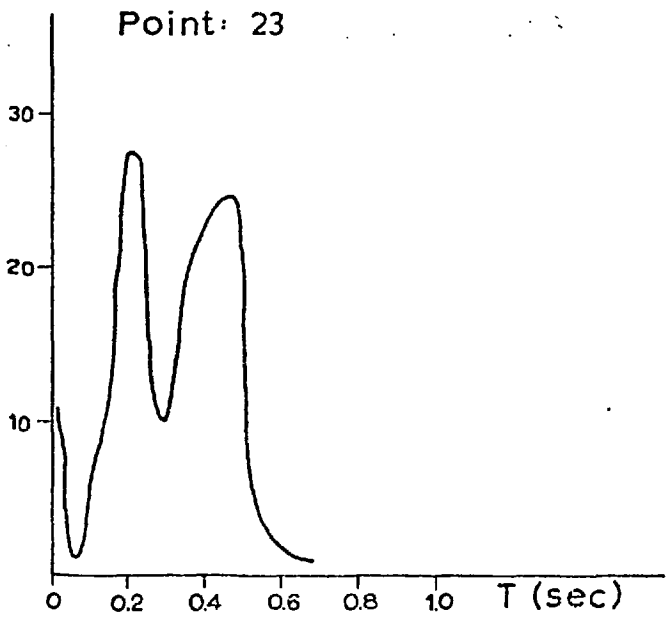

Point : 20
30
20
10
0
0.2
0.4
0.6
0.8
1.0
1.2
T (sec)

FIG 8.8


Point: 21
30
20
10
0
0.2
0.4
0.6
0.8
1.0
T (sec)


Point: 22
30
20
10
0
0.2
0.4
0.6
0.8
1.0
1.2
T (sec)


Point: 23
30
20
10
0
0.2
0.4
0.6
0.8
1.0
T (sec)

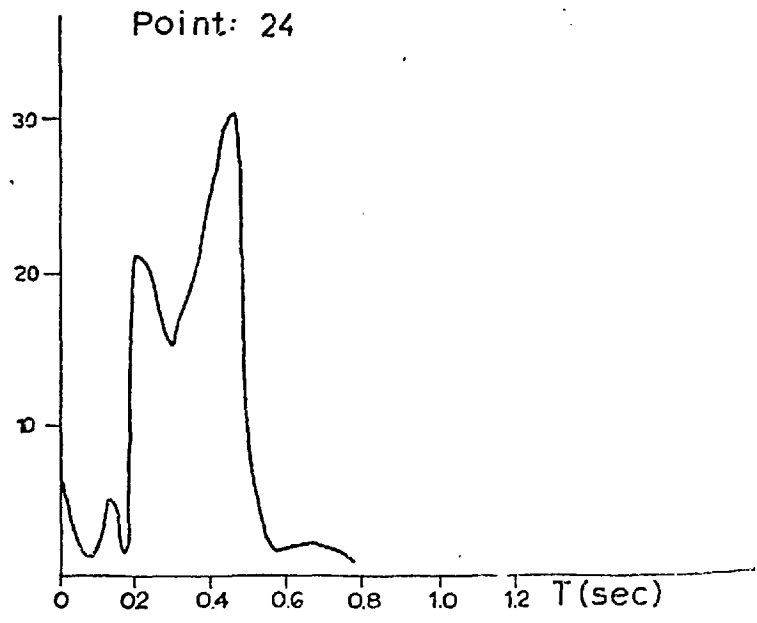
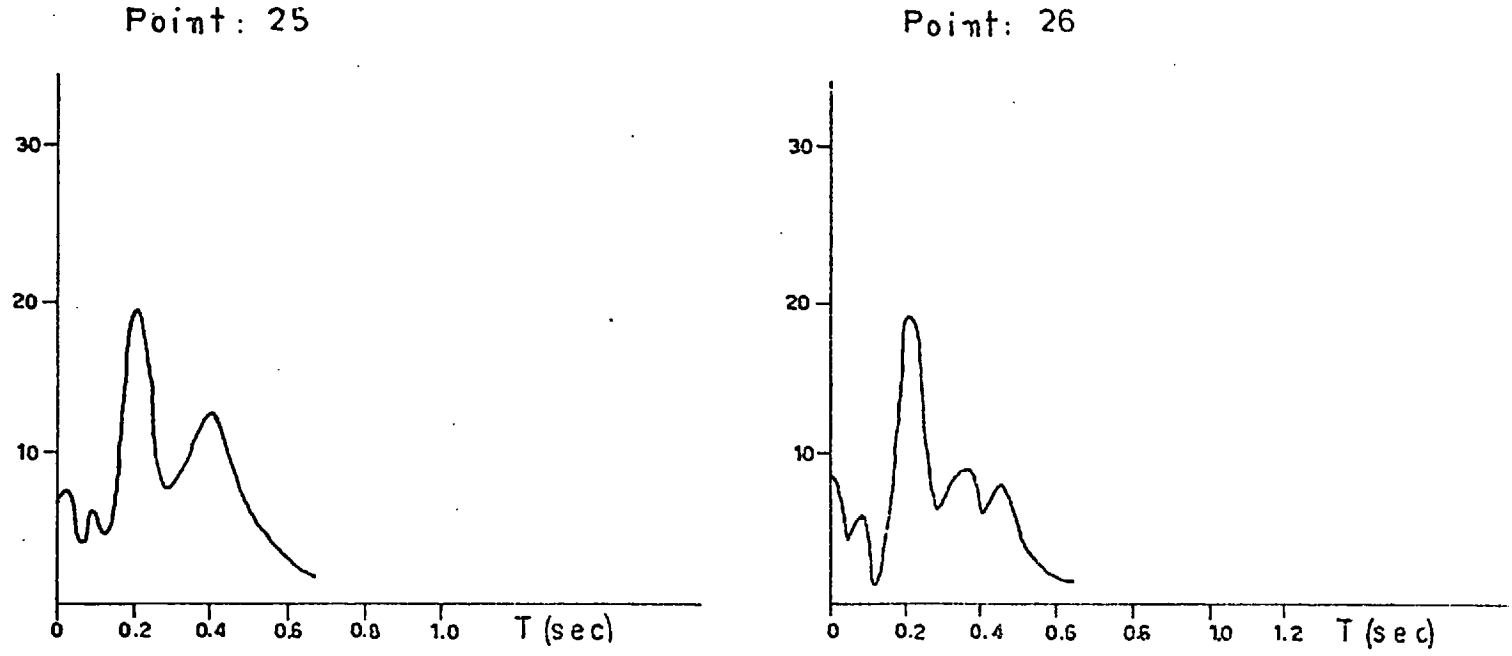

Point: 24
30
20
10
0
0.2
0.4
0.6
0.8
1.0
1.2
T (sec)

FIG. 11.9


Point: 25
30
20
10
0
0.2
0.4
0.6
0.8
1.0
T (sec)
Point: 26
30
20
10
0
0.2
0.4
0.6
0.8
1.0
1.2
T (sec)

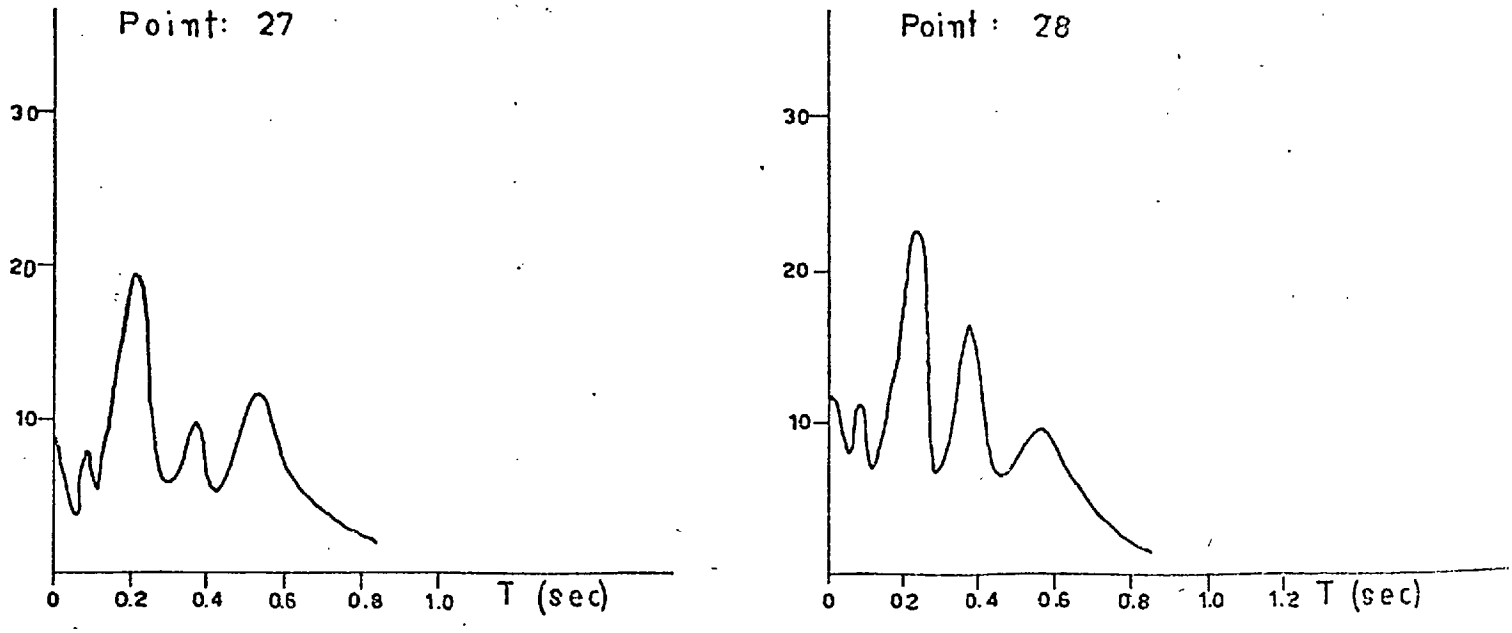
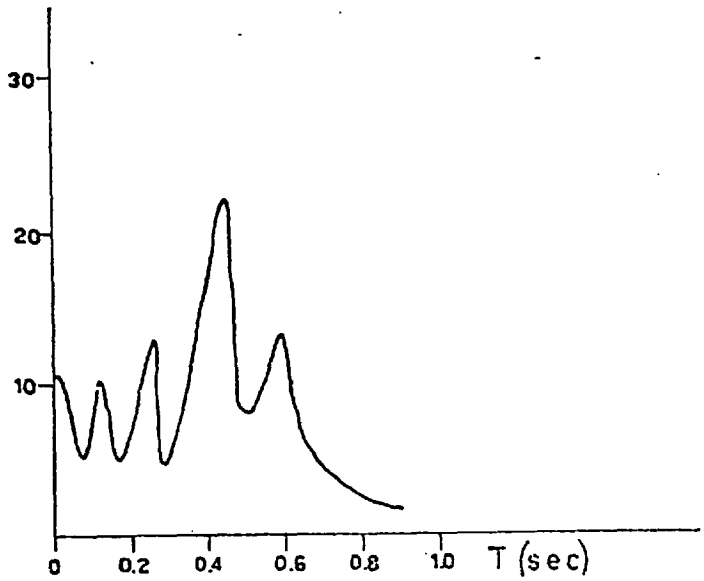

Point: 27
30
20
10
0
0.2
0.4
0.6
0.8
1.0
T (sec)
Point: 28
30
20
10
0
0.2
0.4
0.6
0.8
1.0
1.2
T (sec)

FIG II. 10

Point: 29



Point: 30

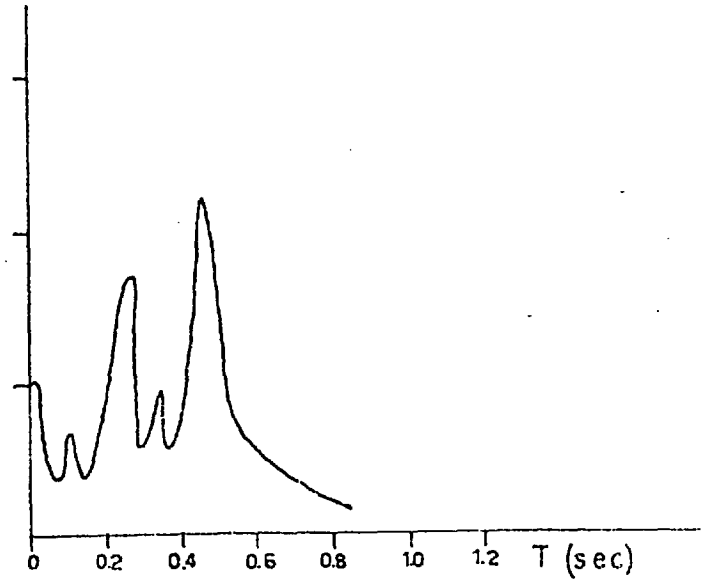


FIG. II

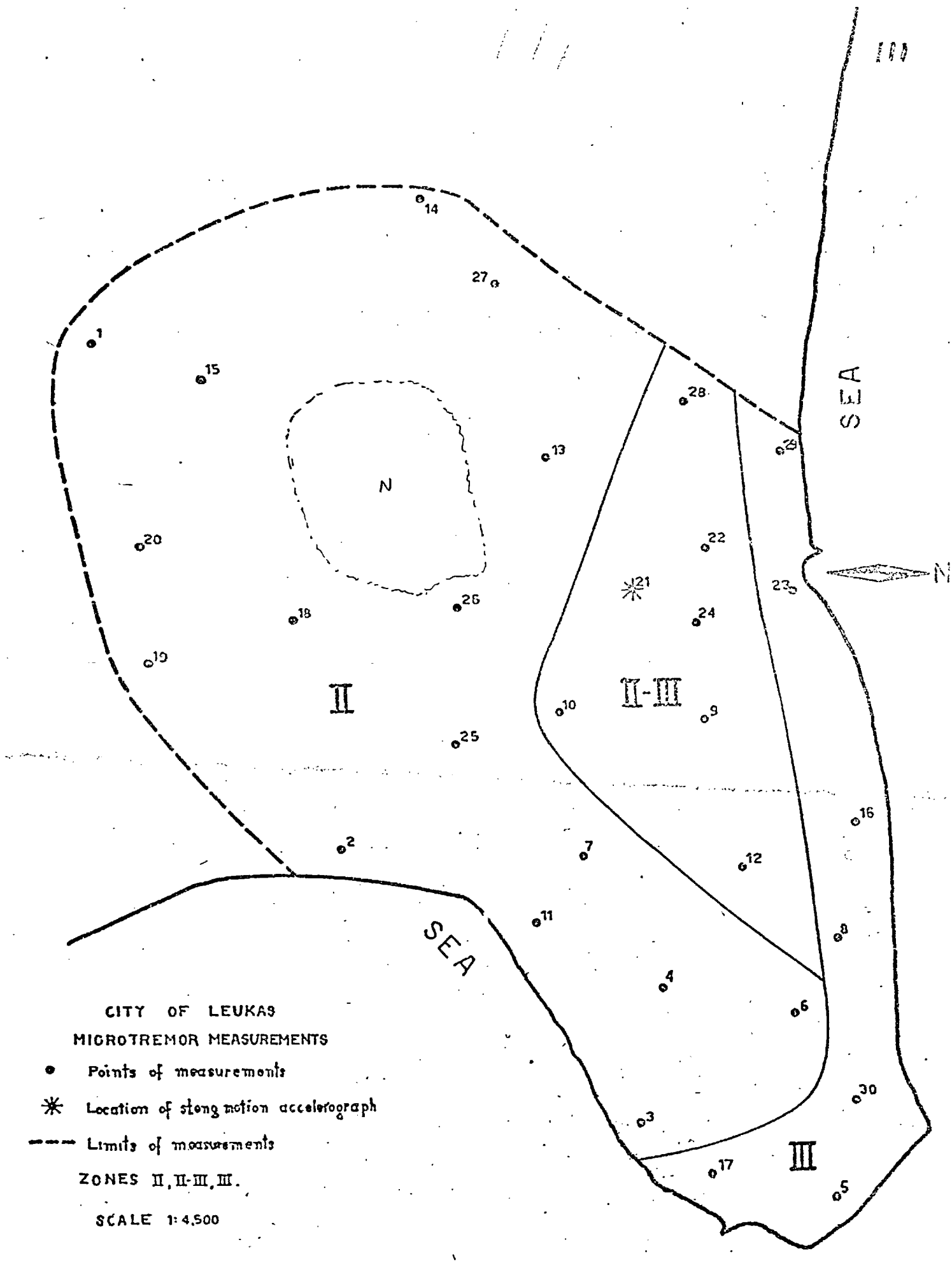

SEA
N
II
II-III
III
SEA
CITY OF LEUKAS
MICROTREMOR MEASUREMENTS
Points of measurements
Location of stong motion accelerograph
Limits of measurements
ZONES II, II-III, III.
SCALE 1:4.500

FIG. D.12

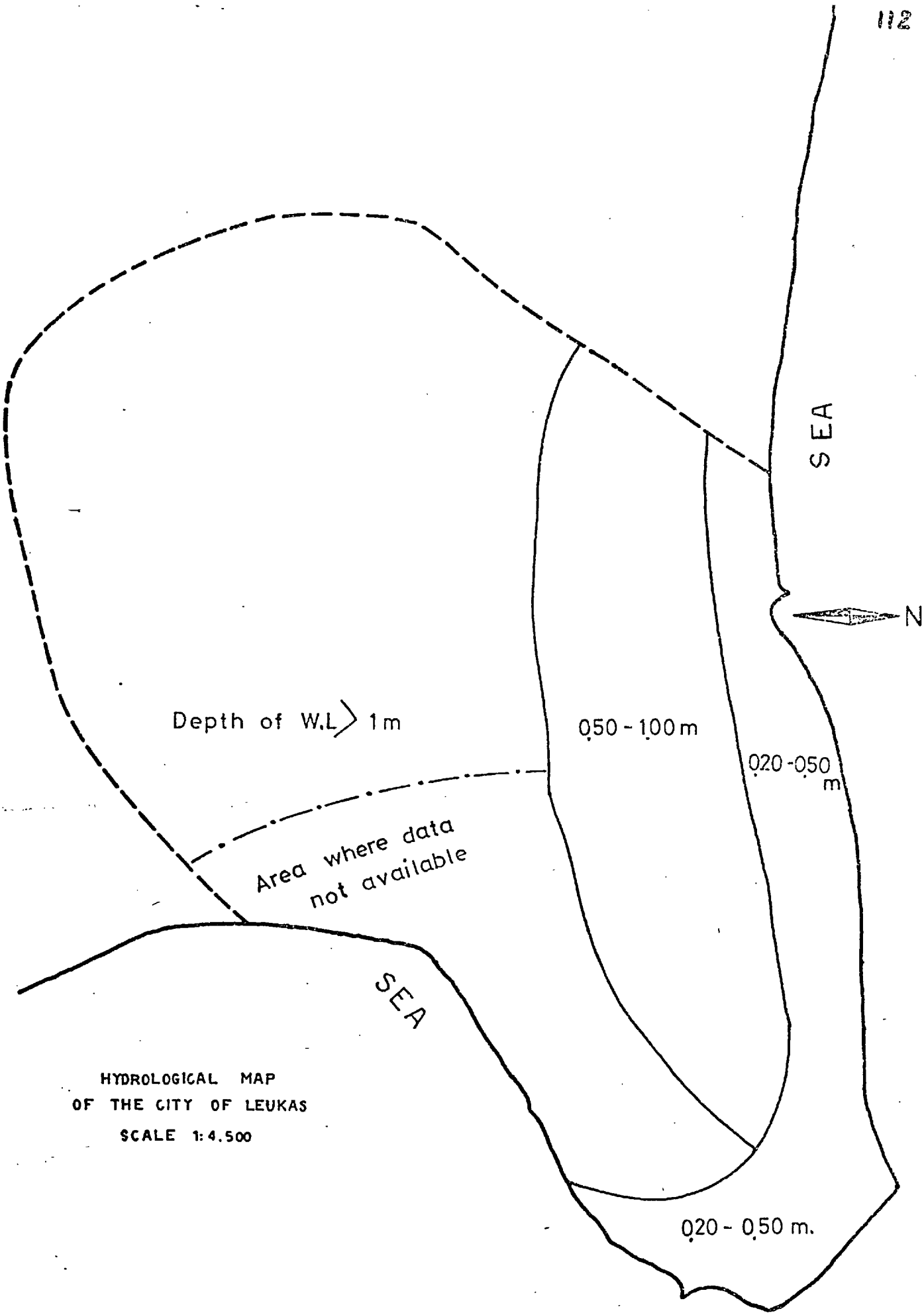
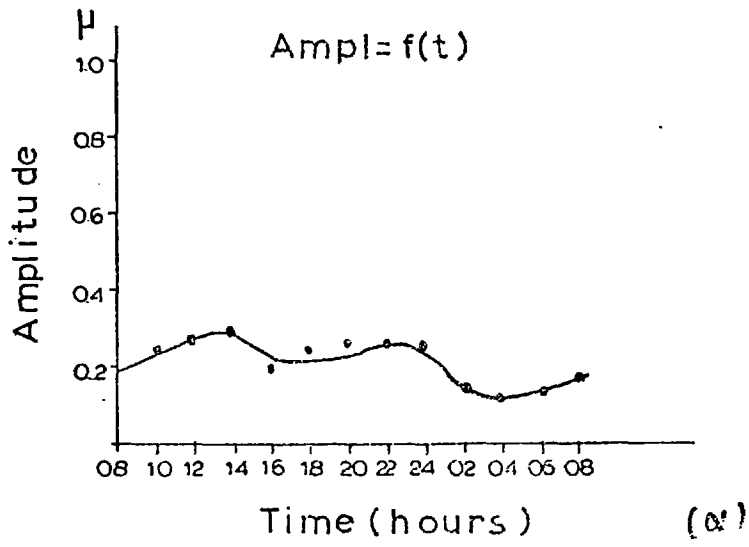

SEA
N
Depth of W.L > 1m
0.50 - 1.00 m
0.20 - 0.50 m
Area where data not available
SEA
0.20 - 0.50 m.
HYDROLOGICAL MAP
OF THE CITY OF LEUKAS
SCALE 1:4.500

FIG. II.13.

24 HOUR MEASUREMENTS LEUKAS



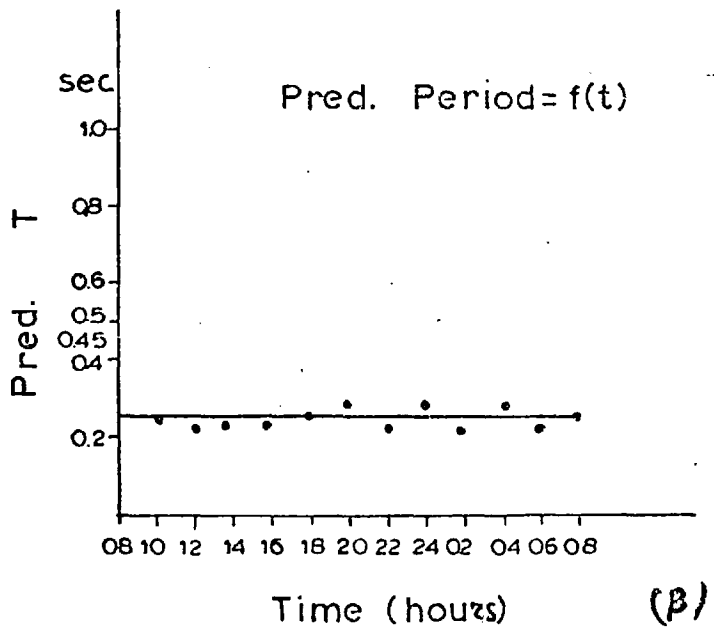


FIG. II. 14

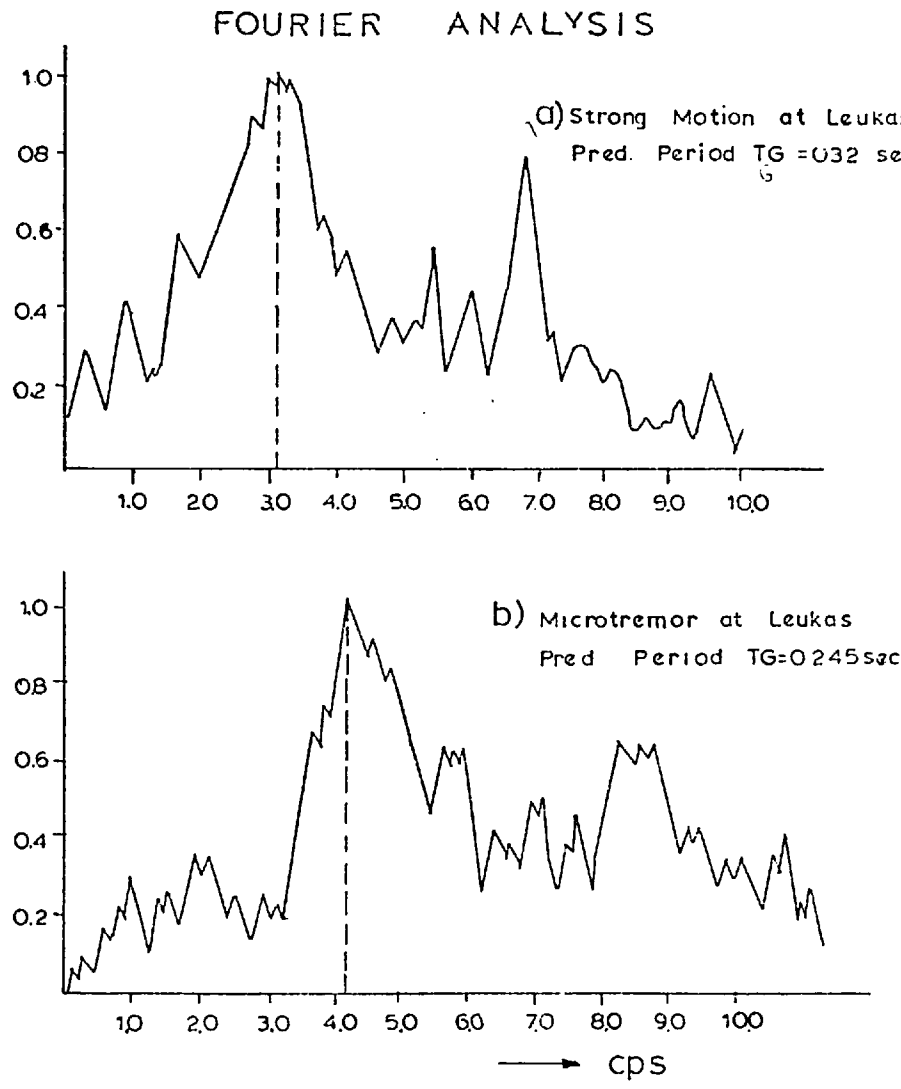
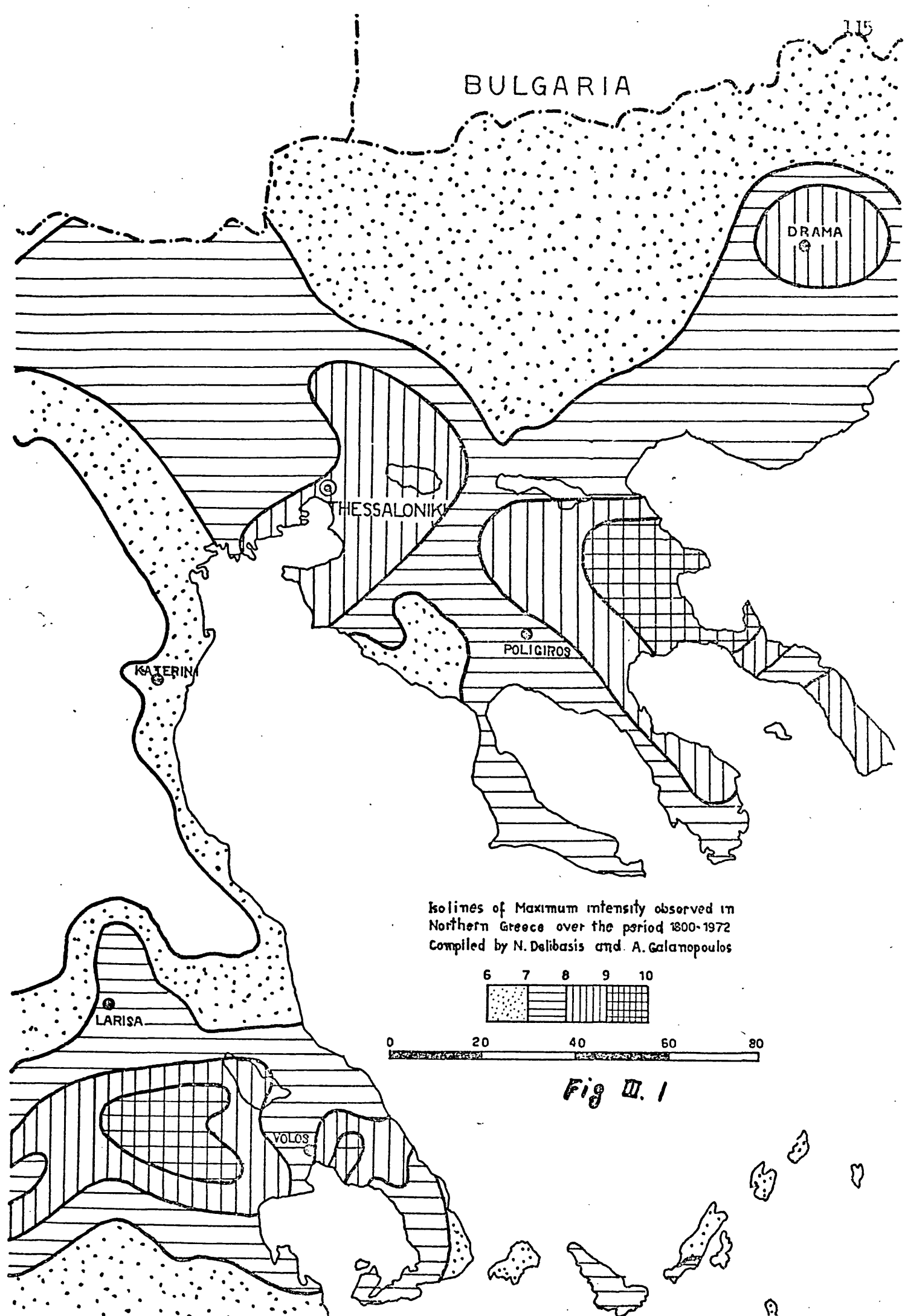


FIG. 15 Comparison of Fourier spectra of microtremors and strong motion accelerogram recorded at Leukas.



Isolines of Maximum intensity observed in Northern Greece over the period 1800-1972
Compiled by N. Delibasis and A. Galanopoulos

Fig III. 1

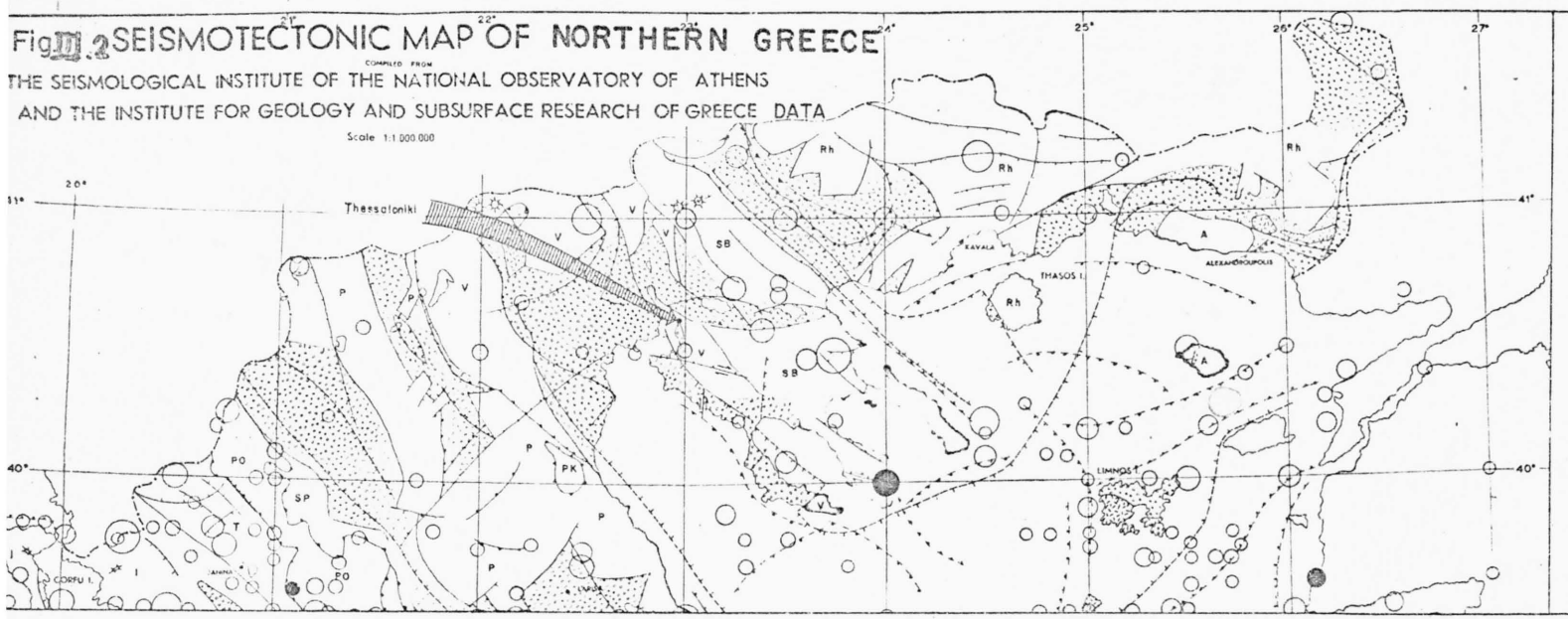
Fig. 2 SEISMOTECTONIC MAP OF NORTHERN GREECE

COMPILED FROM

THE SEISMOLOGICAL INSTITUTE OF THE NATIONAL OBSERVATORY OF ATHENS

AND THE INSTITUTE FOR GEOLOGY AND SUBSURFACE RESEARCH OF GREECE DATA

Scale 1:1.000.000



LEGEND

- Rh — Rhodope massif (Ridge)
- SB — Serbomacedonian massif (Ridge)
- V A — Complex Cenozoic Basin (Vardar) and Axios-Circum-Pelagonian Basin
- P — Pelagonian Ridge
- SP — West Side of Pelagonian Ridge
- PK — Parnassos-Ghiona Ridge
- PO — Olonos - Pindos Geosynclinal
- T — Tripolis Ridge
- I — Ionian Geosyncline
- PX — East Slope of Apulian Plate
- Post Tectonic Deposits
- Neogen and Quaternary Volcanic Rocks
- Outcroppings of diapiric Triassic Gypsum

- Frontline of Lightpoints (Saw Teeth on upthrown side) Dashed when probable
- pre-Pleistocene Normal Fault (Barbs on down-thrown side) Dashed when probable
- Pleistocene Normal Fault (Barbs on down-thrown side) Dashed when probable
- Pre-Pleistocene Volcanos
- Quaternary Volcanos

SHOCKS		CUMULATIVE MAGNITUDE
Shallow	Deep	
○	●	4.3 - 4.9
○	●	5.0 - 5.4
○	●	5.5 - 5.9
○	●	6.0 - 6.4
○	●	6.5 - 6.9
○	●	7.0 - 7.4
○	●	7.5 - 7.9
○	●	> 8.0

Fig. Seismotectonic Map of Northern Greece

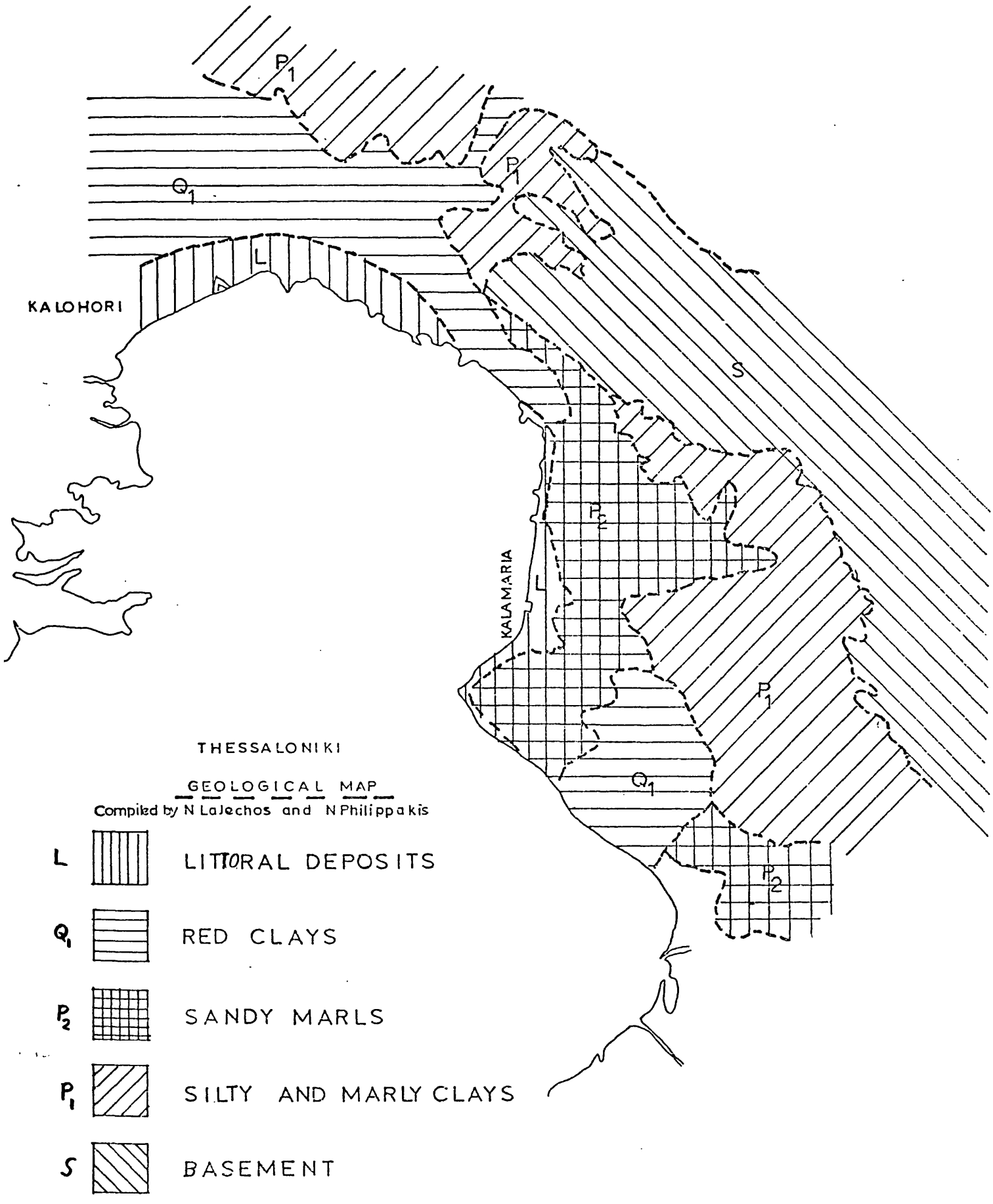

P1
Q1
L
KALOHORI
S
P2
KALAMARIA
P1
Q1
P2
THESSALONIKI
GEOLOGICAL MAP
Compiled by N Lajechos and N Philippakis
L LITTORAL DEPOSITS
Q1 RED CLAYS
P2 SANDY MARLS
P1 SILTY AND MARLY CLAYS
S BASEMENT
SCALE 1:80.000

FIG III. 3

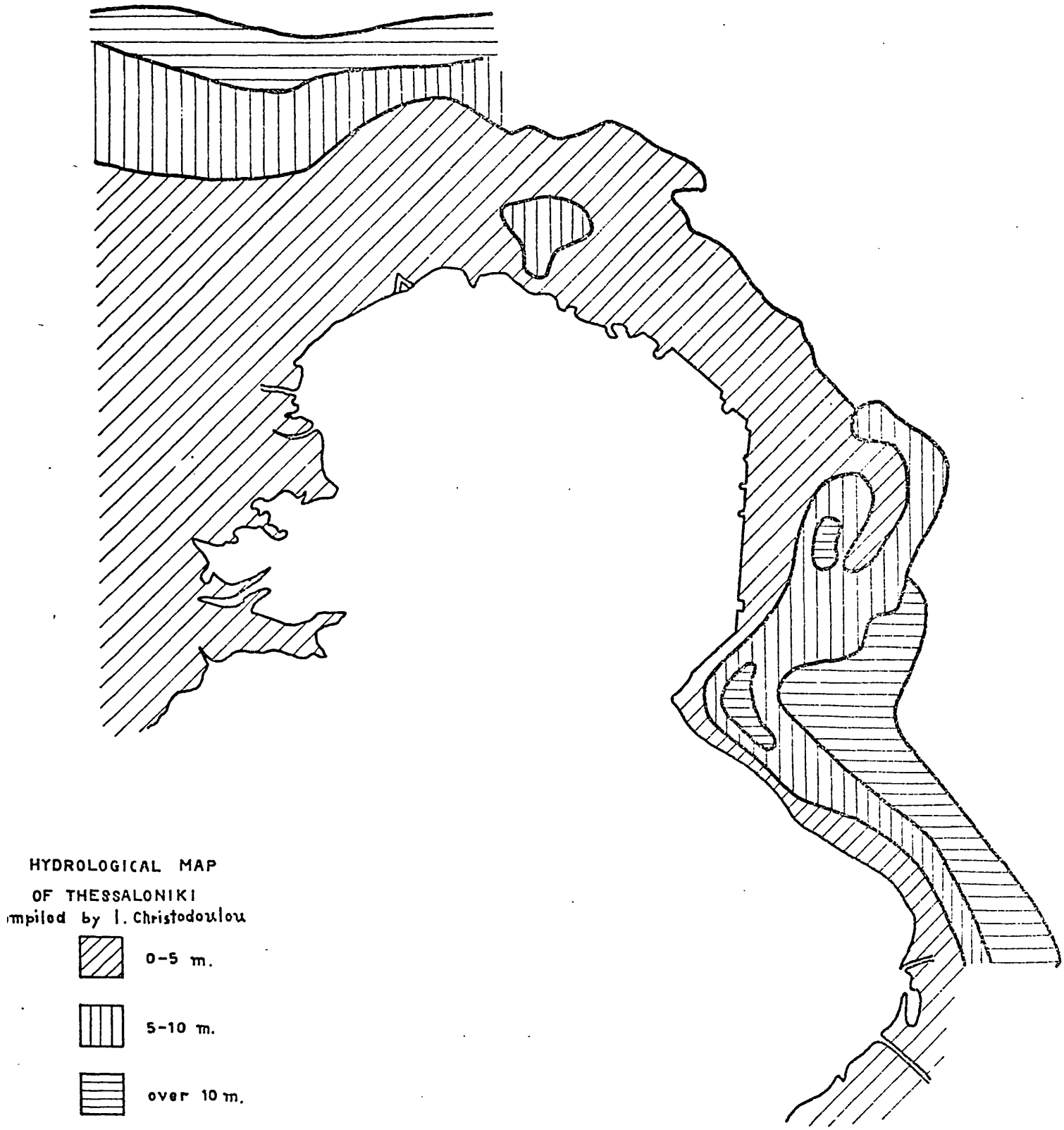
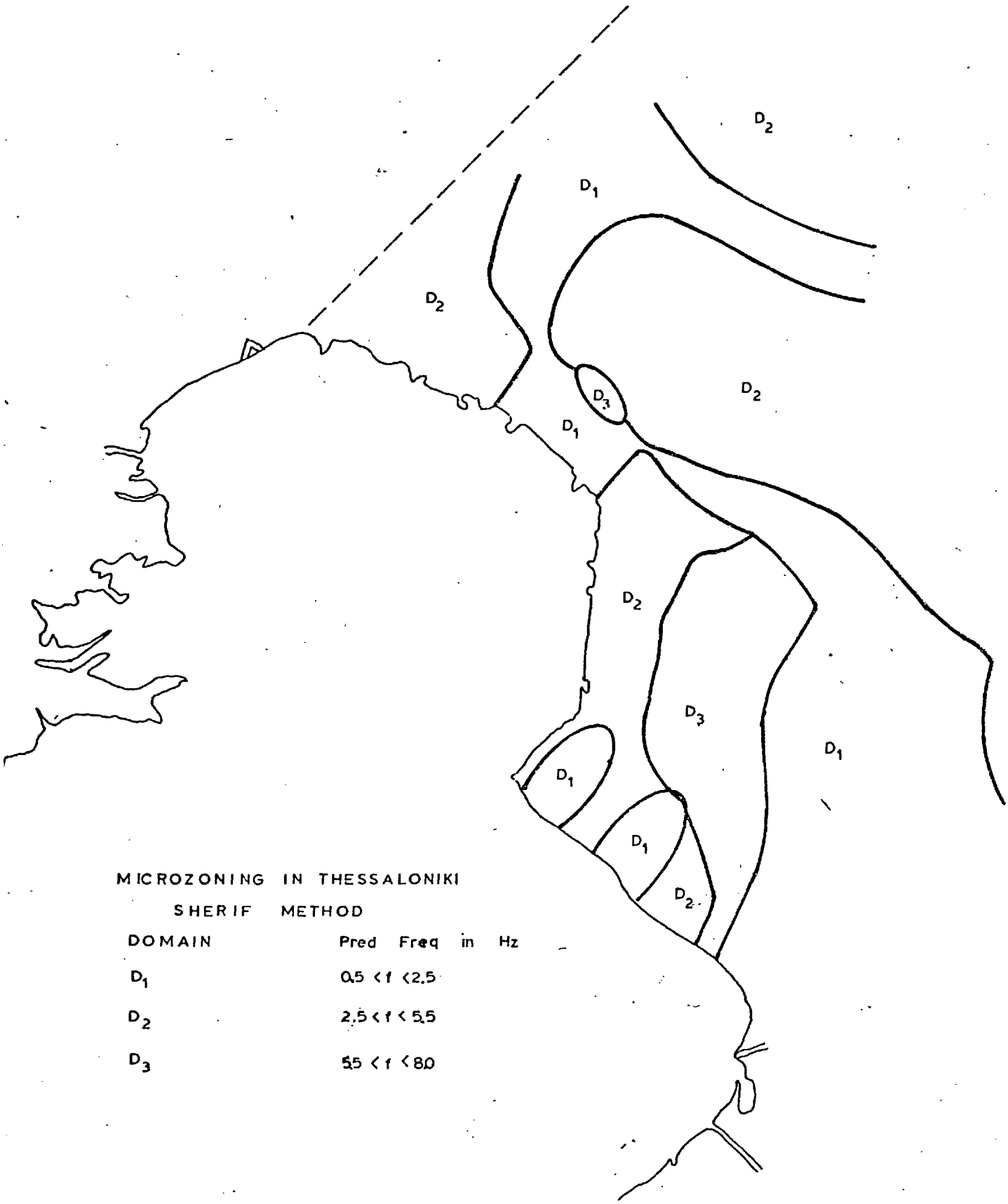

HYDROLOGICAL MAP
OF THESSALONIKI
mpiled by I. Christodoulou
0-5 m.
5-10 m.
over 10 m.
SCALE 1:80.000

FIG. III.4



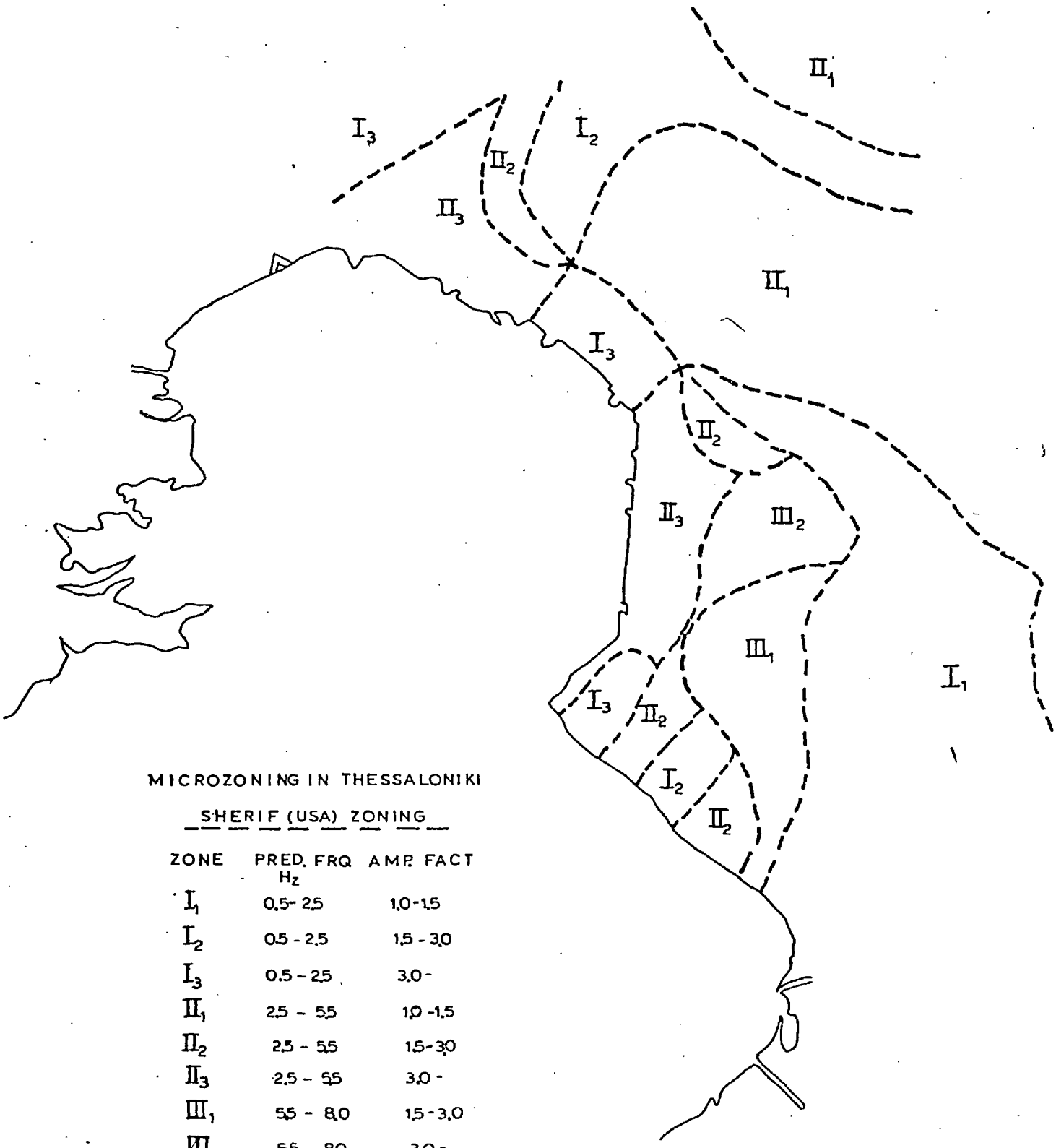
MICROZONING IN THESSALONIKI

SHERIF METHOD

DOMAIN	Pred Freq in Hz
D_1	0.5 < f < 2.5
D_2	2.5 < f < 5.5
D_3	5.5 < f < 8.0

SCALE 1:80.000

FIG III.5



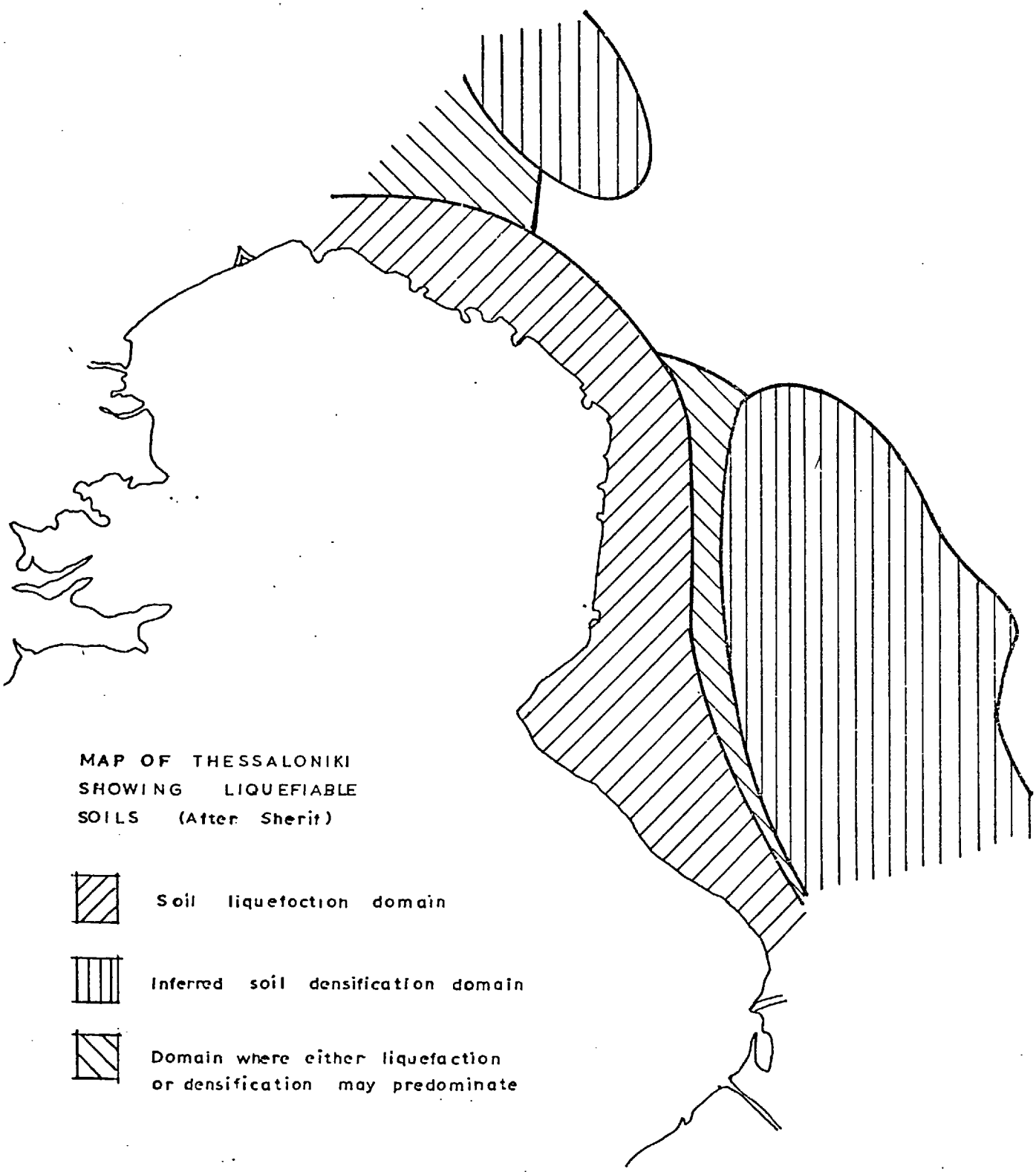
MICROZONING IN THESSALONIKI

SHERIF (USA) ZONING

ZONE	PRED. FRQ Hz	AMP. FACT
I_1	0.5-2.5	1.0-1.5
I_2	0.5 - 2.5	1.5 - 3.0
I_3	0.5 - 2.5	3.0 -
II_1	2.5 - 5.5	1.0 -1.5
II_2	2.5 - 5.5	1.5-3.0
II_3	2.5 - 5.5	3.0 -
III_1	5.5 - 8.0	1.5 - 3.0
III_2	5.5 - 8.0	3.0 -

SCALE 1:80.000

FIG. III. 6



SCALE 1:80000

FIG III.7

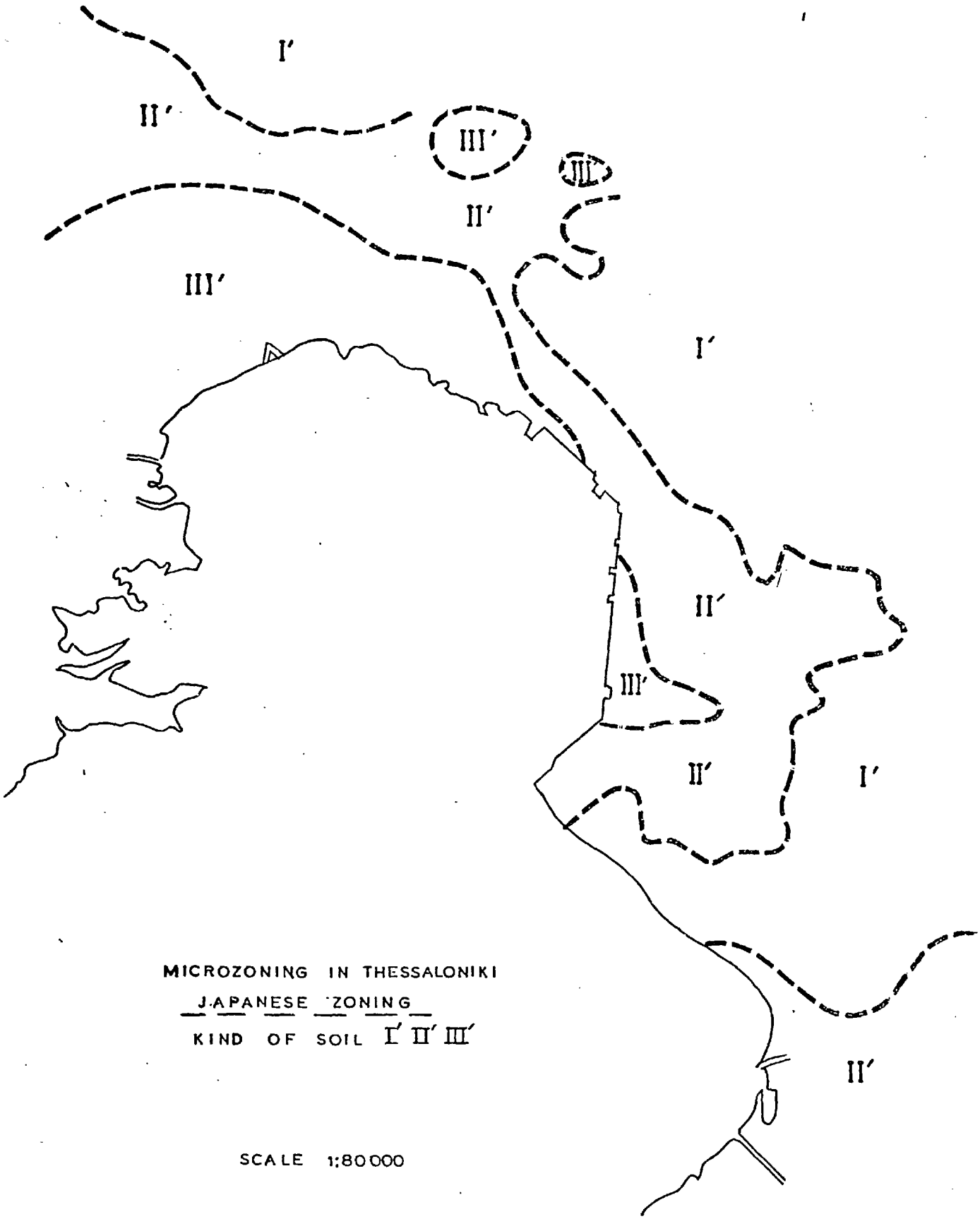
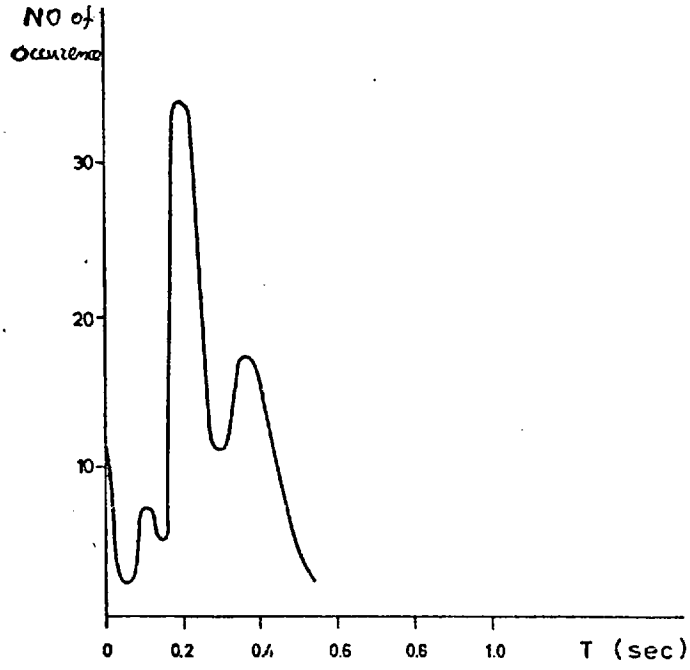
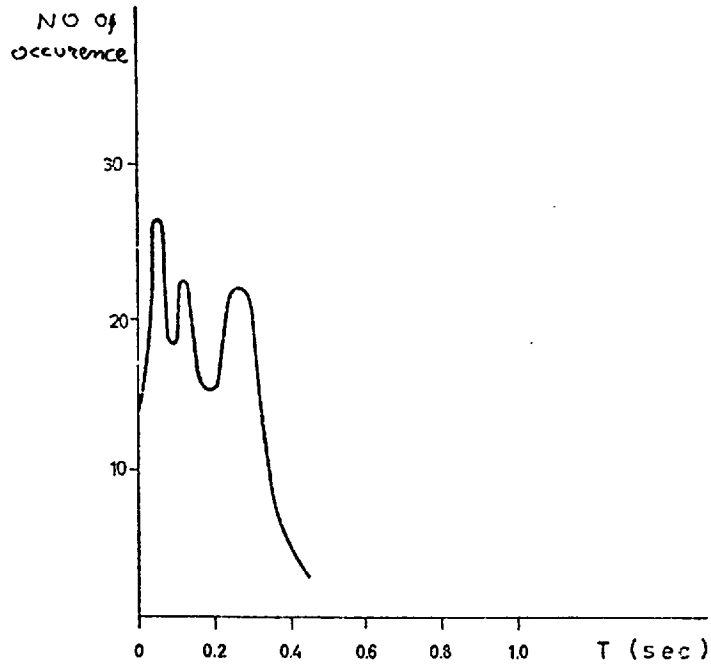

I′
II′
III′
III′
II′
III′
I′
II′
III′
II′
I′
II′
MICROZONING IN THESSALONIKI
JAPANESE ZONING
KIND OF SOIL I′ II′ III′
SCALE 1:80000

FIG. III. 8

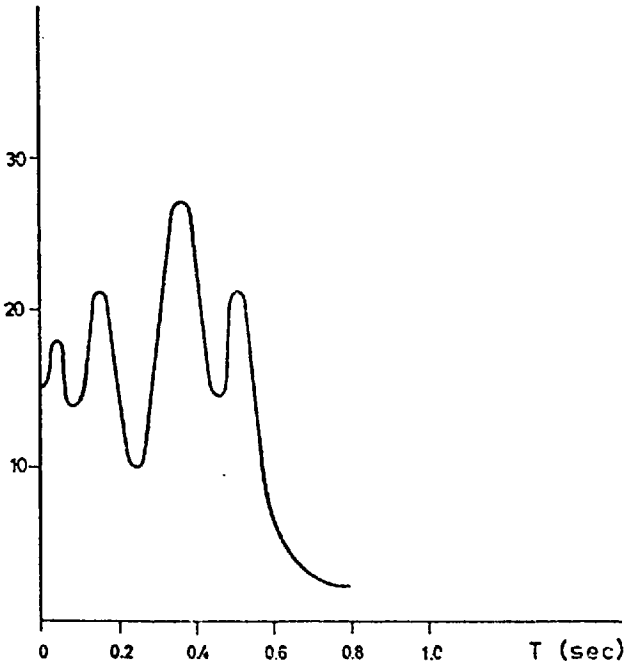
Point: 1



Point: 2



Point: 3



Point: 4

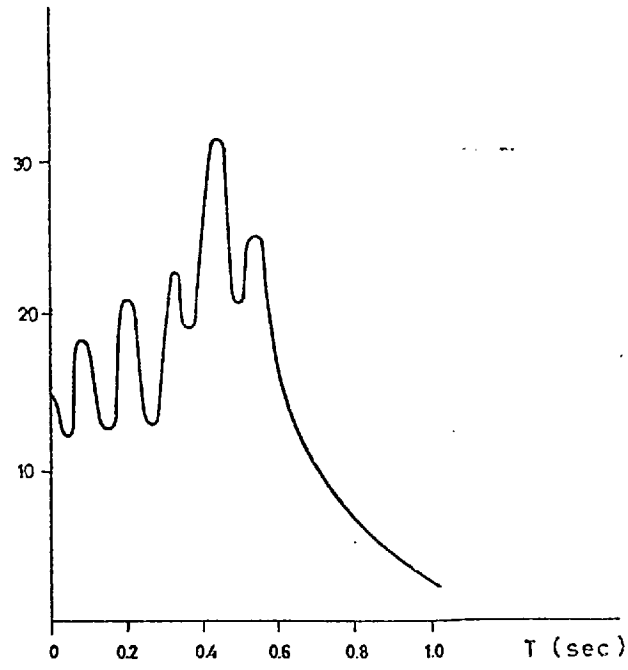
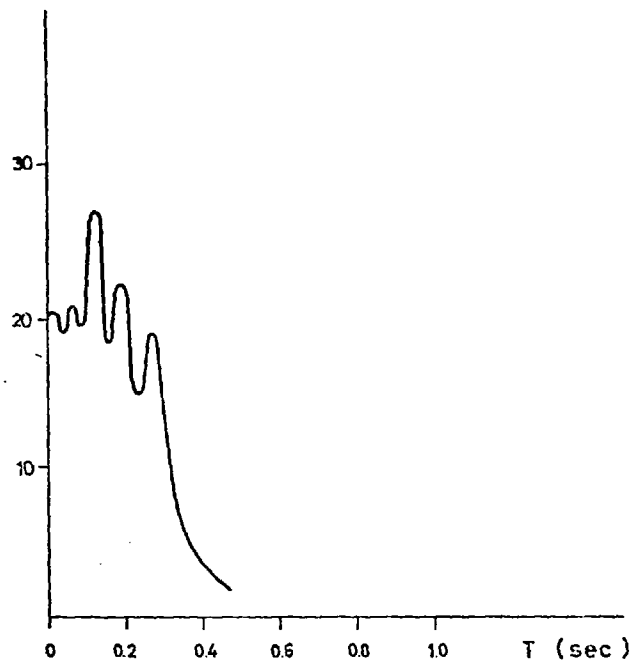
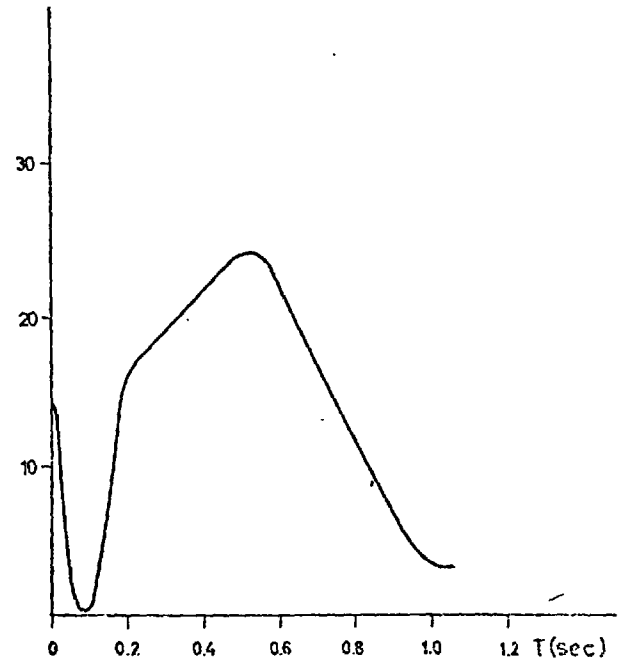


FIG. III. 10

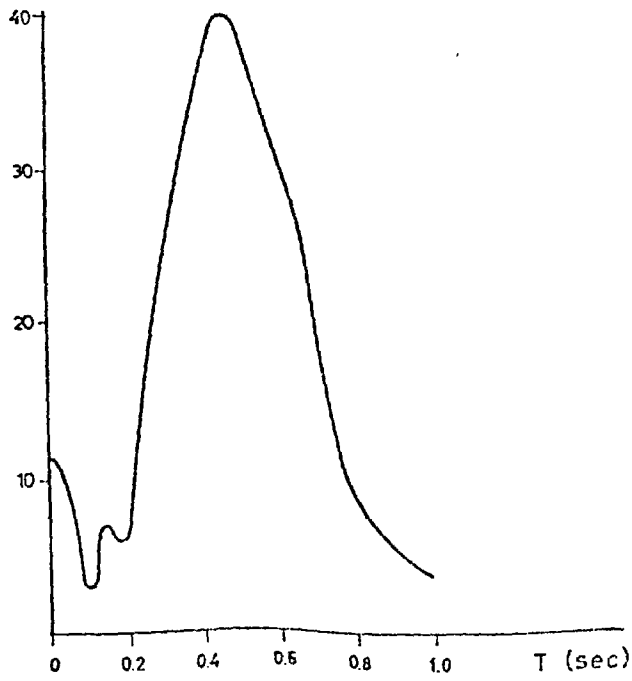
Point: 5



Point: 6



Point: 7



Point: 8

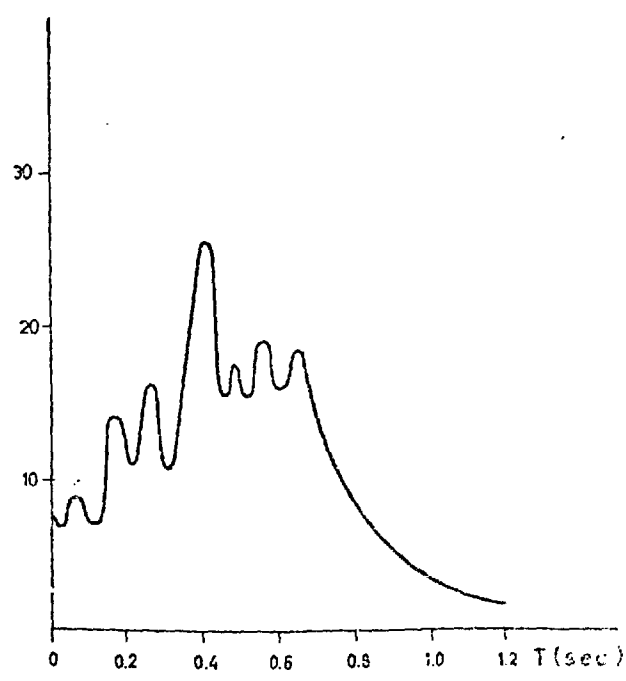
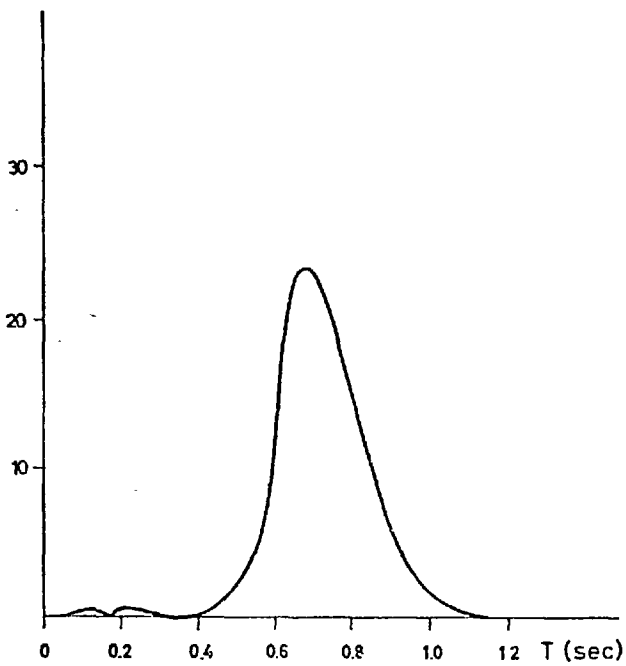
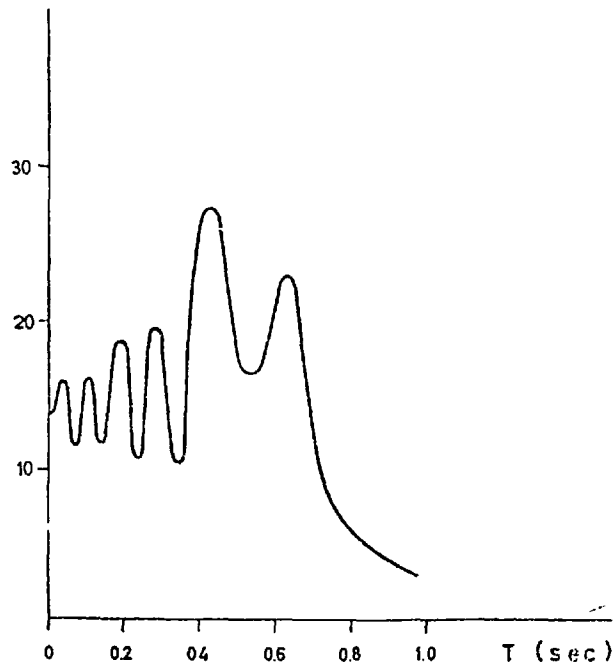


FIG. III. 11

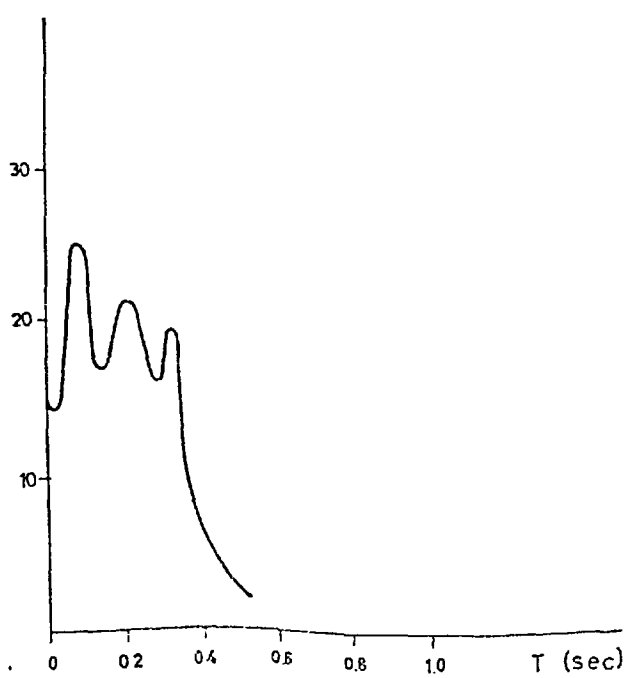
Point: 9



Point: 10



Point: 11



Point: 12

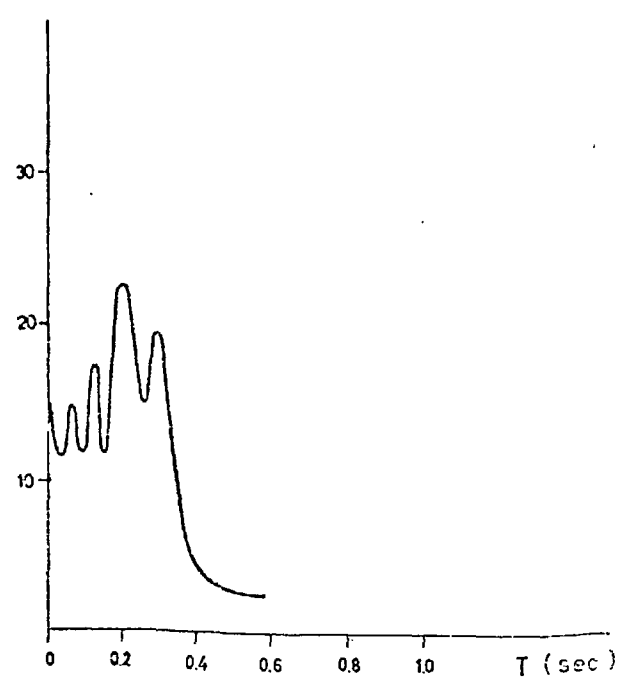
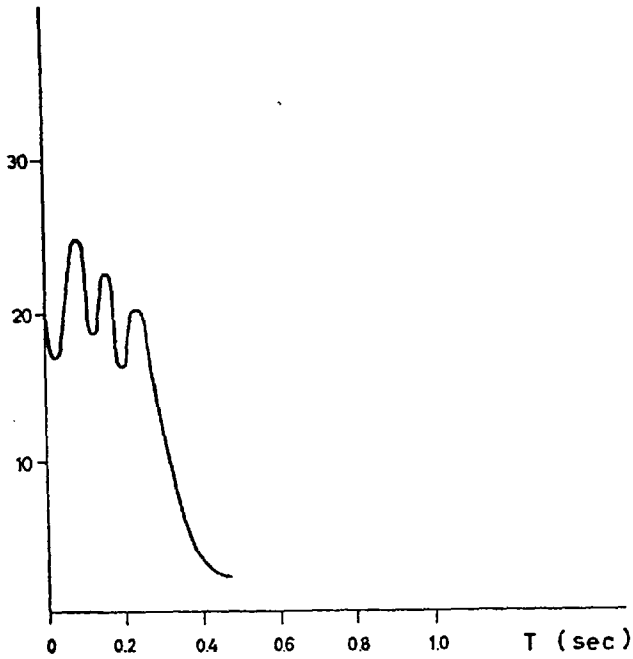
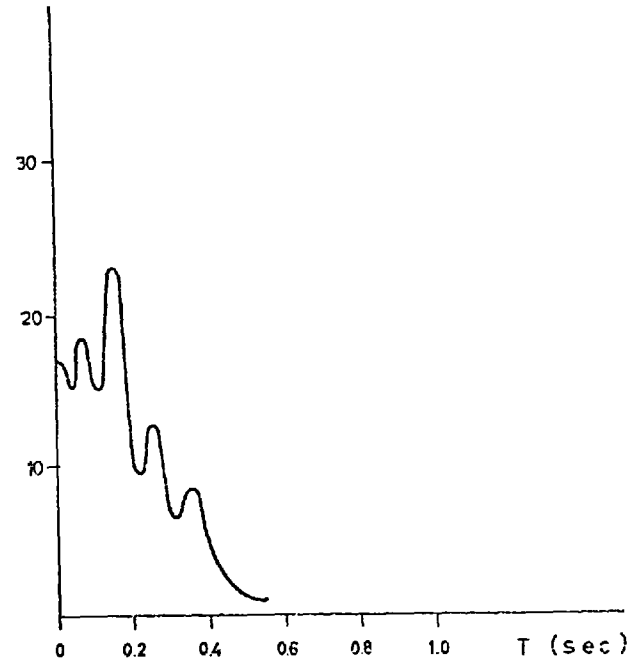


FIG. III, 12

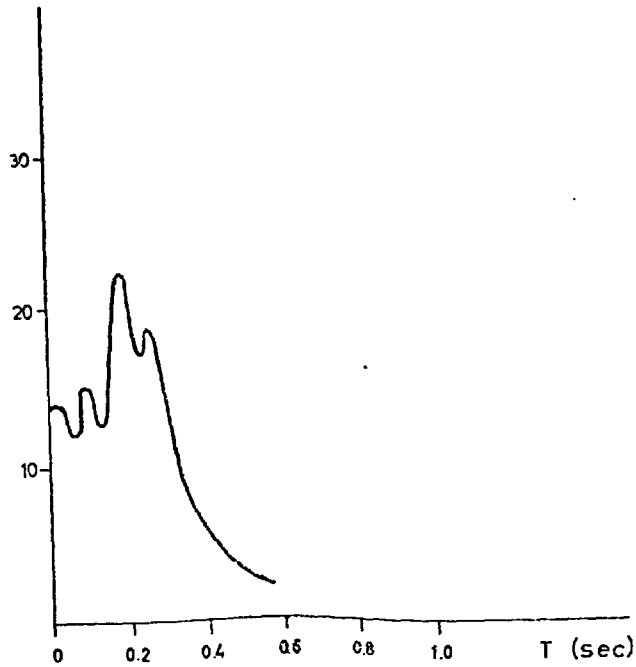
Point: 13



Point: 14



Point: 15



Point: 16

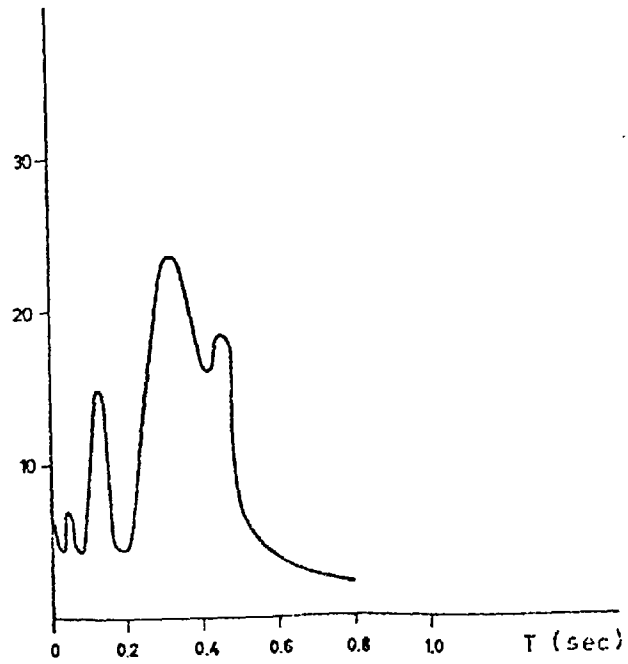
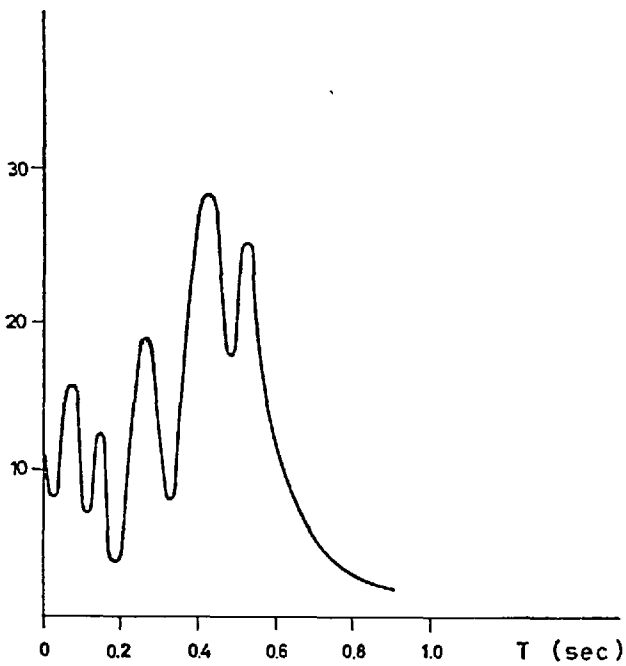
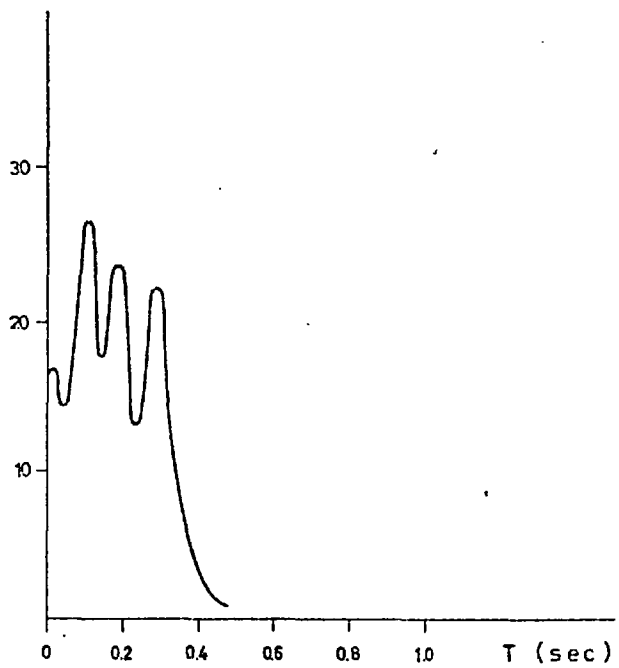


FIG. III. 13

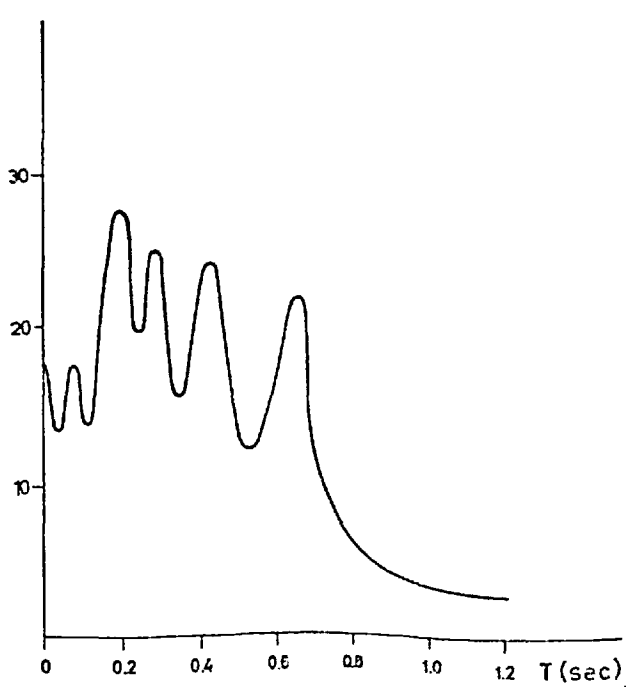
Point: 17



Point: 18



Point: 19



Point: 20

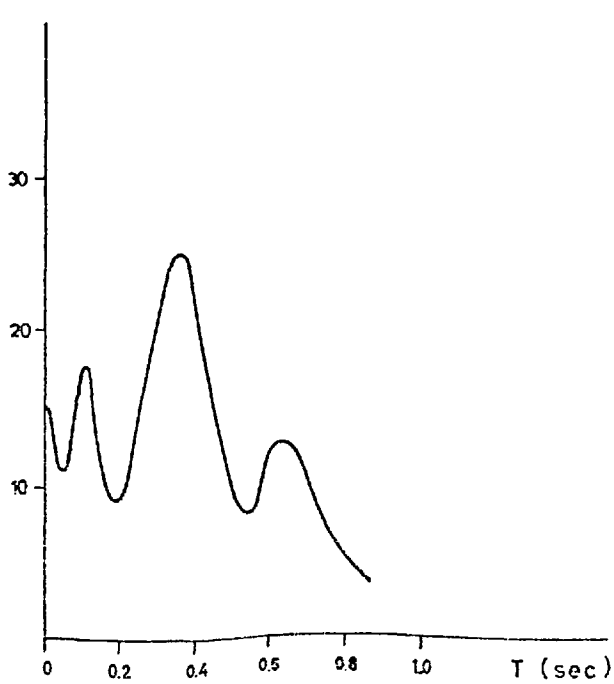
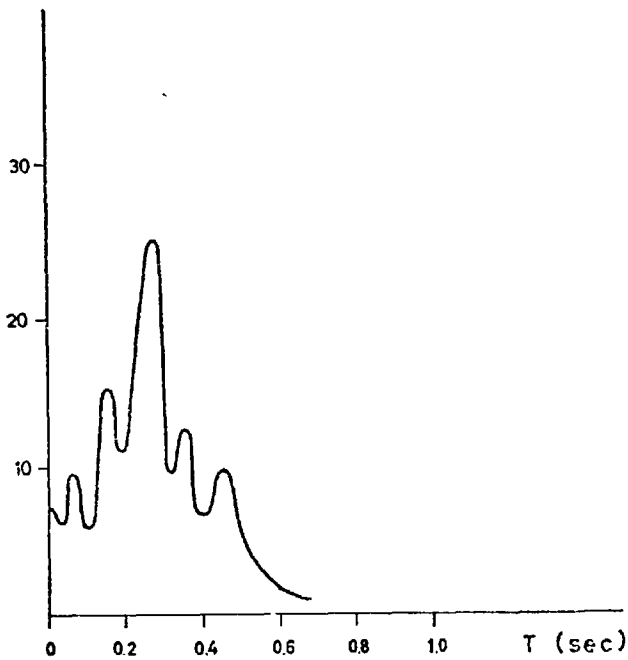
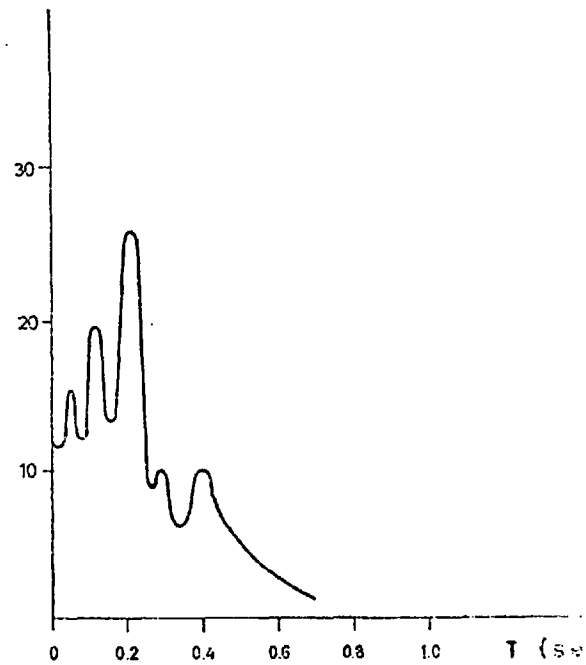


FIG. III. 14

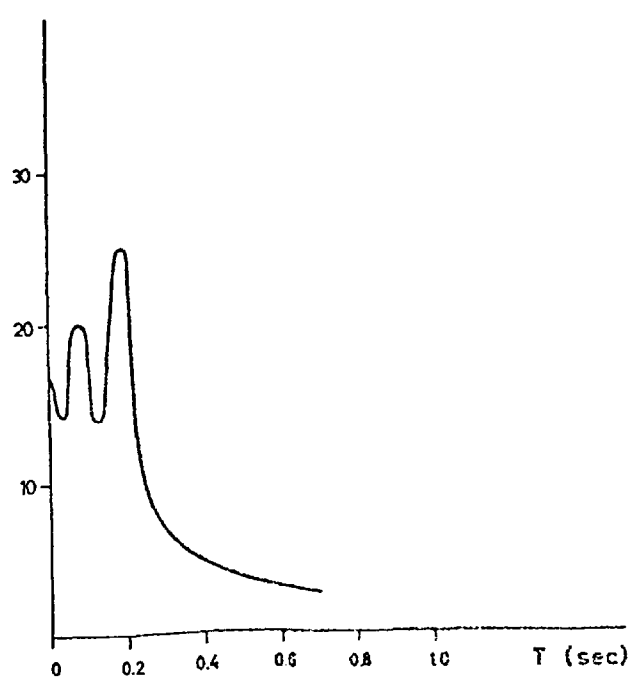
Point: 21



Point: 22



Point: 23



Point: 24

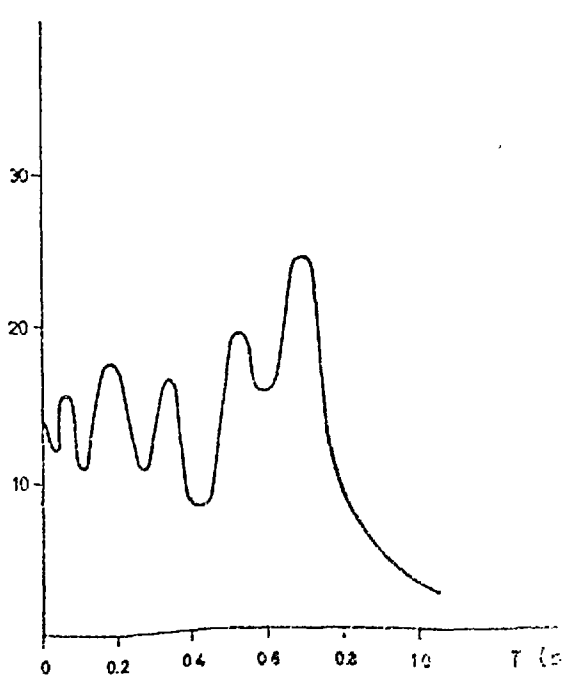
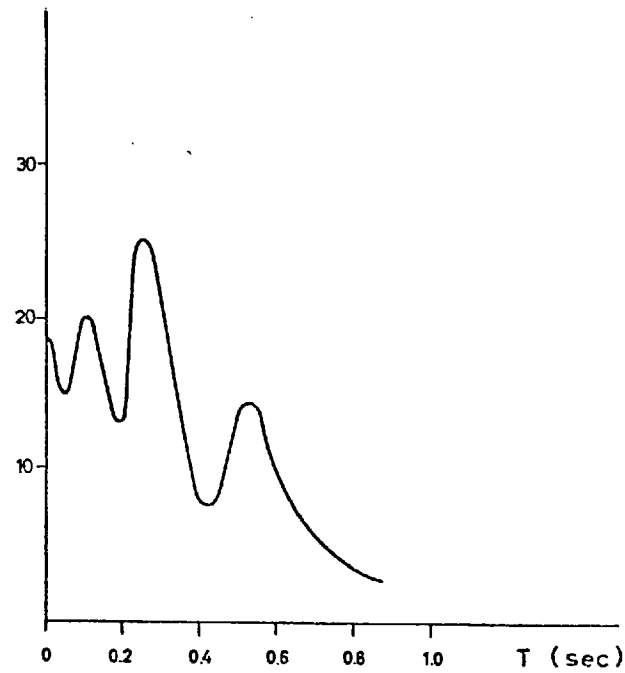
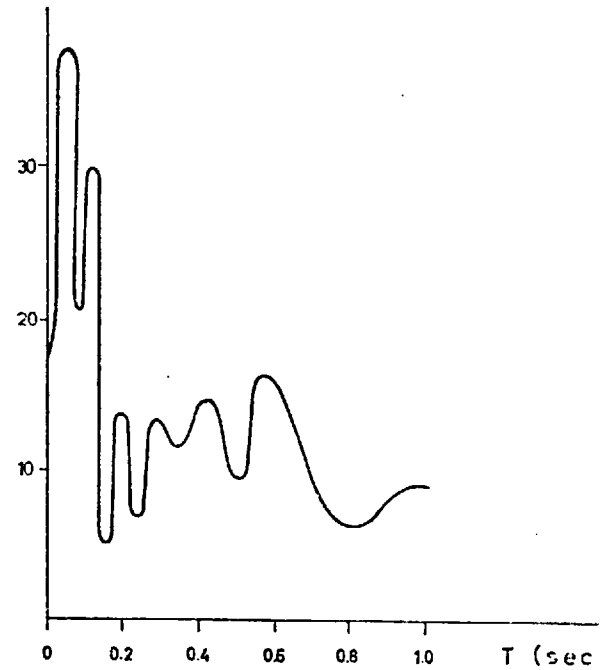


FIG. III. 15

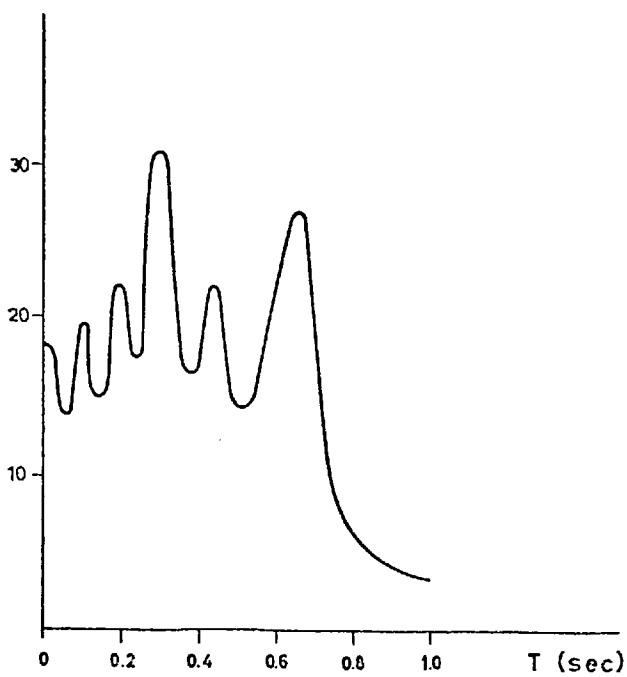
Point: 25



Point: 26



Point: 27



Point: 28

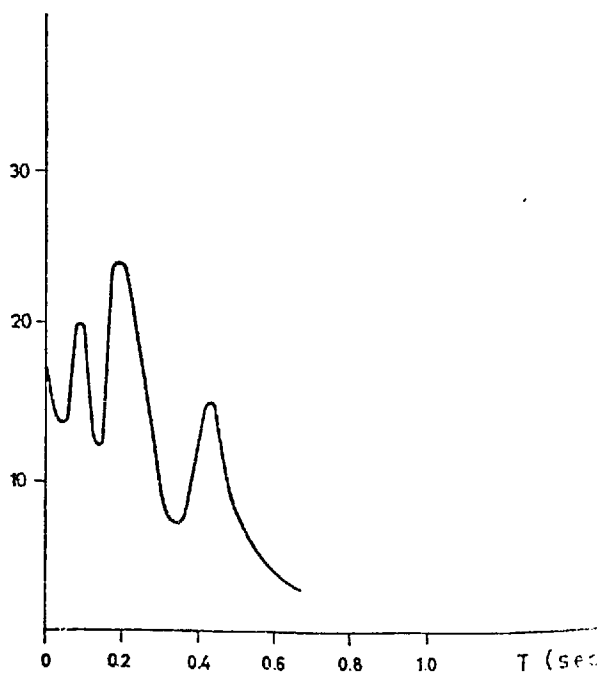
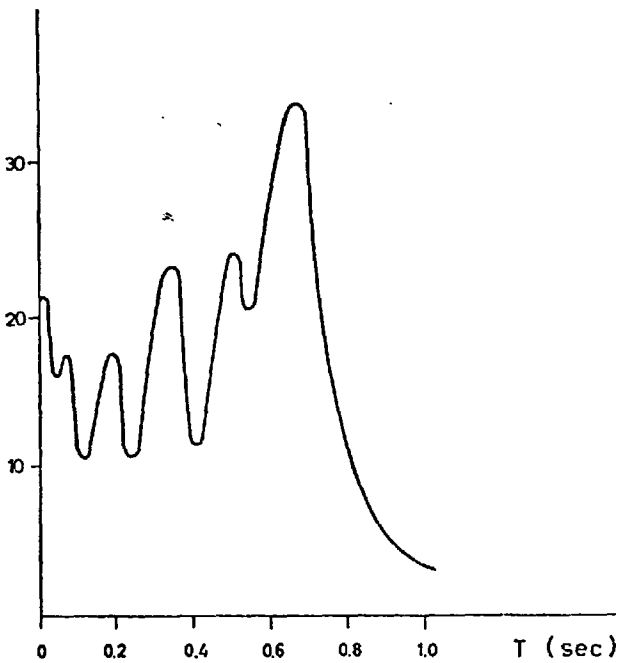
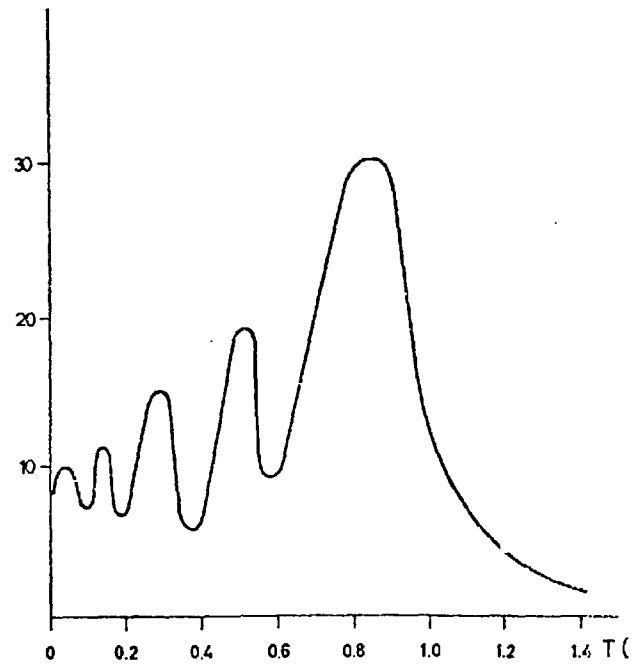


FIG. III. 16

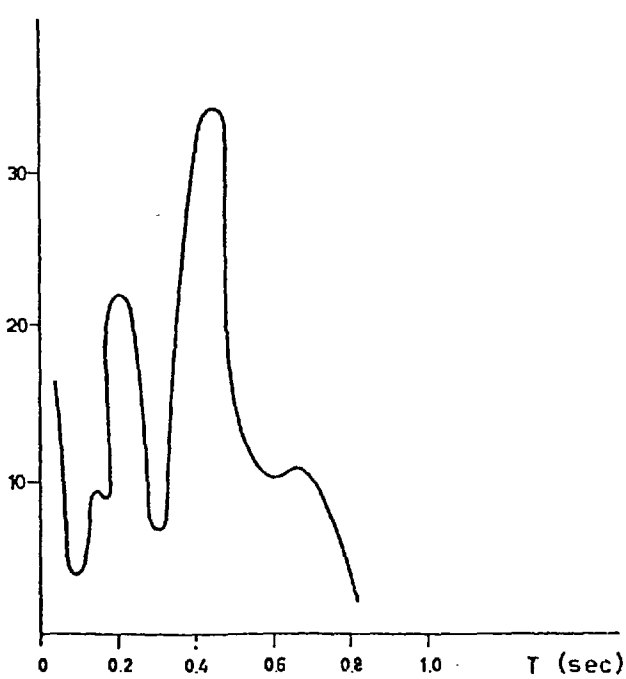
Point: 29



Point: 30



Point: 31



Point: 32

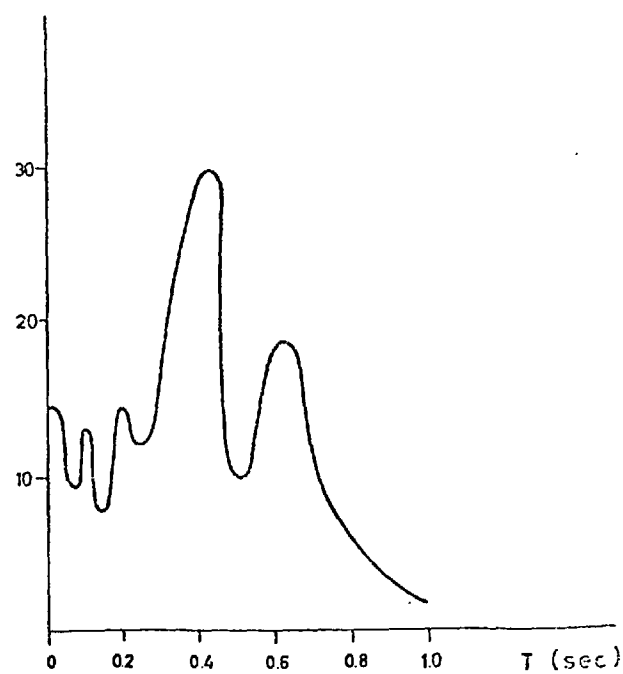
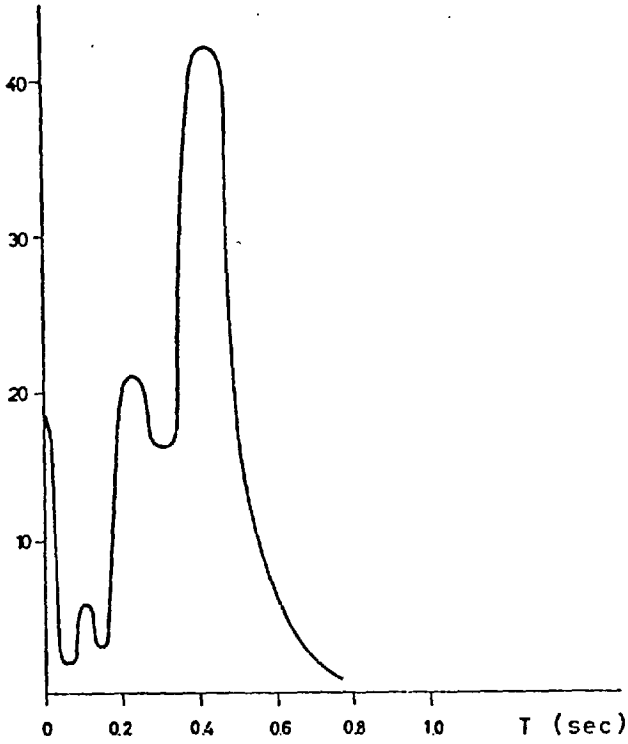
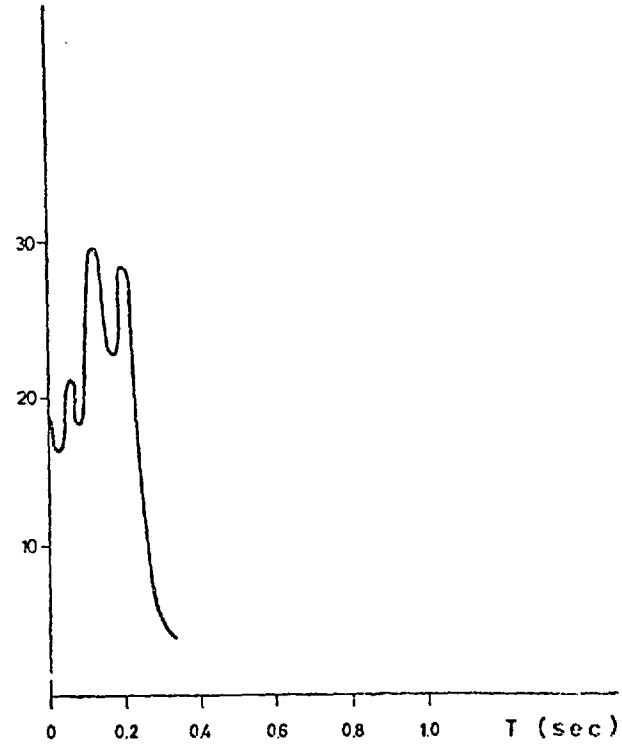


FIG. III.17

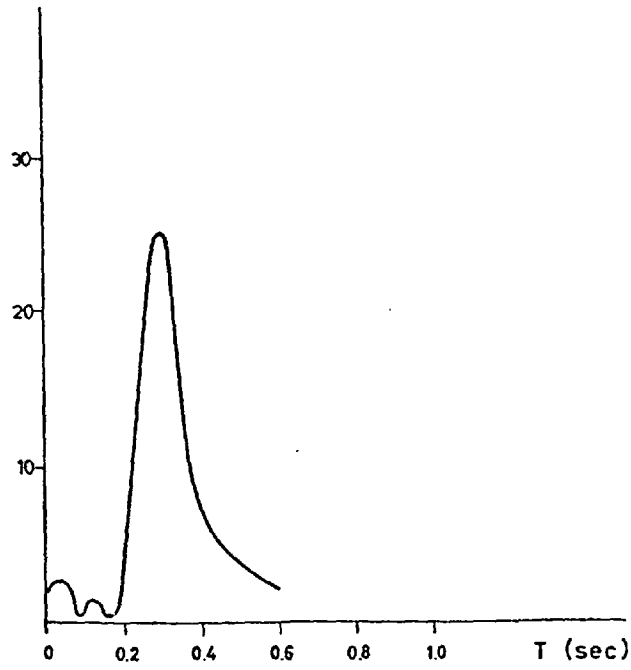
Point: 33



Point: 34



Point: 35



Point: 36

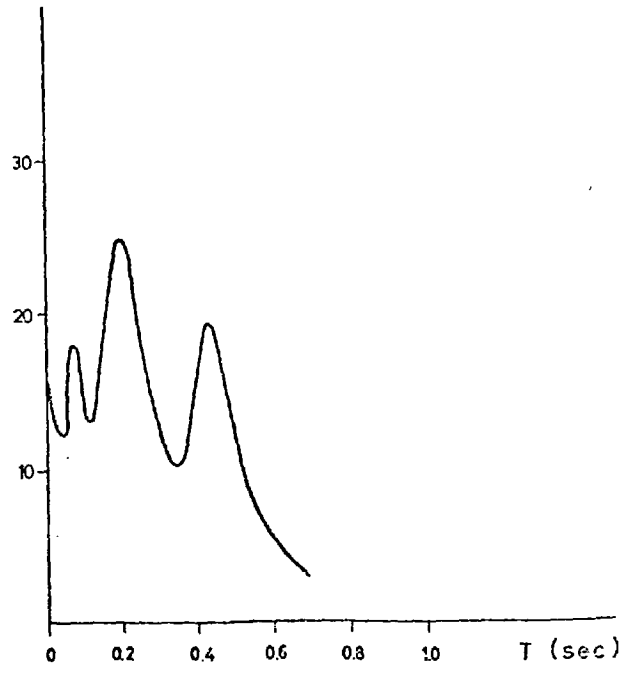
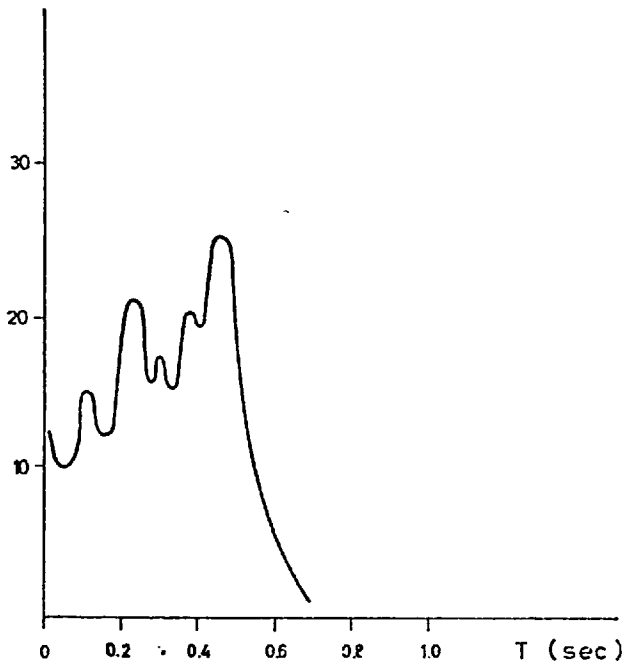
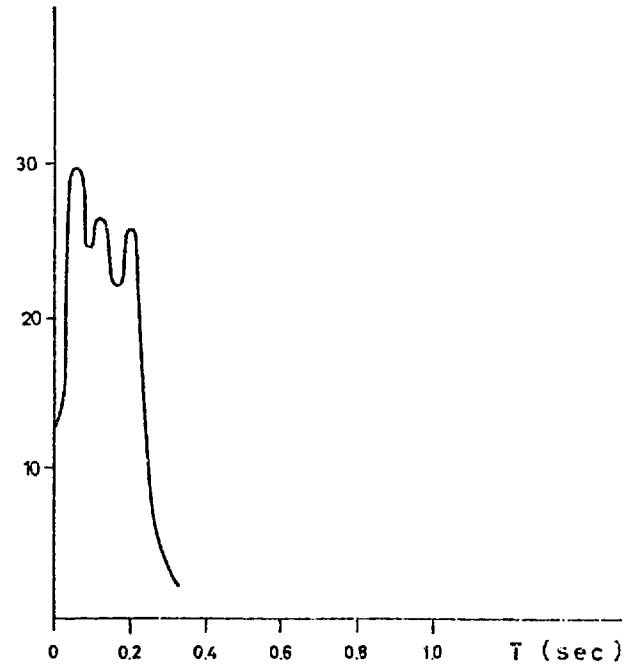


FIG 18

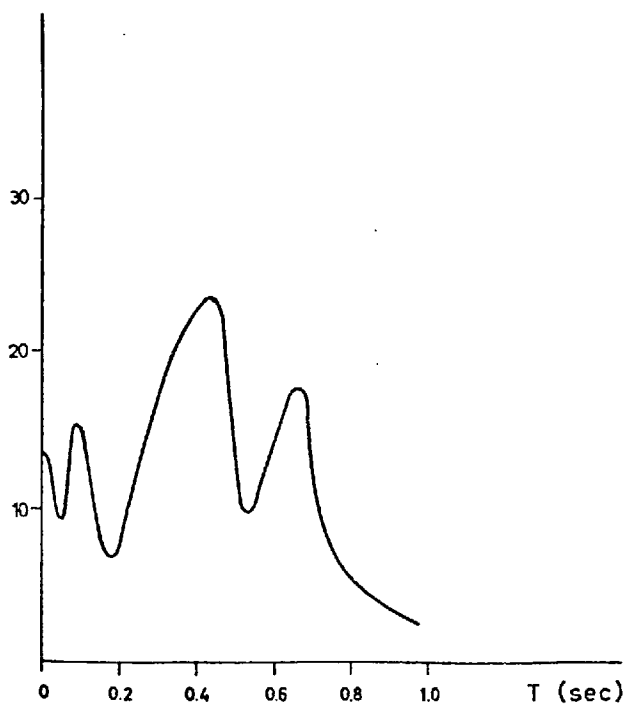
Point: 37



Point: 38



Point: 39



Point: 40

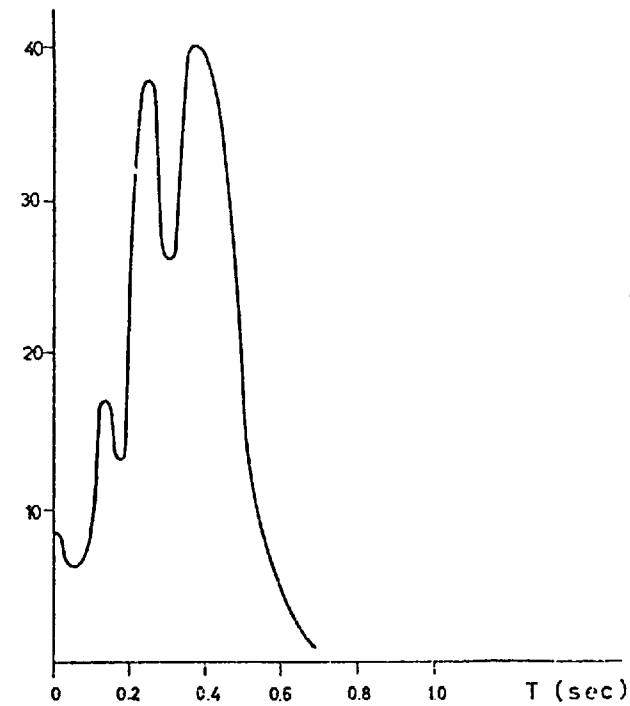
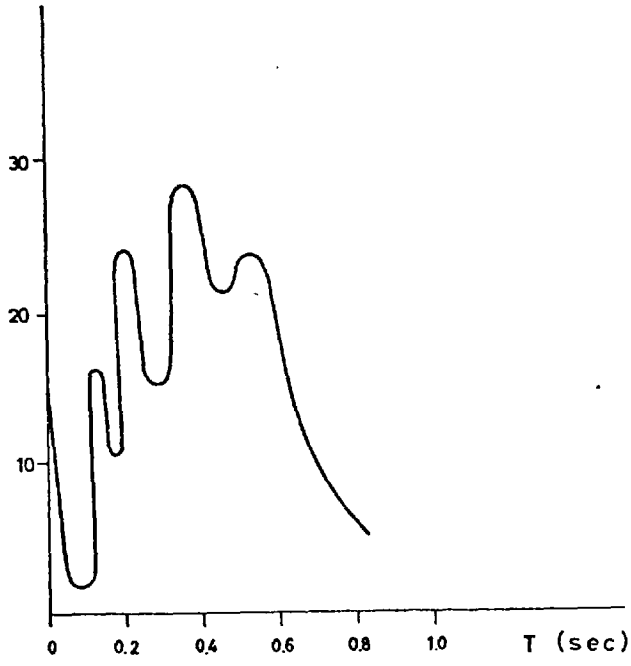
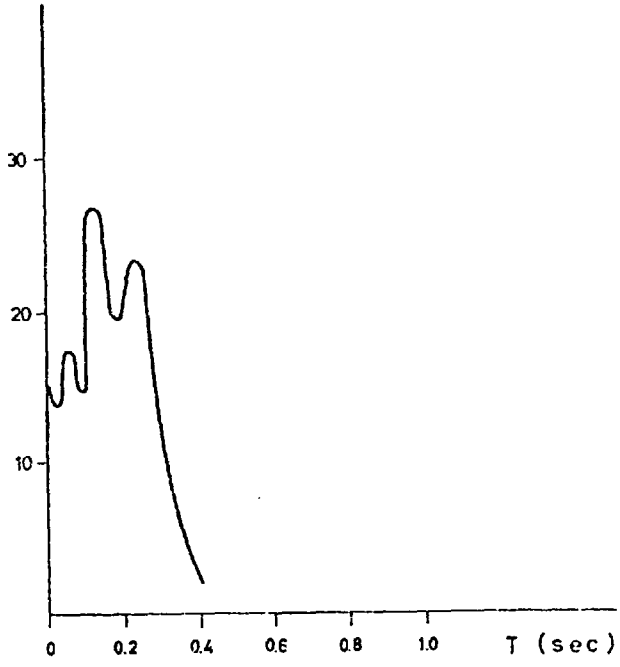


FIG. III. 19

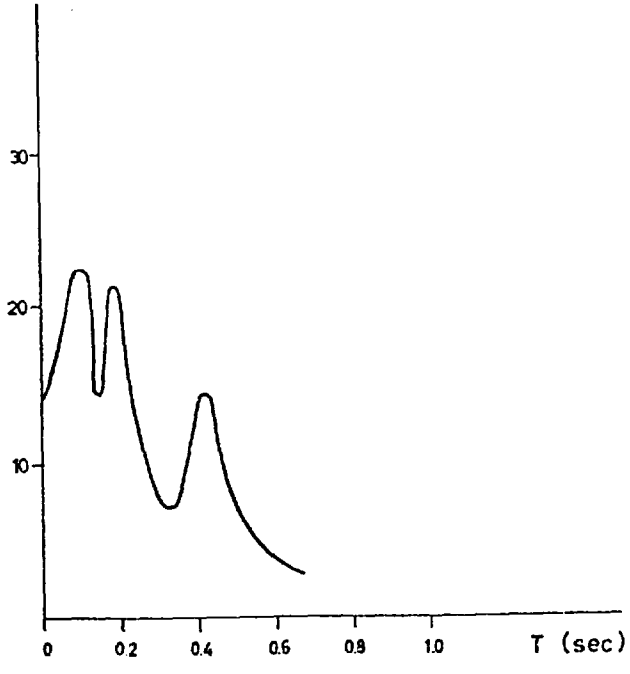
Point: 41



Point: 42



Point: 43



Point: 44

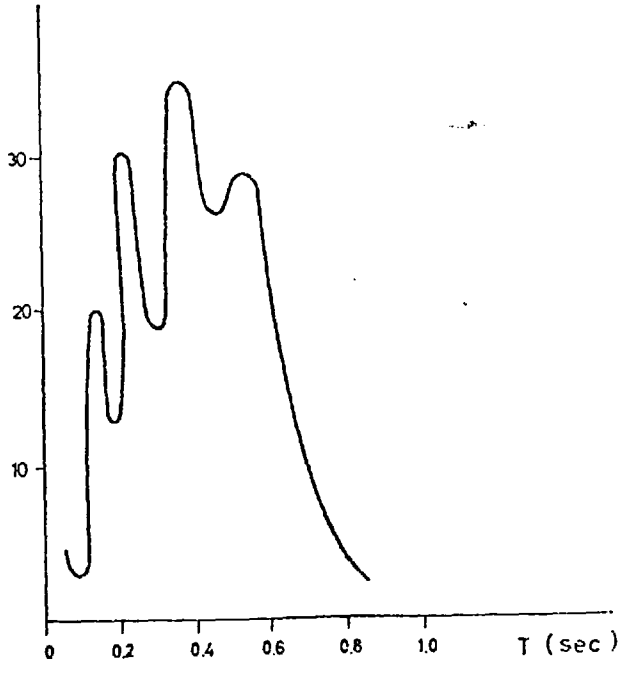
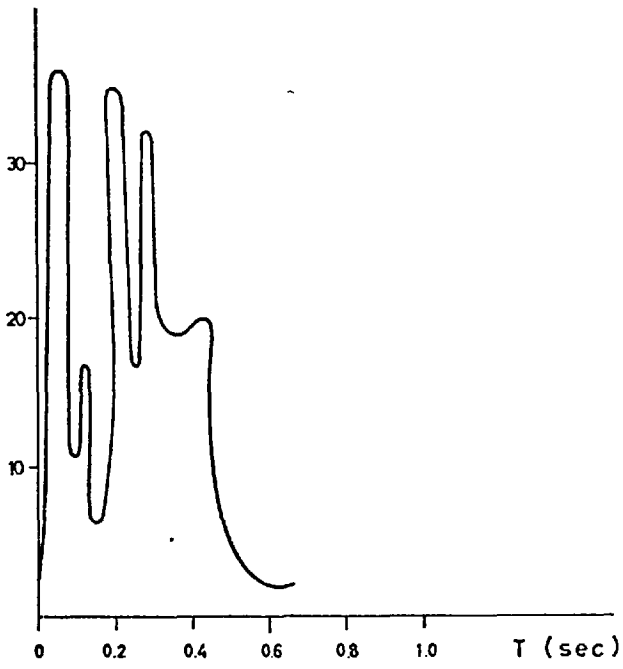
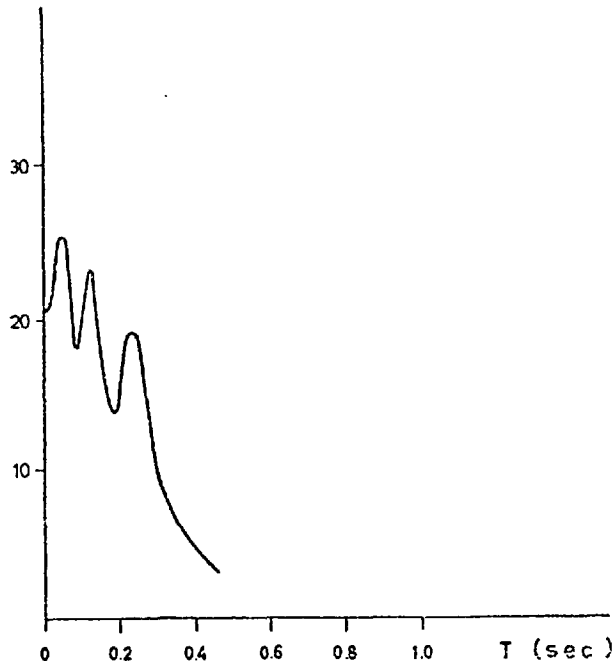


FIG. 29

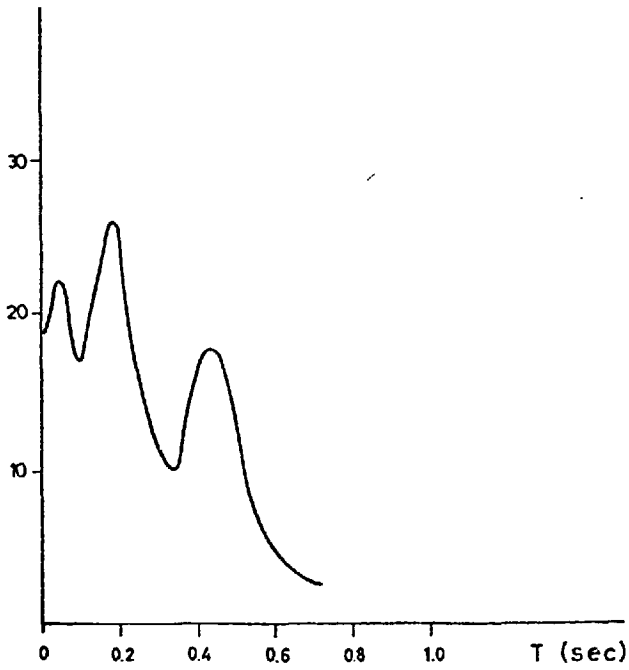
Point: 45



Point: 46



Point: 47



Point: 48

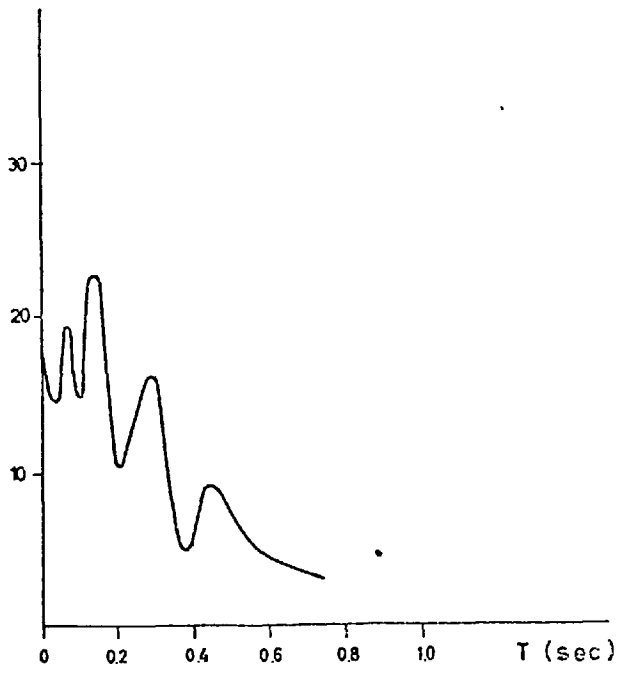
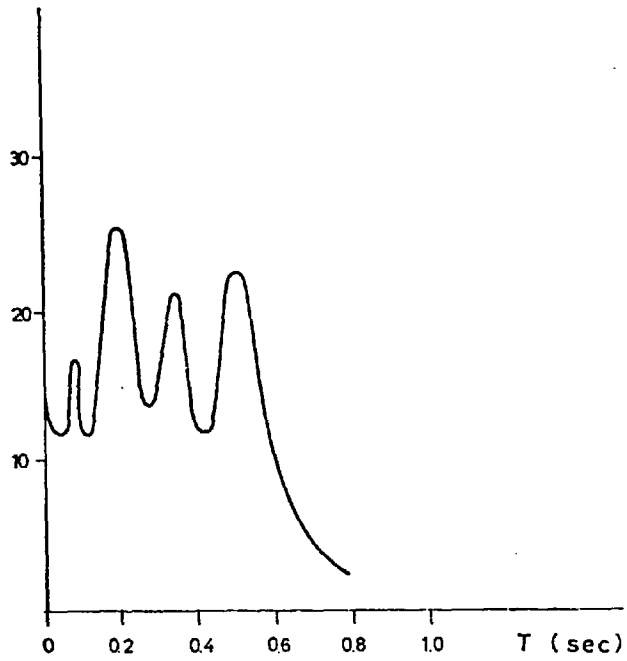
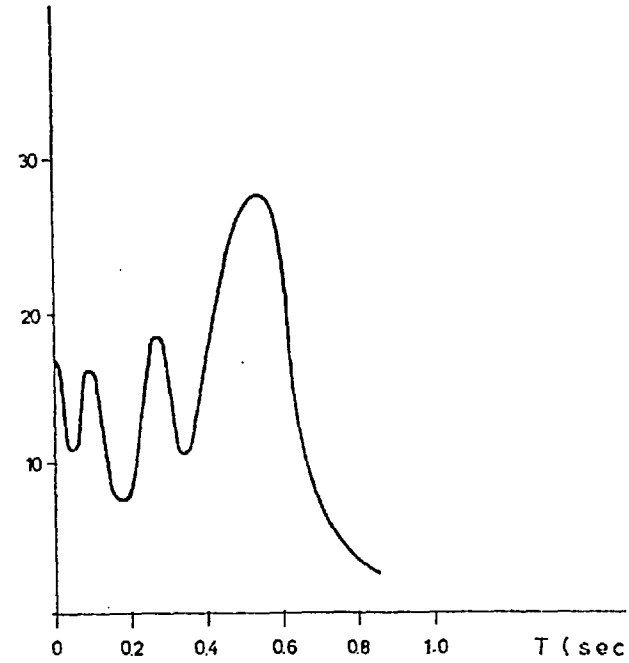


FIG III.21

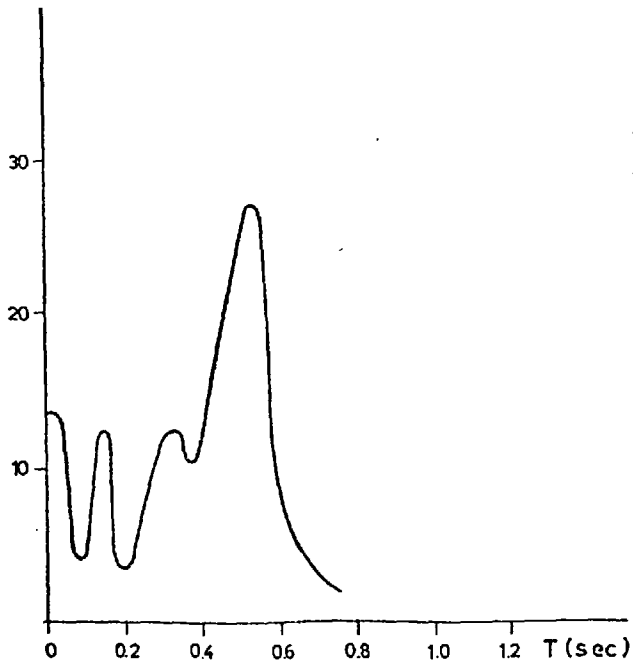
Point: 49



Point: 50



Point: 51



Point: 52

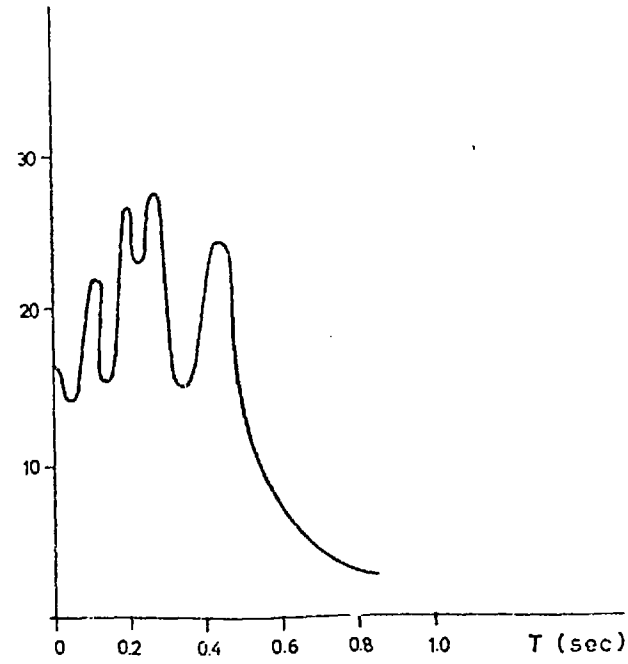
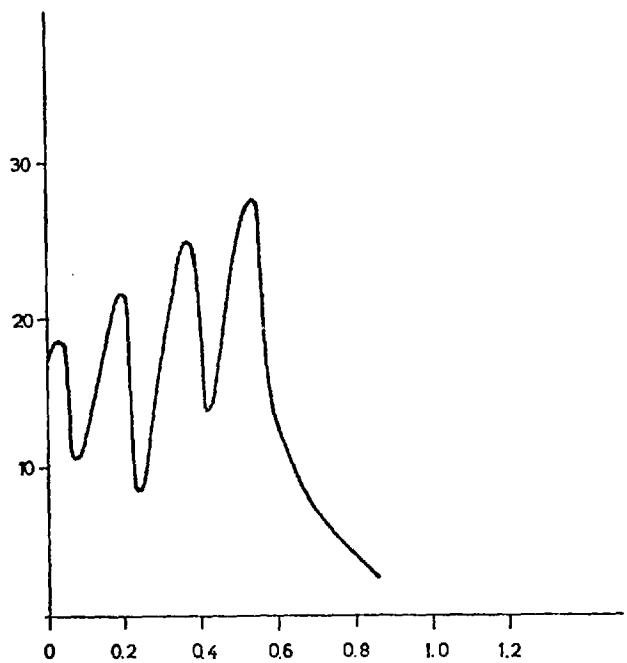
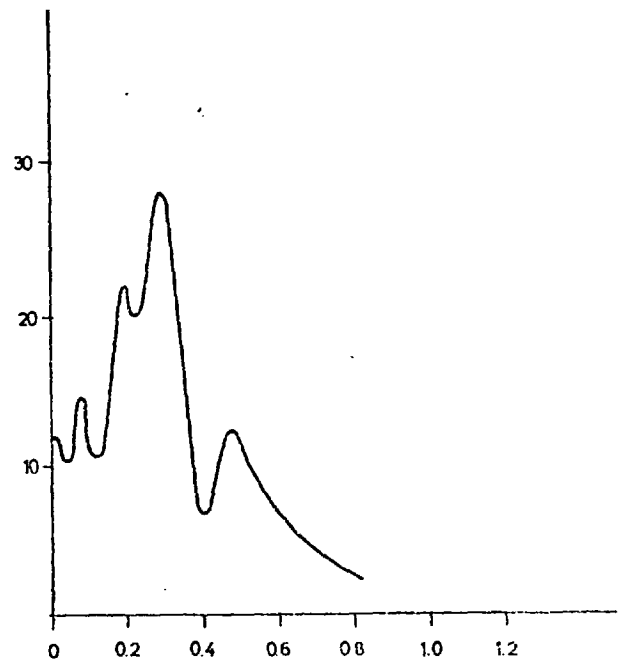


FIG. III. 22

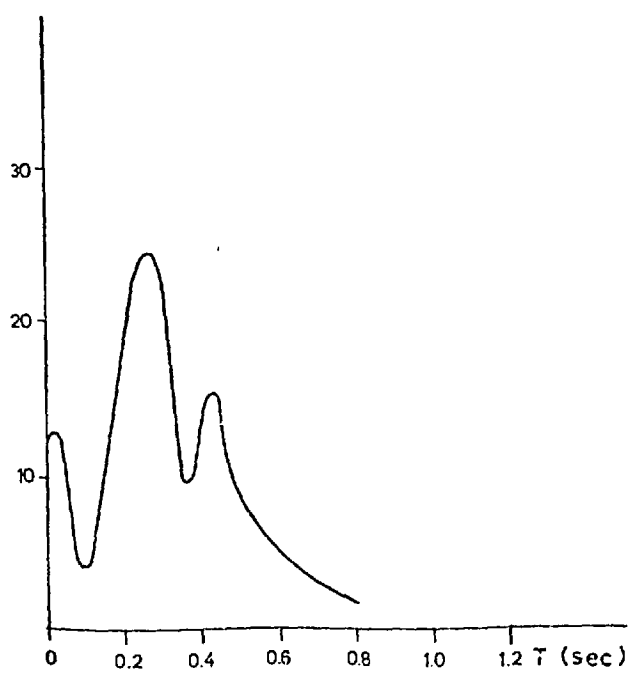
Point: 53



Point: 54



Point: 55



Point: 56

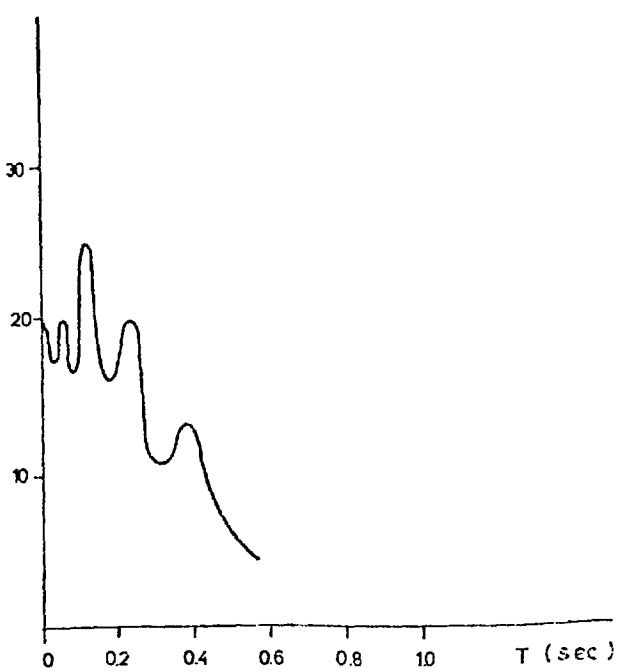
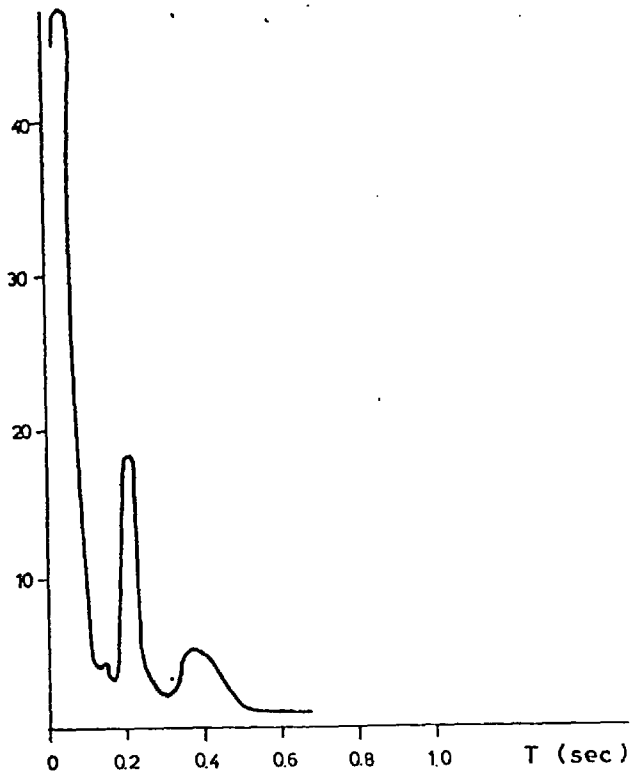
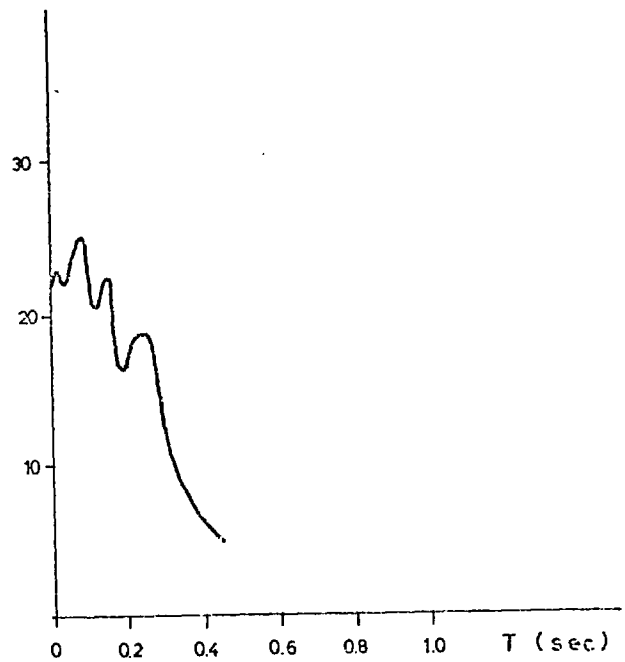


FIG. III.23

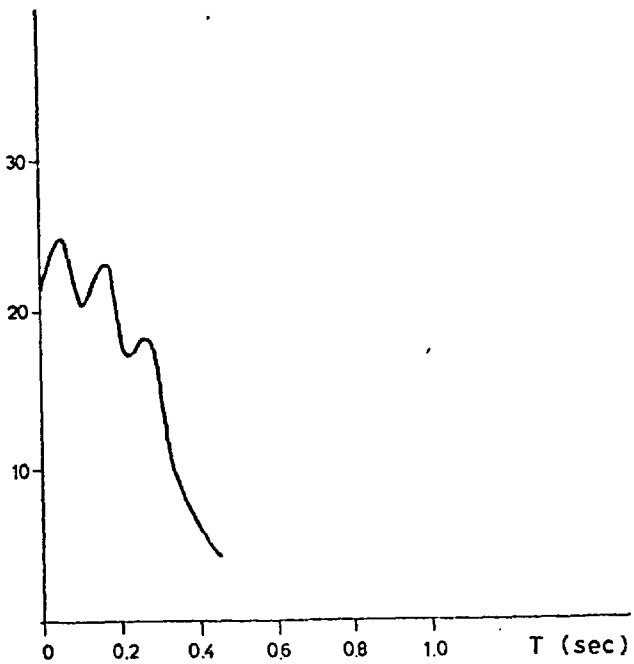
Point: 57



Point: 58



Point: 59



Point: 60

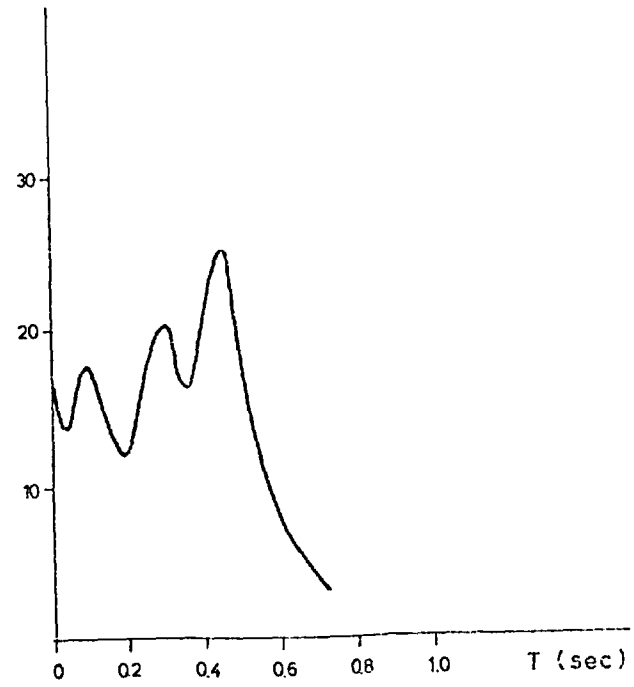
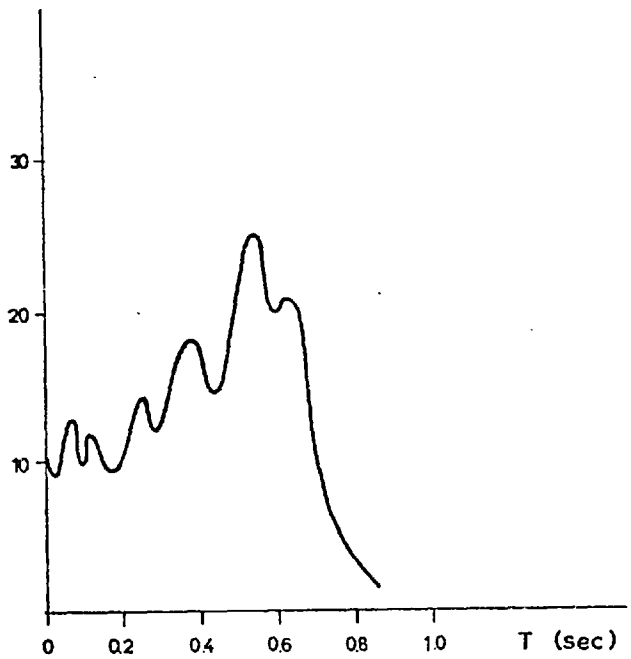
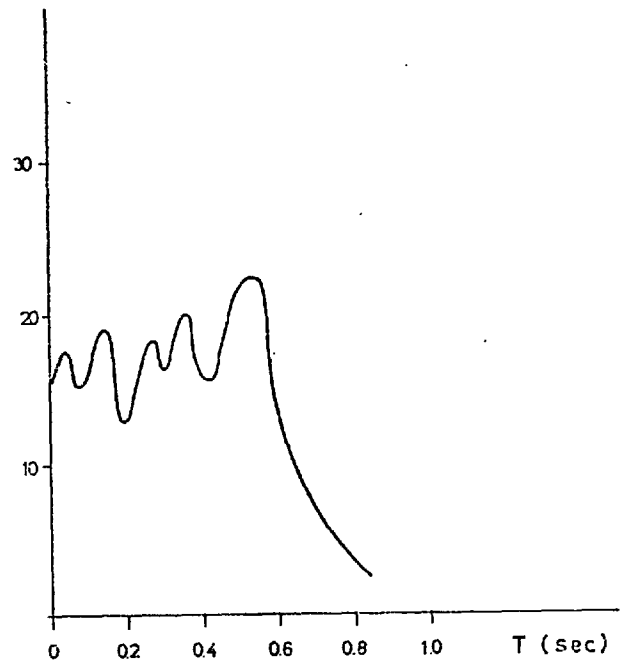


FIG. III. 24

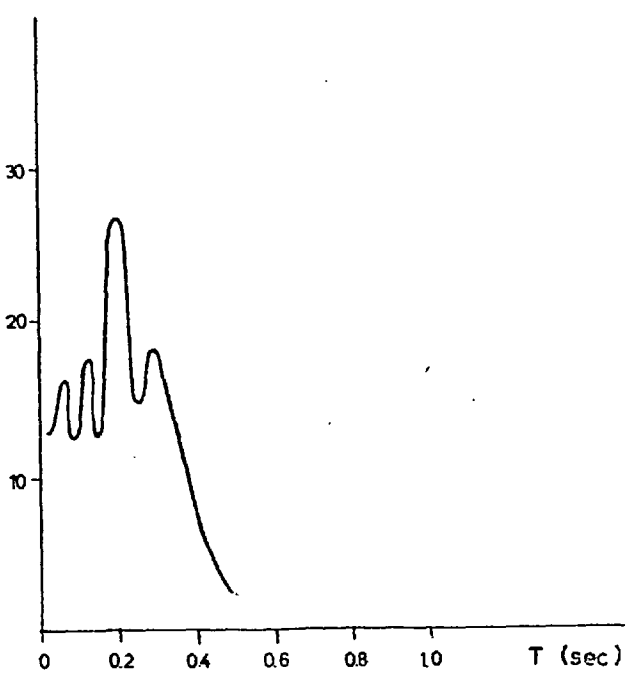
Point: 61



Point: 62



Point : 63



Point : 64

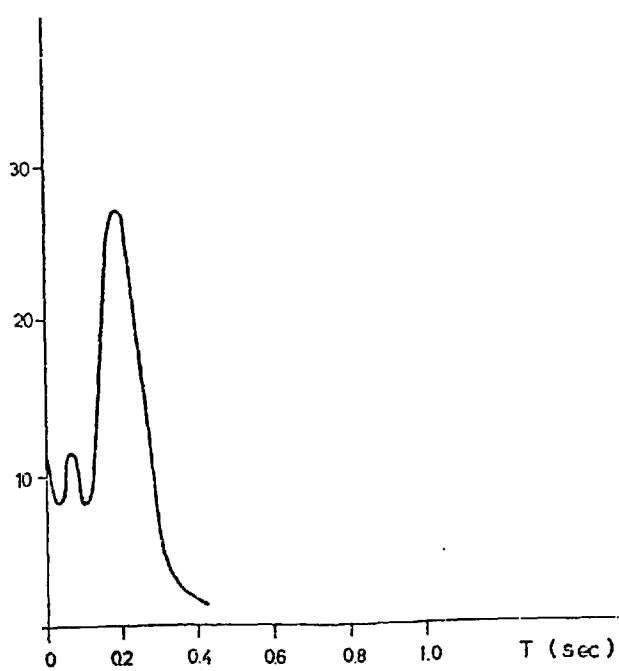
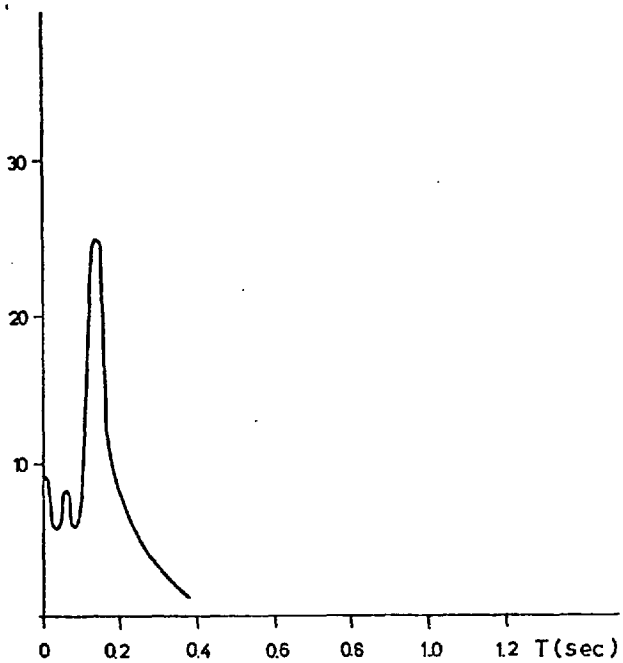
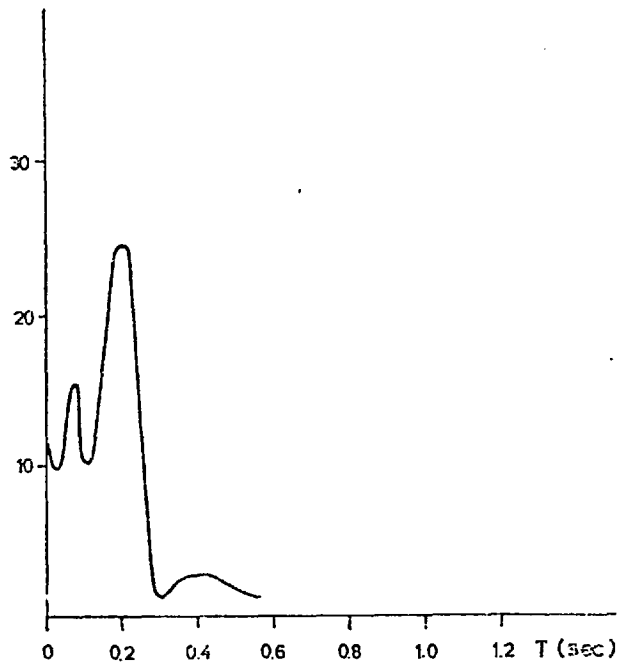


FIG. III. 25

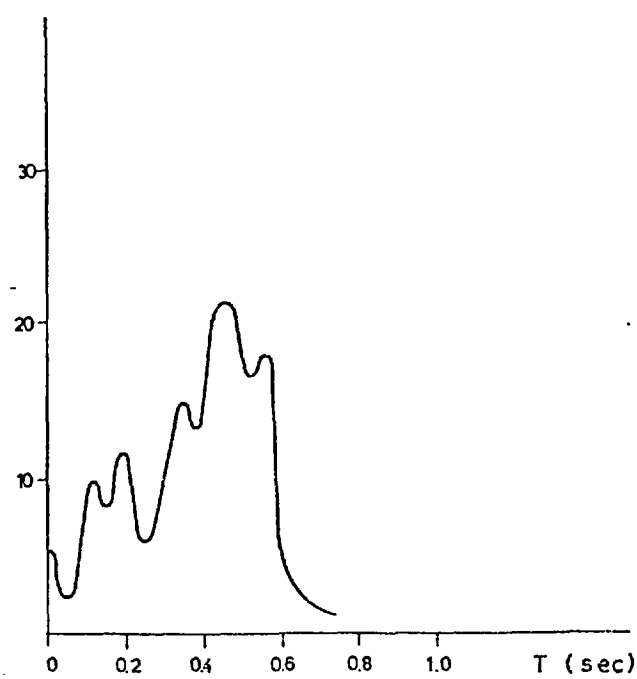
Point: 65



Point: 66



Point: 67



Point: 68

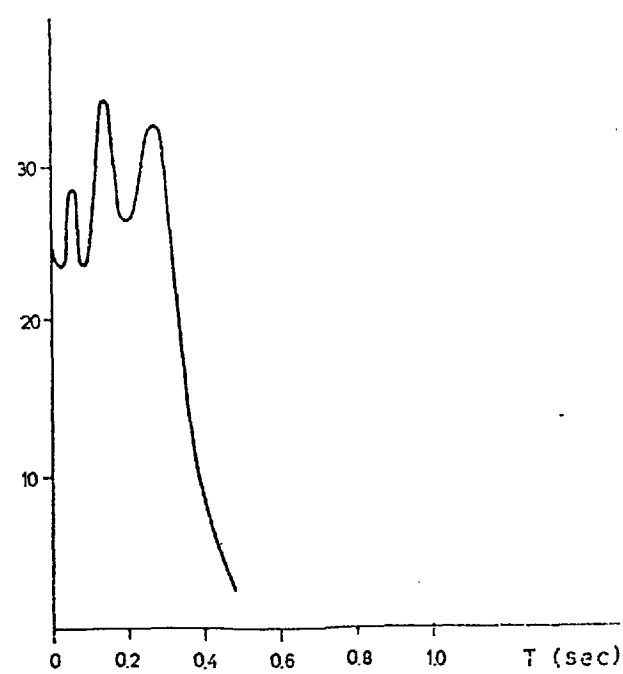
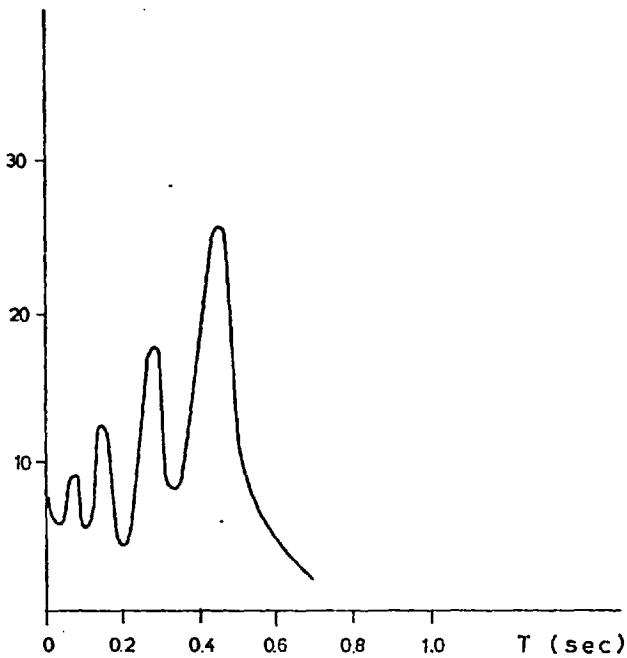
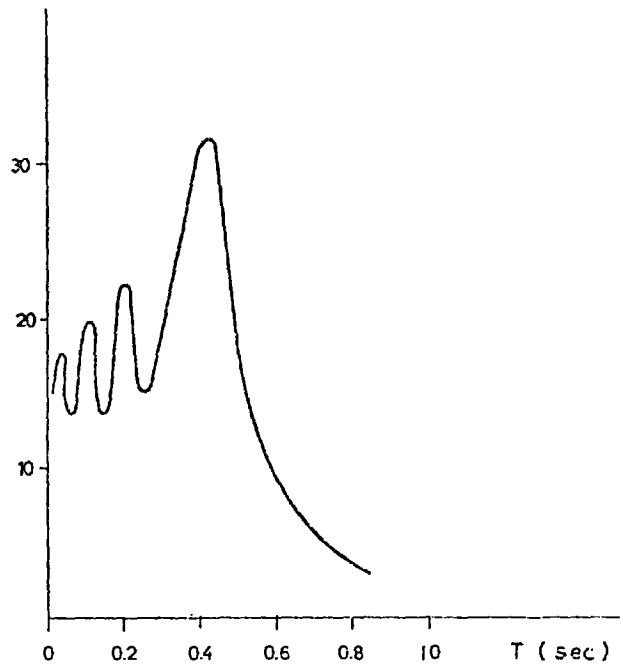


FIG III. 26

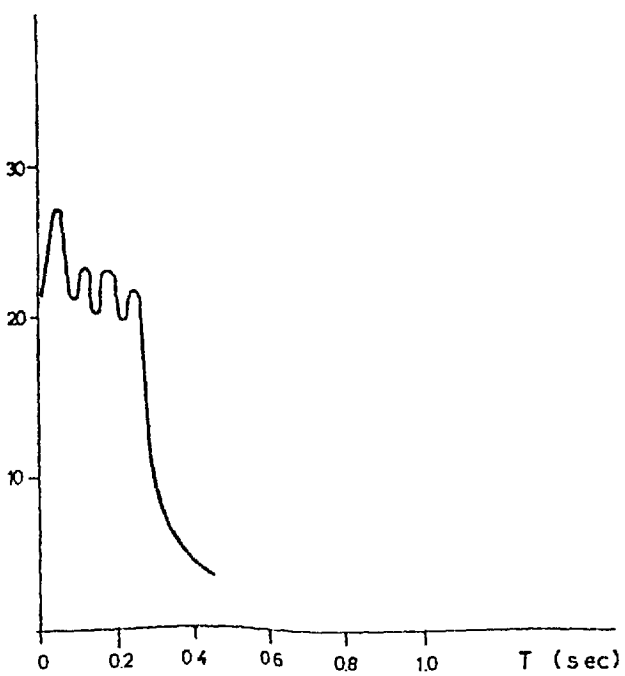
Point: 69



Point: 70



Point : 71



Point : 72

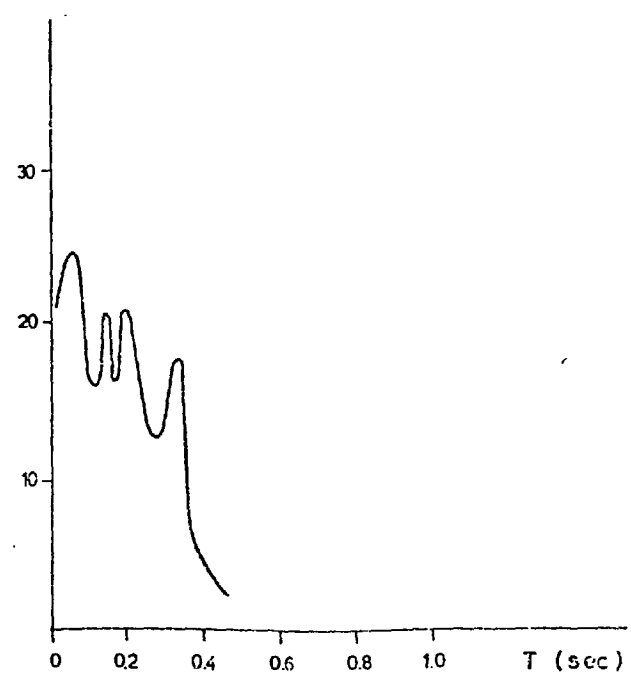
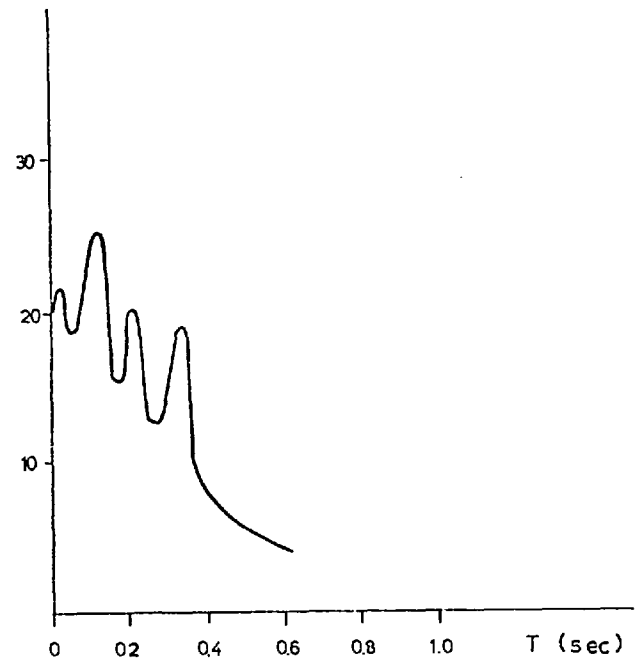
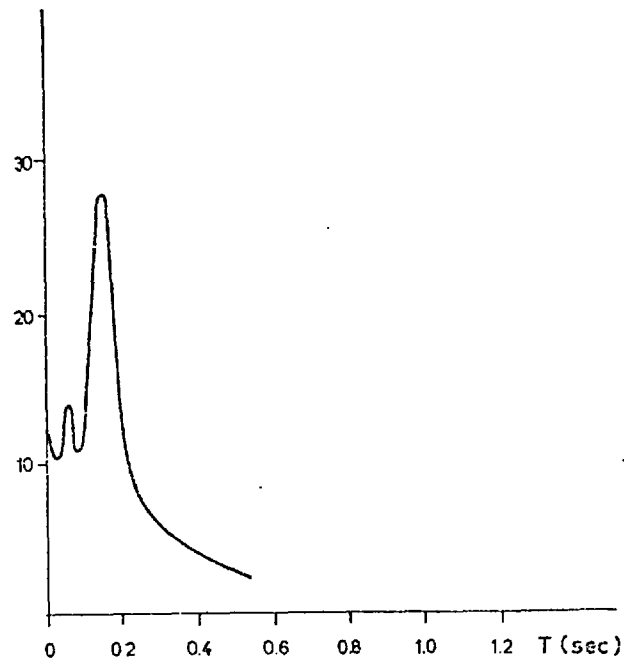


FIG. III.27

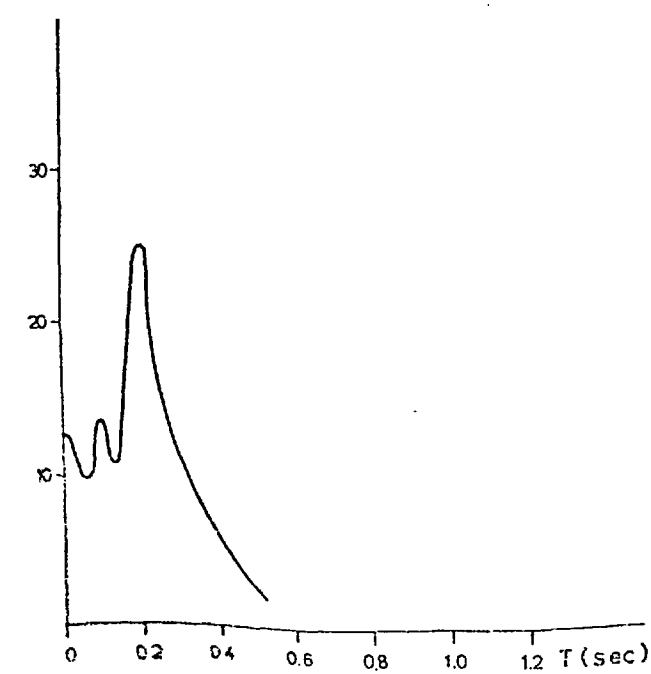
Point : 73



Point : 74



Point : 75



Point : 76

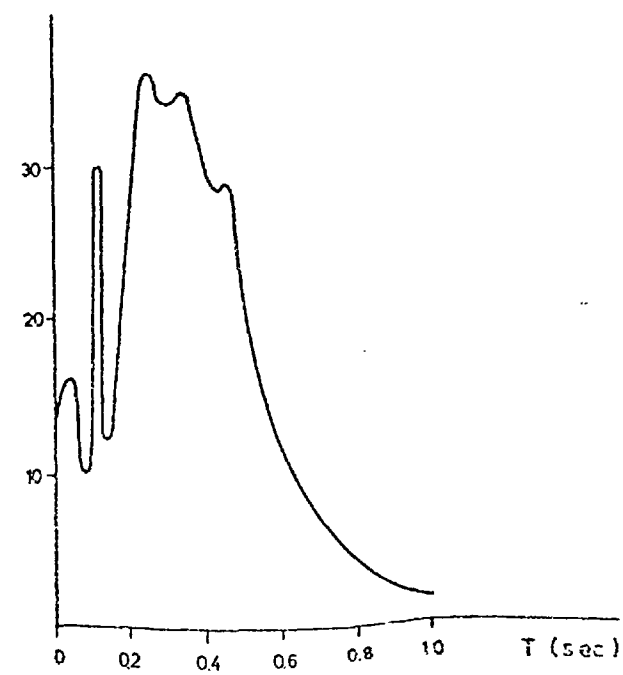
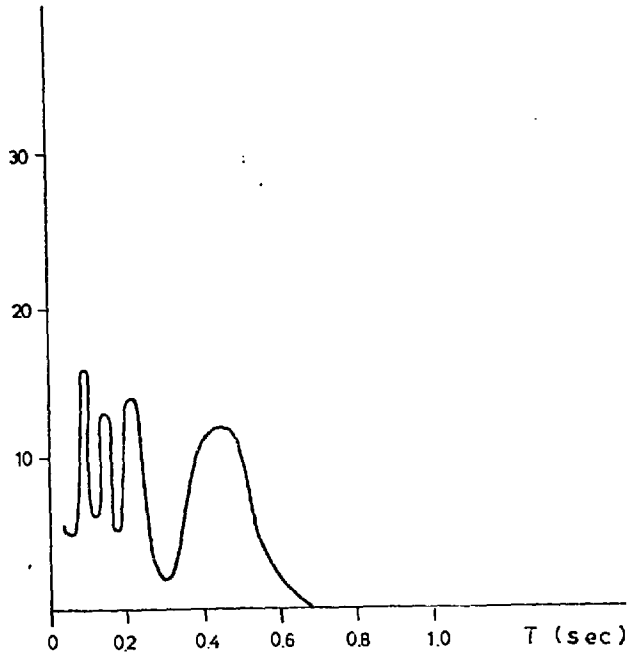
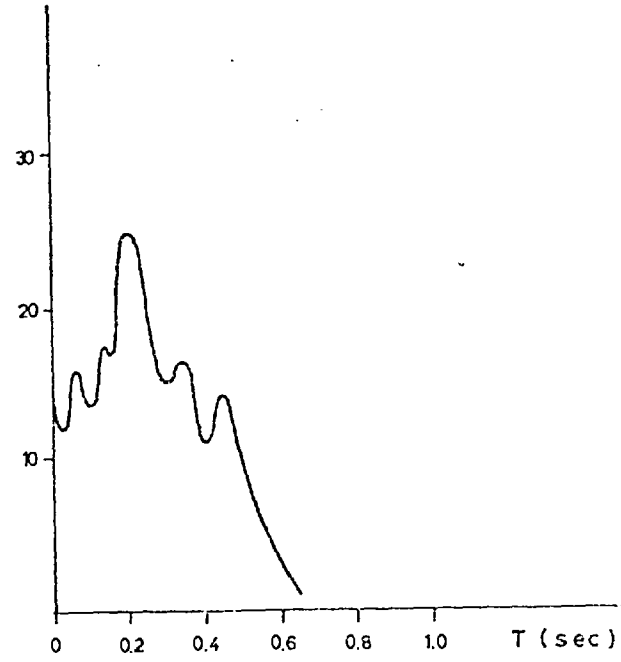


FIG. III.28

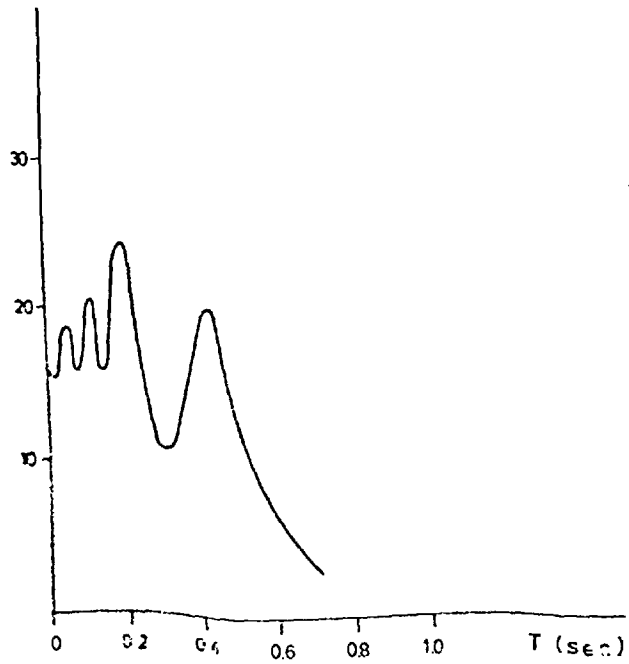
Point: 77



Point: 78



Point: 79



Point: 80

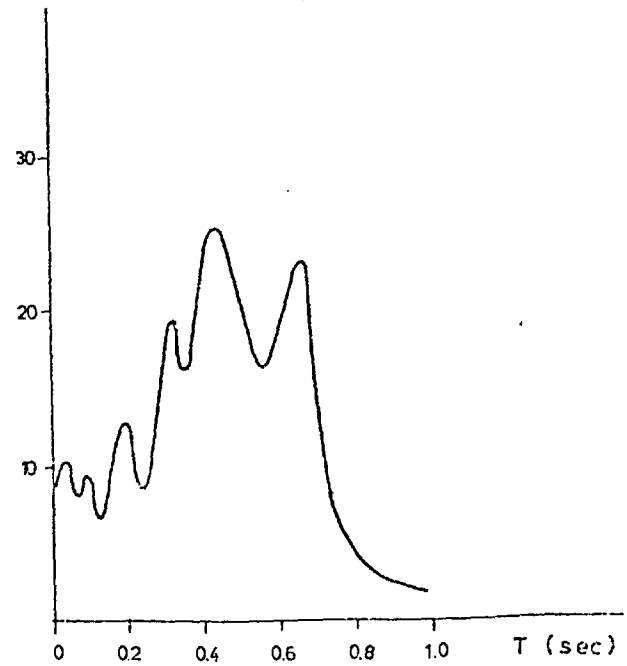
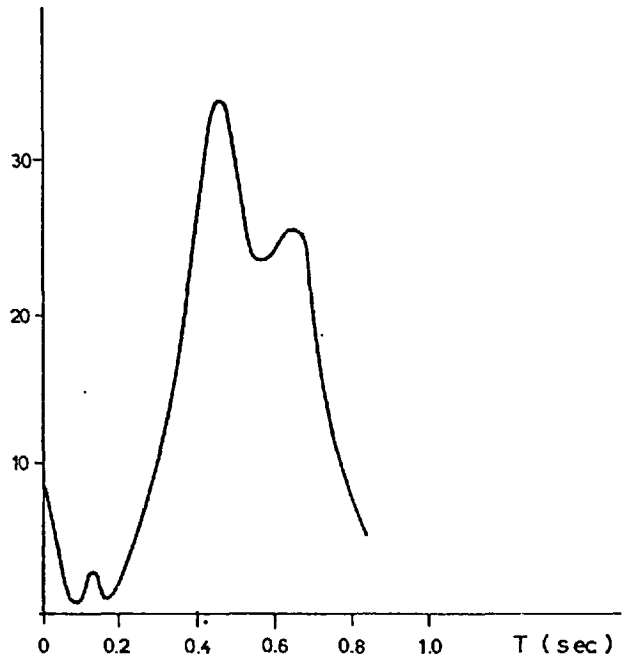
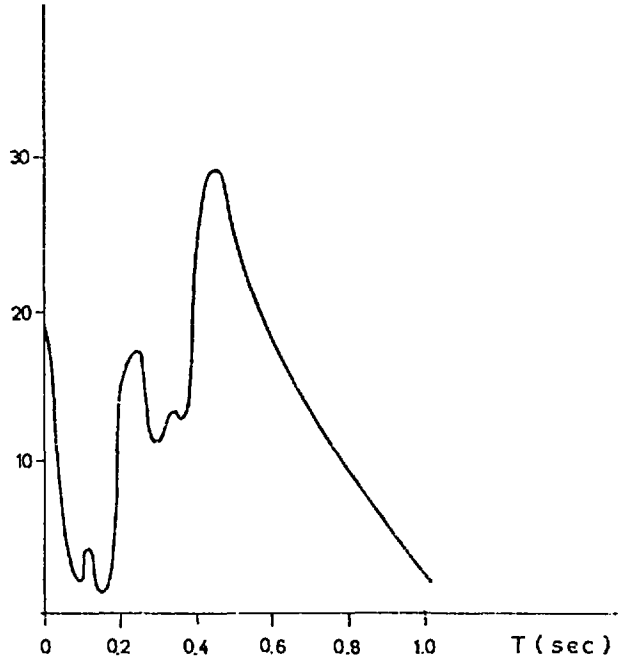


FIG. III.29

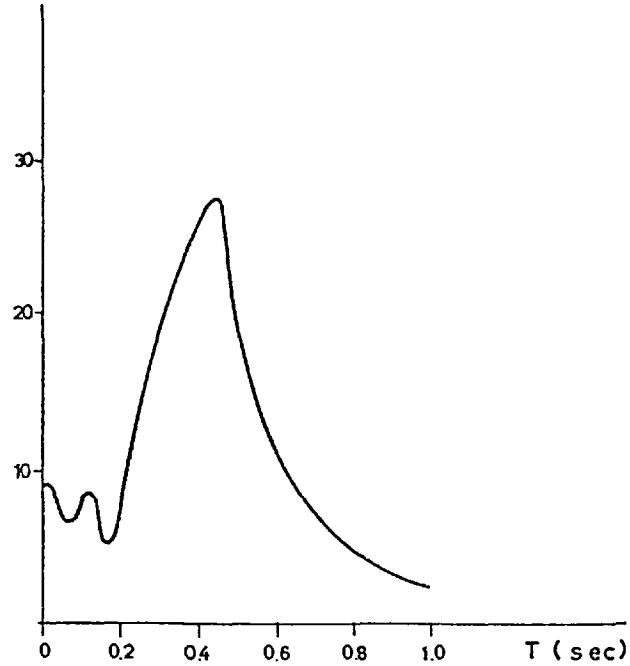
Point: 81



Point: 82



Point: 83



Point: 84

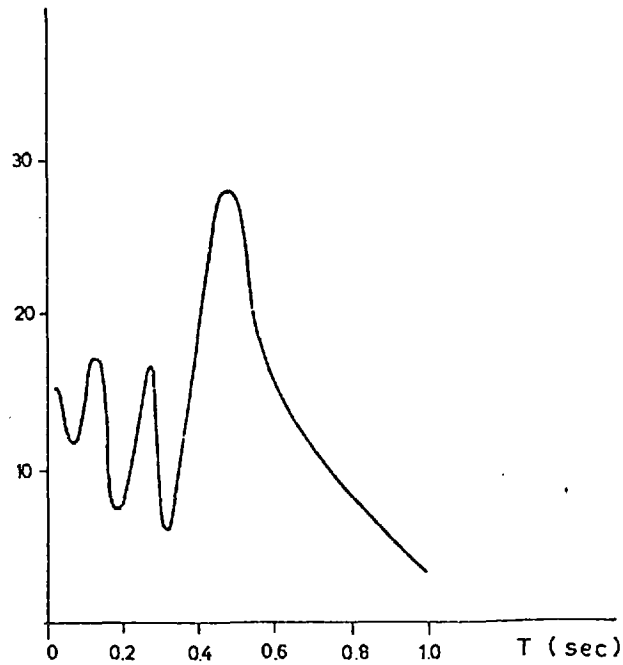
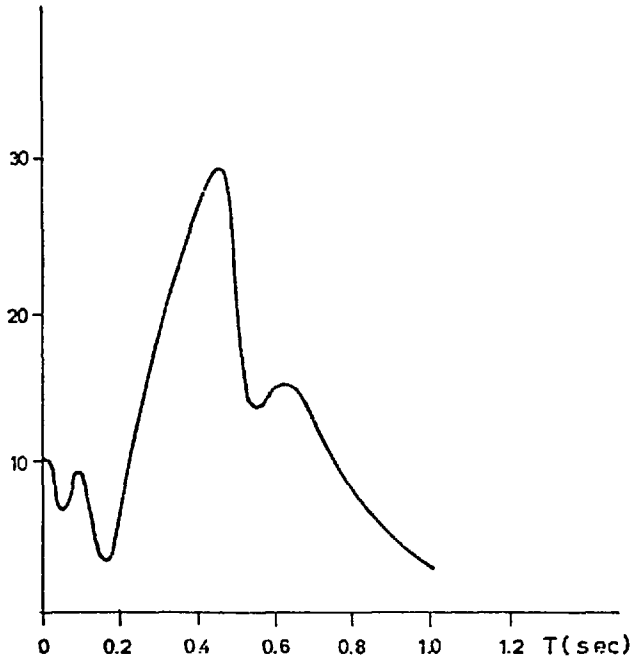
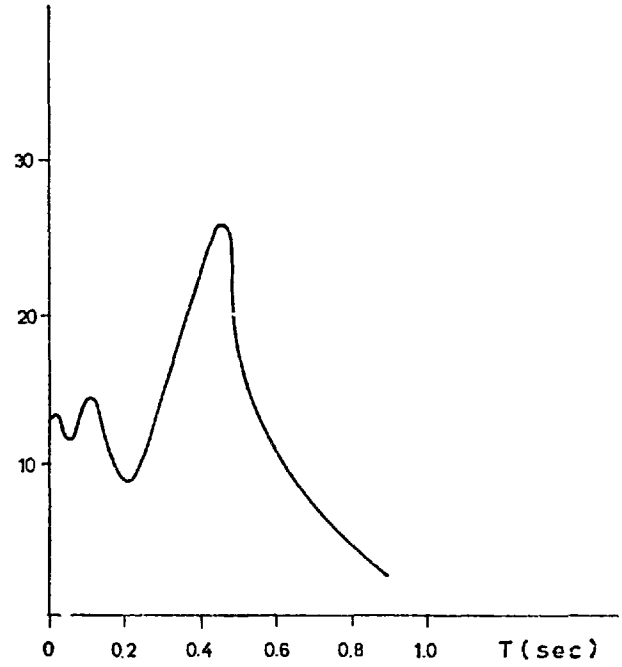


FIG. III. 30

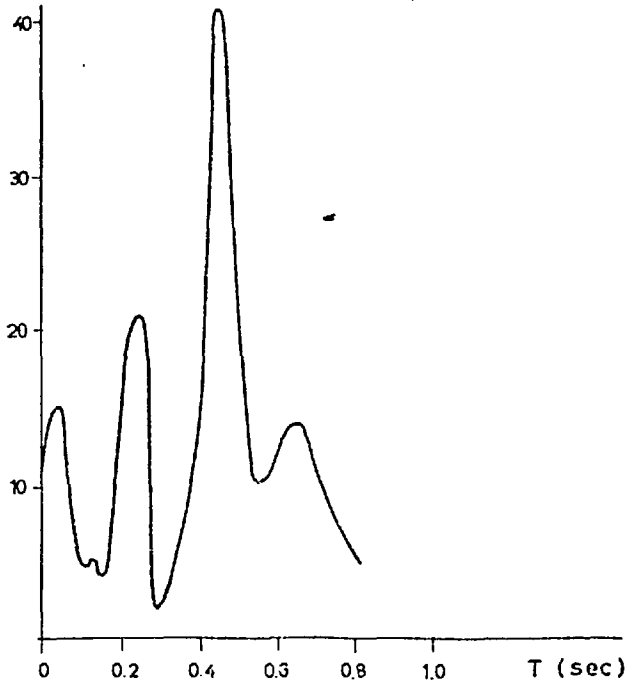
Point: 85



Point: 86



Point: 87



Point: 88

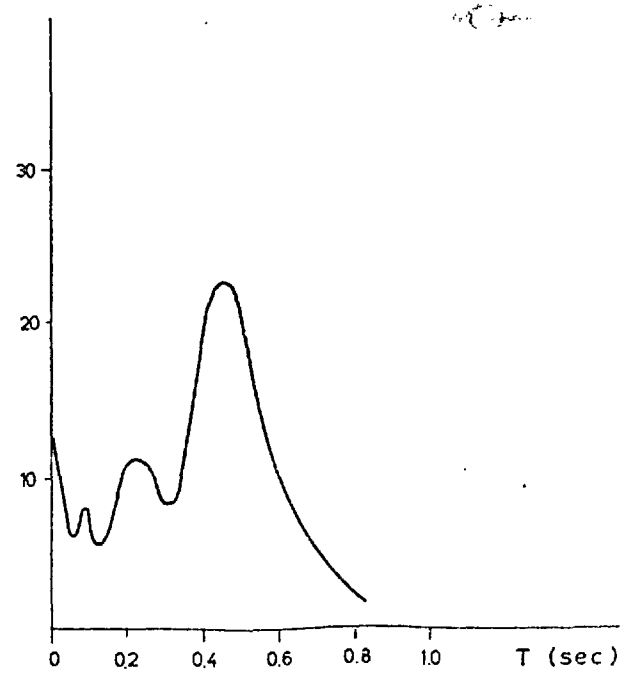
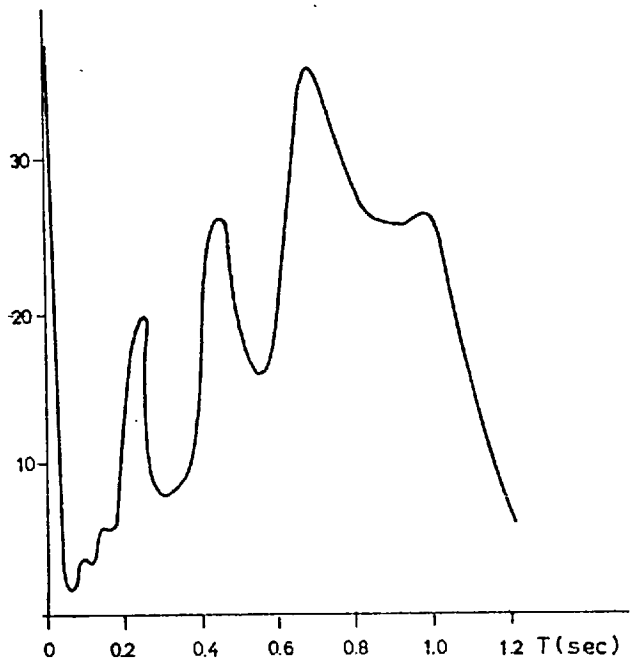
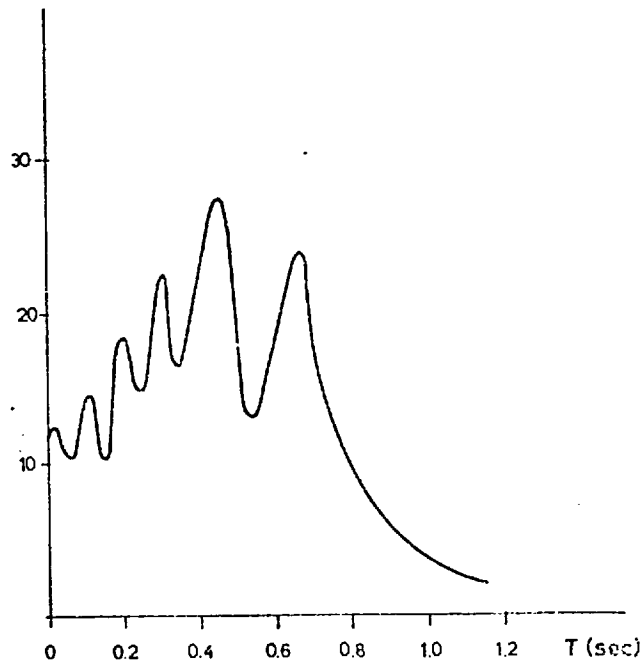


FIG. 33

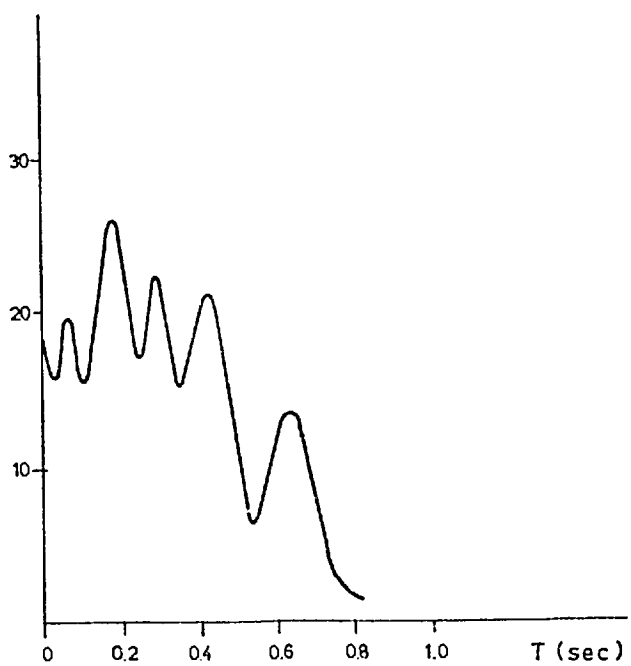
Point: 89



Point: 90



Point: 91



Point: 92

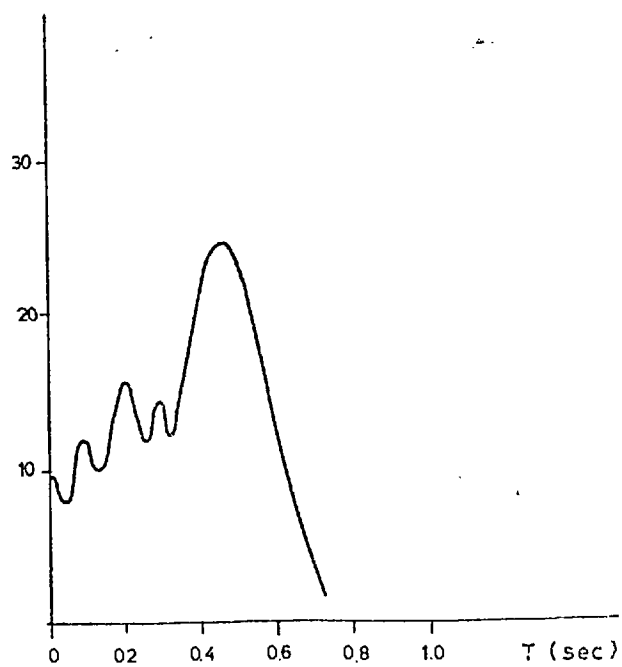
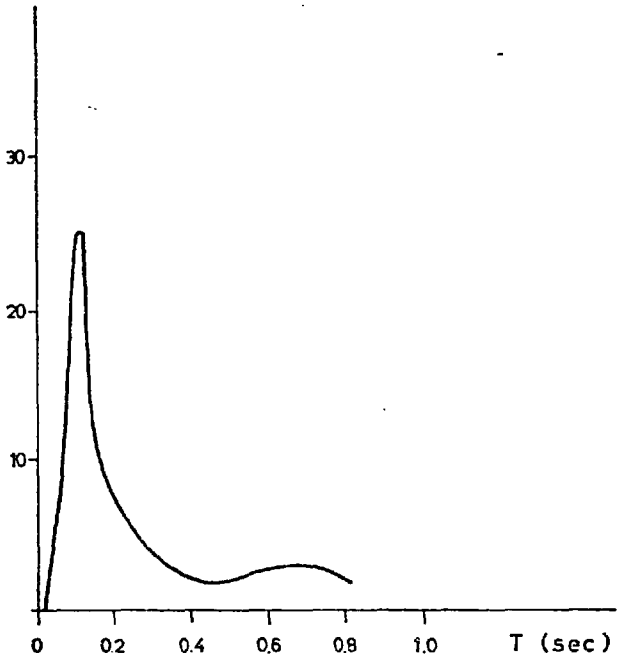
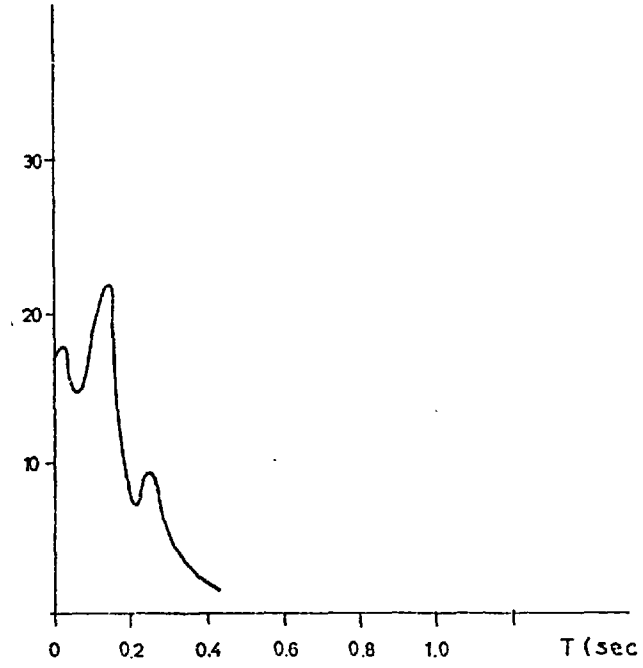


FIG. [illegible]

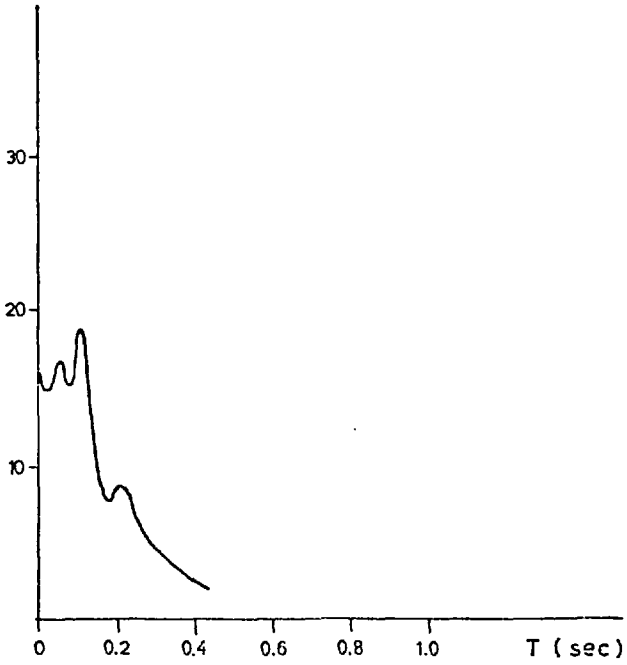
Point: 93



Point: 94



Point: 95



Point: 96

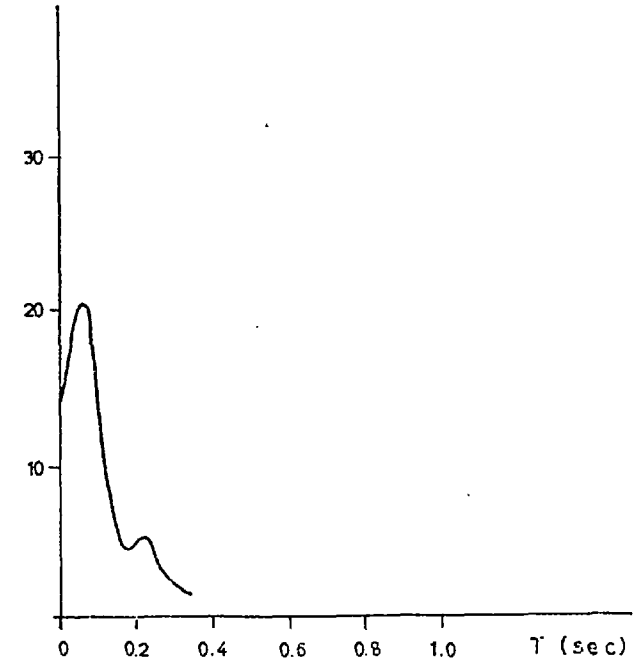
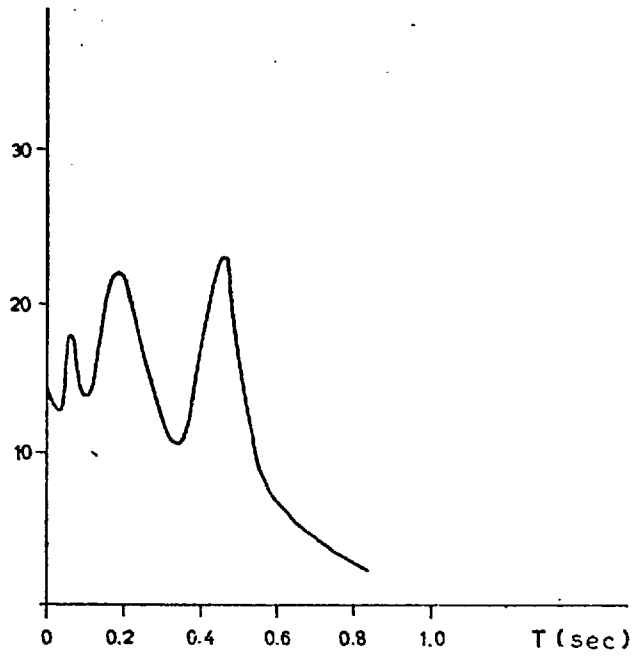
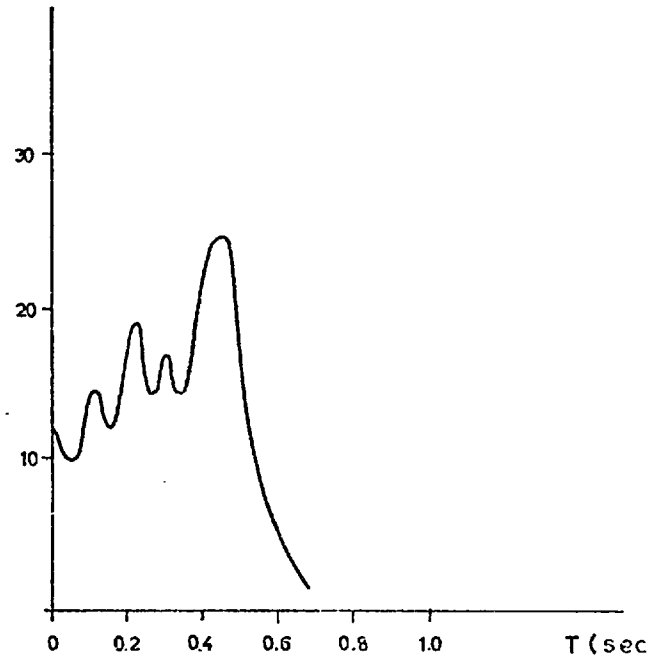


FIG.31.35

Point: 97



Point: 98



Point: 99

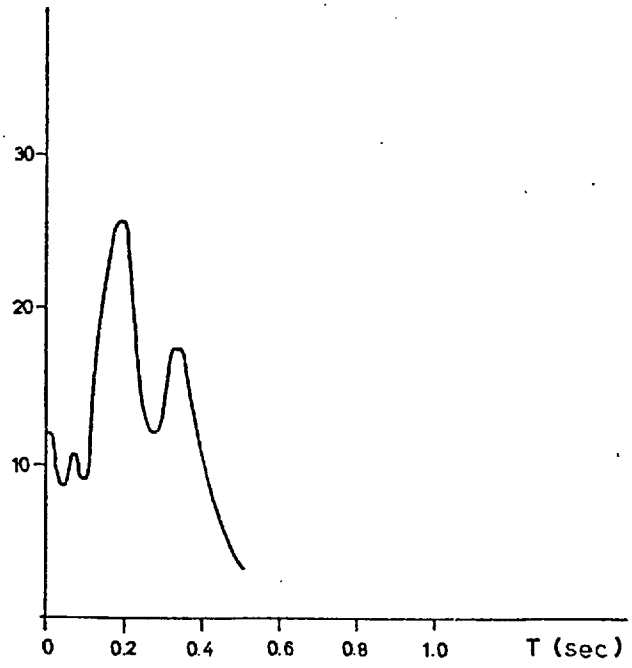


FIG. 23.3

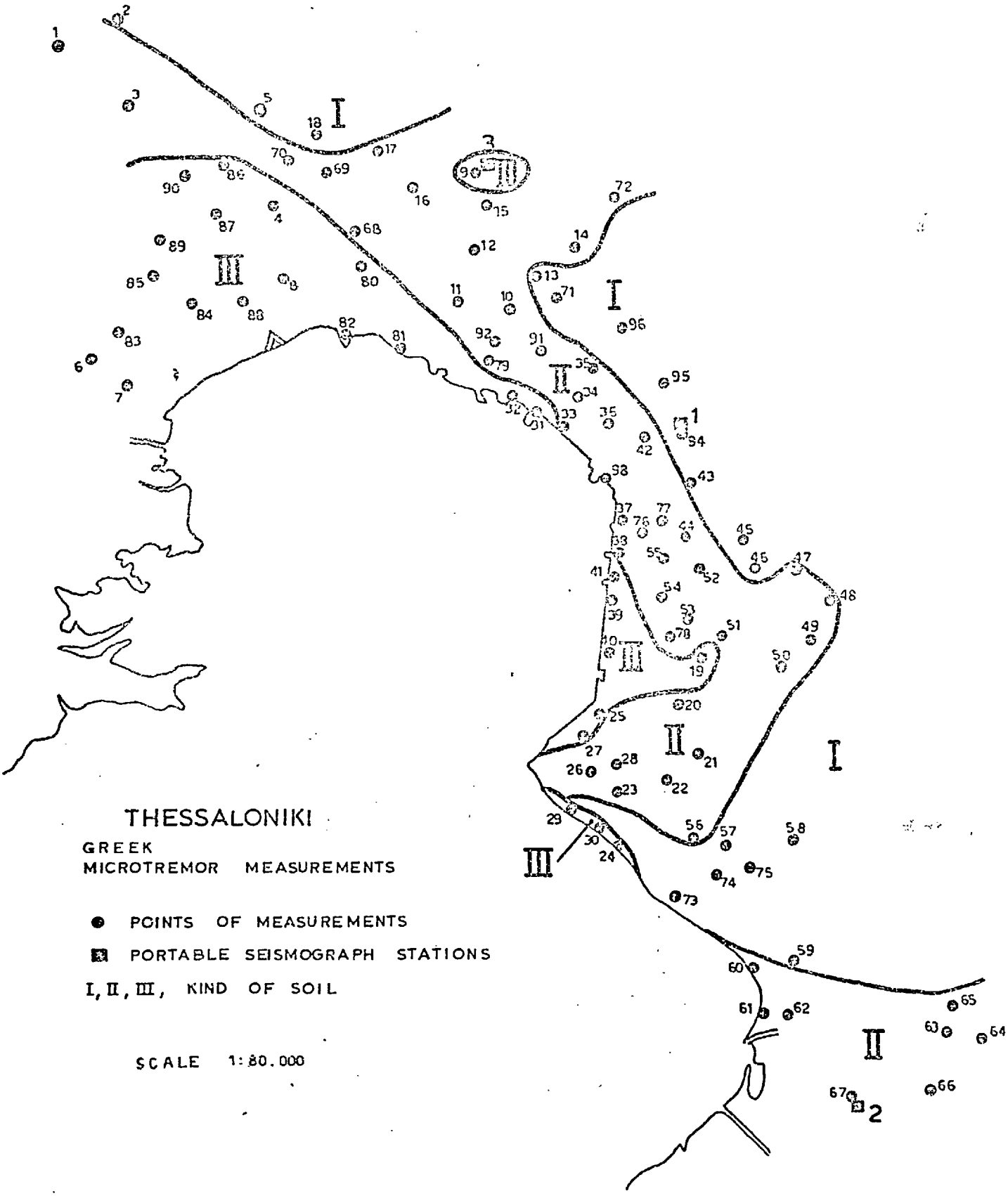
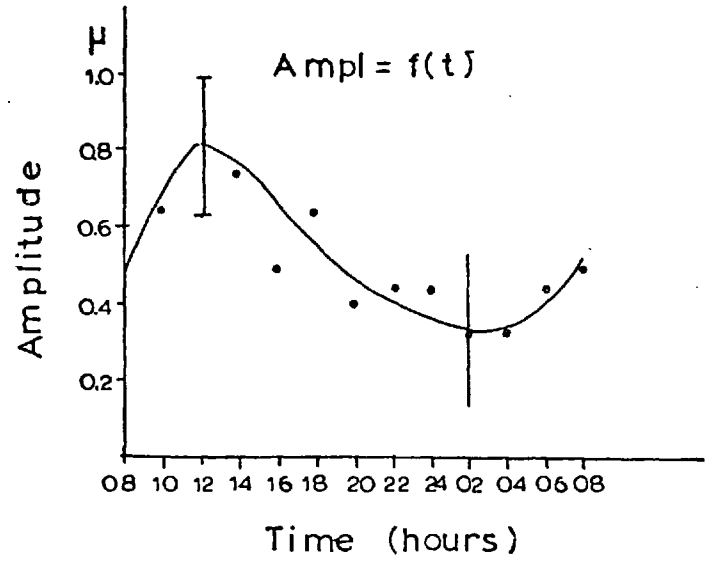
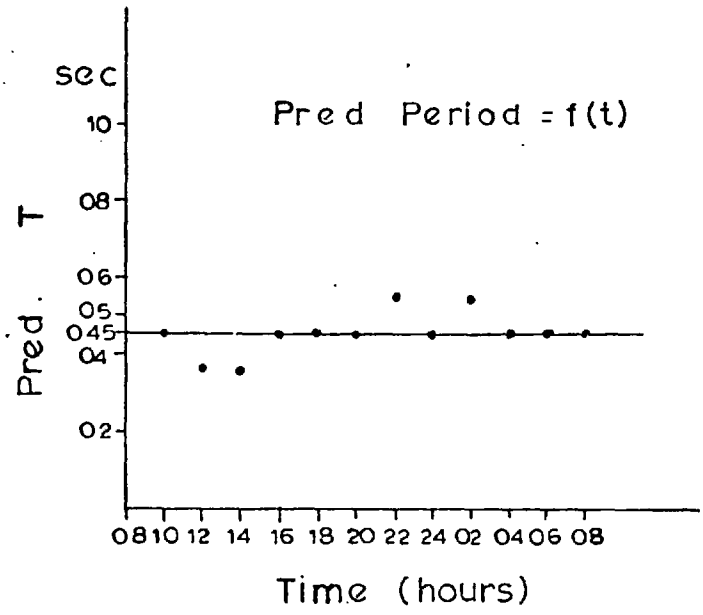

THESSALONIKI
GREEK
MICROTREMOR MEASUREMENTS
● POINTS OF MEASUREMENTS
▣ PORTABLE SEISMOGRAPH STATIONS
I, II, III, KIND OF SOIL
SCALE 1:80.000

FIG. III. 35

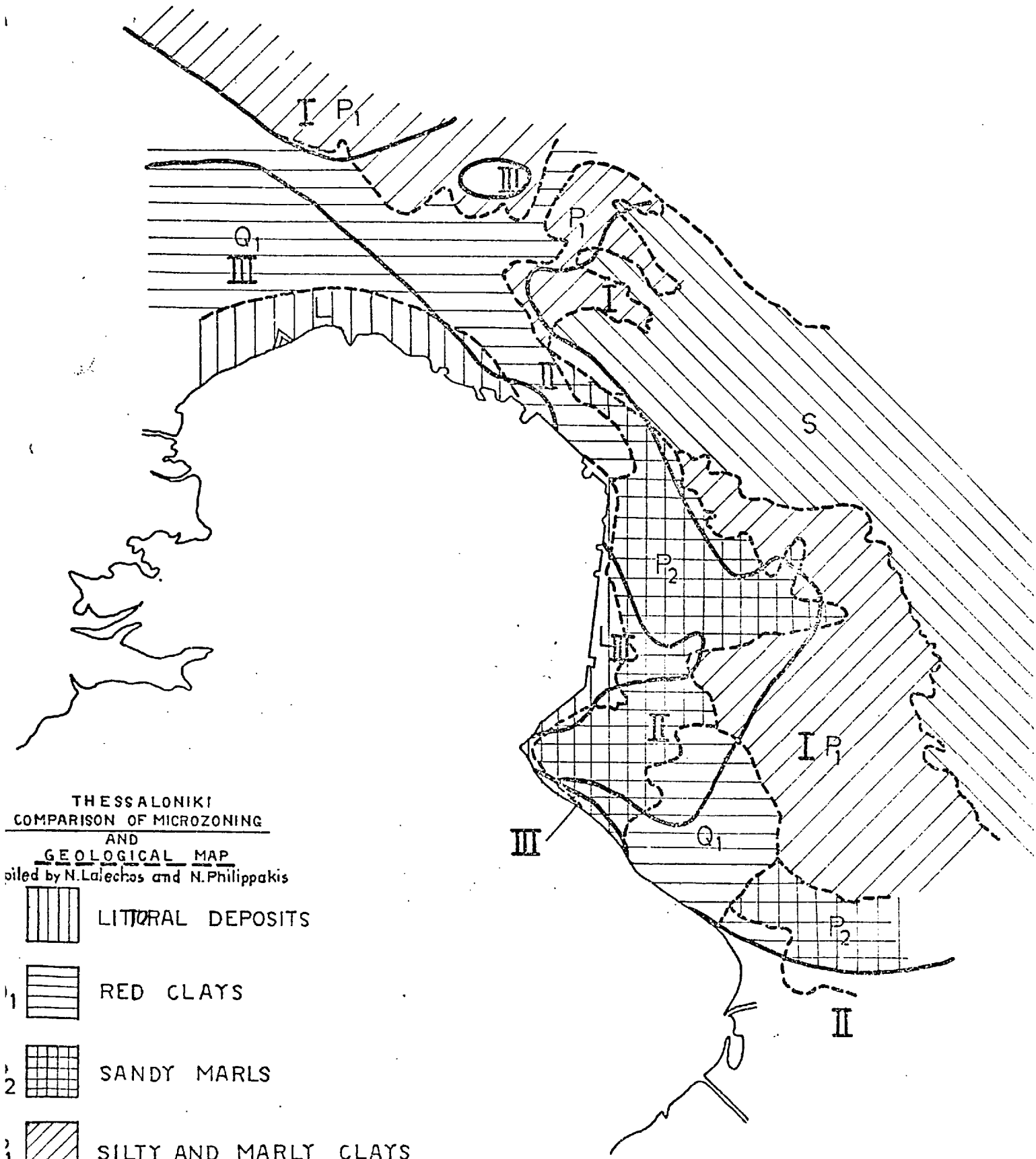

μ
Ampl = f(t)
Amplitude
1.0
0.8
0.6
0.4
0.2
08 10 12 14 16 18 20 22 24 02 04 06 08
Time (hours)

(α)


sec
Pred Period = f(t)
Pred. T
10
08
06
05
045
04
02
08 10 12 14 16 18 20 22 24 02 04 06 08
Time (hours)

(β)

FIG III. 36



THESSALONIKI
COMPARISON OF MICROZONING
AND
GEOLOGICAL MAP
piled by N. Lalechos and N. Philippakis

LITTORAL DEPOSITS

Q1 RED CLAYS

P2 SANDY MARLS

P1 SILTY AND MARLY CLAYS

S BASEMENT

FIG. III, 37

GREEK ZONING
KIND OF SOIL I, II, III.
SCALE 1:80.000

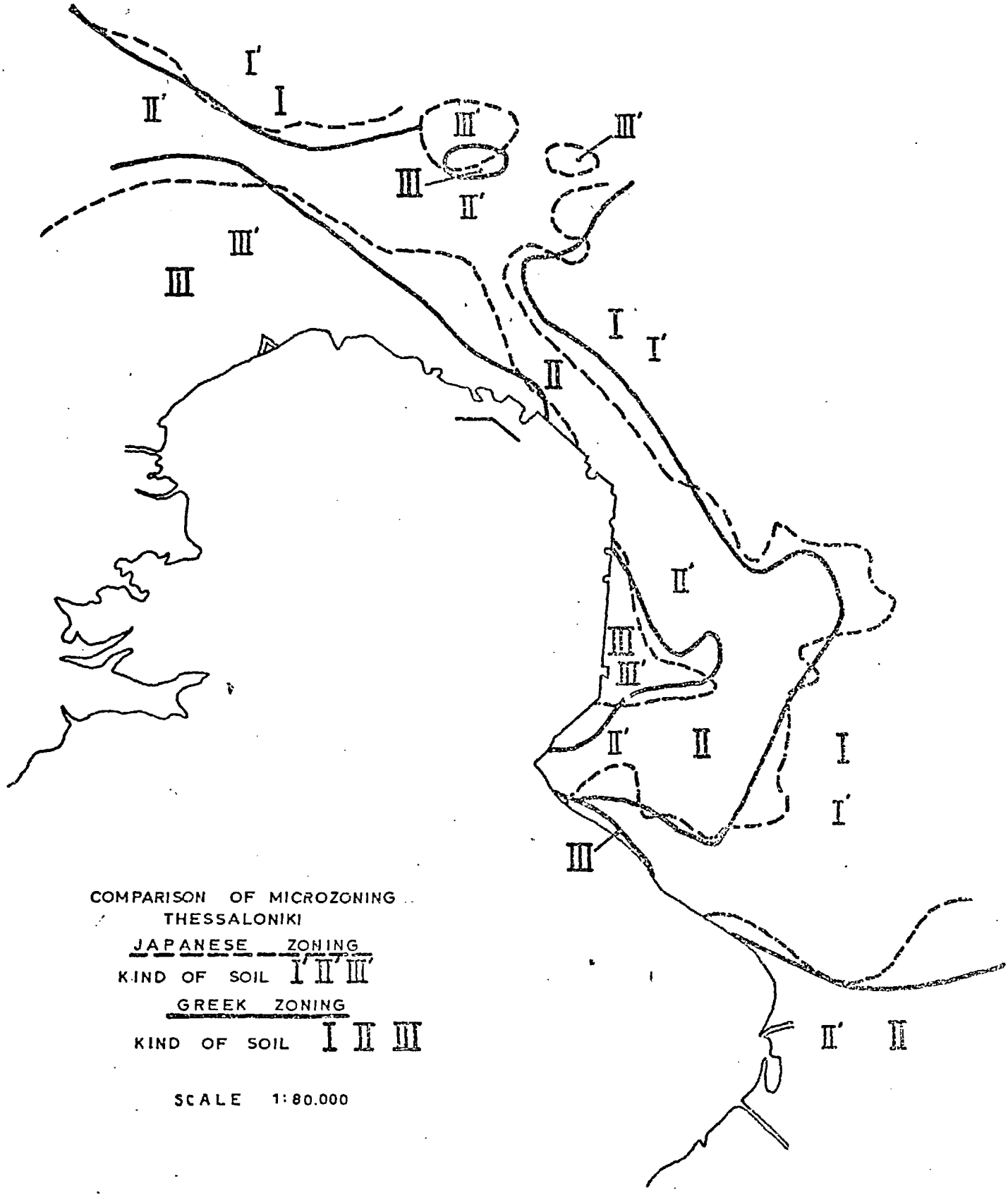
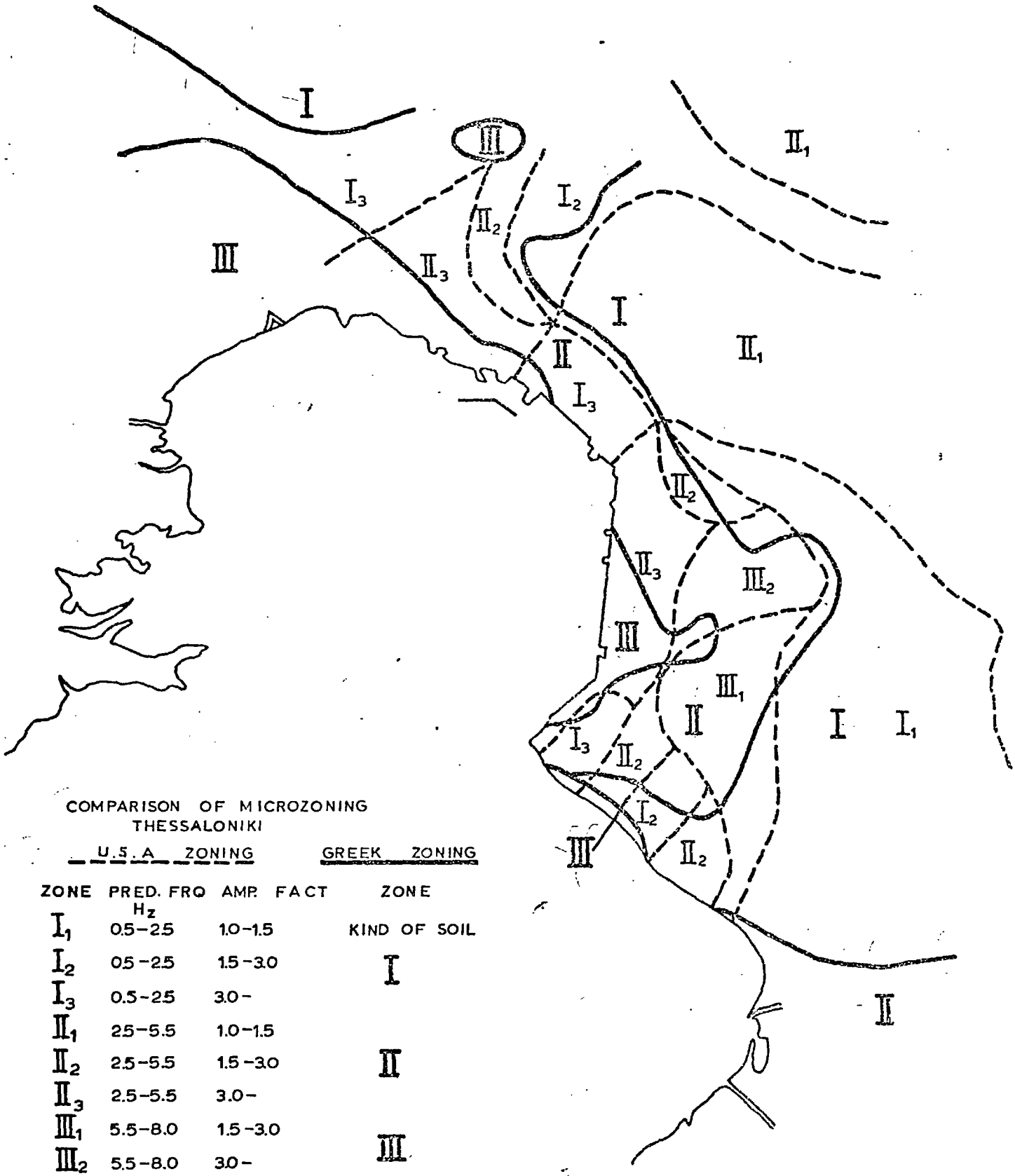

COMPARISON OF MICROZONING
THESSALONIKI
JAPANESE ZONING
KIND OF SOIL I' II' III'
GREEK ZONING
KIND OF SOIL I II III
SCALE 1:80.000

FIG. III.38



COMPARISON OF MICROZONING
THESSALONIKI

U.S.A ZONING			GREEK ZONING
ZONE	PRED. FRQ Hz	AMP. FACT	ZONE
I_1	0.5–2.5	1.0–1.5	KIND OF SOIL
I_2	0.5–2.5	1.5–3.0	I
I_3	0.5–2.5	3.0–	
II_1	2.5–5.5	1.0–1.5	
II_2	2.5–5.5	1.5–3.0	II
II_3	2.5–5.5	3.0–	
III_1	5.5–8.0	1.5–3.0	
III_2	5.5–8.0	3.0–	III

SCALE 1:80.000

FIG. III.39

APPENDIX A
BASE LINE CORRECTION

It is obvious that we can calculate ground velocities and ground displacements by integrating the acceleration data with respect to time. The many computer facilities available can simplify this effort. Usually, however, the velocity and displacement time histories resulting from such integrations drift with increasing time, and end with unrealistically high end-time velocities and displacements. This occurs when other information, as well as common sense, indicate that end-time velocity and displacement are either zero, or at least much less or different from that obtained by integration.

Errors in the acceleration data, introduced either when the data is recorded or in subsequent manipulation, apparently are responsible for the velocity and displacement discrepancies. Several investigators have reported concerning various sources of error and what techniques are available to preclude, correct, or compensate for them. It is generally agreed that the chief source of error is introduced when a base line (zero acceleration) is first inserted into the acceleration data. It can be demonstrated that a base line only slightly shifted from the true zero value - negligible compared with the acceleration peaks - is sufficient to cause the irregularities described. It is also generally agreed that the true base line cannot be determined exactly and some compensating base-line correction must be formulated and applied. The difficulties in determining the base line of an accelerogram are a) the initial part of the shock is not recorded b) the final acceleration or velocity cannot be assumed to be zero,

due to the presence of background noise c) the net displacement is not known.

Initial Condition Uncertainty

It was noted before that the initial part of the shock is not recorded. The triggering sensitivity and the start up time after triggering determines how much of the shock is lost. The adjustment of the trigger sensitivity poses a difficult choice. Since significant acceleration peaks can occur early in the record, it is desirable to have the seismograph triggered as soon as possible. However, if triggering sensitivity is too high, background noise or insignificant foreshocks may exhaust the seismograph paper supply so that a major shock is not recorded.

While the triggering service can be simply and accurately represented mathematically, the analysis of starting times reduces to the first passage time problem, which presents formidable difficulties. Also, a realistic representation of the triggering excitation encounters problems, since no record of this part of the shock has been made. Some results published in Hudson (1963) for the U.S.C.G.S. pendulum starter give an indication of the possible initial velocities and displacements. These results consist of a plot which gives the peak acceleration versus half-sine pulse duration required to trigger the seismograph.

Least - Mean - Square - Velocity Technique

This technique was introduced by Berg and Housner. It adds a time-dependent second order polynomial ($C_0+C_1t+C_2t^2$) to the acceleration, which has the desired effect of producing reasonable velocity and displacement time histories by integration of the acceleration data, rather than the

unrealistic time histories that would occur if the correction were not incorporated. By adding thesecond order polynomial $(C_o+C_1t+C_2t^2)$ the acceleration base line has the shape of a second degree parabola.

The technique which is used for this procedure makes the mean square value of the ground velocity a minimum. This is justified mainly by the feeling that most earthquake ground motions of significant time duration correspond to ground velocities which oscillate approximately symmetrically about a zero axis and approach zero velocity at the end of the earthquake. A similar condition could not be applied to the ground displacement since permanent ground displacements at the end of the earthquake could occur. This imposition of the mean square ground velocity minimization does not correspond directly to any physical requirement, but provides a reasonable technique. However,details on this point will be discussed later on.

The practical effect of the parabolic acceleration base line, combined with a mean square ground velocity minimization is to cause the ground displacement curve to be more closely confined to the vicinity of the zero axis, i.e. longer periods of motion of the order of twice the record length, tend to be suppressed from the displacement picture.

If $\ddot{u}_c$ is the corrected acceleration and $\ddot{u}$ the uncorrected acceleration by introducing the time dependent second order polynomial we have:

$$\ddot{u}_c = \ddot{u} - (C_1 + 2C_2 t + 3C_3 t^2) \qquad \ldots (A.1)$$

hence

$$\dot{u}_c = \dot{u} - (C_1 t + C_2 t^2 + C_3 t^3) \qquad \ldots (A.2)$$

$$u_c = u - (\tfrac{1}{2}C_1 t^2 + \tfrac{1}{3} C_2 t^3 + \tfrac{1}{4}C_3 t^4) \qquad \ldots (A.3)$$

where $\dot{u}_c$, $\dot{u}$ are the corrected and uncorrected velocities and u_c and u are the corrected and uncorrected displacements.

The minimization of the mean square ground velocity requires the quantity $R = \int_0^T \dot{u}_c^2 \, dt$ to be minimum.

So from equation (A.2) we have:

$$R = \int_0^T \left[\dot{u} - (C_1 t + C_2 t^2 + C_3 t^3)\right]^2 dt \rightarrow \min \qquad \ldots (A.4)$$

In accordance with the rules of partial differentiation,

$$\frac{\partial R}{\partial C_1} = 0 \quad \frac{\partial R}{\partial C_2} = 0 \quad \frac{\partial R}{\partial C_3} = 0 \qquad \ldots (A.5)$$

$$\frac{\partial R}{\partial C_1} = -2 \int_0^T \left[\dot{u} - (C_1 t + C_2 t^2 + C_3 t^3)\right] t \, dt = 0$$

$$\frac{\partial R}{\partial C_2} = -2 \int_0^T \left[\dot{u} - (C_1 t + C_2 t^2 + C_3 t^3)\right] t^2 \, dt = 0$$

$$\frac{\partial R}{\partial C_3} = -2 \int_0^T \left[\dot{u} - (C_1 t + C_2 t^2 + C_3 t^3)\right] t^3 \, dt = 0.$$

These three equations give

$$\int_0^T (C_1 t + C_2 t^2 + C_3 t^3) t \, dt = \int_0^T \dot{u} t \, dt$$

$$\int_0^T (C_1 t + C_2 t^2 + C_3 t^3) t^2 dt = \int_0^T \dot{u} t^2 dt$$

$$\int_0^T (C_1 t + C_2 t^2 + C_3 t^3) t^3 dt = \int_0^T \hat{u} t^3 \, dt$$

and finally we get,

$$\frac{T^3}{3} C_1 + \frac{T^4}{4} C_2 + \frac{T^5}{5} C_3 = \int_0^T \hat{u} t \, dt \qquad \ldots (A.6)$$

$$\frac{T^4}{4} C_1 + \frac{T^5}{5} C_2 + \frac{T^6}{6} C_3 = \int_0^T \hat{u} t^2 dt \qquad \ldots (A.7)$$

$$\frac{T^5}{5} C_1 + \frac{T^6}{6} C_2 + \frac{T^7}{7} C_3 = \int_0^T \hat{u} t^3 dt \qquad \ldots (A.8)$$

In these equations $\hat{u}$ is the uncorrected velocity time history obtained by integrating the original acceleration without the correction added, and T is the duration of the acceleration. Initial conditions of zero velocity and displacement are assumed. Hence the C's values can be evaluated.

Brady (1966) details three methods for calculating the integrals and recommends one on the basis of minimizing calculation error. After that the coefficients are readily evaluated and the correction polynomial may be added to the accelerogram. While this technique employs a second-order polynomial, any order polynomial is possible. When the square of the velocity which incorporates the correction is minimized with respect to C's, as many equations as coefficients would evolve by differentiation, and the coefficients could consequently be evaluated. There is a practical limit, however, because if such a series were carried to higher and higher orders, the series

would begin to approximate the negative of the accelerogram and the eventual result would be zero acceleration, velocity and displacement at all times. This interesting situation dramatizes the minimizing, non-conservative characteristic of this technique.

The least-mean-square velocity technique is the more widely used method of base-line correction. There are several possible reasons for this. First, a constant or linear correction-less than second order - seems inadequate, in that the drifting from the base line that usually occurs in the uncorrected velocity seems to be of higher than quadratic curvature. The need for a polynomial of at least second order to add to the acceleration is therefore indicated, and the least-square velocity technique is the only one with such a polynomial that has been advanced. Secondly, on seismic data - and most base-line formulations have been based on seismic data - it is usually very difficult to spot the end time. Therefore the least-mean-square velocity technique, which is not sensitive to end conditions is desirable. Also this technique seems to be attractive to statisticians because it is a least-mean-square manipulation. Incidentally, the squared velocity is related to kinetic energy, but it is not apparent that an earth tremor would have such a minimum-energy characteristic, although there may be some truth in it since in general natural processes involve minimum work.

APPENDIX B

RESPONSE SPECTRA

The response spectra of earthquake ground motion is defined as the plot of the maximum response of a series of single degree of freedom, linear, viscously damped oscillator to a prescribed ground motion, versus the natural period of the oscillator for various fractions of critical damping. The response spectra can be expressed in terms of relative displacement, relative velocity and relative or absolute acceleration. These curves provide a description of the frequency characteristics of the ground motion and give the maximum response of simple structures to the earthquake. By superposition of different modes of response, spectrum techniques can be applied to the design and analysis of complex structures such as buildings and dams. Used in this manner the spectrum technique represents an approach intermediate between a design based on static loads and a complete integration of the equations of motion of the complex structures.

Mathematical solution of response spectra

The response of a single degree of freedom, linear, viscously damped system, at any instant t, to an arbitrary time dependent ground displacement g_o is given by

$$m \frac{d^2}{dt^2}(u + g_o) + c \frac{du}{dt} + Ku = 0 \qquad \ldots (B.1)$$

where m = mass

c = viscous damping coefficient

K = coefficient of stiffness of the system.

u = relative displacement of the mass

$g_o(t)$= displacement of the base from the position of rest.

We can simplify equation (B.1) to

$$m\ddot{u} + Ku + C\dot{u} = -mg(t) \qquad \ldots (B.2)$$

where $g(t) = \frac{d^2}{dt^2}(g_o)$ is the ground acceleration.

If we assume that the motion starts from rest, i.e.

$u = \dot{u} = 0$ at $t = 0$, the solution of the equation is given by:

$$u = -\frac{1}{w_d}\int_o^t g(\tau)e^{-\lambda w_o(t-\tau)} \sin w_d(t-\tau)d\tau \qquad \ldots (B.3)$$

where

$w_o = \sqrt{\frac{K}{m}}$ = undamped natural frequency of vibration of the oscillator.

$\lambda = \frac{c}{2m w_o}$ = fraction of critical damping.

$w_d = w_o(1 - \lambda^2)^{\frac{1}{2}}$ = damped natural frequency of vibration of the system.

From equation (B.3) we can calculate the relative velocity.

$$\dot{u} = -\int_o^t g(\tau)e^{-\lambda w_o(t-\tau)} \cos w_d(t-\tau)d\tau + \frac{\lambda w_o}{w_d}\int_o^t g(\tau)e^{-\lambda w_o(t-\tau)} \sin w_d(t-\tau)d\tau \qquad \ldots (B.4)$$

The relative acceleration is given by

$$\ddot{u} = \frac{w_d^2 - 2\lambda^2 w_o^2}{w_d} \int_o^t g(\tau) e^{-w_o \lambda (t-\tau)} \sin w_d (t-\tau) d\tau$$

$$+ 2 w_o \lambda \int_o^t g(\tau) e^{-\lambda w_o (t-\tau)} \cos w_d (t-\tau) d\tau - g(t)$$

... (B.5)

and the absolute acceleration $\ddot{u}_a$

$$\ddot{u}_a = \ddot{u} + g(t) = \frac{w_d^2 - 2\lambda^2 w_o^2}{w_d} \int_o^t g(\tau) e^{-w_o \lambda (t-\tau)} \sin w_d (t-\tau) d\tau$$

$$+ 2 w_o \lambda \int_o^t g(\tau) e^{-\lambda w_o (t-\tau)} \cos w_d (t-\tau) d\tau$$

... (B.6)

For a given undamped frequency (w_o) and critical damping (λ) the spectrum values are by definition.

S_d = Relative displacement spectrum value = $\left|u\right|_{max}$.

S_v = Relative velocity spectrum value = $\left|\dot{u}\right|_{max}$.

S_a = Absolute acceleration spectrum value = $\left|\ddot{u}_a\right|_{max}$.

For small λ we can see that the quantity $(1-\lambda^2)^{\frac{1}{2}}$ is close to one and the above equations, (B.3)(B.4)(B.6), may be simplified to:

$$u_p = -\frac{1}{w_o} \int_o^t g(\tau) e^{-\lambda w_o (t-\tau)} \sin w_o (t-\tau) d\tau \quad \text{... (B.7)}$$

$$\dot{u}_p = -\int_o^t g(\tau) e^{-\lambda w_o (t-\tau)} \cos w_o (t-\tau) d\tau \quad \text{... (B.8)}$$

$$\ddot{u}_{ap} = w_o \int_o^t g(\tau) e^{-\lambda w_o (t-\tau)} \sin w_o (t-\tau) d\tau \quad \text{... (B.9)}$$

If we replace in equation (4.8) the cosine term by sine, the maximum value of the velocity response is not affected. So we can write

$$S_{dp} = |u_p|_{max} \qquad \ldots (B.10)$$

$$S_{vp} = |\dot{u}_p|_{max} = w_o S_{dp} \qquad \ldots (B.11)$$

$$S_{ap} = |\ddot{u}_{ap}|_{max} = w_o^2 S_{dp} \qquad \ldots (B.12)$$

where S_{dp}, S_{vp}, S_{ap} represent the "pseudospectra" of the ground movement. For $\beta = 0$ we have

$$S_d = S_{dp}$$

$$S_a = S_{ap}$$

$$S_v \neq S_{vp}$$

APPENDIX C

NUMERICAL CALCULATION OF SPECTRUM.

We can write the equation of motion for a linear, viscously damped, single degree of freedom oscillator as follows:-

$$m\frac{d^2u}{dt^2} + c\frac{du}{dt} + Ku = -mg(t) \qquad \ldots (C.1)$$

By getting the ground acceleration $g(t)$ in a digitised form $g(t) = a_i(t - t_{i-1}) + b_i$, we can write equation (c.1) as

$$\frac{d^2u}{dt^2} + 2\lambda w_o\frac{du}{dt} + w_o^2u = -a_i(t - t_{i-1}) + b_i \qquad \ldots (C.2)$$

where

$$w_o^2 = \frac{K}{m} \text{ and } 2\lambda w_o = \frac{c}{m}$$

We can obtain the complementary function by solving

$$\frac{d^2u}{dt^2} + 2\lambda w_o\frac{du}{dt} + w_o^2u = 0 \qquad \ldots (C.3)$$

put $u = Ae^{-\rho(t-t_{i-1})}$

$$\rho^2 - 2\lambda w_o\rho + w_o^2 = 0$$

$$\rho = \lambda w_o \pm \left[\lambda^2 w_o^2 - w_o^2\right]^{\frac{1}{2}}$$

$$= \lambda w_o \pm iw_o(1 - \lambda^2)^{\frac{1}{2}}$$

so

$$u = \left[A\sin w_d(t - t_{i-1}) + B\cos w_d(t - t_{i-1})\right]e^{-\lambda w_o(t-t_{i-1})} \qquad \ldots (C.4)$$

where $w_d = w_o(1 - \lambda^2)^{\frac{1}{2}}$.

To find the particular integral, we put $u = c_1(t - t_{i-1}) + d_i$

$$2\lambda w_o c_1 + w_o^2 c_1(t - t_{i-1}) + w_o^2 d_1 = - a_i(t - t_{i-1}) - b_i$$

and by equating the constants

$$c_i = - \frac{a_i}{w_o^2}$$

and $2\lambda w_o c_1 + w_o^2 d_i = - b_i$

$$\text{or } d_i = \left[-b_i + 2\frac{a_i}{w_o}\right]\frac{1}{w_o^2}$$

So we get the complete solution of the equation of motion for

$t_{i-1} \leq t \leq t_i$ which is:

$$u = e^{-\lambda w_o(t-t_{i-1})}\left[A \sin w_d(t - t_{i-1}) + B \cos w_d(t - t_{i-1})\right]$$

$$- \frac{a_i}{w_o^2}(t - t_{i-1}) - \frac{1}{w_o^2}(b_i - \frac{2\lambda a_i}{w_o}) \qquad \ldots (C.5)$$

where the constants A and B can be determined from the initial conditions of the step.

$$t = t_{i-1} \quad u = u_{i-1} \quad \dot{u} = \dot{u}_{i-1} \qquad \ldots (C.6)$$

From (C.5) (C.6), we have

$$u_{i-1} = B - \frac{1}{w_o^2}(b_i - 2\frac{\lambda a_i}{w_o})$$

$$B = u_{i-1} + \frac{1}{w_o^2}(b_i - 2\frac{\lambda a_i}{w_o}) \qquad \ldots (C.7)$$

Differentiating (C.5) for t

$$\dot{u} = -\lambda w_o e^{-\lambda w_o(t-t_{i-1})}\left[A \sin w_d(t-t_{i-1}) + B \cos w_d(t-t_{i-1})\right]$$
$$+ w_d e^{-\lambda w_o(t-t_{i-1})}\left[A \cos w_d(t-t_{i-1}) - B \sin w_d(t-t_{i-1})\right]$$
$$- \frac{a_i}{w_o^2} \qquad \ldots (C.8)$$

From (C.6) (C.8) we get

$$\dot{u}_{i-1} = -B\lambda w_o + Aw_d - \frac{a_i}{w_o^2}$$

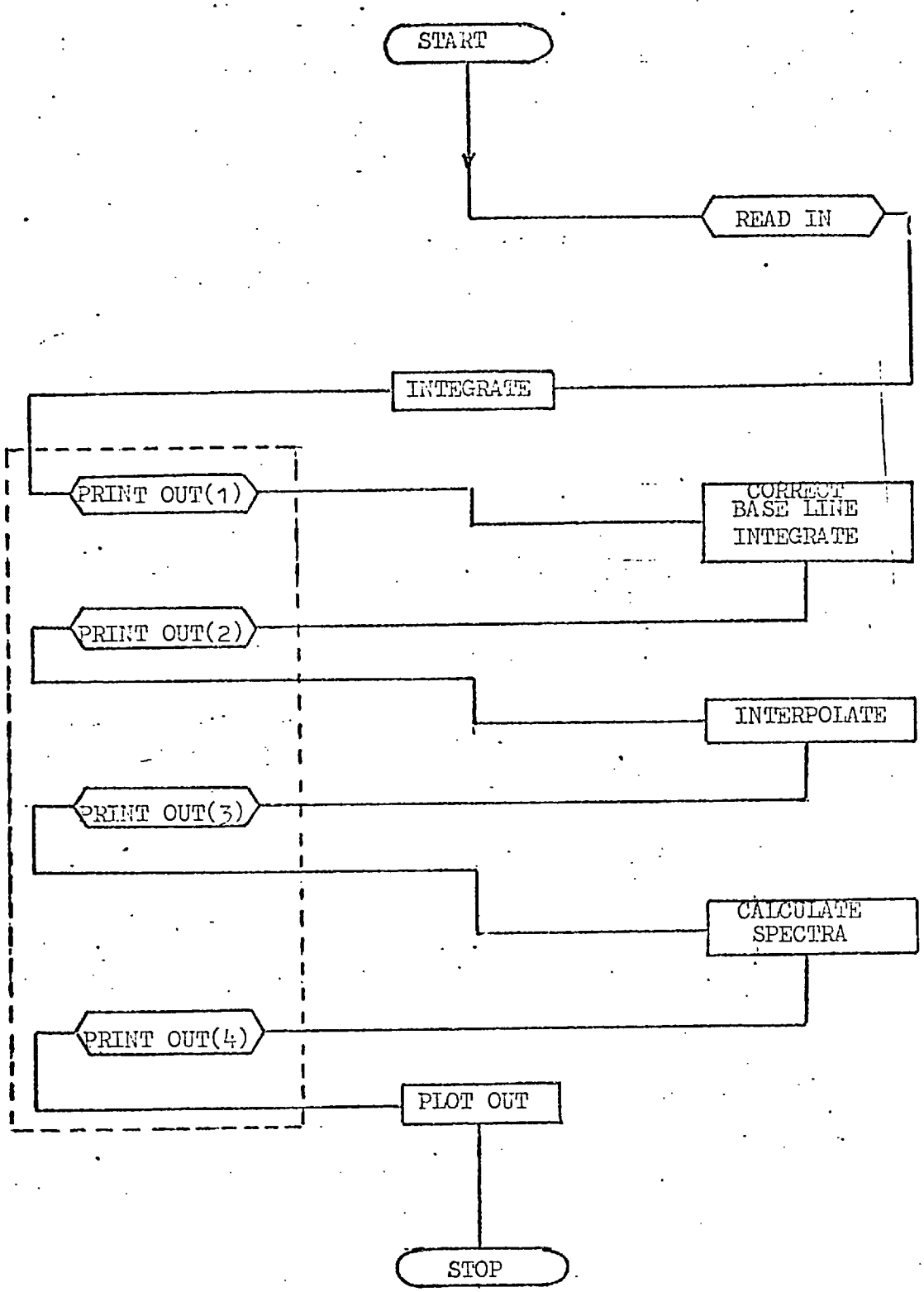
$$A = \frac{1}{w_d}\left[\dot{u}_{i-1} + B\lambda w_o + \frac{a_i}{w_o^2}\right] \qquad \ldots (C.9)$$

The absolute acceleration is given by

$$\ddot{u}_a = \ddot{u} + g(t) = -(2\lambda w_o \dot{u} + w_o^2 u) \qquad \ldots (C.10)$$

Thus having the solutions of the equations for u, $\dot{u}$, $\ddot{u}_a$ and with the initial conditions known, i.e. t = 0, u = $\dot{u}$ = 0, we can calculate the displacement, velocity and absolute acceleration of the oscillator by a step-by-step process at any required instant.

So we can plot the maxima values of displacement, velocity and acceleration versus the corresponding periods of the oscillators involved.



APPENDIX D

COMPUTER PROGRAM

```
(S)
ACH(CALCOMP,CALCOMP)
ECT(D,L=CALCOMP)
URN(CALCOMP)
UEST(TAPE27,HI,S)IC CALCOMP TAPE,PERMIT.
(LC=11610)

   PROGRAM SPEC1(INPUT,OUTPUT,TAPE5=INPUT,TAPE6=OUTPUT,TAPE27)
FTC    ROUSSO
   DIMENSION          V(600),D(600),T(600),AC(600),VC(600),EC(600),
  1DC(600),TT(2400),AA(2400),AM(400),VM(400),DM(400),NUM(6),TO(400),T
  86(400),T7(400)
   COMMON A,V,D,T,AC,N,ASCALE,TSCALE,J,VC,EC,DC,NU,JN,TT,AA,AM,VM,DM
   COMMON PN,K,CG,CX,CY,M,TO,TD,KOUNT
   J=2
   V(1)=0.0
    D(1)=0.0
    RECORDS OF ACCELERATION,TIME, AND VELOCITIES CALCULATION
   CALL READEN
    N=1
10 TIM1=T(N)
   ACC1=AC(N)
   N=N+1
   TIM2=T(N)
   ACC2=AC(N)
   TG=TIM2-TIM1
   V(J) =((ACC2+ACC1)*0.5)*(TG)+V(J-1)
   D(J)=((ACC2+(2.0*ACC1))/6.0)*(TG*TG)+(V(J-1)*TG)+D(J-1)
   J=J+1
    IF (J.LE.JN)  GO  TO  10
    CALL   WRITE  (1)
   CALL  BASECO
   CALL  INTERP
   KOUNT=0
   CALL  SPECTR
   DO 99 JJ=1,JN
   V(JJ)=V(JJ)*981.
   VC(JJ)=VC(JJ)*981.
   DC(JJ)=DC(JJ)*981.
99 CONTINUE
   CALL START
   NUM(1)=JN
   CALL GRAF (T,EC,NUM,1,0,12HTIME SECONDS,12,21HCORRECTED ACCEL IN
  5G,21,8.0,5.0)
   CALL SYMBOL(3.0,-.5,0.14,26HN S PORTHUNEME EGE 18/3/57,0.0,26)
   CALL GRAF(T,V,NUM,1,0,12HTIME SECONDS,12,27HUNCORRECTED VELOCITY C
  5M/SEC,27,8.0,5.0)
   CALL SYMBOL(3.0,-.5,0.14,26HN S PORTHUNEME EGE 18/3/57,0.0,26)
   CALL GRAF(T,VC,NUM,1,0,12HTIME SECONDS,12,25HCORRECTED VELOCITY CM
  5/SEC,25,8.0,5.0)
   CALL SYMBOL(3.0,-.5,0.14,26HN S PORTHUNEME EGE 18/3/57,0.0,26)
   CALL GRAF(T,DC,NUM,1,0,12HTIME SECONDS,12,20HCORRECTED DISPLAC CM,
  520,8.0,5.0)
   CALL SYMBOL(3.0,-.5,0.14,26HN S PORTHUNEME EGE 18/3/57,0.0,26)
   DO 2 I=1,6
   NUM(I)=M
   DO 97 K=1,KOUNT
   VM(K)=VM(K)*981.
```

```
   DM(K)=DM(K)*981.
97 CONTINUE
   DO 9 I=1,KOUNT
   T6(I)=TO(I)
 9 T7(I)=TO(I)
   CALL GRAF(TO,AM,NUM,6,0,14HPERIOD SECONDS,14,20HACCEL SPECTRUM IN
  5 G,20,8.0,5.0)
   CALL SYMBOL(3.0,-.5,0.14,26HN S PORTHUNEME EQE 18/3/57,0.0,26)
   CALL GRAF(T6,VM,NUM,6,0,14HPERIOD SECONDS,14,24HVELOCITY SPECTRUM
  5CM/SEC,24,8.0,5.0)
   CALL SYMBOL(3.0,-.5,0.14,26HN S PORTHUNEME EQE 18/3/57,0.0,26)
   CALL GRAF(T7,DM,NUM,6,0,14HPERIOD SECONDS,14,19HDISPLAC SPECTRUM C
  5M,19,8.0,5.0)
   CALL SYMBOL(3.0,-.5,0.14,26HN S PORTHUNEME EQE 18/3/57,0.0,26)
   CALL ENPLOT(22)
   STOP
   END
```

```
S18FTC READDK
      SUBROUTINE  READEN
C  THIS ROUTINE READ DATA FOR GROUND ACCELERATION OF
     DIMENSION          V(600),D(600),T(600),AC(600),VC(600),EC(600) ,
     1DC(600),TT(2400),AA(2400),AM(400),VM(400),DM(400),NUM(6),TO(400),T
     86(400),T7(400)
      DIMENSION   NAME (12)
      COMMON A,V,D,T,AC,N,ASCALE,TSCALE,J,VC,EC,DC,NU,JN,TT,AA,AM,VM,DM
      COMMON PN,K,CG,CX,CY
C     THIS ROUTINE READ DATA FOR GROUND ACCELERATION OF EARTHQUAKE
      READ (5,4)  NAME
      WRITE (6,4)  NAME
    4 FORMAT  (12A6)
      READ (5,5) TSCALE,ASCALE
    5 FORMAT  (2F10.4)
       WRITE  (6,5)  TSCALE  ,ASCALE
C     SIMULTANEOUS READING OF TIME-ACCELE DATD UDER THE NAME OF A(N)
C     PN IS THE TIME INCREMENT
C     NU IS THE TOTAL NUMBER OF A(N) READING
C     JN IS NU/2 TOTAL NUMBER OF TIME-ACCELE COUPLE
      READ  (5,1000)  NU,JN,PN
 1000 FORMAT  (2I3,F6.4)
      WRITE  (6,1000 )NU,JN,PN
      READ (5,1020)   (T(I),AC(I),  I=1,JN)
 1020 FORMAT (12F6.3)
C     TIME DATA CHECK
       DO  30  I=2,JN
C     TIME ERROR MESSAGE
      IF(T(I) .LT.T(I-1)) WRITE (6,1012)  T(I),I
 1012 FORMAT  (14H ILLEGAL TIME2,4X,F6.3,10X,I3)
   30 CONTINUE
      DO  300  N=2,JN
      T(N) = (T(N)-T(1))*TSCALE
       AC(N) =(AC(N)-AC(1))*ASCALE
  300 CONTINUE
      T(1) =0.0
      AC(1)=0.0
      RETURN
      END
```

```
$IBFTC WRITDK
      SUBROUTINE WRITE  (L)
      DIMENSION          V(600),D(600),T(600),AC(600),VC(600),EC(600),
     1DC(600),TT(2400),AA(2400),AM(400),VM(400),DM(400),NUM(6),TO(400),T
     86(400),T7(400)
      COMMON A,V,D,T,AC,N,ASCALE,TSCALE,J,VC,EC,DC,NU,JN,TT,AA,AM,VM,DM
      COMMON PN,K,CG,CX,CY,M,TO,TD ,KOUNT
   70  FORMAT (1X,15HORDER NUMBER J=,4X,12I9)
   71 FORMAT (1X,16HTIME . IN.  SEC.,3X,12F9.4)
   72 FORMAT (1X,18HACCLE. IN.CM/SEC2.,X,12F9.4)
   73 FORMAT (1X,17HVELOC. IN.CM/SEC.,2X,12F9.4)
   74 FORMAT (1X,13HDISPL. IN.CM.,6X,12F9.4)
      IF(L.LT.1.OR.L.GT.20)  GO  TO  99
      GO TO  (7,8,9,10 ),L
    7 M=1
      WRITE (6,3)  NU ,JN
    3 FORMAT  (1X,3HNU=,I3,3HJN=,I3)
  785  K=M+11
       IF  (K.GE.JN)  K=JN
      WRITE  (6,70) ( J ,J=M,K   )
       WRITE  (6,71) (T(J), J=M,K  )
       WRITE  (6,72) (AC(J) ,J=M,K )
      WRITE  (6,73)( V(J)  , J= M,K )
      WRITE  (6,74) (D(J)  , J=M,K)
      M=M+12
      IF(K.LT.JN)  GO  TO  785
      RETURN
    8 M=1
  786 K=M+11
       IF  (K.GE.JN)  K=JN
      WRITE (6,70)  (J,J=M,K)
      WRITE (6,71) (T(J), J=M,K)
      WRITE  (6,72)  (EC(J),J=M,K)
      WRITE  (6,73)  (VC(J),J=M,K)
      WRITE (6,74) (DC(J),J=M,K)
      M=M+12
      IF(K.LT.JN)  GO  TO  786
      IF(M.LT.JN)  GO  TO  786
      RETURN
    9  WRITE (6,313)  (TT(I),AA(I), I=1,K)
  313  FORMAT (6(3X,F8.4,2X,F8.4))
      RETURN
   10  WRITE(6,53)TO(KOUNT),TD,AM(KOUNT),VM(KOUNT),DM(KOUNT),M
   53  FORMAT (6X,5(F9.5,10X),I5)
      RETURN
   99 WRITE  (6,1013)
 1013 FORMAT (33HERROR IN COMPUTED GO TO IN ,ERRR,)
      RETURN
      END
```

```
$IBFTC BASECO
      SUBROUTINE  BASECO
      DIMENSION          V(600),D(600),T(600),AC(600),VC(600),EC(600),
     1DC(600),TT(2400),AA(2400),AM(400),VM(400),DM(400),NUM(6),TO(400),T
     86(400),T7(400)
      COMMON A,V,D,T,AC,N,ASCALE,TSCALE,J,VC,EC,DC,NU,JN,TT,AA,AM,VM,DM
      COMMON PN,K,CG,CX,CY
C        THIS IS THE  BASE-LINE CORRECTION  SUBRUOTINE
      J=1
      WRITE (6,3)  NU ,JN
    3 FORMAT  (1X,3HNU=,I3,3HJN=,I3)
      B1=0.
      B2=0.
      B3=0.
  120 TP=T(J)
      TS=T(J+1)
      TK=TS-TP
      AK  =AC(J+1)-AC(J)
      P=AK/TK
      IF (TK.LT.0.00001)  GO TO  121
      TS2=TS*TS
      TS3=TS2*TS
      TS4=TS2*TS2
      TS5=TS4*TS
      TS6=TS5*TS
      TP2=TP*TP
      TP3=TP2*TP
      TP4=TP2*TP2
      TP5=TP4*TP
      TP6=TP5*TP
      TK2=TS2-TP2
      TK3=TS3-TP3
      TK4=TS4-TP4
      TK5=TS5-TP5
      TK6=TS6-TP6
      CO2 =T(J)*T(J)
       G=(0.5* P)*(0.25*TK4-2./3.0*T(J)*TK3+0.5*CO2*TK2)+1./3.*AC(J)*TK3
     1-0.5*AC(J)*T(J)*TK2+0.5*V(J)*TK2
      X=(0.5*P)*(0.2*TK5-0.5*TK4*T(J)+1./3.*TK3*CO2)+0.25*TK4*AC(J)-1./3
     1.*TK3*AC(J)*T(J)+1./3.*TK3*V(J)
      Y=(0.5*P)*(1./6.0*TK6-0.4*TK5*T(J)+0.25*TK4*CO2)+0.2*TK5*AC(J)-0.2
     15*TK4*AC(J)*T(J)+0.25 *TK4*V(J)
      B1=B1+G
      B2=B2+X
      B3=B3+Y
  121 J =J+1
      IF (J.LT.JN)  GO TO 120
      Z=T(JN)
      Z2 =(Z*Z)
      Z3=Z2*Z
      Z4=Z3*Z
      Z5=Z4*Z
      E3=B1/Z3
      E4=B2/Z4
      E5 =B3/Z5
      PA1=1.0/Z
      PA2=1.0/Z2
      CG=(300.0*E3)-(900.0*E4)+(630.0*E5)
      CX=((-900.0*E3)+(2880.0*E4)-(2100.0*E5))*PA1
```

```
      J=1
   85 CO2=T(J)*T(J)
      CO3=CO2*T(J)
      CO4=CO2*CO2
      EC(J)=AC(J)-(CG+2.0*CX*T(J)+3.0*CY*CO2)
      VC(J)  = V(J) -(CG*T(J)+ CX*CO2 +CY*CO3)
      DC(J)=D(J)-(0.5*CG*CO2+0.333*CX*CO3+0.25*CY*CO4)
      J=J+1
      IF (J.LE.JN)  GO  TO  85
      WRITE  (6,502)  B1,B2,B3,CG,CX,CY
  502 FORMAT  (///6(5X,E15.6)///)
      CALL  WRITE  (2)
      RETURN
      END
```

```
$IBFTC INTER
      SUBROUTINE  INTERP
      DIMENSION          V(600),D(600),T(600),AC(600),VC(600),EC(600) ,
     1DC(600),TT(2400),AA(2400),AM(400),VM(400),DM(400),NUM(6),TO(400),T
     86(400),T7(400)
      COMMON A,V,D,T,AC,N,ASCALE,TSCALE,J,VC,EC,DC,NO,JN,TT,AA,AM,VM,DM
      COMMON PN,K,CG,CX,CY
      J=1
      K=1
      X =1.0
      TT(1) =T(1)
      AA(1)=EC(1)
 12   TP =T(J)
      TS=T(J+1)
      AAC1 =EC(J)
      AAC2 =EC(J+1)
      TK =TS-TP
      AB =AAC2 -AAC1
      PP =AB/TK
 13   K=K+1
      TT(K)=TP+PN*X
      AA(K)=AAC1+PP*PN*X
      X=X+1.0
      IF (TT(K).LT.TS) GO TO 13
C
      TT(K) =TS
      AA(K) =AAC2
      X =1.0
      J =J+1
       IF (J.LT.JN ) GO TO 12
      CALL WRITE (3)
       RETURN
      END
```

```
$IBFTC SPEC
      SUBROUTINE  SPECTR
C THIS PROG IS CALCULATIN OF SPECTRUM IN ELASTIC RANGE
      DIMENSION           V(600),D(600),T(600),AC(600),VC(600),EC(600),
     1DC(600),TT(2400),AA(2400),AM(400),VM(400),DM(400),NUM(6),TO(400),T
     86(400),T7(400)
      COMMON A,V,D,T,AC,N,ASCALE,TSCALE,J,VC,EC,DC,NU,JN,TT,AA,AM,VM,DM
      COMMON PN,K,G,CX,CY,M,TO,TD,KOUNT
      WRITE  (6,1)  K
    1 FORMAT  (6X,I6)
   21 READ(5,30)NCHECK,DA
   30 FORMAT (I6,F6.4)
      WRITE (6,35)DA
   35 FORMAT (10X,F6.4)
       IF (NCHECK.GT.0)  RETURN
       WRITE (6,51)
   51 FORMAT (5X,12HNATUR PERIOD,5X,10HDAMP PEIOD,5X,14HSPECT ACCELERA,
     25X,14HSPECT VELOCITY,5X,18HSPECT DISPLACEMENT)
       WRITE (6,52)
   52 FORMAT(8X,6HSECOND,10X,6HSECOND,12X,5HPER G,12X,9HCM/SEC(G),12X,
     16HCM (G))
      KOUNT=KOUNT+1
      TO(KOUNT)=0.05
      M=1
   31 WO =2.0*3.14159/TO(KOUNT)
      DA2=DA*DA
      WD=WO*SQRT(1.0-DA2)
      TD=2.0*3.14159/WD
      J=1
       SA=0.0
       SV=0.
       SD=0.0
      SAMAX=0.0
      SVMAX=0.0
      SDMAX=0.0
   32 TP=TT(J)
      TS=TT(J+1)
      AAC1=AA(J)
      AAC2=AA(J+1)
      TT1=TS-TP
      PP=(AAC2-AAC1)/TT1
      X =SIN(WD*TT1)
      Y =COS(WD*TT1)
       R=1.0/(WO*WO)
      EX=EXP(-DA*WO*TT1)
C
      B=SD    +R*(AAC1-2.0*DA*PP/WO)
      C=1.0/WD*(SV    +B*DA*WO+PP*R)
C
      SVV     =-DA*WO*EX*(C*X+B*Y)+WD*EX*(C*Y-B*X)-PP*R
      SDD     =(C*X+B*Y)*EX-(PP*R*TT1+R*(AAC1-2.0*DA*PP/WO))
      SAA     =-(2.0*DA*WO*SVV     +SDD/R)
        IF(ABS(SDD     ).GT.ABS(SDMAX))  SDMAX=SDD
       IF(ABS(SVV     ).GT.ABS(SVMAX))  SVMAX =SVV
       IF(ABS(SAA     ).GT.ABS(SAMAX))  SAMAX =SAA
      SV=SVV
      SA=SAA
      SD=SDD
      J=J+1
```

```
      IF(J.LT.K )      GO  TO  32
      VM(KOUNT)=ABS(SVMAX)
      DM(KOUNT)=ABS(SDMAX)
      AM(KOUNT)=ABS(SAMAX)
      CALL WRITE (4)
      IF(KOUNT.EQ.60.OR.KOUNT.EQ.120.OR.KOUNT.EQ.180.OR.KOUNT.EQ.240.OR.
     4KOUNT.EQ.300.OR.KOUNT.EQ.360) GO TO 21
      KOUNT=KOUNT+1
      TO(KOUNT)=TO(KOUNT-1)+0.05
      M=M+1
      IF(M.LE.60) GO TO 31
       GO .TO  21
      END
```

REFERENCES

ALFORD, J.L., HOUSNER, G.W. & MARTEL, R.R. Spectrum Analyses of Strong-Motion Earthquakes. Pasadena: California Institute of Technology, Earthquake Research Laboratory, 1951.

AMBRASEYS, N. Maximum intensity of ground movements caused by faulting. World Conf. Earthquake Eng. 4th, Santiago, Chile, pp. 154-171.

AMBRASEYS, N. (1963) The Buyin-Zara (Iran) Earthquake of Sept. 1962. Bull. Seism. Soc. Am. 53(4).

AMBRASEYS, N. (1970) Factors controlling the Earthquake Response of Foundation materials: Proceedings of the 3rd European Symposium on Earthquake Engineering, Sofia, pp. 309-317.

AMBRASEYS, N. (1973) Dynamic and Response of Foundation Materials in Epicentral regions of Strong Earthquakes. 5th W.Conference on Earthquake Engineering, Rome (Invited Paper).

AMIN & ANG (1966) A non-stationary stochastic model for strong motion earthquakes. Civil Eng. Stud., Structural Research Series No. 306, University of Illinois, Urbana.

BENIOFF, H. The physical evaluation of seismic destructiveness. Bull. of Seismol. Soc. of America, 1934, pp.39 -403

BIGGS, J.M. Introduction to the Structural Dynamics. McGraw-Hill Book Co., 1964.

BERG & HOUSNER (1961) Integrated velocity and displacement of strong earthquake ground motion. B.S.S.A. Vol.51 no.2, pp. 175-189.

BERG, G. (1963) A study of error in response spectrum analysis. Primeras Jornados Chilenas de Sismologia e Ingeniera Antisisma. Vol.1, 1963, Santiago, Chile.

BERG & HOUSNER (1961) Integrated velocity and displacement of strong earth ground motion. Bulletin of Seismological Society of America, Vol. 51.

BORNOVAS (1964) Geological Study of Leukas island, Athens.

BOSTROM, R.C. & SHERIF, M.A. (1972) United States Microzonation Procedures. Proceedings of the International Conference on Microzonation, Seattle, Vol. I, pp. 183-190.

BRADY, A.G. (1966) Studies of Response to Earthquake ground motion. California Institute of Technology, Pasadena, California, 1966.

CLOUD, W.I.K. & HUDSON, D.E. A Simplified Instrument for Recording Strong Motion Earthquakes. Bulletin Seism.Society of America. Vol.51, No.2, April, 1961.

CLOUD, W.K. (1967) Intensity Map and Structural Damage, Parkfield, California, Earthquake of June 27, 1966. Bull. Seismol. Soc. Am., 57(6).

GALANOPOULOS Seismology. Athens 1961.

GALANOPOULOS The large conjugate fault system and the associated earthquake activity of Greece. Ann. Géol. des Pays Helleniques, 18, 119-134, 1965a.

HUDSON (1956) Response spectrum technique in engineering seismology. Proc. 1st W.C.E.E. Berkeley, California.

HOUSNER, G.W.,R.R. MARTEL & J.L.ALFORD Spectrum Analysis of Strong-Motion Earthquakes. Bulletin of the Seismological Society of America, Vol.43, No.2, April 1953.

HUDSON, D.E., WIGAN, N.C. & TRIFUNAC Analysis of Strong-motion Accelerograph Records. California Institute of Technology, Pasadena, California, 1969.

HUDSON, D.E. (1962) Some problems in the application of spectrum techniques to strong motion earthquake analysis. B.S.S.A. Vol. 52, No.2.

HALVERSON, H.T. Modern Trends in Strong Movement (Strong-Motion) Instrumentation. San Gabriel, California, U.S.A.

HALVERSON, H.T. The strong motion accelerograph. Proceedings of the Third World Conference on Earthquake Engineering. Vol. I, New Zealand, 1965.

HUDSON, D.E. (1963) The measurement of ground motion of destructive earthquakes. Bulletin of Seismological Society of America.,Vol.53.

HOUSNER, G.W. Characteristics of Strong-Motion Earthquakes. Bulletin of the Seismological Society of America, Vol.37, No.1, Jan. 1947, 19-31.

HOUSNER, G.W. Properties of Strong Ground Motion Earthquakes. Bulletin of the Seismological Society of America, Vol.45, No.3, July 1955, 197-218.

JACOBSEN & AYRE, R. Engineering Vibrations. McGraw-Hill Book Co. Inc. New York, 1958.

JENNINGS, P.C.(1968) Equivalent Viscous Damping for yielding Structures. J.Eng.Mech.Div.ASCE, 94 (EM1).

JENSCHKE, V.A., CLOUGH, R.W. & PENZIEN, J. Characteristics of Strong Ground motions. Proceedings of the Third World Conference on Earthquake Engineering, Vol.I, New Zealand, 1965.

KOBAYASHI, H. (1974) Microtremor measurements in the Balkan Region. Report on the Seminar on Microzoning, Ankara.

MEDVEDEV, S.V.(1965) Engineering Seismology; Israel Program for Scientific Translations, Jerusalem.

NIGAM, N.C. (1967) Inelastic Interactions in the Dynamic Response of Structures, Pasadena, California: Report of Earthquake Engineering Laboratory, California Institute of Technology.

NIGAM, N.C. & JENNINGS, P. Calculation of Response Spectra from Strong-Motion Earthquake Records. Bulletin of the Seismological Society of America, Vol. 59, No.2, pp.909-922,April 1969.

OHSAKI, Y. (1972) Japanese Microzonation Methods. Proceedings of the International Conference on Microzonation, Seattle, Washington.

OKAMOTO, S. (1973) Introduction to Earthquake Engineering. University of Tokyo Press, Tokyo.

POCESKI, A. The ground effects of the Skopje July 26, 1963 earthquake B.S.S.A., Vol.59, No.1, pp. 1-22, February, 1969.

POPPITZ Velocity and Displacement of Explosion-Induced Earth tremors derived from acceleration. Bull. Seismol. Society of America, Vol.58, No.5, pp.1573-1582, Oct.1968.

RICHTER, C. Elementary Seismology. Freeman and Company. San Francisco,1958.

ROSENBLUETH,E. & BUSTAMANTE. Distribution of Structural Response to Earthquakes. Proceedings ASCE, Vol.88, No. EM3 (June 1962), pp. 75-106.

RAVARA, A. Spectral Analysis of Seismic Actions. Proceedings of the Third World Conference of Earthquake Engineering, Auckland and Wellington, New Zealand, 1965.

SARMA, S.K. Energy flux of Strong Earthquakes. Tectonophysics. Elsevier Publishing Company, Amsterdam (1970).

SARMA, S.K. Response characteristics and stability of earth dams during strong earthquakes. Ph.D.Thesis, University of London, 1968.

SCHIFF, A. & BOGDANOFF, J. (1967) Analysis of current methods of interpreting strong-motion accelerograms. B.S.S.A., Vol. 57, No. 5.

SEED, B. & IDRISS, M. (1969) Influence of Soil Conditions on ground motions during earthquakes. Proceedings of the American Society of Civil Eng., Soil Mechanics and Foundation Division, SM 1, pp. 99-137.

SEED, B. & SCHNABEL (1972) Soil and Geologic effects in site response during earthquakes. Proceedings of the International Conference on Microzonation, Seattle, Washington.

SHERIF, M.A. (1973) Microzonation of Thessaloniki using the Sherif-Bostrom (U.S.A.) Method, Seattle, Washington.

THOMSON, W.T. Spectral Aspects of Earthquakes. Bulletin of the Seism. Soc. of America, Vol.49, Jan 1959, pp. 91-98.

TAKAHASI, R. The SMAC strong motion accelerograph and other latest Instruments for measuring Earthquakes and Building Vibrations. Proc. World Conference on Earthquake Engineering. Earthquake Engineering Research Institute and the University of California, Berkeley (1956).

UDWADIA, F.E. (1972) Investigation of Earthquakes and Microtremor Ground Motions, Ph.D. Thesis, California Institute of Technology.

ZATOPEK, A. Sur le movement du seismograph sous l'influence de deux formes du choc. Union Geodesique et Geophysique Internationale Association de Seismologie. Serie A. Travaux Scientifiques Fascicule 17. Communications presentées à la Conférence d'Oslo, Août, 1948.